Université catholique de Louvain
Ecole polytechnique de Louvain
Institute of Condensed Matter and Nanosciences
Institute of Mechanics, Materials and Civil Engineering

Mechanical and physicochemical properties of EPDM type cable polymers after thermal and radiochemical ageing

---

Thèse présentée le 27/02/2019
par Tamara Šarac
en vue de l'obtention du grade de
Docteur en Sciences de l'Ingénieur

Composition du jury

Prof. Eric Gaigneaux (Président)	Université catholique de Louvain, Belgique
Prof. Jacques Devaux (Promoteur)	Université catholique de Louvain, Belgique
Prof. Thomas Pardoen (Promoteur)	Université catholique de Louvain, Belgique
Dr. Milan Konstantinović (Promoteur)	SCK • CEN, Belgique
Prof. Christian Bailly	Université catholique de Louvain, Belgique
Dr. Frederic Monnaie	ENGIE Laborelec, Belgique
Prof. Agnés Rivaton	Université Clermont Auvergne, France
Dr. Gregory Marque	EDF, France

Louvain-la-Neuve, February, 2019.

Acknowledgement

This thesis is organized through a cooperation between Université catholique de Louvain (UCL), SCK • CEN, and ENGIE Laborelec. I thank to UCL and SCK • CEN for a strong scientific input and to ENGIE Laborelec for an industrial input and sponsoring of the thesis. I would like to thank to all the institutions for organizing this doctoral thesis and choosing me to perform it.

Foremost, I would like to express my sincere gratitude to my closest advisors Dr. Milan Konstantinović (SCK • CEN) and Prof. Jacques Devaux (UCL), for continuous support during my Ph.D study, for their patience, motivation, enthusiasm, and immense knowledge.

Besides my direct advisors, I would like to thank Prof. Thomas Paroden (UCL) and Dr. Andrei Goussarov (SCK • CEN), for their encouragement, insightful comments, and hard questions. Special thanks goes to ENGIE Laborelec for providing the industrial samples and Dr. Andrei Goussarov, for ageing of samples.

I am thankful to DOW Chemicals for providing the neat samples. I thank to Mr. Mat Celina and Dan Gillen from SANDIA National Laboratories (USA) for their hones reviews of my work and nano-indentation measurements provided on selected samples.

With Engie Laborelec, I have experienced support and guiding through close collaborations with Tanguy de Schoutheete, Dr. Nicolas Quiévy and Dr. Frederic Monnaie and I thank them for their instructions and help.

It was honor to be a part of the Nuclear Material Science (NMS) institute at the SCK • CEN and a pleasure to work within the group of

Lambrecht Marlies. I specially thank to my colleagues in SMT (structure material test) group Jan Knaeps, Jasper Joris, Geert Berkmans and Roel Vanuytven for their support in experimental work and positive oriented working environment.

The enthusiastic intern Laurent Remy provided important input for my thesis and he has gradually contributed to the experimental work. I thank to him. Pascal Van Velthem from the Bio and Soft matter department (BSMA) of the Institute of condense matter and nanosciences, was a great support, not only in practical work performed at the UCL university, but also in advising and guiding. I would like to express my gratitude to him, as well as to Sabine Bebelman for helping me with the FTIR experiments.

An introduction to a world of nuclear power plant cables was given to me through a collaboration with Dr. Vit Places, who I was visiting in UJV, Rez, (Czech Republic), and through contacts with EDF (France), where I have spend two weeks getting to know their program for cable qualification. These were done within the framework of ADVANCE project. I thank them for having me on their site and for the knowledge and experience passed on.

I would like to thank to Boris Minov, an office fellow, not just for academic support, but also for being my friend.

I am grateful to my dear friends, also PhD or master candidates, that shared the good and the bed with me, even the same roof. Thanks to all my friends from Serbia and to the new ones, I have met in the SCK • CEN campus for constant support and for being a part of this journey.

I thank to all the jury members for accepting to make this thesis better and bring me to the final steps.

Last, but not the least, I would like to thank my family: my husband for endless support, for daring to change his life, leave job and follow me to Belgium so that I can complete the Ph.D journey; my daughters Una and Tara, for motivating me in a special way and keep me going even in a less successful periods; my parents that doubtless believed in me and my sister who was always there for me, even to sit in a plane leaving her obligations behind, fly from Serbia to Belgium and unselfishly help with

whatever I call for. Beside my close family I need to mention cousins and neighbours, they were all supporting me strongly.

This was not an easy journey, but I am grateful for everything it brought to me: a bit less good things, to learn from them and to strengthen me and a good things to celebrate and to remember them.

Abstract

Instrumentation, control and power cables are related to the fundamental safety systems of Nuclear Power Plants. Their safe operation must be ensured in order to secure current and possibly extended NPP operation, under normal and accident conditions. Operating environment of these cables implies harsh ageing factors, including increased temperatures and radiation. Degradation with ageing might jeopardize cable functionality and cable integrity has to be regularly monitored. Cable structural integrity is often monitored by studying mechanical and electrical properties of cable insulation, which is mainly made out of polymers.

This study aims to contribute to the plant life extension validation and plant life management improvement through a better understanding of physico-chemical processes responsible for the cable insulation ageing, in parallel with development of cable life time prediction model. In order to do so, accelerated ageing with a broad ageing condition matrix was applied to the industrial and non-industrial (neat) polymer samples. The non-aged and aged samples were investigated using mechanical, microstructural and physico-chemical investigation techniques. Attempt was made to correlate the properties on macroscopic and microscopic scale with respect to the ageing processes and ageing mechanisms. Issues related to the necessity and the limitations with respect to the usage of accelerated ageing, with the emphasis on the diffusion limited oxidation effect were discussed and the results are incorporated into the life time predicting model.

Regarding the mechanical properties, elongation at break is generally used as a benchmark criterion for cable insulation ageing assessment.

However this is a destructive technique and attempts are being taken to develop an alternative non-destructive, rapid, and on-site monitoring technique. The indenter measurement test conforms to the above requirements and this technique is proposed to be implemented to assess the condition of cables installed in a nuclear plant.

The present thesis aims at the analysis of the elongation at break and indenter modulus data for polymer insulation materials, with the challenging goal of establishing correlations between the two techniques. The setting up correlations will provide the capability of assessing the condition of cable materials by use of an in-situ, non-destructive technique. In order to establish such a correlation, a modelling based on a phenomenological approach of the polymer ageing, as well as an experimental characterization of polymer degradation is required. Empirical modelling, supported by a phenomenological background is further used for predicting the evolution of elongation at break under long-term operating conditions, in order to estimate the time for reaching a given end - of - life criteria.

Contents

Chapter 1

Introduction

1.1 Cables in Nuclear Power Plant

When built, nuclear power plants (NPP) were foreseen to work up to 40 years. A few years ago, the first Belgian NPP reached this critical age. In the meantime, the nuclear industry was evaluating the safety issues related to the lifetime extension of existing power stations. The current design life of NPPs could potentially be extended to 60 or possibly even 80 years [1]. The lifetime extension of existing NPP relies on the long term stability of many of its components. For that purpose it is of outmost importance to demonstrate the structural and functional integrity of the components for extended time usage.

Power, control and instrument cables are important for safe and reliable NPP operation. Unlike other NPP components, such as reactor pressure vessel, specific cable surveillance program was never established. International experience has indicated that, as operating plants have aged, the number and rate of cable failures has increased, implying that degradation due to ageing may be a contributing factor [2]. Age-related degradation indeed might contribute to the appearance of cable failure.

Generally, and so in NPP, the cables can be grouped as: low (<1000 V), medium (1000 V-35 kV), and high voltage (>35-230 kV) cables. Low

voltage cables are separated into three basic categories: instrumentation, control and power cables [3].

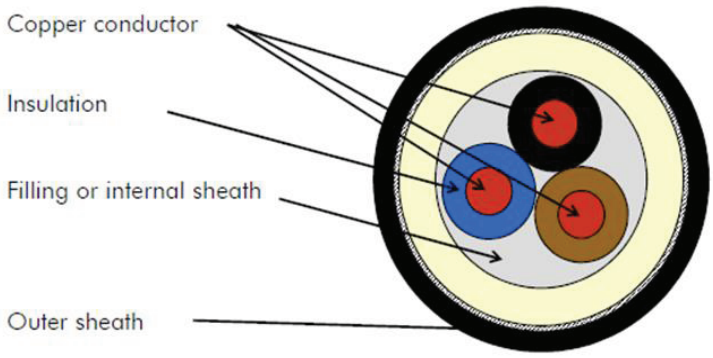

Figure 1.1: *Basic cable components.*

Basic cable components are presented in Figure 1.1 and they are: metallic conductor, an insulation that surrounds the conductor, an internal filling (paper-like or rubber-like material), an outer insulation (known as jacket or outer sheet). Shielding can be employed between the insulation and the conductor, and over the insulation to grade the voltage stress. Conductor is a metallic component that conveys electrical power or signal. Copper and aluminum are the most employed metals for this purpose, due to their low resistivity (i.e. increased amount of current in the circuit in comparison to the other conductors), and due to the fact that they are relatively cheap (especially in comparison to silver which has the lowest resistivity but it is more expensive) and easy accessible. Low resistivity of these conductors ensures decreased Joule heating, which is desired with respect to the surrounding insulation and possible thermal ageing effects that could be caused by wire heating. Conductors are insulated from other conductors and environment in order to prevent short circuit. Electrical insulation is provided to largely isolate the conductor from other paths or surfaces through which the current might flow. Insulation material must possess required electrical properties (a high resistance to the flow of electric current and good dielectric properties) and adequate mechanical properties. If present, shield layer is made out of flexible polymers blended with conducting carbon black

that imparts semiconducting characteristics or out of braided or winding conducting material (copper or aluminum) tapes. The jacket serves as inner cable insulation protection. It protects underlaying layers from mechanical damage, direct contact with chemicals, fire etc. Actually, the jacket is the most exposed part to the environmental ageing factors, so it is expected that it degrades faster than an inner insulation.

Variety of cable designs exist and they mainly depend on cable application and operating location. Cable designs differ in number of conductors, insulation and jacket thickness and configuration in which cable is put together. Some of the possible designs are presented in Fig. 1.2. In most cases actual insulation composition is not known due to proprietary nature of the company manufacturing process [3].

Figure 1.2: *Examples of cable designs.*

In one nuclear reactor, there are several thousands of kilometres of cables, and more than a thousand kilometres for instrumentation and control only. Cables are therefore a difficult component to replace. There are numerous environmental stressors in NPP that are affecting the cable insulation degradation: heat, irradiation, oxygen containing atmosphere, humidity, mechanical stressors like vibration, electrical surges, etc. Radiation and heat are predominant parameters of concern in many un-

dergoing studies, since they are found to have the biggest effect on cable ageing. [3] Despite numerous activities, an effective condition monitoring method for NPP is still under development.

The aim of this study is to investigate the ageing mechanisms relevant for NPP operating conditions, and to develop the methodology to assess the level of cable insulation degradation, with respect to the expected service life time.

1.2 Historical application of cable materials

Polymer materials are suitable as insulation materials, firstly due to their properties (mechanical and electrical), and then because they are easy to work with, not so costly, and widely available. Material intended for insulation around the conductor itself (inner insulation) is more required to fulfill expectation regarding electrical properties, while jacket material primarily has to be resistant to the environmental conditions [4].

Before the synthetic substitutes appeared, natural rubber was used for electrical insulation purposes, but polyethylene (PE) was found to be superior to rubber for moisture resistance and easier to handle in manufacturing procedure. Since 1950s, when PE was introduced for power distribution cables, application for extruded insulation material was increasing continuously together with improvements of these materials. PE was widely used through 1970s but then improved synthetic polymer materials were developed. [4] PE material itself has excellent dielectric strength, high insulation resistance, and a low dissipation factor at all frequencies making it an ideal insulator, however it is limited in its application temperature range. Still, PE is a homopolymer that is used as a basic constituent for some more advanced synthetic materials. Some of the most common synthetic polymer-based materials for cable insulation application beside polyethylene are polyvinyl chloride (PVC), ethylene-propylene elastomers (EPR, EPDM), cross-linked polyethylene (XLPE). [5, 6]

Ethylene-propylene elastomers and cross-linked polyethylene are introduced about the same time, around 1960s, for cables up to 1500 V (low

and medium voltage cables). By cross-linking a PE to become XLPE, a material of increased operating temperature range is obtained while good electrical properties of PE are maintained. The chemical and oil resistance at elevated temperatures are also improved for XLPE in comparison to PE. EPR has high dielectric strength (it is also a PE-based material), but it is often used as a jacket material due to wide operating temperature range (for a polymer material), excellent weathering resistance and resistance to a wide range of chemicals including many acids, alkalis organic solvents and ozone. It is also highly resistant to moisture, but it does not offer high resistance to oils. With respect to the mechanical properties both material are superior in comparison to the PE, but also to many others. XLPE offers great tensile strength, elongation and impact resistances. EPR rubber is a soft material and it can be used in many applications. When needed, increased hardness might be achieved by blending with some harder (for example more crystalline) polymer. Its mechanical properties include good resistance to compression, cutting, impact, tearing and abrasion. [4–6]

1.3 Industrial process for cable production and cross-linking

Insulation is mainly produced via extrusion process. The basic industrial set up for cable coating is schematically presented in Fig. 1.3. and consists of conductor pay off, extruder with a crosshead die, cooling/curing shaft, cupstan (pulling) and take up.

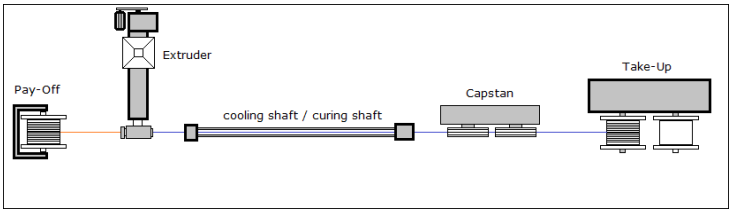

Figure 1.3: *A basic industrial set up for cable coating.*

Pay off is loaded with the conductor (wire) which needs to be coated i.e.

insulated. As already mentioned in Section 1.1 copper and aluminium are the most suitable materials to be used as conductors and they are received as large coils of round rod. Conductor pay off feeds the extruder where manufacturing of insulation and jacket is performed. Extrusion process is the step in which the cable is actually formed.

An extruder could be described as a screw that rotates in a barrel (see Fig. 1.4). Extrusion process is used to produce the material of a certain cross sectional shape and it includes mixing and melting of the (in this case) insulation compounds, shaping and cooling down of the final product.

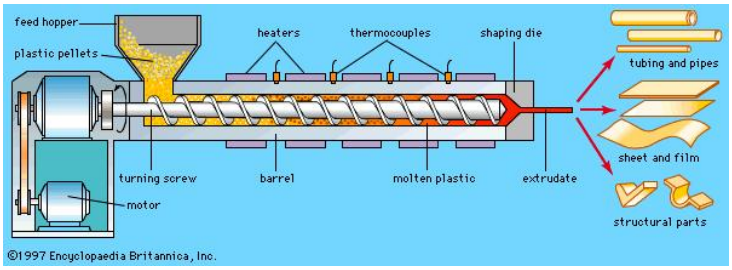

Figure 1.4: *Basic parts of an extruder.*

The type of extrusion that is the most widely used in wire coating and cable production is crosshead extrusion. This means that the process proceeds by introduction of the substrate, that is meant to be coated, to cross with the melt flow at the head of the extrusion process, see Fig. 1.5. Depending on the design of the product, un-coated wire or already coated wire (one or more together), could be introduced through a "crosshead", which can be single layer, co-extrusion or multi-layer type.

Extruders main parts are feeder (feed hopper) through which the compounding materials are introduced, motor which turns the screw, heating, cooling systems and pressure adjusting systems, and a die of a desired cross-section shape (see Fig. 1.4).

To manufacture a product from polymer material, not just polymer type constituent are used. Polymer (sometimes more than one) is used as a matrix, but many additional components are also present (10 to 15,

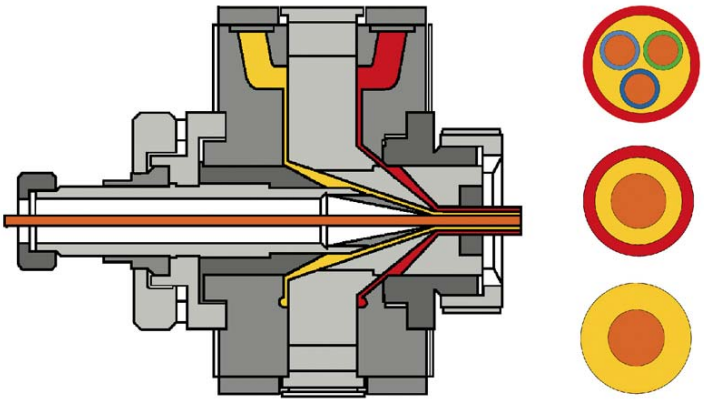

Figure 1.5: *The scheme of a crosshead extrusion head.*

sometimes even more). There are fillers (inorganic) and additives for different purposes. This means that the possibilities for composing compounding materials are practically countless. Compounding materials might be supplied as already prepared for extrusion, which means that they can be used "as received" and shaped in a desired form, but this option is rather expensive so producers prefer to mix the ingredients themselves to obtain a desired material. The feeding (compounding) material is the most often in the form of pellets or strips.

Detailed formulations of the final polymer material are protected by proprietary rights and known by the manufacturing company only, but there are few standard components that are publicly familiar. In order to get a material, suitable for industrial application above its glass transition, a cross-linking process (vulcanisation) is needed. Prior vulcanisation process material which contains very few cross-links is soft, sticky, with poor resistance to abrasion. [7, 8] Cross-linking of material usually demands addition of cross-linking agent into the compounding mixture. The cross-linking process follows the extrusion process and it will be discussed in more detail later in this chapter.

Besides cross-linking agents many inorganic fillers are being added. Rubbers can generally be mixed with high amounts of fillers. Fillers mainly have reinforcing role, but flame retardant fillers are especially important

in cables made for application in NPP industry. Zinc oxide was widely used to improve sulfur vulcanisation process, but it was observed that it also provides better heat stability for EPDM, so it is often present as one of the compounding materials even when peroxide curing is applied. Red Lead oxide (simply referred as red lead) acts as an ion scavenger and it improves electrical properties under wet ageing. Processing aids (wax or an oil that acts as a lubricant) are added in order to improve processing during extrusion and make it easier. Pigments are also included in the formulation and black coloured insulation is observed to offer better ageing stability in comparison to the light-coloured pigments.

To decrease (or prevent) polymer degradation during extrusion, but also afterwards, antioxidants are present. When the temperature is raised during manufacturing, material might be subjected to oxidative degradation, which is very common for polyolefins. Manufacturing temperatures are significantly higher than the service ones, which accelerates oxidation process. Significant oxidative degradation may be very harmful as it can lead to chemical changes within the insulation that introduce more polar species that may, in turn, introduce changes in electrical properties and make the cable more prone to failure during ageing. To prevent potential oxidation at processing temperature, antioxidant are incorporated into the pellets. The common antioxidant types have historically been either an organic amine-type (yellowish) or phenolic (white) compounds, again exact formulations are often known only by the manufacturer. Unreacted antioxidant together with antioxidant degradation by-products that are not volatile would stay in the amorphous regions after cooling upon manufacturing. Higher quantities of antioxidant can be included in the insulation formula in order to prevent/postpone/slow down oxidation reactions at service temperature. The antioxidant nature, when not known can be determined by an infra-red spectrum and the antioxidant efficiency, can be estimated by an oxidation induction time measurement via thermal analysis. [4]

All the material introduced through the feeder progresses down the screw. Screw is rotating in the barrel and the material inside is being pushed toward the extrusion head where the die is. The barrel is divided into the temperature controlled zones and material is being melted and

mixed on its way toward the die. Depending on ongoing chemical reaction, cooling of the barrel might be required sometimes. Parameters as temperature and pressure inside the barrel as well as the screw rotation rate are very important in material processing. The properly formed material is being pushed through the die and the extruded cable comes out as a final product. [9]

Several methods are used to cross-link the polymers: use of organic peroxides; use of high energy radiation; vulcanisation with sulfur; modification of the backbone structure (silane cross-linking). Since the peroxide curing was employed in the case of EPDM cable that is under investigation within this thesis, this type of curing will be explained in more details.

Peroxide cross-linking is generally the most common method for low and medium voltage cables. The most common organic peroxide for commercial application is dicumyl peroxide (DCP), which chemical formula is presented on in Fig. 1.6.

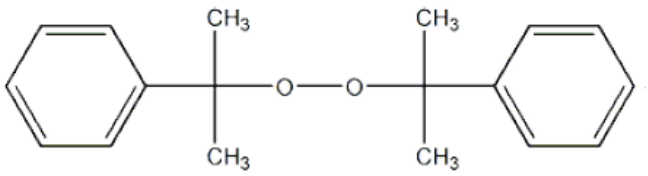

Figure 1.6: *Chemical formula of dicumyl peroxide.*

DCP is a strong free radical source that is traditionally already incorporated in the material (polymer) pellets by the material suppliers. Peroxide decomposes at certain elevated temperature and it creates free radicals. The peroxide is supposed to remain stable during the extrusion process, so the extrusion temperature should be lower than the peroxide decomposition temperature. DCP decomposes at temperatures above PE melting temperature, which is one of the reasons for its broad application. DCP decomposes giving cumyloxy radicals (see Fig. 1.7).

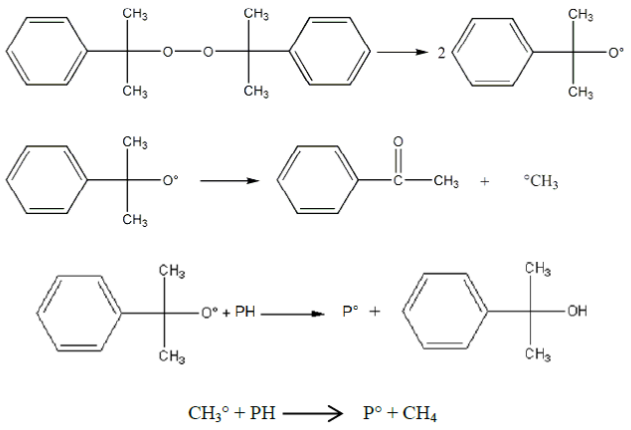

Figure 1.7: *Scheme of dicumyl peroxide decomposition and reaction with polymer.*

Free radicals are very unstable and they react fast. The created radical can subtract a hydrogen from polymer macromolecule which leads to generation of a macroradical. Cumyloxy radical can also reorganize via β chain scission and give acetophenone and a methyl radical which can also subtract a hydrogen from polymer and forms a methane molecule and a polymer macroradical. Created macroradicals finally create covalent bonds.

During the curing process, several byproducts are ultimately formed. The major ones are dimethyl benzyl alcohol, acetophenone and methane. [4] Byproducts migrate out of the insulation with time. The most important issue after cross-linking of EPDM with peroxide is the lack of knowledge on residual concentration of double bonds and their further effect on ageing.

During extrusion and (especially) curing process temperatures are higher than the polymer crystallites melting temperatures, so the entire polymer is amorphous (molten), which means that crystalline regions are not

hindering dispersion of the peroxide and uniformity of cross-linking process. When possible, recrystallization, will take place during the cooling process which follows.

Insulated cables undergo cooling process. Cooling process might be carried out as water-cooling or as dry cooling. During the water cooling care must be taken to avoid quenching and creation of locked-in mechanical stresses which cause material shrink-back. As insulation layer gets thicker, cooling has to be more gradual. In dry cooling, nitrogen can be used as cooling medium, and cooling is generally sufficiently gradual to avoid "locked-in" stresses, but the method of dry cooling is still not frequently used in cable production. [4]

After cooling, fully insulated cable goes to assembling. Capstan and take up are the final product assembling machines. Capstan is a system of pullays that is pulling extrudate through extrusion process toward take-up unit which is at the end of an extrusion line and, as its name indicates, it collects the final product.

Fast improvements in the materials and extrusion procedure in the 1980s has led to production of cables that can be qualified to operate for 30, 40, or perhaps even 60 years [4–6].

1.4 Industrial context of the thesis

This thesis aims to address the industrial issue, related to the cable ageing in NPP stations (see Section 1.1). The investigation was focused on the cable insulation. Research activities were carried out by running in parallel development of empirical/engineering model of the ageing and the attempt to better understand the fundamentals of polymer ageing process, by studying aged and non-aged samples. It is expected that these two research lines benefit from each other in such a way that empirical model gets physical background in order to generate a predictive model of polymer degradation and a better understanding of the ageing process.

Several mechanical and physico-chemical testing methods were employed in order to analyse polymer ageing at both, at macroscopic and micro-

structural level. Special focus was given to non destructive or low destructive techniques, that are practical for in situ testing, which does not require NPP cable disassembling. In order to contribute to a better understanding of the ageing process attempt was made to correlate macroscopic and microstructural changes caused by ageing. Additionally, a very important issue of accelerated versus ageing under operating conditions was analysed. Namely, in order to make predictive modeling it is convenient to bring the sample to a certain state (in this case to reach an end of operational life criterium) for a shorter time, so the samples are aged under irradiation dose rates and on temperatures that exceed those in the NPP. An engineering model will be developed on the basis of elongation at break, which is standardly used in industry for assessment of the cable integrity.

The main samples that are used for this investigation are obtained from the industrial storage i.e. NPP cable storage. These samples are made out of insulation stripped of a low voltage cable that is in use in the Belgian NPPs. Low voltage cables are mainly applied in instrumentation and control systems. Design of low voltage cables is more simple in comparison to the high voltage cables.

Samples from the industrial cables used for the investigation are made out of the cable marked as "Eupen ERR cable" on the outer sheet of the investigated cable. This means that the cable is produced by "Kabelwerk Eupen AG" (Belgium), while ERR stands for E-energy; R-inner insulation made out of EPDM; R- outer insulation made out of EPDM. Cables of this type were produced and installed during the ’70 and the ’80. This cable has four conductors, each insulated with the insulation of a different colour. The insulation that is around the conductor itself is named "inner insulation". This four wire insulated system is packed together and surrounded with the "outer insulation" layer also known as jacket. There is also an inlay material within the insulated conductors. An inlay material can be made out of different materials and in this case it is an sticky rubbery material. The investigation was performed on the samples made out of both, inner and outer insulation. It should be emphasized that generally an inner insulation is produced in a way that special care is given to its electrical properties, while outer sheath

is required to protect from the outer degradation factors, so the special attention is given to its mechanical properties and to its resistance toward humidity or chemicals.

In the insulation production (inner or outer) polyolefin polymer materials were employed. PE is the most present material, used as homopolymer but also as a component of many copolymers. The EPDM studied within this thesis is a copolymer of ethylene, propylene and diene - ethylidene norbornene (ENB).

Next to the industrial samples, "model" polymer samples were produced in the laboratory of the Université catholique de Louvain (UCL), aged and tested afterwards. These samples were made of neat polymers (EPDM and ethylene-octene copolymer) kindly provided by "The Dow Chemical Company". These model samples were made out of neat polymer pellets "as received" without addition of the fillers or cross-linking agent. The choice of such materials relays on an attempt to study the behaviour of the polymer itself under the environment that involves increased thermal and radiative stresses. It is expected that the results on neat polymers would help to better understand the chemistry behind the polymer ageing, by using less complex samples, regarding the composition, in comparison to the industrial material. Many groups of polymers are used in production of cable insulation. The exact composition of old insulation formulas, insulating the cables build in 30-40 years ago, are not even known. From that time, polymer industry developed gradually, and the modern formulations are available. Still, the NPP industry strains toward obtaining an "universal" ageing indicator, that ideally can be used regardless the particular formulation or even on different types of polymers. It is not easy to meet this expectation, since behaviour of a polymer under ageing will depend on its unique chemical composition and structure, plus each component added to a polymer is expected to influence its properties and ageing mechanism. However, comparing the ageing behaviour of an industrial polymer (the one that includes additives) with a "neat" polymer sample (model polymer), could indicate about direction, regarding possible consolidation of ageing indicators toward some universal, most relevant parameter, which can be used to assess the state of majority of the cable insulation

materials in use in NPP.

As a result, all the above mentioned activities, should provide better plant life management plan and support the possible plant life extension.

1.4.1 Structure and properties of the class of cable polymer of interest

The overview of the main chemical and physical properties for several polyolefin, PE based is given in Table 1.1. Polymers are listed starting from the data for PE monocristal (which does not exist in practise but the data are obtained theoretically), through the data for high and low density PE (HDPE and LDPE respectively), toward the data for PE and PP copolymers (EPR and EPDM).

Table 1.1: *The selected data for several PE based polymers.*

Type	Monomer(s)	Density, g/cm^3	Crystallinity, %	Tm, ^{0}C
PE monocrystal	$CH_2 = CH_2$	1.0	100	$\pm$142 ([1])
HDPE ([2]) Philips	$CH_2 = CH_2$	0.955-0.970	82-73	130-135
HDPE ([2]) Zn	$CH_2 = CH_2$	0.955-0.970	82-73	128-130
LLDPE ([2])	$CH_2 = CH_2, butene, octene$	0.915-0.935	60-46	120
LDPE	$CH_2 = CH_2$	0.915-0.935	60-46	110
VLDPE ([2,3])	$CH_2 = CH_2, octene$	0.857-0.908	34-13	38-104
EPR	$CH_2 = CH_2$, $CH_2 = CH - CH_3$	0.860-0.855	Very low, if any	/
EPDM	$CH_2 = CH_2$, $CH_2 = CH - CH_3, diene$	0.860-0.855	Very low, if any	/

(1)Weeks J., Journal of Research of the National Bureau of standards - A.Physics and Chemistry Vol.67A, No.5, 1963.; (2)HDPE, LLDPE and VLDPE can be synthesized by Metallocenes catalysts; (3) DOW ENGAGE data sheet

It is known that, depending on its structure, PE can differ in its density. HDPE is obtained when PE with less branches is produced, so mainly linear chains can easily form crystalline structure. Crystalline structure ensures higher density, since the aligned chains are more closely packed together. LDPE is characterised by branched structure which hinders chain aligning, and it is softer in comparison with HDPE. LLDPE and VLDPE stand for linear low density polyethylene and very low density polyethylene. Both are commonly obtained by copolymerization of ethylene with longer-chain olefins in the case of LLDPE, and short-chain polyolefins in the case of VLDPE. It is common to use octene or butene in copolymers in cable industry. Such copolymers give possibilities for some property improvements and these materials can be used

as inner insulation or jacket. These polymers are also characterised by lower density, but instead of long branches they rather posses significant number of short branches. Both, long chain branches and short chain branches, hinder the ability of the polyethylene main chain to crystallize.

Ethylene-propylene polymers are dominated by linear $-CH_2-$ and branched $-CH-$ units. Ethylene and propylene monomer are mixed in a gaseous state prior to polymerization in order to obtain EPR. By copolymerization of ethylene and propylene with certain catalysts of Ziegler-Natta type amorphous rubbery material can be obtained. Ratio of ethylene to propylene employed in the polymerization process will influence the ethylene to propylene ratio in the ultimate EPR insulation material. But even if it is possible to manufacture a wide variety of EPR copolymers each with different ethylene to propylene (E/P) ratios, not all E/P propylene ratios are suitable as insulation materials. E/P ratio of 50 to 70 % is typical for most insulations. EPR copolymer should be distinguished from blend of polyethylene and polypropylene. They have largely different properties and blends are prone to phase separation of different polymers, which does not happen with true copolymer. Ethylene-propylene does not contain unsaturation, except when a third monomer, a diene, is added to the ethylene-propylene monomer blend prior to polymerization. Diene monomer contains unsaturated bonds and it can facilitate certain (non-peroxide) cross-linking processes. Possible examples of the termonomer are 1,4-hexadiene, ethylidene norbornene or dicyclopentadiene (see Fig. 1.8). Copolymers that contains diene are more correctly called EPDM, but it is not uncommon to refer all ethylene copolymer or terpolymers to EPRs or EPs.

Propylene segments in the EPR (EPDM) interfere with the natural tendency of polyethylene to align. As the amount of co-monomer increases in the polymer, there is a decrease in crystallinity and copolymer may appear as completely or almost completely amorphous polymer, usually with short chain branched structure. Crystalline regions contribute to polymer density, toughness, modulus and moisture and gas permeation resistance; while, the amorphous regions increase the ductility, flexibility, and also facilitate processing.

It is worth saying that the same principles that apply to ethylene co-

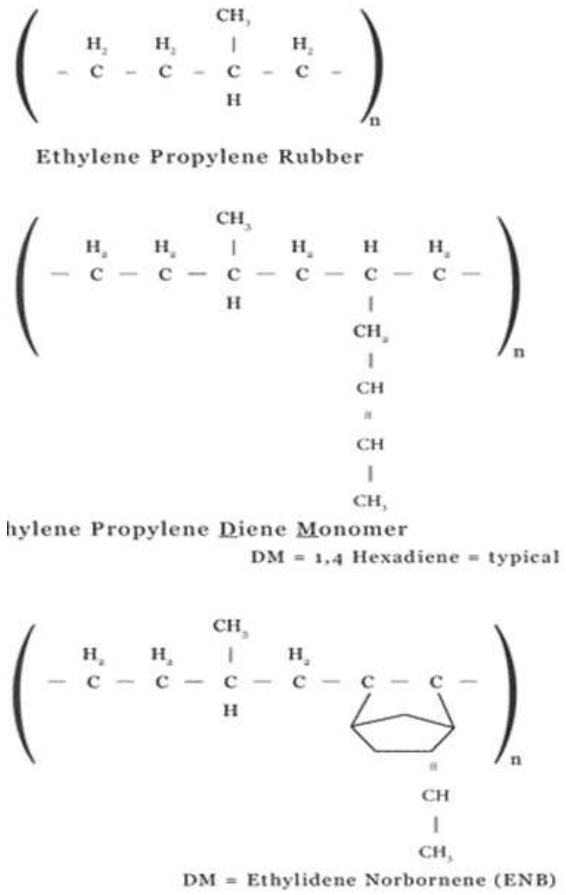

Figure 1.8: *Scheme of EPR and EPDM with different diene monomers.*

polymers with propylene also apply to ethylene copolymers with other monomers like vinyl acetate (VA) or ethyl acrylate. [4] Ethylene vinyl acetate (EVA) will be shortly discussed here, since it is also present in the formulation of the studied industrial cable insulation. VA is a polar comonomer, which indicates that an increase of its percentage in the formulation, increases EVA polarity and decreases crystallinity percent.

Properties and an application of EVA depend on VA percent. EVA that contains about 50 % of VA is completely amorphous and it has predominantly rubber-like behaviour, which means that by cross-linking it becomes suitable for cable insulation applications. Its density is 0.99 g/cm^3. [10] All EVA polymers, except the ones with very low VA content, offer very good environmental stress cracking resistance, which increases with VA content. This makes EVA very desirable in cable industry.

Polymers composed only of main chains are known as linear polymers, while polymers composed of chains that contain branches are called branched polymer. Next to these two groups there are cross-linked polymers, which are specially important in cable industry, due to their enhanced mechanical properties in comparison to the raw elastomer gum, especially due to their flexibility. PE and its copolymers are being cross-linked mainly following the procedure described in Section 1.3.

In cross-linked polymers macromolecular chains are connected to each other by covalent bonds and they form a three-dimensional cross-linked network. With the increase of cross-linking the molecular weight gets so high that the cross-linked polymer can be considered to have an "infinite" molecular weight. Three-dimensional network is the characterized by the cross-link density which can be expressed as average mass of sub-chains between two cross-links and the functionality of cross-links, which is the average number of chains ending into (or going out from) a cross-link.

Chains between cross-links which takes part in elastic properties of the network are called elastically active. In an ideal network, all chains are elastically active, but in reality there are always polymer chains that are not a part of "infinite" network and these chains are considered as "network defects". Chain loops, dangling chains, and free chains are examples of "network defects".

Cross-linking affects significantly the solubility of polymer. In a suitable organic solvent chains of the polymer interact with solvent and when that interaction overcomes chain-chain (polymer-polymer) interaction chains move apart and the polymer dissolution occurs. The chains of a cross-linked polymer that are connected by covalent bonds will never move so far apart and instead of dissolution, swelling in a solvent will happen

and so called "gel phase" will be formed instead of solution. Contrary to swelling of three-dimensional network, chains that are not part of the network created by cross-linking will dissolve. Two parameters "gel fraction" and "sol fraction" are used in describing the cross-linking extent of a polymer.

Unvulcanized elastomer, which contains very few cross-links, is soft with poor resistance to abrasion, and it is not applicable in practical application. Cross-linking increases modulus of elasticity, tensile strength, and resistance to degradation by oxidation, but with increasing the cross-link density rubber hardens and the extensibility is being reduced. There is always a cross-linked and a not cross-linked part of the material however, the physical and electric properties are mainly controlled by the cross-linked regions of the polymer.

Mechanical properties of a polymer at a given temperature are not characteristic for the polymer as a substance, but of the physical state which the polymer has at a given temperature (semi-crystalline, glassy, rubbery or viscous). So depending on their structure and operation temperature, polymers can show various mechanical behaviors. The majority of polymers that are used for cable insulation are actually elastomers (rubbery polymers), which are characterized by their specific elastic properties. Elastic properties of insulation are one of the most studied non-electrical properties and maybe the most important one. Therefore, it is considered that degradation of cable polymer insulation is often closely related to its embrittlement i.e. loss of elasticity [3].

Elastomers are specific for their ability to withstand very large deformations together with deformation recoverability after the stress is removed. Rubbery materials can undergo large deformation under applied stress and then recover their initial shape after the stress is removed. To undergo large deformations, the polymer chains must have a high degree of flexibility and deformability. Long macromolecular chains, their entanglement and bonding of chains by covalent bonds, or chain aligning, contribute to polymer elasticity.

Elastic properties of rubber have entropic origin. Entropy is a measure of the degree of disorder within a system. When it is extended under stress,

rubbery material tends to go back to a higher entropy state. During the extension the entangled and cross-linked chains straighten and align, less disordered system is formed and entropy lowers. When the applied stress is removed, the system goes back to its thermodynamically preferred state [8].

Break of the elastomer sample originates from a high local stress to which a limited number of chains are exposed. When these chains break, a crack is formed which gradually propagate through neighbouring chain fracture until complete failure of the sample occurs. Network defects and damage such as voids and cracks, constitute initiating source of break. [11].

Fillers have an important influence on the mechanical properties. As a rule, the charged (filled) material has a larger elastic modulus than the matrix. Elastic modulus of filled rubber will depend on the properties and nature of the filler, its morphology and size, amount and distribution through the matrix. The interaction between the matrix and filler is a key feature, i.e. is the quality of the adhesion and interface strength. Sometimes surface treatment of the filler is performed to achieve better adhesion to the matrix. Increase in the tensile strength of a filled rubber in comparison to the unfilled reference is also observed. [12] The effect on the elongation at break can vary, but the elongation at break decreases in majority of cases.

Aside from mechanical properties, polymer has to fulfill certain electrical properties so it can be used as an insulation material. For several polymers, the magnitudes of these properties are given in Table 1.2. [6] Since electrical properties of insulation are out of scope of this study only the basic explanation of each listed property will follow table.

Table 1.2: *The electrical properties of some polymers [6].*

Material	Resistivity (Ωcm)	Diel. Strength (kV/mm)	Diel. constant (1 kHz)	Dis. factor (1 kHz)
Natural rubber	10^{15} - 10^{17}	2.36-31.5	2.1-3.7	0.0023-0.0030
EPR	10^{15} - 10^{17}	35.4	3.17-3.34	0.0066-0.0079
EPDM	10^{15} - 10^{17}	35.4-41.3	3.0-3.5	0.004 (at 60Hz)
PE	$> 10^{22}$	17.7-27.6	2.28-2.35	1-2 $\times$ 10^{-4}
XLPE	$> 10^{15}$	21.7-98.4	2.3	3-5 $\times$ 10^{-4}

The electrical resistivity measures the current flowing through the sec-

tion of material under imposed voltage (its called volume resistivity). Useful insulation material have resistivity of at least $10^6 \Omega cm$.

The dielectric strength of an insulating material is the maximum electric field that a pure material can withstand under ideal conditions without breaking down (without experiencing failure of its insulating properties).

The dielectric constant or relative permittivity is the ratio of the capacitance of a capacitor based on the material as a dielectric, compared to a vacuum. It indicates how easily a material can become polarized by imposing an electric field on an insulator.

The dissipation factor is a measure of loss-rate of energy of a mode of oscillation (mechanical, electrical, or electromechanical) in a dissipative system. Insulation materials should have low values of electrical dissipation factor, to avoid dielectric losses.

Beside a polymer, the final cable material will contain a lot of additives and fillers as well (10 to 15, sometimes even more) and some of them are described in more details in Section 1.3. Properly formulated, an EPR compound will exhibit excellent electrical properties, excellent high temperature performance, low water permeability, as well as resistance to water trees, acids, bases, ozone, and UV. Even if many EPR compounds that are used as insulations for cables possess proprietary ingredients and the formulations in detail known only to the manufacturer, some basic and often used components and their purpose are familiar.

1.5 Ageing of cable polymer insulation

1.5.1 Ageing mechanism

Ageing of some component (essentially of the constituent material) is seen as a loss of functionality of that component with time. Ageing process could be defined and monitored at different levels. At the macroscopic level, ageing can be detected as a change of mechanical or electrical property with time. Degradation usually begins in the localized regions and then propagates through the material. The changes at the macroscopic scale are caused by changes at the microstructural level.

Many factors contribute to the material ageing: temperature, oxygen, moisture, presence of chemicals, mechanical stressors and, especially within the NPP industry, irradiation. Within this thesis, ageing of polymer material, used as a cable insulation, under elevated temperature and irradiation was studied. In order to understand the ageing process the focus is given to the understanding of correlation between microstructural properties and macroscopic mechanical behaviour.

High energy radiation is either electromagnetic radiation (X and γ rays) or particle radiation (α rays, fast electrons, neutrons, nuclear fission products). Polymer macromolecules are capable of interacting with all kinds of radiation. Still, interaction of radiation with atomic nuclei can be neglected when the photon kinetic energies are lower than 10 MeV and if the material consists only of light nuclei, which is the case for polymer materials. The flow of the resulting reactions depend on the chemical composition of irradiated material and on the nature of radiation. The term "high irradiation" refers to the types of radiation that have significantly higher kinetic energies than the bond dissociation energies. In NPPs the cables are only exposed to γ radiation, so accelerated ageing based on γ is used in this work. γ rays constitute one type of electromagnetic radiation. They are photons so they are neutral (neither is positively nor negatively charged) and they have no mass. Because of this, their interaction with matter is via electrons, but they can also transfer some part or all of their energy to the matter.

When γ ray interact with electrons of polymer atoms three possible processes may occur: the photoelectric effect, the Compton effect and the pair formation. In all three processes secondary electrons are ejected and they usually possess enough kinetic energy to induce further ionization or electronic excitations in surrounding system. The energy of secondary electrons is usually less than 100 eV so they lose this energy very close to their source (react with surrounding neighbouring atoms). Created instable species (radicals) further react easily with intact molecules and oxygen. [13]

The photoelectric effect takes place when a photon hits the electron which is bound to an atom. An incident photon completely disappears upon interaction while an energetic photoelectron is ejected by the atom.

In such a way an ionized atom with a vacancy in one of its bound shells is created. This vacancy is then shortly filled by an electron from a shell with a lower bonding energy or by capture of a free electron from the material. Important is to notice that the emission of photoelectron by photoelectric effect is only possible when photon reaches or exceeds the binding energy of the electron.

The Compton effect is an inelastic scattering effect. Namely, the gamma-ray photon is scattered from its initial pathway, by a charged particle usually an electron, and deflected through certain angle with respect to its original pathway. The photon transfers the part of energy to the recoil electron depending on scattering angle.

Pair formation dominates at the high energies and what happens is that the energy is directly converted into matter. It can be seen through the creation of electron and positron when the photon passes close to atomic nucleus. The electromagnetic energy of the photon must overcome or at least to be equal to the rest mass energy of the two particles so that pair formation can happen. The situation must allow both energy and momentum to converse and in order for this to happen the atomic nucleus must receive some momentum.

Gamma radiation is very penetrating through a polymer material and it is considered to create radicals very uniformly. High energy radiation is supposed to cause random main-chain degradation, rather than specific side-attack on macromolecular chain. [13] Presence of impurities incorporated in the macromolecule chain can promote specific site attack. Presence of so-called "weak links" will also lead to a non random polymer degradation process. Olefinic unsaturations, especially if they are terminal are a typical example of weak links. In comparison to radiation induced degradation, thermal degradation is considered to be more of a selective nature.

Thermal degradation refers to the case when chemical changes in polymer are the only consequence of elevated temperature without the involvement of another compound. Still, in practice it is difficult to distinguish it from other forms of degradation, like thermo-chemical degradation.

Polymer materials are, with few exceptions, stable below the temperature range of 100 - 200 ^{0}C. Their thermal sensitivity is due to the fact that they are bonded by covalent bonds. This is where the selectivity comes from. We could expect that the bonds having the lowest dissociation energy will break primarily. These bonds are prone to break at temperatures between 400 - 600 ^{0}C, but at lower temperatures, like 150-300 ^{0}C, bond scission can initiate chemical reaction like oxidation. The initiated reaction will further proceed faster at higher temperatures but significant conversion can be achieved at slightly elevated temperatures as well. So, the scission of chemical bonds as a result of temperature influence will cause rapid polymer decomposition at highly elevated temperatures, but rates of chemical reactions are very temperature dependant and they can cause significant decomposition even at milder temperatures with respect to the one where polymer bond dissociation energy is overcome. Increase in crystallinity, incorporation of polar groups, incorporation of aromatic and heteroaromatic rings, intermolecular chemical cross-linking and less branched polymer structure increase thermal stability of polymer. Increased thermal stability leads to better resistance to oxidation at higher temperatures. [14]

Ageing mechanism of polymers that were exposed to irradiation and/or high temperatures, has been widely studied [15–19]. Still, considering the complexity of cable polymer system, it is not always easy to describe the process at the mesoscale and correlate it to the macroscopic changes, so there is no complete understanding yet. Studying of polymer decomposition mechanism on molecular level indicates that polymer decomposition reactions are free radical reaction type. Which means that by both ageing factors of interest here (irradiation and heat) free radicals are created out of intact polymer.

Kinetically, single step and chain reactions are distinguished. While in single step reactions, the reaction rate is directly proportional to the rate of initiation step, in chain reactions initiation reaction creates the products that can further react with original (intact) molecules. Therefore, the once started chain reactions are characterized by self-propagation. Often one initiation reaction causes several propagation reactions, which multiplies damaging effect. Under continuous initi-

ation process conversion increases exponentially with reaction time(not directly proportional like in one step reaction). Auto-acceleration is followed by auto-retardation after long enough time and depletion of the oxygen concentration in the bulk of the material is a good example of that. Propagation can be inhibited by reaction products. [13, 14]

The interaction of irradiation and/or heat with polymer will cause ageing that proceeds through free radical chain reaction. Three basic ageing mechanisms are generally accepted for cable polymer macromolecules: cross-linking, chain scission and oxidation. In practice, cables are operating in air, so it means in oxygen containing atmosphere, hence oxidation is very important ageing mechanism. Cross-linking and chain scission can appear in both atmospheres with or without oxygen. There are three main steps of oxidation (ageing) process: initiation; propagation and termination.

Initiation step is given by the Eq. 1.1, which simplifies the previously described process of polymer decomposition via thermal influence or via reaction with irradiation. [13, 14] Creation of radical is essential in this step (Eq. 1.1) and it proceeds either by hydrogen abstraction or by the scission of a carbon-carbon bond.

$$P \rightarrow P^* \tag{1.1}$$

The Eq. 1.2 and 1.3 describe so called propagation step. At ambient temperatures chemical structures of polymers are quite stable against the attack of molecular oxygen, but if any process initiate creation of free radicals they will further react rapidly with oxygen, see Eq. 1.2.

$$P^* + O_2 \rightarrow POO^* \tag{1.2}$$

Result of the reaction presented by Eq. 1.2 is creation of POO* type of radical (peroxy radical) that can easily attack intact molecule (typical for chain reactions) and accept hydrogen.

$$POO^* + P \rightarrow POOH + P^* \tag{1.3}$$

The created hydroperoxide (POOH) can remain as such at low temperatures, but can easily undergo thermal decomposition presented by Eq. 1.4 and this is considered to be of outmost importance in oxidation process.

$$POOH \rightarrow PO^{*} +^{*} OH \tag{1.4}$$

The reaction 1.4 is important because decomposition of hydroperoxide means that each initiating radical can produce two new radicals, which demonstrates the possibilities for decomposition process acceleration. The scheme of so called "double chain mechanism", which is presented schematically in Fig. 1.9, representing the complex nature of polymer oxidation process.

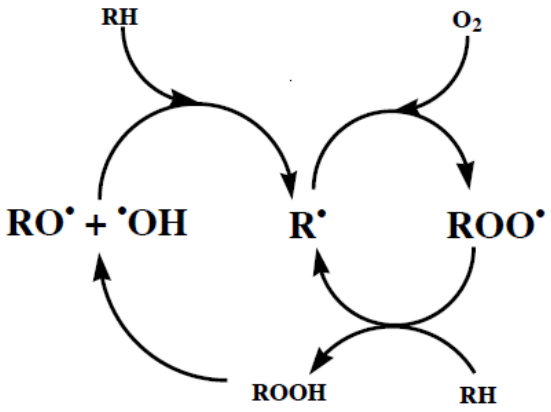

Figure 1.9: *The double chain mechanism during the oxidation process.*

OH* radical created via hydroperoxide decomposition is very reactive with organic molecules commonly by hydrogen abstract reaction with aliphatic organic compound, which is presented by Eq. 1.5.

$$OH^{*} + PH \rightarrow P^{*} + H_2O \tag{1.5}$$

Polymer radical created via reaction presented by Eq. 1.5. can initiate oxidative degradation (when oxygen is available) and give peroxyradical. This peroxyradical can further again form hydroperoxy radical and these reactions are very important as propagation steps of auto-oxidation.

Alkoxy radical, PO*, is created from hydroperoxide decomposition (Eq. 1.4) as well and it is prone to abstract hydrogen from intact molecules (which is presented by the Eq. 1.6) or to addition to a double bond in the case of polyenes. It can also undergo a β scission, see Eq. 1.7.

$$PO^* + PH \rightarrow POH + P^* \tag{1.6}$$

$$PO^*P' \rightarrow PC = O + P^* \tag{1.7}$$

Finally process is terminated by one of the following termination reactions (Eq. 1.8 - Eq. 1.10):

$$a)2POO^* \rightarrow POOP + O_2 b)2POO^* \rightarrow PO + POH + O_2 \tag{1.8}$$

$$POO^* + P^* \rightarrow POOP \tag{1.9}$$

$$P^* + P^* \rightarrow P - P \tag{1.10}$$

P* has the highest reactivity among the other radicals and it is active even at very low temperatures. Reaction 1.10 can proceed as recombination or disproportionation reaction. Disproportionation reaction is often present in polyethylene and it requires transferable hydrogens. Radical recombination reaction depends on radical mobility since it is encounter controlled process. In Fig. 1.10 the example of recombination and disproportion reactions is presented.

While the recombination reaction contributes to a creation of a new bond and in an increase of the molecular weight and cross-linking density, disproportionation results in the decrease of the molecular weight

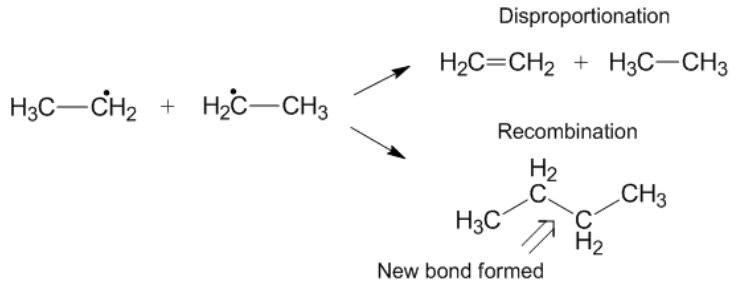

Figure 1.10: *Recombination and disproportionation reactions.*

and it promotes chain scission. The possibility for recombination and disproportionation reaction exist for POO* radicals as well, and it is presented by the Eq. 1.8 where reactions a) and b) are recombination and disproportionation reactions, respectively. An increase in temperature generally reduces the probability for cage reaction (like radical recombination) since the mobility of molecules is increasing.

Radicals created by decomposition of hydroperoxide can also undergo termination reaction, instead of removing the hydrogen from the polymer for example. These termination reactions are schematically presented by the Eq. 1.11 and 1.12.

$$PO* + P* -> POP \tag{1.11}$$

$$OH* + POO* -> POH + O_2 \tag{1.12}$$

Which termination reaction will dominate depends on polymer type and ageing conditions. Polyolefins with short alkyl side groups (like polypropylene) and unsaturated polymers undergo predominantly chain scission, while cross-linking is observed to be dominant for polyethylene, and rubbers with somewhat less active double bonds.

As already mentioned PE is more prone to cross-linking whereas PP to chain scission once the oxidation process is terminated. Mechanism of PE cross-linking is presented on Fig. 1.11.

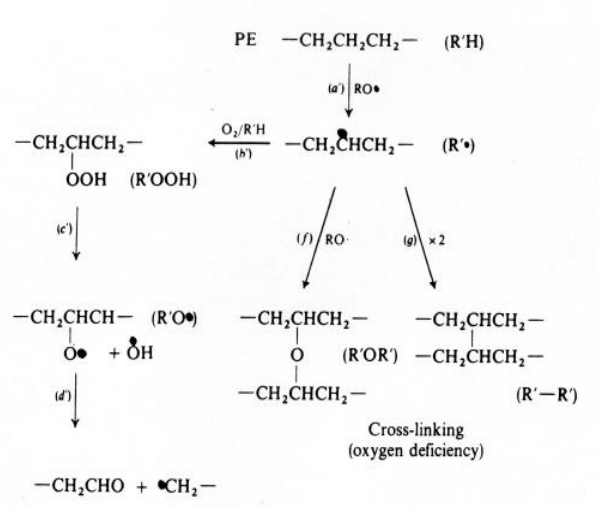

Figure 1.11: *PE oxidation scheme.*

The first reaction presents the hydrogen abstraction from PE chain, and forming of alkyl radical (a' reaction). When there is enough oxygen this radical will form a hydroperoxide (step b'), which is presented by the arrow that is going toward (b'). Formed hydroperoxide is very liable and it will decompose giving alkoxy and hydroxyl radical (c'), which can further attack intact polymer or alkoxy radical can undergo β scission leading to aldehyde and alkyl radical, which is presented as d' reaction. In the absence of oxygen, after alkyl radical is created (a') the reactions presented by the arrows facing down will proceed. So the alkyl radical might encounter other alkyl radical (g) or alkoxy radical (f) and for a new bond (cross-link).

Oxidation scheme is presented for PP on Fig. 1.12:

The carbon atom that is the most convenient for hydrogen abstraction is tertiary carbon because the C-H bond of tertiary carbon has the lowest dissociation energy in comparison to the other carbons (primary and secondary). The reaction a presents the creation of alkyl radical and the reaction b creation of hydroperoxide, which further decomposes (c,d). In the absence of oxygen, tertiary radicals rather undergo chain scission

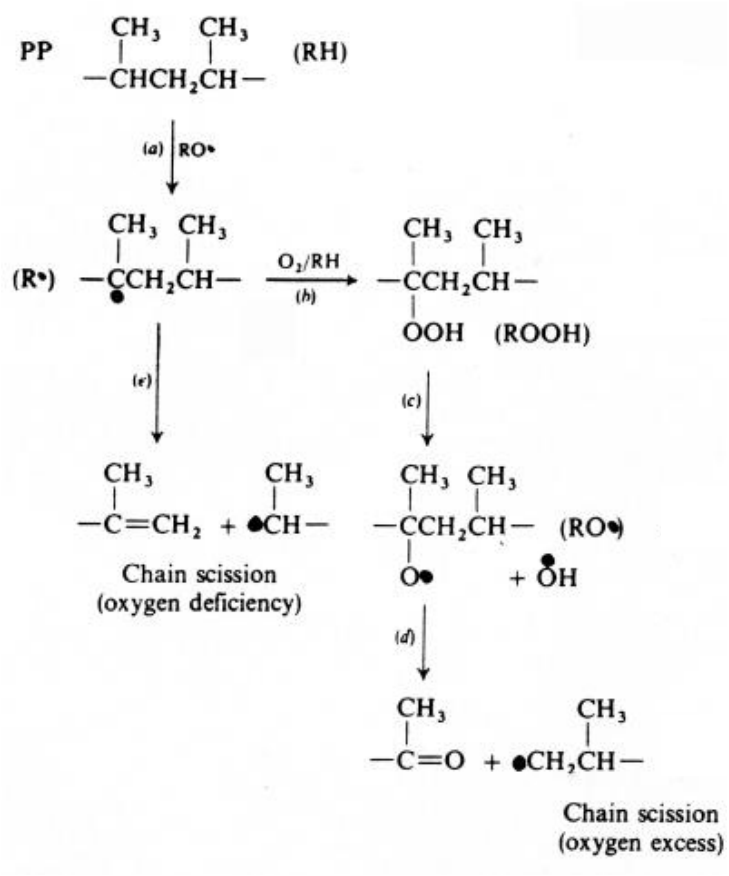

Figure 1.12: *PP oxidation scheme.*

and alkyl radical is created (reactions e).

When it is used as a cable insulation, polymer is a solid and its oxidation process is actually reaction with a gas. Gas is of limited solubility with respect to the amorphous region of polymer and if we talk about the crystalline region it is inaccessible for oxygen and many other penetrants (at the temperatures below the crystalline melting temperature). Beside oxygen solubility, oxygen diffusion is very important for the kinetics of

oxidation. These parameters determine the rate of degradation and the uniformity of the oxidation i.e. is it going to be homogeneous through the sample thickness or it will be restricted to the sample surface.

Heterogeneity or homogeneity of the oxidation influences importantly the mechanical properties. Rubbers are known to be sensitive to surface cracking. When the sample oxidation is localised to the surface this might give surface cracks, which can propagate deeper toward the sample bulk, and when they overcome the critical size sample will become brittle or sample failure can occur. Still, for the same amount of oxidation, but uniformly dispersed through the sample, failure may not happen.

Oxygen uptake depends not only on original material properties, it is changing with oxidation process. Generally, polymers containing carbon black have decreased oxygen uptake. Saturation values of oxygen uptake can be due to the consumption of oxygen within the sample or due to inaccessibility of polymer reactive sites. The question of oxidation homogeneity is very important for accelerated ageing which will be discussed within the Section 1.4.3.

The environmental and operational stressors acting on a cable system will cause aging and degradation mechanisms that, over time, will result in degradation, and ultimately, failure of the dielectric integrity of the cable insulation.

To sum up, it could be supposed that an oxidative chain reaction (autooxidation process) initiated by temperature and radiation is relevant for EPDM cable insulation. This reaction proceeds by free radical mechanism. Free radicals that are created in the initiation step are very prone to react with surrounding oxygen. Oxidation in these cases refers to an autooxidation that proceeds as a chain reaction with molecular oxygen. Solubility and diffusion rate of oxygen are dependent on sample morphology, presence and distribution of additives, presence of stabilizers(antioxidants), and ageing conditions (temperature and the dose rate).

It can be anticipated than in the presence of oxygen and at lower dose rates chain scission percentage will be higher than in its absence. Oxygen

is expected to react with lateral macro-radicals, thus it hinders cross-linking.

Stabilizers or Antioxidants

Generally, there is no correlation between thermal stability and radiation resistance. So if one polymer is by nature (its composition) stable against thermal decomposition it does not mean that it is stable against radiation as well and vice versa.

Two types of antioxidants are used in order to block oxidation reactions. Term "stabilisation" refers to retardation of propagation reactions, since initiation reaction or thermally activated "bond breaking" can not be prevented. Stabilisers are antioxidants that in most cases act as free radical scavenger or hydroperoxide decomposers, which is presented by Eq. 1.13.

$$P - O - O^* + XH -> POOH + X^* \tag{1.13}$$

X* is a less reactive free radical that will not propagate chain reaction. Phenols and amines are often used in this sense, because they act as hydrogen donors and this reaction is in competition with hydroxyperoxide creation reaction, see Eq. 1.3.

Hydroxide decomposers, act with hydroperoxides that are formed during propagation step. Compounds that can effectively react with products of hydroperoxide decomposition are added, in order to prevent chain branching reactions. They can be, for instance, sulfur containing products (disulfides). Two types of antioxidants are often employed together.

Generally, in order to protect from radiation, external shielding of cable is a possibility, but since γ radiation is highly penetrating it means that rather thick layer of shield of strongly absorbing material (like lead) is needed. Here more significant method is incorporation of protective components into the cable polymer material which are called anti-rads. These anti-rads are only effective to a limited extent since they can not prevent the absorption of energy by polymer (again initiation reactions

can not be prevented). Mainly they prevent oxidative chain reaction (act like antioxidants) or transfer excitation energy from the polymer to the additive (energy sink effect). Generally, aromatic compounds, inorganic fillers or carbon black exhibit protective properties. [4]

1.5.2 Accelerated ageing

In order to demonstrate the cable functionality for the long term operation, accelerated cable ageing experiments which are often focusing on the cable insulation, since the loss of insulation properties might lead to the loss of cable functionalities, are required. In order to predict the behaviour of a cable, methods of accelerated ageing are used and they involve ageing under elevated temperatures and dose rates in comparison to the operational ones. It is important to make sure that ageing mechanisms during the accelerated ageing are representative of the ageing mechanisms of long term degradation. For instrumental and control (I&C) cables normal operating conditions include temperatures between 25-65 ^0C and dose rates that are not exceeding 1 Gy/h. The gray (Gy) is defined in the International System of Units (SI) as the absorption of one joule of radiation energy per kilogram of matter. The total dose depends on the dose rate that the cable is exposed to and on its service life time, but we can safely estimate it to about 500 kGy (∼40 years, normal operating conditions) [20], with suitable margin of error. In practise, in Belgium and France an approximation of about 1kGy/year is used giving then about 40 kGy for 40 years of normal operating conditions. Accelerated ageing might also be applied to imitate the NPP accidental conditions: very high temperatures and dose rates. The example is so called "LOCA" (loss of coolant accident) test, where extremely high dose rates and temperatures are used to simulate a loss of coolant type of accident in NPP.

Accelerated ageing can be only thermal ageing, only radiation ageing or it can combine both temperature and radiation. If ageing considers both, then it can be performed simultaneously, which means that elevated temperature and dose rate are applied at the same time, or sequentially where thermal ageing is followed by radiation or vice-versa.

Simultaneous ageing is considered to be the best to perform whenever it is possible. First of all, it represents the condition from reality where both ageing factors (temperature and radiation) are acting together and also this is considered to be the most severe ageing condition. In the cases when simultaneous ageing can not be applied, sequential ageing may be preformed as well. For a majority of materials, radiation followed by thermal ageing is considered to be more severe than vice-versa. The fact that simultaneous ageing is shown to be more severe than sequential raised the question about synergetic effects. Cable insulation degradation is often measured as a loss in elongation at break. When measuring of elongation at break loss for PE, it was established that the loss is the highest when simultaneous ageing is applied. Regarding sequential ageing, more severe degradation is observed when radiation is followed by thermal ageing. [1, 21]

Accelerated ageing should be performed in a way that it is representative for natural age-related degradation, but there are still many drawbacks in practise that need to be analyzed and understood better. This is needed in order to obtain the validation of applied accelerated conditions. For example, the application of, Arrhenius equation based, activation energy estimation method is under debate. Very important is the question of oxygen limited diffusion, and dose rate effects for the ageing performed under the air. Chosen ageing temperature should not cause changes of physical state of polymer material. Crystallinity is very important property, it can gradually affect mechanical and chemical material behaviour. If temperature chosen for accelerated ageing exceeds the melting temperature of polymer crystalline structures then significant change of material will be made and the degradation results for accelerated ageing may not be representative for degradation under operating condition. [1, 3]

Arrhenius equation is often used in order to estimate accelerated ageing temperature and activation energy for degradation reactions. It is used as well for an extrapolation of the results from accelerated to real conditions and vice-versa. But there are many limitations of using Arrhenius behaviour. First of all, in NPP there is no constant thermal environment, and sometimes elevated temperatures can cause more than one

degradation mechanisms. As a result non-linear Arrhenius behaviour can occur, making a linear extrapolation of the results non reliable. Estimations of activation energy, that are usually done using three points method, will not be correct if material exhibits non-linear Arrhenius behaviour. There are studies that have shown that EPR has non-linear Arrhenius behaviour, regarding the elongation at break decrease, for temperatures higher than 100 ^0C and that Arrhenius methodology is not applicable when more than one degradation mechanism is active [3]. Some polymers exhibit so called "inverse behaviour" where more severe degradation occur at lower temperature. Recovery mechanisms that appear at higher temperatures, due to increase of chain mobility, are responsible for this phenomenon.

Diffusion of oxygen is also very dependent on temperature. Since reaction with oxygen is actually one of the main degradation mechanisms when polymer ages under air, the presence of oxygen is an important factor for the process of ageing. For service life conditions, oxygen consumed by degradation reactions is being replaced by diffused oxygen. However, at higher temperatures which are used for accelerated ageing, polymer oxidation is accelerated. If oxidation rate is faster than oxygen diffusion rate, oxidation in the material bulk will decrease due to the lack of oxygen. Then the material degradation can be heterogeneous, with the surface being more degraded than the bulk. One of the very important questions when using accelerated ageing is: "does this reduction of oxygen diffusion time affects the qualification and how". [3,22,50]. Increase of oxygen pressure reduces radiation dose rate effects that are attributed to the oxygen diffusion [23, 50]. Still, in many studies it was observed that there is no difference in performance for the cables with and without oxygen diffusion when subjected to LOCA testing, which includes extremely high dose rates and temperatures [3].

The concept of equal dose - equal damage that assumes that degradation depends only on dose and not on the dose rate is being questioned nowadays, after many researches have shown that dose rate may play a role in degradation. The dose rate effect leads to the observation that degradation is more severe at lower dose rates. The dose rate effect has not been resolved completely. For some investigations it appears to be

important, in others not. The same goes for different materials, some exhibit stronger dose rate effect, but in others it was not confirmed. Although it is found that this effect is secondary when accident doses apply [3], it should be studied and better understood in order to improve general understanding of polymer radiation ageing process.

Variation in composition of cable polymer insulation probably effects the ageing process, but the problem is that the exact composition is not always known. Besides polymer or polymer mixture which varies a lot as well, there is a high amount of fire retardants, antioxidants, anti-rads, pigments, numerous of additives and fillers. So, even if the producers (which are many) use the same generic polymer, the final products differ a lot. Type of the component, its presence or absence, the way of mixing, and curing processes may have high impact on ageing. These effects should be handled as well. Question of cable ageing characterization and prediction can become even more complex when one includes existence of hot spots, elevated vibration spots, installation configurations like bends, overhangs and so on. In some previous works [3] it was concluded that fire additives have negligible influence on EPR degradation and that, in the case of EPR, fire retardant loss rate is not significantly affected by radiation. Still, there are other works [12] that claim that fire retardant may influence the ageing of EPDM polymer. Regarding the pigments, it was found for PE that they do affect the characteristics of the ageing process [3]. Namely, PE with the same composition, but different in colour (pigments), were observed to differ in stability going from the most toward less stable as follows: black > red > white. Presence of antioxidant will for sure influence material stability.

1.5.3 Techniques to monitor polymer ageing

Techniques that are used in NPP industry to monitor cable ageing are known as Condition Monitoring (CM) techniques, since they are used to evaluate the condition of the cable. Cable CM techniques involve methods that can be used to determine the performance of cable insulation material or try to identify problems in cable conductors [1]. Except the cable itself, other parts of instrumentation and control system, like

connectors or splices, are also controlled by several techniques. Detailed reports related to the cable inspection in NPP environment and CM techniques have been published. Techniques that are applied to cable insulation are of interest in this work. Some of these are well established, some are being developed. The ones used for the sample investigation within this thesis are presented in this chapter.

In order to determine the cable condition, or to make a qualification, several properties of cable insulation are measured and compared to certain acceptance criteria. Electrical properties are the most important with respect to the cable functionality. This thesis is devoted to the mechanical properties of cable polymers, so techniques for analysis of electrical properties will not be discussed. Mechanical properties are not directly related to the functionality of an cable, but they demonstrate its integrity, flexibility and ability to withstand movement during normal operation or accidents [1]. Regardless of what property is measured (electrical, mechanical or physico-chemical), the most important is that the measured parameter is valid to indicate the cable condition. So the chosen parameter has to change in accordance with the state of the cable and the monitoring of parameter evolution has to be correlated to the condition or functional performance of the cable on which it is applied. Moreover, it is desirable to link the measured cable state indicators with an independent parameter, such as time, in order to attempt to observe the trend in cable performance and enable the prediction of the cable behaviour, especially with respect to the cable ageing under operation.

The size of a sample that techniques are using is very important. Some techniques require long cable samples, some few centimeters, and their application to NPP cables requires cable dismantling. There are techniques which are very low destructive or non-destructive and these techniques are very welcome, because they offer possibility for in situ testing, witch does not include cable dismantling. The most common one is visual inspection. If during a visual inspection any indication of defects or degradation is identified then further more intrusive testing is required i.e. application of additional CM technique(s). Many of these techniques are still under development and for the majority standard techniques attempts to improve the result interpretation and to explain

the structure-property correlation is constantly running.

Standard CM technique in industrial practise is tensile test and the elongation at break is well established as valid parameter to monitor state of an cable. Cable insulation polymers tend to loose their ductility with ageing and elongation at break is a parameter that changes nicely with sample embrittlement. Namely, the elongation at break mainly decreases as material gets brittle, which has been demonstrated through extensive research testing [19, 21, 24–28]. In order to define when a certain cable has reached the end-of-life (end-of-service), certain criteria has been set up. The last recommendation [29] defines the end-of-life criteria only as 50% of absolute elongation at break value, but many studies report relative elongation at break values. The exact definition of the relative and absolute elongation at break values are given in Chapter 2.2.1. Next to the elongation at break, the stress at break (ultimate tensile stress) and Young's modulus are often determined from tensile test as well.

Tensile properties may vary depending on sample preparation and testing conditions, so they must be well controlled and it is recommended to test at least 5 samples [31]. Even it is very common and mainly reliable to use elongation at break value for cable condition qualification, significant number of samples is required and industry aims for applying less destructive techniques than tensile test. Indentation techniques, which involve probe penetration just few hundred microns into the sample surface, appear as potentially convenient non-destructive cable CM techniques.

Generally, the compressive modulus of a material, defined as the ratio of compressive stress to compressive strain below the proportional limit, will increase with polymer ageing in the case when polymer hardens. Compressive modulus can be measured using the indentation method which measures the force required for the resulting displacement, while indenter is penetrating into the material and it is expressed as N/m^2 [32, 33]. These data are later used to calculate the indenter modulus (from a plot of the penetration force versus depth), which is closely related to compressive stiffness, see Fig 1.13. It has to be noted that in NPP industry indenter modulus is a term used in relation to the indenter

system for describing the ratio of the change in the applied force to material deformation, expressed as N/mm [33]. Advantage of this method is that in can be used in a laboratory, but also in situ in a NPP. Speed of the probe is an important test set-up characteristic, because polymer properties are time dependant. Generally, increase in probe speed will induce increase in IM value. The "relaxation modulus" parameter, which is a ratio between change in a force and the corresponding penetration right after indentation needle stopped penetrating into the sample, can be also determined from indentation test. Namely, before testing starts, maximum force for the needle is predetermined and needle travels inwards until it reaches the maximum force value then it stays still for a while and finally goes back after stress is released. Until the needle is going back, force and displacement are decreasing and relaxation modulus can be calculated. It has been already observed that indenter modulus can be useful for degradation monitoring for EPR [34].

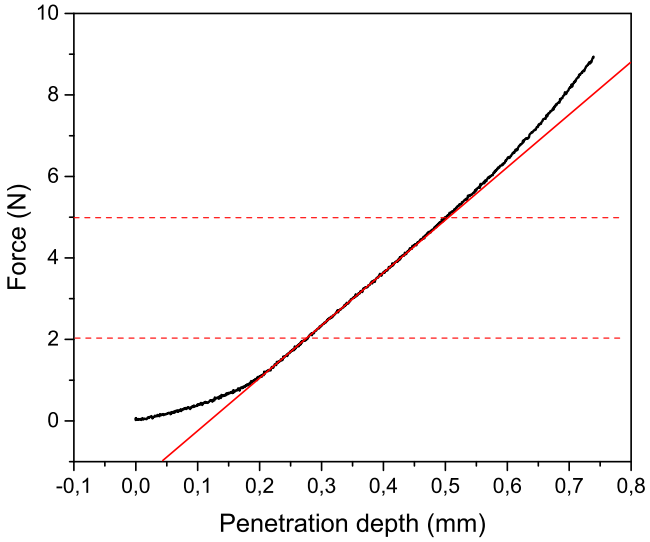

Figure 1.13: *Example of the Indenter Modulus calculation.*

An indenter method is the most appropriate for the low voltage cable insulation, and cable polymers that are not semi-crystalline. It was ob-

served that the IM mainly stays constant with ageing, when test is performed on semi-crystalline polymers. This is probably because hardness is gradually controlled by the crystalline regions, which do not change as much with sample ageing. [1] Regarding the test on-site performance, it is only possible to measure outer cable insulation (jacket) and it could be expected that the obtained data will be sensitive to cable construction.

Technique that is based on similar principles, but invented for different purpose is modulus profiling technique. This technique is used to measure the modulus/hardness of a polymer through its thickness in order to demonstrate the sample (non)homogeneity. The potential issue of sample inhomogeneity, induced by an accelerated ageing, was already addressed (Chapter 1.4.3). The experiment involves pressing of a well characterized probe onto a sample at time 0 with a small contact mass, which is then followed by the addition of a larger mass at time t_1. With a properly shaped probe tip, the change in penetration occurring between t_1 and $2t_1$ allows calculation of the tensile compliance, which is reciprocal of Young's Modulus [35]. Very detailed description of the apparatus that is developed to give very precise tensile compliance values per sample cross-section is given by Kenneth et al. [35]

Measuring of materials chemical properties usually does not require large samples. Only few milligrams of sample is often enough for tests like DSC (differential scanning calorimetry), IR (infra red), density measurement, DMA (dynamic mechanical analysis), swelling test. The fact that these techniques are of low intrusion type, with respect to the cable installation, makes them desirable for cable state monitoring; but broad investigation needs to be done in order to correlate a parameter measured by one of these techniques to the change in sample structure (microstructure) that is caused by ageing factor(s).

Thermogravimetric analysis (TGA) provide measurement of a sample mass loss as a function of the temperature and time, while the sample is heated in a controlled environment. Sample can be heated in a controlled heating rate or isothermally. Test can be conducted either in nitrogen or in air (oxygen presence) atmosphere. The experimental record is a thermal curve of some form of weight change (in mass units, in percents) versus time or temperature, see Fig. 1.14. Analysis is often extended

by calculating the first derivative of a mass loss.

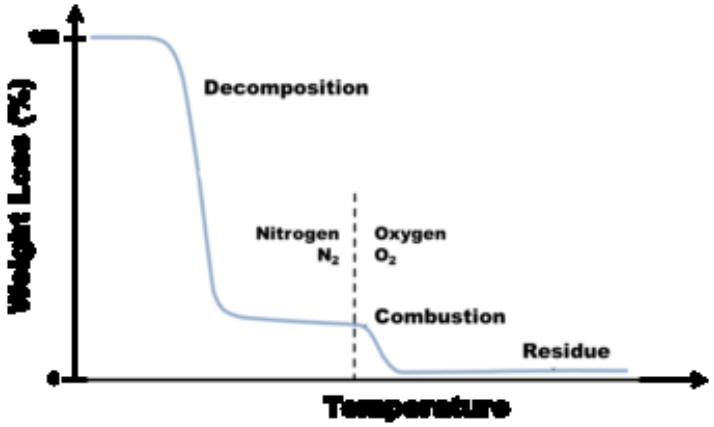

Figure 1.14: *Schematic TGA curve.*

TGA is a low destructive test, for an experiment, a sample of about few mg is needed. Principal application of TGA is to detect thermal stability of a polymer, but it is also often used for composition detection and for determination polymer thermal decomposition kinetics. Despite the fact that a lot of polymer degradation kinetics studies have been already carried out using TGA [36–39], not much work has been reported regarding the aged cable polymers. Sample decomposition during TGA takes place at temperatures much higher in comparison to a cable operation temperatures, and it is difficult to imagine that TGA decomposition will contribute to a better understanding of sample ageing. Still, authors reported shift of thermogravimetric curve toward higher temperatures (increase of thermal stability) after sample irradiation for some polymers [40–43] and dependence of EPDM thermal stability on its cross-linking degree and filler content [44–46]. There are indications that ageing can produce chemical and structural changes that later can affect sample thermal decomposition, so it might be that sample ageing could be indirectly monitored by TGA.

FTIR is already well established technique for characterising a sample on molecular level. During polymer ageing evolution of macroscopic

properties are monitored, but all these macroscopic changes are caused by the structural changes. It is not simple to monitor chemical changes of an industrial polymer material, since its structure is very complex. Still, it is possible to observe some changes that are typical for oxidation process, and an example is given in Fig. 1.15. Formation of carbonyl and hydroperoxide species is typical when oxidation is the dominant ageing mechanism, so an increase of absorbance in the C=O and O-H vibration domains can be observed in aged sample in comparison to the non-aged ones [1, 47–49]. Same technique can be used for sample profiling when an "oxidation-sensitive" peak is monitored as a function of sample thickness [50]. Within this work more detailed profiling was not performed, but the comparison between sample surface and bulk spectra using ATR-FTIR is presented.

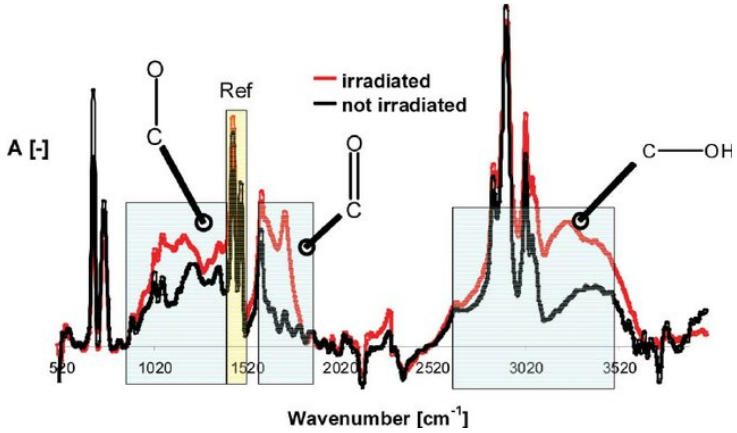

Figure 1.15: *An example of FTIR spectra of irradiated and non-irradiated sample.*

Hyphenated thermal analysis are considered to be a step forward in material characterization and analysis. Coupling of TGA with FTIR is convenient in order to detect gases and volatiles that are evolving as a result of material decomposition during TGA test. During a sample decomposition created gasses are transported through a heated transfer line by a carrier gas flow toward gas measuring cells of the spectrometer, where evolved gas analysis is preformed continuously. As an output from

TGA-FTIR test, beside the TGA and DTGA curves, Evolved Gas Profile (EGP) can be constructed from stored interferograms and it is also called Gram-Schmidt (GS) profile. Each point in EGP corresponds to a spectrum of the evolved components. The GS profile essentially shows the total change in the IR signal relative to the initial state. For a selected wavenumber a Specific Gas Profile or Functional Group Profile can be constructed as well. Comparison of EGP and TGA data as a function of time can be made. TGA-FTIR is a cost-effective and informative method to perform compositional analysis or to study degradation reaction mechanism. [51]

Swelling test is often used in order to characterise macromolecular structure of a polymer i.e. polymer three-dimensional network [11, 47, 52, 53]. It is expected that cross-linking and chain scission ageing mechanisms will induce change in network structure. Swelling test is based on a property of cross-linked polymer to absorb the solvent without complete dissolution due to covalent bonds that exist between the chains. The swelling ability depends on the interaction between solvent and polymer macromolecules and the chain length between the cross-links. Swelling test is performed by putting a sample in a solvent in which sample swells, and then drying out a sample in a vacuum chamber. Sample is weighted before putting in solvent, when swollen, and after drying. These weights are used in several existing equations for calculation of few parameters that are related to network properties, like swelling ratio, gel fraction and soluble fraction. The choice of the swelling procedure, solvent and the equations for parameter calculation depends on sample composition, presence of fillers, ... Swelling ratio is the ratio of the gel volume in the swollen state to its volume in un-swollen state and it indicates the extensibility of the network due to the penetration of the solvent. High swelling ratio indicates that there is a long molecular weight between cross-links i.e. less cross-linking and contrary lower swelling ratio values indicate more tightly bonded structure which means more cross-linking. Gel fraction indicates extent of swollen part of the sample structure and soluble fraction an extent (percentage) of the structure that is dissolved by the solvent. Swelling ratio is a good technique to follow changes in network structure, but there is an issue

with highly oxidised samples, where polymer structure is more polar than initially which induces changes in polymer-solvent interaction and decreases swelling ability of the solvent. [1, 11]

DMA is a technique where a sinusoidal force or stress is applied and resulting sinusoidal deformation or strain is monitored. DMA measures viscoelastic properties of the material through the changes in stiffness and dumping, that are reported as modulus (G) and tan delta ($tan\delta$). A strain response lags behind input stress and this lag is known as phase angle, δ. A ratio of the dynamic stress to dynamic strain gives a complex modulus. A complex modulus has two components: storage and loss modulus. Storage modulus measures the elastic properties of sample ı stiffness, and it describes ability of the material to store energy. Loss modulus is related to the dumping characteristics of the sample and it is related to the heat dissipated by the sample as a result of the material molecular motions. Tan δ is a ratio of the loss and storage modulus. Peaks on tan δ versus temperature curve are representing different relaxations of the material. An example of glass temperature detection is given in Fig. 1.16. All these values (storage modulus, loss modulus and tan delta) depend on temperature and time, since polymers are viscoelastic materials. When non-aged and aged samples are compared, increase of storage modulus is considered to be a consequence of increase of cross-linking degree of sample. Still, one has to be careful with semi-crystalline materials, where storage modulus is also affected by the crystallites. [54–56] When material relaxation is studied, the position and the height of the peaks on tan δ - temperature curve are analysed. The peak that is related to the movement of the high chain portions and that appears at glass temperature (Tg) is monitored. Shift of this peak (or shift of Tg) towards higher temperature usually is correlated with sample stiffening and decrease in molecular mobility, which is considered to be consequence of dominance of cross-linking as an ageing mechanism. [55, 56] Viscoelastic properties of the material are often compared with its dielectric properties.

DSC can be used in several manners in cable CM. Beside being used to detect glass and melting temperature and to monitor these processes, it is often used for oxidation induction tests, which serve to detect a

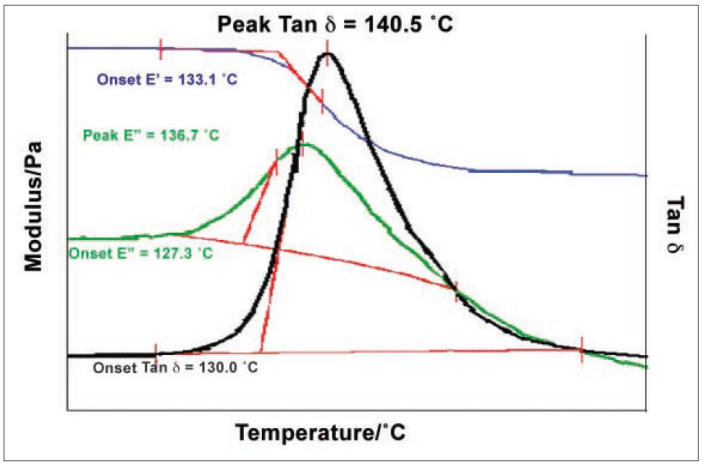

Figure 1.16: *An example of glass temperature detection via DMA.*

level of antioxidant in sample. Antioxidants are obligatory component in cable polymers and they are being consumed during material processing (cable production) as well as during the cable operation. It was observed that after antioxidant is consumed, polymer often starts to degrade more rapidly [1]. Oxidation induction time and temperature are two parameters that could be measured by DSC and they are considered to be indicators of antioxidant level in the sample [1, 57]. DSC is also used to measure percent of crystallinity in the sample and to monitor changes in crystalline structure of semi-crystalline polymers. Increased temperatures can cause melting of crystallites if the temperature exceeds the polymer melting temperature. Radiation chain-scission may cause changes in structure of crystalline domains, while oxidation should not affect crystalline domains, since oxygen diffusion into crystallites is negligible. [14]

Since regular cable qualification was not standardized and performed, like this is the case for other NPP components such as pressure vessel, cable CM techniques are still under development. Within this study tensile test, technique that is already established as a benchmark [1], is

used, but cable ageing monitoring via several other techniques, that still need to be validated as suitable for cable state monitoring, were performed and discussed. The attempt has been made to monitor material changes, caused by ageing, at macrostructural and microstructural level, as well as to correlate them.

1.6 Literature review on EPDM/EPR ageing studies

The studies of thermal and/or radiochemical (accelerated) ageing of EPDM and EPR suggest that ageing is characterized by the competition between chain scission and cross-linking and emphasize the importance of oxygen diffusion through the sample thickness on the ageing mechanism. The competition between these two ageing mechanisms is observed to depend on many factors like ageing conditions, material composition (PE/PP ratio, presence of the diene) and also initial cross-linking degree of the polymer. The presence of fillers was shown to influence the ageing mechanism, and it was assumed that matrix-filler interphase plays key role in it.

The radiochemical ageing of EPDM and EPR elastomer under non-oxidative and oxidative atmosphere is studied by A. Rivaton and presented through three papers reporting the identification of the chemical changes resulting from the radiochemical ageing of the EPDM and EPR films under argon atmosphere [15], the identification and quantification of chemical changes in EPDM and EPR γ-irradiated films under oxygen atmosphere [16] and finally the mechanism of radiooxidation is proposed [17].

The evolution of the mechanical behavior of aged filled and un-filled EPDM elastomers has been investigated via tensile and swelling tests within the work of A. Shabani [11] and E. Planes [58]. The work of A. Shabani includes as well analysis of the evolution on the chemical level (mainly FTIR), in order to attempt to contribute to a better understanding of EPDM ageing at different structural scales. Both studies include thermal only ageing of the EPDM as well. The changes of the

mechanical properties of various kinds of ethylene-propylene copolymer with the irradiation in air, in oxygen of 10 atm, and under vacuum were reported by T. Seguch et al. [59] The same authors report the evolution of the swelling parameters for samples aged by γ-irradiation in oxygen under pressure [60].

The understanding of the evolution of polymer network characteristics under ageing is important in order to understand the evolution of the macroscopic properties. Therefore molecular dynamics of polymer chains was often studied in order to characterize polymer network. N. Cellete et al. performed the ageing and DMA testing on non-cross-linked and cross-linked EPDM with and without antioxidant [54, 55]. This relaxation behavior studies are completed by the investigation that included infra red spectroscopy and gel fraction measurements [61] and tensile testing [62].

Heterogenous oxidation intimately related to the diffusion limited oxidation present at high dose rates and temperatures is appearing to be the key issue in order to obtain valid accelerated ageing that is comparable to the material ageing ongoing under operating condition. Investigation of the oxidised and non-oxidised regions within the aged EPR samples were performed by T. Seguch et al. [23] Several adequate profiling techniques to monitor the sample heterogeneity/homogneity were proposed and applied on the aged EPR by R.L. Clough, K. Gillen et al. [22] The dose rate effects on swelling and mechanical properties are reported by T. Seguchi et al. [98] The attenuation of the diffusion limited oxidation at high dose rate, by increasing the irradiation temperature within the certain temperature range is reported by A. Shimada et al. [28]

The thermal only ageing of the EPDM was also studied [11, 64, 65]. Regarding the prediction of polymer life time duration, an existing methodology application on the EPR material is reported [24, 25].

Investigation of EPDM radiochemical ageing mechanism at physico-chemical level

The polymer samples that are meant to be studied in order to monitor evolution of chemical and/or physical material properties with ageing

are often made in the forms of film. Especially when it is intended to avoid any possible DLO. These samples are also often made in laboratory having more simple composition in comparison to the industrial one. A. Rivaton et al. studied aged EPDM and EPR samples in a form of $\sim$ 100 μm thick films. The films were irradiated under argon or oxygen flow (0.5 L/min) under the dose of 1000 Gy/h and temperature of 20^0C at doses between 5 and 455 kGy. The analysis of the aged film proceed by using mainly UV-Vis and IR analysis with derivatisation reactions and chemical titration. Swelling method was used to evaluate the cross-linking.

The results of the irradiation under the argon were shown that creation of *trans*-vinylene, vinyl, vinyldiene, and dienic type unsaturation, the cross-linking of the matrix, the emission of the hydrogen are the main modification of the chemical structure of both, EPDM and EPR samples, resulting from the radiochemical ageing under non-oxygen atmosphere. Similar chemical changes of the EPDM aged under the inert atmosphere were observed by other studies [61]. The radiochemical yields of these products were observed to be similar for EPDM and EPR. The increase of the intermolecular bond density of the EPDM in comparison to the EPR was explained by the presence of the diene, whose double bonds were consumed with a high radiochemical yield.

The major oxidation products resulting from the oxidative radiochemical ageing were found to be (in the decreasing concentrations): hydroperoxides, ketones, carboxylic acids and alcohols and peroxide. The oxidation product concentration was found to be about two times higher in EPDM than in EPR. According to the evolution of the products concentration with the dose it was observed that hydroperoxides may be decomposed under exposure and that the diene plays an important role in the radical oxidation of the EPDM, since it was observed that the oxidation of ENB (the diene type present in the EPDM) moieties increases the formation rate of the major oxidation products, especially ketones. The radiochemical yield of the ENB double bonds consumption was found to be much higher during the irradiation under oxygen atmosphere in comparison to the one under the argon (32.1 versus 4.5). Moreover it was observed that oxygen accelerates the cross-linking reactions in EPDM as

long as the ENB double bonds are not completely consumed by radiooxidative reactions. The total consumptions of the ENB double bonds was observed to occur at the dose of about 200 kGy, but it significantly decreased already at about 100 kGy. According to the evolution of the gel fraction parameter as a function of the dose, it was established that cross-linking density increases for the doses up to the 95 kGy and then decreases. The decrease of the gel fraction with dose is explained by the decrease of the cross-linking rate which is assumed to be a consequence of the oxidative chain scission process, that became dominant once when almost total saturation was achieved ($\sim$ 100kGy). Interestingly, the cross-linking rate (increase of the gel fraction with dose) is observed to be faster in oxygen containing irradiation atmosphere (before the almost total ENB unsaturation consumption occurs) in comparison to the inert atmosphere. This could confirm that indeed oxygen accelerates cross-linking reaction in EDPM until double bonds of the ENB are not totally consumed and then cross-linking rate is antagonised by oxidative chain scission reactions.

Regarding the EPR the gel fraction was observed to increase significantly, but after an "induction period", while under the argon increase of the gel fraction has been observed as soon as irradiation began. It was assumed that oxidative chain scission inhibits the cross-linking at doses belove 250 kGy.

It is also important to mention that the oxidation product distribution of 200 μm films, aged under 1000 Gy/h at doses from 100 - 450 kGy under oxygen atmosphere, was investigated by micro-FTIR and no oxidation profile was observed which indicated that the oxidation was homogeneous.

The detailed mechanism of EPDM polymer radio-oxidation at 20^0C, that was proposed [17], is presented in Fig. 1.17. Unselective interaction of radiation and material leads to scission of C-H bonds, while C-C bonds are less affected. C-H and C-C bond scission results in creation of alkyl radical ($P^{\cdot}$). The random interaction of the irradiation with orbital electrons mainly involves the ethylene units in both EPDM and EPR polymers. When oxygen is present alkyl radicals react easily with it forming peroxy radicals ($PO_2^{\cdot}$), which further may react in two ways:

1) to create hydroperoxides by abstraction of hydrogen atoms on the polymeric backbone or 2) to recombine giving ketones and alcohols as final products and terminate the chain oxidation.

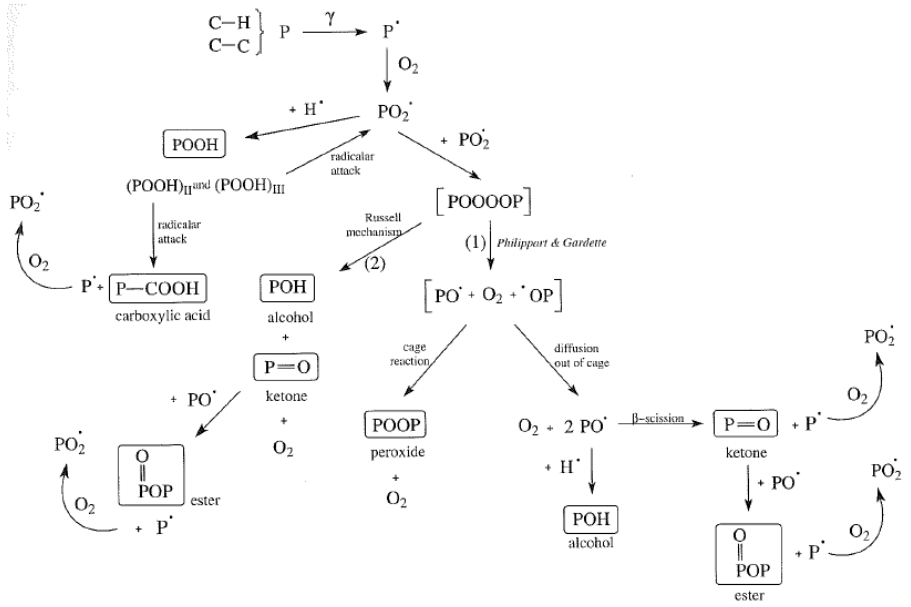

Figure 1.17: *The proposed mechanism of EPDM radio-oxidation [17].*

The reaction od hydroperoxide creation is enhanced with temperature increase, which is important to consider when simultaneous thermal and irradiation ageing is performed. The reaction of hydrogen abstraction is selective reaction, since the most labile hydrogens are abstracted. In the case of the EPDM there are two labile hydrogens: hydrogen on the *tert*-carbon atoms of propylene units and hydrogen on C atom in the position α to double bonds of ENB. The macroradicals formed by hydrogen abstraction react with oxygen giving the hydroperoxides.

The NO treatments prior FTIR, were performed by in order to detect the formation of alcohols and hydroperoxides and to identify their structure

(primary, secondary or tertiary). By this treatment it was concluded that mainly secondary hydroperoxides were formed on ethylene units by random initiation (due to radiation), while selective propagation (hydrogen abstraction) leads to formation of tertiary hydroperoxides on propylene units and secondary hydroperoxides on ENB units.

The stability of the created hydroperoxides was studied by vacuum irradiation of the pre-radiooxidised EPDM and it was established that direct decomposition of hydroperoxide by O-O bond dissociation, that is typical in the case of thermal ageing, is not likely to happen from direct radiolysis. It was proposed that created hydroperoxide undergo one of the two reactions: radical attack of the hydrogen atom in α-position to a *sec*-hydroperoxides giving carboxylic acid and primary radical, which continues chain oxidation reaction; or radical attack to a hydrogen from *sec*- and *ter*- hydroperoxides site generating peroxide radical, which can undergo recombination and terminate the chain oxidation process.

It was already mentioned that radicals created by random reaction of the irradiation with polymer, beside reacting with oxygen and creating hydroperoxides, can also recombine. Recombination of two *sec*-peroxyl radicals is possible to proceed by a Russel-type mechanism giving sec-alcohols and ketones, but since it was observed that *sec*-alcohols are present in lower concentration with respect to ketones (ratio 1/5) it was proposed that beside the Russel-type mechanism, there is a recombination mechanism via formation of tetroxide intermediate ([POOOOP]->[$PO^{\cdot}$]+O_2+$PO^{\cdot}$]). Tetroxide intermediate can be created by both *sec*- and *ter*- peroxy radicals and they are very unstable. The major route of the alkoxy radicals ($PO^{\cdot}$) is the diffusion out of cage, followed by a β-scission where ketons and alkyl radicals are formed; but alkoxy radicals can also attack polymer matrix giving alcohols and alkyl radicals or undergo in cage reaction, which is cross-linking and formation of peroxide bridges. It is also possible that *sec*-alcohols are present in lower concentration because they are not stable. Namely, it is proposed that the *(ter)*-CH site might be attacked by oxygen giving ketones and water as reaction products.

The work of A. Rivaton et al. proposes and explains mechanism of EPDM radiooxidation at room temperature, but at higher irradiation

temperatures some modifications are expected, especially regarding the hydroperoxide formation (out of peroxy radicals) and possible dissociation.

Thermal ageing of EPDM

The long therm thermal ageing of the 2 mm thick EPDM samples was performed by D. Bouguedad et al. [64] The ageing time was 6070h at 80^0C, 5040h at 100^0C, 3520h at 120^0C and 980h at 140^0C. The first published paper [64] presents the evolution of the mechanical and dielectric properties under thermal ageing, while the second one [65] presents the result of physicochemical analysis (ATR-FTIR, DSC and TGA). For all ageing temperatures it was observed that the tensile strength increases at the beginning, reaches maximum and decreases afterwards. Moreover, it was observed that the decrease is faster at higher ageing temperatures (120^0C and 140^0C). The increase of the tensile strength was attributed to the cross-linking phenomenon, while the decrease was related to the domination of the chain-scission. Regarding evolution of the elongation at break, significant change with respect to the value of the non-aged sample was not observed for the samples aged at 80 ^{0}C. For the other ageing temperatures the decrease of the elongation at break was observed and it was faster for the higher ageing temperatures. Regarding the spectroscopic analysis, important changes with respect to the spectrum of unaged sample, were not observed for the samples aged at 80^0C and 100^0C. Standard changes of the chemical structure that are consequence of the oxidation (evolution of carbonyl and hydroxyl species) were observed for the samples aged at 120^0C, 5040h and 140^0C. However, for the samples aged at 140^0C it was observed that the chemical changes are limited only to sample surface, while the bulk seemed not to be affected by the oxidation. This is the most probably an indication of the DLO.

Evolution of EPDM network under ageing

The modification of EPDM polymer, formulated without and with ATH as a fire retardant filler, under the thermal and irradiation ageing, was studied by A. Shabani [11]. The main objective of that study was to contribute to a better understanding of EPDM ageing at different structural scales. The samples out of three types of EPDM material were produced and cross-linked by peroxide. Two types of ATH filler were used, treated and non-treated.

The filler/matrix interphase was analysed. It was proposed that it can be divided into two different phases: the glassy hard phase, which is in contact with filler surface; and the sticky hard phase, linked to the EPDM matrix. The thickness of glassy hard phase was assumed to be negligible comparing to the thickness of sticky hard phase. This latter was considered to build up an interpenetration network in a parallel system with the matrix network, which is unaffected by filler particles. This two-phased system was proposed to be model the reinforcement effect of fillers.

One set of the samples that involve 100 μm thick film and 2-3 mm thick plate samples was only thermally aged in air at the temperatures of 90, 110 and 130 ^{0}C. In order to monitor a thermal oxidative ageing the evolution of the film samples mass with ageing was monitored. It was observed that after an initial induction period, the samples mass increases, which was attributed to the oxygen absorption during the propagation step, and decreases afterwards, which was attributed to the evaporation of the volatile products of the sample oxidation. The formation of oxidation products has been followed by FTIR and the presence of hydroxyl and carbonyl group bearing species detected. The consumption of the ENB double bond after an induction time was confirmed by FTIR and several possible mechanism were proposed. The induction time for the sample oxidation was observed to decrease with ageing temperature increase.

The FTIR imaging technique was used on thick plate samples and it was observed that heterogeneous oxidation appears for the samples aged at 110 and 130^{0}C, while the oxidation profile of the samples aged under

90^0C was observed to be flat, which means the oxidation was homogenous. The heterogeneous oxidation was correlated to the diffusion control oxidation process.

The kinetics of the thermal oxidation was studied and it was revealed that the formation of hydroperoxides is the determining step of the oxidation rate. Moreover, it was found that the formation of hydroperoxide was less in the case of filled samples and it was decreasing with the increase of the filler concentration. Since hydroperoxide decomposition is the main source of chain scission, it is expected that the presence of filler particles affect the changes in the macromolecular characteristics of the EPDM network.

It was observed through the swelling measurement (the increase of soluble fraction with ageing time) and tensile test (the decrease of Young's modulus) that the predominant ageing mechanism for the neat EPDM samples is chain scission, except for the samples aged at 90^0C where a minor cross-linking was observed for the short ageing times. Introduction of the filler was found to change this predominance. Namely, the presence of 33 phr of ATH was observed to nullify the effect of chain scission, and the presence of 100 phr of ATH counterbalanced this predominance and replaced it by a toughening. Such effect of the filler particles presence was explained by the formation of strong filler/matrix interactions throughout thermal exposure ie the interphase densification with oxidative ageing. As this effect is more pronounced for EPDM matrices filled with untreated ATH, it was concluded that the interactions must be related to the chemical functions at the filler surface, i.e. hydroxyl functions. Moreover, these interactions were observed to still exist when the samples are swelled, which was an indicator of their chemical nature.

The same effect (the interphase densification) was used to explain the uncertainties of the swelling measurements. At unaged state, the interaction between filler particles and polymer chains is due to the weak Van der Waals forces induced by the polar surface of ATH particles. But with oxidative ageing, highly polar oxidation products, such as hydroperoxides, alcohols or carboxylic acids, are being produced and stronger dipole interactions can be established. These interactions could lead

to a modification of the swelling measurement parameters and together with the decrease in swelling ability of solvent due to formation of polar oxidation products, they are giving uncertainties to the swelling measurements of highly oxidised samples. Since it was observed that the apparent filler/oxidised matrix interactions do not disappear when the samples are swelled, their chemical nature is assumed.

The analysis of the elongation at break evolution with ageing was performed and it was proposed that, at early stages of exposure, when the number of chain scission is fairly low, the ultimate elongation is governed by the functionality of cross-links, while when the number of chain scission becomes important, the ultimate elongation is governed by the number of cross-links. The cross-links of the EPDM tridimensional network were assumed to be tetrafunctional initially. At the beginning of thermal exposure, as the chain scission happens, the concentration of elastically active chains, and consequently the Young's modulus was observed to decreases. Meanwhile, the functionality of cross-links dropped from four to three, due to the chain scission, but the number of junctions remained constant. This alteration of functionality was proposed to create a network with higher elongations at break, that was observed for the lower ageing times. However, when the number of chain scissions became important, the junctions disappear and the ultimate elongation decreases, which was observe for higher ageing times.

The irradiation ageing was performed on 2-3 mm thick samples, at the dose rates of 0.1, 1 and 10 kGy/h, under a dried air flow at a temperature ranged between 35^0C and 45^0C. The profiling using the FTIR was performed and carbonyl profiles were analysed for each dose rate in order to monitor the oxidation homogeneity/heterogeneity through the sample. The homogeneous oxidation was only observed for the samples aged at 0.1 kGy/h and for the samples aged at 1 and l0 kGy/h the oxidation profile was observed, which was correlated to the diffusion controlled kinetics.

The evolution of the hydroperoxide concentration with time was observed to differ from what was observed for the thermally aged samples. The overall tendency in radiochemical oxidation was observed to be a continuous increase in the hydroperoxide concentration. The rate of hy-

droperoxide accumulation was observed to reach its maximum at the beginning of the exposure and then to decrease as exposure continues. Moreover, it was observed that the rate of hydroperoxide accomulation with time increases with the dose rate. The main chemical reaction is formation and accumulation of hydroperoxides, which start to decompose at a specific received dose. The most probable reason for this would be the proposed difference in the initiation step of radiation ageing in comparison to the thermal. The main source of radicals during the radiation ageing is created by the direct interaction of irradiation and matter, when the bond dissociation happens. The creation of the hydroperoxides from the radicals created during the initiation proceeds later, during the propagation step and it is also possible for some termination reactions. While in the case of ageing initiation by thermal factor, the hydroperoxide decomposition is the main source of radicals,since the O-O bond has the lower dissociation energy in comparison to the C-H an C-C bonds. Therefore, the step of initial hydroperoxides accumulation was not observed in the case of thermal ageing.

The change of the soluble fraction of the samples aged at 1 kGy indicated that by the dose of 150 kGy cross-linking is a dominant mechanism, while above 150 kGy the chain scission becomes dominant. Interestingly, it was observed that the alteration of the hydroperoxide accumulation of the samples aged at 1 kGy happens at the same dose, $\sim$150 kGy. This indicated that the decomposition of hydroperoxide is related to the chain scission dominance and network structure destruction.

The matrix/filler interphase densification phenomenon and its increases with the filler content, was also observed, but in a less extent in comparison to the thermal ageing. This was explained by the fact that the interphase mobility is increased at higher temperatures, and the thermal ageing temperatures were higher, while diffusion of oxygen molecules is facilitated as well at higher temperature. Therefore higher number of densification acts is supposed to happen at higher temperatures.

The importance of the initiation step for the subsequent reactions is evident and it is discussed as well within the life-time prediction studies [24, 25]. Generally, three initiation mechanisms are proposed in the case of radiation ageing [11]:

1) Purely thermal initiation: at low dose rates the irradiation induced initiation is negligible and the main act is the decomposition of hydroperoxides;
2) Purely radiochemical irradiation: at high dose rates the consumption of hydroperoxides is negligible and the main act is polymer radiolysis. Therefore the hydroperoxides remain stable and accumulate in the system.
3) Combined radiochemical and thermal initiations: at the beginning, the accumulation of hydroperoxides is predominant. When the concentration of hydroperoxides attains a critical value, the decomposition rate of hydroperoxides increases sharply.

The so called 'synergetic effect', that might influence simultaneous radiation and thermal ageing, is often discussed. This effect understands that the rate constant of the reaction under the combined thermal and radiation ageing is higher in comparison to the simple addition of the heat and the radiation individual rate constants. [21, 66]

The effect of the γ-radiation on EPDM network evolution was studied by Planes et al. [58]. The samples were exposed to γ-radiation at a dose rate of 1 kGy/h at room temperature in an oxygen atmosphere for doses 50, 165, 300, 510 kGy. The sample oxidation profiles for the maximum irradiation doses were checked by IR profiling via variation in absorbance at 1713 cm^{-1} across the sample thickness and they were observed to be nearly flat; which lead to a conclusion that the oxidation processes are homogeneous within the sample thickness. The main techniques used for analysing the evolution of the EPDM network with ageing were tensile test and swelling measurement.

The uncross-linked and EPDM samples of different cross-linked degrees were studied and it was observed that under irradiation cross-linking is dominant mechanism in the case of non cross-linked EPDM. The same was observed by other authors [54, 55, 61, 62]. For the samples that already have high degree of cross-links, the cross-linking was observed only at the lowest radiation doses, while at higher doses chain scission was found to be dominant and moreover it was observed to increase linearly with the dose for the doses above $\sim$ 100 kGy. Assuming such a scission kinetic, a cross-linking kinetic was estimated, and it was

found that, contrary to the chain-scission, the cross-linking kinetic is not proportional to the radiation dose. The cross-linking mechanism was observed to saturate when the cross-linking density is close to that estimated for non-irradiated cross-linked EPDM. This suggested that the cross-linking mechanism during the ageing should be very similar to that induced by either irradiation or by chemical (peroxide) curing.

The consequences of the chain scission on the mechanical properties of the initially cross-linked EPDM, were observed to be a decrease of the Young's modulus and decrease of the elongation at break. The decrease of the elongation at break was explained by the presence of the defects in the network. The network architecture of the material was supposed to become very irregular due to the degradation, containing more and more weakened zones, which deteriorate the material ultimate properties. It was proposed, given the distributed character of these chain lengths,that the elongation at break is likely controlled by the shortest chains which percolate through all samples; whereas the increase in the average length of the active chains control the material modulus.

The uncross-linked and cross-linked EPDM containing ATH filler were also investigated. It was observed that the soluble fraction at high irradiation doses is higher in comparison to the the EPDM without filler, which suggested the higher chain scission. The author assumed that the degradation was enhanced due to the presence of the filler, which might be explained by the formation of supplementary radicals at the filler surface.

Interestingly, the elongation at break was observed to increase for all the filled samples; while the ultimate stress of EPDM filled by untreated ATH increase with ageing which was contrary for the EPDM samples filled with untreated ATH where the ultimate stress mainly decreased. It was supposed that with fillers, the degradation promotes filler-matrix decohesion and cavitation which enables larger strains at break during the tensile test in comparison to the unfilled EPDM.

In order to investigate the influence of the temperature on irradiation ageing, additional ageing was performed at 80^0C. The oxidation profiles were observed to be almost flat and the oxidation was assumed to be

homogeneous.

An increase in the swelling ratio and a decrease in the elastic modulus were observed to be faster for the samples irradiated at 80^0C in comparison to the samples irradiated at 25^0C. This was explained by the crystallinity melting, but since the sample crystallinity was not very high (11%) additional factor was determined as reason for faster degradation at higher ageing temperature and that is thermal activation of the reactions. Moreover, during thermal ageing, hydroperoxides decomposition is enhanced and so is formation of radical species, which accelerates degradation mechanism. The acceleration of the degradation induced by the filler presence, previously observed for ageing at higher temperatures, was less pronounced during the irradiation at 80^0C.

Evolution of EPDM molecular dynamics with ageing

In order to monitor the evolution of the molecular dynamics of polymer chains with ageing, N. Cellete et al. performed ageing and DMA testing of 1 mm thick non-cross-linked and cross-linked EPDM with and without antioxidant [54, 55]. The γ irradiation ageing was performed in air at 1 kGy/h for total integrated doses ranging from 50 to 450 kGy. Additionally, the electron irradiation ageing under inert atmosphere was performed at dose rates of 500 kGy/h for the doses of 100 and 500 kGy. The relaxation behaviour of non-aged and aged samples was monitored through the evolution of tanδ, the elastic and the loss modulus, as a function of the irradiation dose. It was observed, by the increase of the relaxation peak temperature together with the decrease of its amplitude as a function of the irradiation dose, that there is a decrease in the molecular mobility. The decrease in the molecular mobility was associated to the dominance of the cross-linking, which was observed to be more important for non-vulcanised samples, while antioxidant was not observed to influence the magnitude of the cross-linking importantly. Additionally, it was observed that cross-linking is more important for γ irradiation under air in comparison to the electron irradiation under inert atmosphere, but since the irradiation was not performed under the same or similar dose rate it was difficult to compare. Nevertheless, the authors proposed

that the presence of oxygen and longer irradiation time in the case of γ irradiation enhances chain scission which leads to more recombinations. The further investigations of the authors included infra red spectroscopy and gel fraction measurements [61] and tensile testing [62] confirmed that at the higher irradiation doses, over 100 kGy for the samples and ageing conditions applied within their study, chain scission becomes more dominant in presence of oxygen. Moreover, additional investigation of relaxation phenomena evolution with ageing was performed by including the measurement of dielectric relaxation parameters [55]. Dielectric relaxation spectroscopy (DRS) enables detection of molecular dynamics through dipolar labeling, so it can be used to monitor polar species created by oxidation. Indeed, it was confirmed that, by irradiation under oxygen, the amount of polar species increases and DRS was observed to be suitable as complementary technique with the mechanical relaxation measurements. Moreover, the DRS appeared to be more sensitive for detecting early steps of degradation, while mechanical relaxation measurements seemed to be better in detecting cross-linking phenomenon. The same was observed by the other authors that studied ageing effects on EPDM by measuring the mechanical and dielectric material relaxations, [56]. These authors confirm that DMA properties seem to be more sensitive to long-term ageing effects, especially cross-linking, while dielectric loss parameter is very convenient to detect sample oxidation even at early phase of ageing.

The effect of atmosphere and oxygen pressure to the ageing process of EPR

The changes of mechanical properties of various kinds of 1 mm thick ethylene-propylene copolymer (EPR) with the irradiation in air, in oxygen of 10 atm, and under vacuum were investigated [59]. The samples were irradiated up to the 1200 kGy with a dose rate of 5 kGy/h. The EPR were cross-linked by DCP, they were formulated without and with antioxidants and they did not contain any mineral filler. The ultimate tensile strength was observed to decrease strongly with dose at initial stage, up to the 250 kGy, then the decrease becomes gradual, in both

oxygen and vacuum. The values of the ultimate tensile strength of the samples aged under vacuum is very similar to the values of the samples aged under oxygen. The elongation at break of EPR irradiated under vacuum decreases with dose. Contrary, the elongation at break of the samples aged in oxygen, decreases with dose at initial stage, but it increases at the higher dose, taking the minimum at the doses about 400-700 kGy (see Fig. 1.18). The dose at which the minimum is positioned was observed to depend on the type of antioxidant and it was the lowest for the sample that was containing no antioxidant. The minimum followed by an increase of the elongation at break was explained by the sample network degradation due to the chain scission and lost of the elasticity. The value of the elongation at break of the samples aged under air was observed to have the intermediate values between ones for oxygen and vacuum. The evolution of the ultimate tensile strength was not shown, but it was explained to be complex, probably due to the heterogeneous ageing phenomenon: cross-linking in the sample bulk vs. chain scission near the sample surface. The evolution of the modulus at 200% elongation with dose, of the samples irradiated in oxygen and under vacuum was presented. It was observed to increase with dose for the samples aged under vacuum, which was explained by the dominance of the cross-linking. Expected modulus decrease was observed for the samples aged in air. The rate of decreasing was observed to be dependant on the types of antioxidants.

The properties of the samples irradiated under the 10 atm oxygen were studied by swelling measurement [60]. The gel fraction was observed to decrease, while the swelling ratio was increasing with the dose, which is in accordance with the domination of the chain scission degradation mechanism, which is assumed to deteriorate the polymer network during the irradiation under oxygen. Moreover, the logarithm of the swelling ratio exhibited a linear relation with the dose, which is in accordance with the observation of E. Planes et al. [58] Additionally, it was found that the slopes of the log(swelling ratio) vs. dose lines are dependent on the initial cross-link density i.e. the initial swelling ratio and the equation is proposed to calculate swelling ratio at any dose, from the initial swelling ratio. The results indicated that the samples with higher

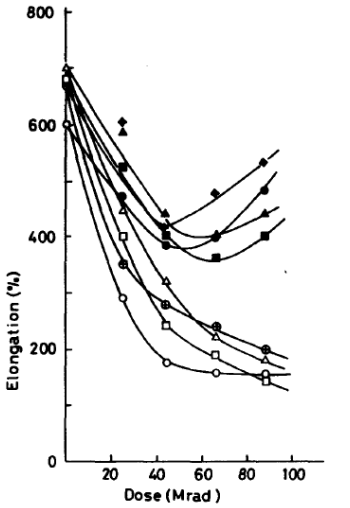

△, EPR (No. 7) with NBC under vacuum; ▲, EPR (No. 7) with NBC in oxygen; □, EPR (No. 8) with DPPD under vacuum; ■, EPR (No. 8) with DPPD in oxygen; ○, EPR (No. 9) with I-1010 under vacuum; ●, EPR (No. 9) with I-1010 in oxygen; ⊕, EPR (No. 6) without antioxidant under vacuum; ◆, EPR (No. 6) without antioxidant in oxygen.

Figure 1.18: *The evolution of elongation at break with dose, irradiated under different conditions, for EPR with and without antioxidant [59].*

initial cross-link density are more resistant to the oxidative degradation induced by irradiation.

Heterogeneous oxidation

The oxidation is proven to be the most important cause of the EPDM degradation under the thermal and irradiation stressors. The dominant mechanism of ageing was shown to be dependant on the oxygen availability. The issue of heterogenous oxidation of bulk samples due to the oxygen limited diffusion through the sample thickness is often studied together with the investigation of the methods to determine the extent of the sample oxidation. By theoretical analysis of the oxidation depth

in a polymer film it was shown by T. Seguchi et al. [23] that the depth of oxidation region was proportional to the square root of the oxygen pressure/dose rate ratio. The polymers for experimental analysis were irradiated under pressurized oxygen atmosphere (0.21 - 10 atm) at high dose rates ranging from 0.5 to 1 Mrad/h (5 - 10 kGy/h) in order to accelerate the oxidative degradation. The gel fraction measurements on 1, 2 and 3 mm thick EPR films were observed to correspond to the oxygen penetration range, calculated according to the theoretical analysis. Accordingly, the method was proposed for accelerated ageing of polymer materials by irradiation at higher dose rate, which aims avoiding the heterogeneous oxidation. This method assumes ageing at high irradiation dose rate in oxygen under pressure. Diffusion and solubility of oxygen were measured for EPR and the diffusion coefficient was observed to scarcely change up to the 200 kGy, while solubility constant increased slightly by increasing the dose. The reported values were following: the diffusion coefficient (cm^2/sec) was measured to be: 1.6x10^{-6}; 1.6x10^{-6}; 1.5x10^{-6}; the solubility coefficient (mol/(g*atm)) was 4.3x10^{-6}; 4.6x10^{-6}; 4.6x10^{-6}; for the non-irradiated sample; sample irradiated in vacuum up to the 200 kGy and sample irradiated under oxygen up to the 200 kGy, respectively.

The dose rate effects on the radiation induced oxidative degradation of cross-linked EPRs mechanical and chemical properties was investigated by the tensile properties, gel fraction, and dielectric tangent loss [98]. It was found for the polymers that are not containing antioxidant that the degradation at a given dose depends on the dose rate: $Deg/r = k*I^{-1/3}$; where Deg is degradation, r-dose, I-dose rate and k-constant. Interestingly, for the polymers containing antioxidant the dose rate effects was not observed.

In their studies K. Gillen, M. Celina and R. L. Clough gradually investigated the dose rate effects during ageing [22, 35, 67–69]. The report from 1984. [22] addresses several techniques adequate to investigate the heterogeneous oxidation in irradiated polymers, especially in industrial ones. The two EPR materials appear among the studied polymers. For the oxidation profiling relative hardness measurement across cross-sectioned samples was performed together with measurement of the densities of pieces of the degraded samples. All irradiation was car-

ried out at 70 ^{0} C and the sample thickness was 3.15 mm. The probe penetration profiles indicated changes in relative hardness on cross-sectioned samples of the EPR material are presented in Fig. 1.19. For the unirradiated material the profile was essentially flat. For the samples aged at the highest dose rate (6.7 kGy/h) up to the total dose of 1650 kGy and 2970 kGy the U-shaped profile was obtained, and it was observed to be a somewhat more shallow in the case of the sample irradiated up to the 1650 kGy. For both samples the oxidation seemed to be penetrating only about up to the $\sim$ 20 % of the thickness from each side, while for the interior $\sim$ 60 % the cross-linking seems to be dominant, which was an indicator of strong oxidation heterogeneity induced by accelerated ageing. The profile of the sample aged at 1.1 kGy/h up to the 1750 kGy was observed to approach a more homogeneous oxidation, exhibiting rather flat profile with a shallow curvature. The probe penetration profiles were observed to be in a good correlation with density measurement. The density was observed to increase for the oxidised part of the sample, which was creating a profile when samples were taken across the sample thickness, and the profile is observed to be nicely correlated to the relative hardness profile. It was demonstrated that the profiling techniques as probe penetration and density measurement seem to be adequate to demonstrate the sample oxidation heterogeneity / homogeneity.

Regarding the attenuation of the diffusion limited oxidation at high dose rate, according to the study of A. Shimada at el. [28] it is possible to decrease the DLO by increasing the irradiation temperature. It was explained by the fact that the diffusion of the oxygen increases with increasing the temperature, but still it was recommended not to exceed the temperature of 100^0C, since the contribution of the thermal degradation would increase importantly then. The thickness of the tested samples was 1 mm. Within this research it was observed by monitoring the elongation at break decay that the radiation ageing at 250 Gy/h at room temperature for 400h seems to be equivalent with the radiation of 1000 Gy/h at 100^0C for 400h. The only thermal ageing was performed at 100^0C and 155^0C for 400h; and while the elongation at break decay starts being significant after more than 200h of ageing at 155^0C, at the 100^0C the degradation was scarce within the 400h. Due to that it was

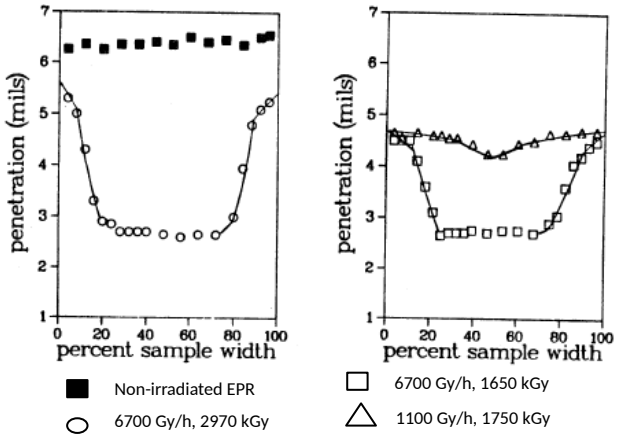

Figure 1.19: *The probe penetration profiles on cross-sectional samples of the EPR [22].*

assumed that most of the degradation in the case of irradiation at 100^0C was induced by irradiation. By FTIR it was confirmed that the main oxidation product were carboxylic products and profiling of the carboxylic products was performed in order to investigate the homogeneity of the oxidation thorough the sample thickness. It was confirmed that profiles are flat for ageing conditions of 250 Gy/h at room temperature and 1000 Gy/h at 100^0C.

Prediction of EPDM behaviour under ageing

A scientific approach together with accurate diagnostic tool are necessary to determine precisely the mechanism of polymer insulation degradation, which is essential in order to enable reliable prediction of the cable polymer life duration. In the paper of B. Pinel and F. Boutad from 1999. a methodology to predict the life duration of polymers used in nuclear power stations was presented and applied on the EPR cable polymer [24]. This study was performed on the samples made out of

cables that are in use in NPP and the accelerated ageing was performed on the 30 cm long cables. The same authors presented the lifetime prediction for the EPR industrial samples which were striped out of the aged cable. The combined radiation was performed at the temperatures from 50 - 90 and 100 Gy/h for the total dose of 10 - 100 kGy in air. The irradiation at 40^0C was entitled as purely irradiation ageing and it was performed in air at several dose rated ranging from 10 up to the 2200 Gy/h, for the dose range of 10 - 100 kGy.

The principles of the life-time prediction kinetic model that is used, are presented in the Section 2.2.1. By the fitting EPRs elongation at break versus time data, experimentally obtained for different dose rates and temperatures, the irradiation constant rates were calculated using the described kinetic model. The constant rate diagram was constructed, showing the dependance of the irradiation rate constant from the dose rate, see Fig. 1.20. The "break point" was observed at $\sim$ 500 (455) kGy/h and it was equivalent to so called "critical dose rate" i.e. a minimal dose rate from which the DLO can be expected. Thus, for the dose rates lower than critical homogeneous oxidation is expected, while for the higher ones heterogenous oxidation is expected. Additionally, a "predominance diagram" (ln(dose rate) vs. (1/T)) was constructed which supposed to indicate the main stress contribution for a given ageing condition. It was already mentioned within this chapter that in the cases of simultaneous thermal and irradiation ageing several ageing "domains" are often defined according to the stressor responsible for the dominant initiation mechanism. There are domains of thermal stressor domination, irradiation domination, thermal and radiation coexistence and the one where DLO appears. Interestingly, according to the diagram of predominance that was constructed by B. Pinel and F.Boutad using their experimental data, the dominant ageing factor at operating conditions (i.e. 40 ± 50^0C and 0.1-1 Gy/h) supposed to be irradiation, see Fig 1.20.

The end of the life-time prediction of EPR cable material was performed as well. [26] The tensile test was performed. It was observed that for the dose rates below the 500 Gy/h the ultimate tensile stress does not change importantly, while for the dose rates above 500 Gy/h it consid-

erably increases. So the dose rate of the 500 Gy/h was again enabled as the critical dose rate regarding the oxygen diffusion control of the ageing process. For the combined ageing it was stated that the temperature has only limited influence on the life-time. Within the applied temperature range the dependence of the temperature related rate constant was found to obey the Arrhenius law, which means that the extrapolation to the operating conditions (40^0C) can be performed. The kinetic model was applied to the elongation at break versus time data, and the constant rates for irradiation and thermal activated reactions were determined, together with the activation energies for each process and several modelling parameters. The modelling results were observed to be in accordance with the experimental ones and the prediction for the life-time of the material under the operating conditions (0.01 Gy/h and 40 ^{0}C) was made using the obtained parameters. It was observed that the end life criteria - 50% absolute elongation at break, is never reached before 50 years.

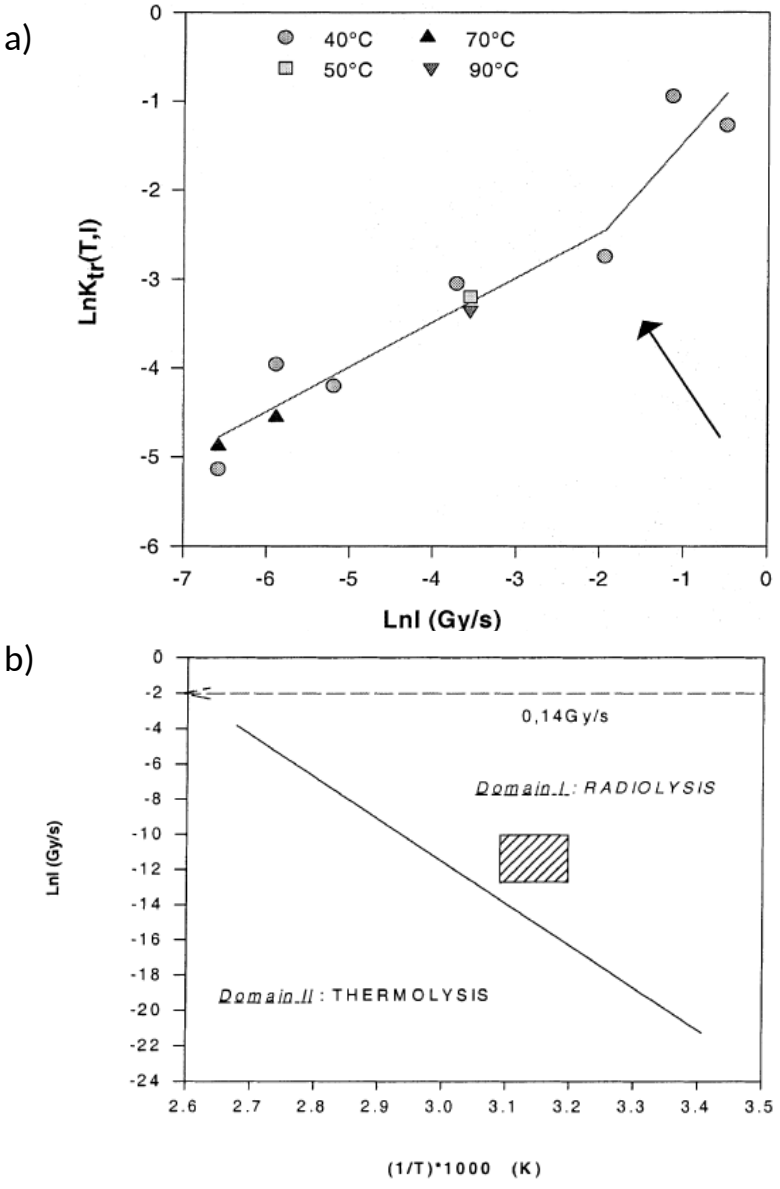

Figure 1.20: *The constant rate (a) and predominance (b) diagrams [24].*

1.7 Objectives of the thesis

At present, there are over four hundred operational nuclear power plants (NPPs) in the world [70]. Operating experience has shown that ineffective control of the ageing degradation of major NPP components can jeopardize plant safety and also plant life. Among these elements, cables are vital components of Instrumentation and Control (I&C) systems in NPPs [1]. To ensure their safe operation various maintenance programs, in-service inspections, and testings of structures, systems and components important to safety are being updated and developed.

The safety and effectiveness of the cable wire depend on its insulation. Insulation resists electrical leakage, prevents the wires current from coming into contact with other conductors and preserves the material integrity of the wire by protecting against environmental. The evolution of a cable insulation, which is mainly produced out of polymer material, with ageing is gradually investigated in order to assess the state of the cable.

Accelerated ageing can be employed in many ways, and the way it is designed will affect the outcome of the aged sample experimental investigation. Within this thesis, the simultaneous thermal and radiation ageing is performed, covering a rather broad temperature, dose rate and dose matrix. Ageing parameters were designed in order to ensure that an end - of - life criterium will be reached for the majority of ageing conditions, as well as to address the investigation of diffusion limited oxidation and the dose rate effect, which are still not completely resolved, despite the fact that they were observed relatively early in the cable insulation investigation.

Next to the ageing condition, sample composition and geometry are important for an accelerated ageing study. Although it is not uncommon to age an entire cable, it is not very practical and it requires a lot of space in ageing chambers. Simple sample compositions or film samples are good in order to study chemical properties and basic ageing mechanism, but these might lack in important observations related to the ageing behaviour of "real" systems. Two types of industrial samples

were investigated in this thesis. They were extracted from outer and inner cable insulation (aged as extracted, not as assembled on the cable). The inner insulation sample is about 2 times thinner in comparison to the outer. Next to them, the neat polymer samples, made out of the raw polymers, designed to match the properties of polymer originally used in the composition of industrial samples, and manufactured in the lab to match the dimensions of outer insulation samples, were investigated as well. The neat polymer samples were aged under the same conditions as industrial samples, in order to attempt to assess better the chemical evolution of polymer with ageing, without the influence of additives and fillers gradually present in industrial polymers.

Accelerated ageing is done in order to bring the cable to the end - of - life state in a faster way, so that the prediction, when it will happen under operating conditions, could be made. This prediction is often made on the basis of empirical investigation. In order to make it more reliable, a physico-chemical background should be provided for such a prediction. In another words, the better understanding of the ageing at physico-chemical level together with a correlation with the evolution of the macroscopic properties is needed. Several condition monitoring techniques, measuring physico-chemical, microstructural and macrostructural properties, were performed within this thesis, in order to attempt to find suitable parameters to monitor the cable ageing. Furthermore, an attempt is made to correlate these parameters, focusing on the origin of the correlation, where observed.

The objectives of the proposed work can be summarized as follows:

- to perform experiments on accelerated ageing of cable polymers and to develop improved experimental methodology for performing such tests; to improve existing methodologies applied for the analysis of accelerated ageing experiments;

- using both phenomenological approach to the radiation-assisted relaxation and ageing effects and understanding of microscopic transformations involved, to establish correlations between the elongation at break and indenter measurement data to provide the capability of assessing the state of cable materials by use of in-situ, non-destructive techniques;

-to improve the physical understanding of the polymer ageing-degradation making the link between the changes of mechanical properties, chemical evolution and microstructural properties, related to ageing;

- to develop methodology for providing estimations of the residual lifetime of partially aged cables.

1.8 The thesis outline

The thesis is organized as follows:

Main issues of the NPP cable ageing are presented in the introduction (Chapter 1).

Chapter 2 contains the description of materials and methods which were used in this study. Besides, the ageing matrix, the applied investigation techniques and calculation methods/models are explained. The cable insulation (outer and inner) mainly made out of EPDM was stripped out of a cable from the NPP storage (the cable type is in use in NPP) and kindly provided for investigation by ENGIE Laborelec. The dumbbell shape samples were made from the outer insulation and tubular from the inner. Since industrial cables are complex with respect to the composition, neat dumbbell samples were produced in the Université Catholique de Louvain laboratory from the polymer materials that are analogous to the matrix EPDM type polymer of the industrial cable, in order to obtain more a simple system for the investigation and to compare the behaviour of industrial and neat polymers. The detailed description of the material chemical composition and sample production is also given in this chapter.

The results are discussed in Chapters 3 and 4. The results related to the industrial polymer are presented and discussed in Chapter 3. Mechanical results, elongation at break modelling and microstructural and physicochemical results are first presented for outer insulation samples and then for inner insulation specimens. The tensile and indenter modulus test results are discussed and compared. Tensile parameters are calculated and monitored as a function of the ageing time and dose.

The elongation at break model is applied to the experimental data and the model application is discussed. Correlation between indenter modulus test and elongation at break results are analyzed. With respect to the microstructural techniques used, the focus is given to thermogravimetry, since an original correlation between thermal decomposition of the industrial polymer in air and the change of the elongation at break as a function of the dose is found. These results are compared to other non-mechanical test results as well.

Chapter 4 contains the results and discussion for the neat polymer. Three ageing conditions, similar to the one applied to the industrial samples, are applied to two types of raw materials. The data are obtained for polymers known as Nordel 3722 and Engage 8100 polymer. The change of the tensile properties as a function of the ageing dose and time is presented together with the elongation at break modeling and compared to the results obtained for industrial polymer. The results of the non-mechanical test are presented, once again with a focus on comparison between the TGA results of neat and industrial polymers.

General conclusions, as well as possible future work were summarized in Chapter 5. This chapter describes in detail the methodology for obtaining estimations of the residual lifetime of partially aged cables, in particular what concerns diffusion limited oxidation effect.

The results of IAEA bench-marking program, which included the thermal ageing and tensile investigation of several NPP cable insulations from the producers world-wide, are presented in Chapter Appendix A. The result of the bench-marking tests were used to confirm the validity of tensile test procedure.

Chapter 2

Materials and Methods

2.1 Materials and ageing conditions

Accelerated simultaneous thermal and radiation ageing was performed on two types of samples, both based on a EPDM as the main component. The first one, extracted from the cable coming out from NPP storage, were named industrial EPDM samples and described in Section 2.1.1. The second one were produced in the university laboratory from the polymer pellets obtained by "DOW Chemicals"; and they were named neat EPDM samples. The neat EPDM samples are presented in Section 2.1.2. Ageing conditions were designed in order to reach high enough level of sample degradation to satisfy end-of-life criteria, and to have a variety of ageing conditions, broad enough for the evaluation of dose rate effect. Accelerated ageing of samples is presented in Section 2.1.3 and conditions that could possibly cause diffusion limited oxidation are discussed in Section 2.1.4.

2.1.1 Industrial samples

The industrial samples were kindly provided by ENGIE, Laborelec. These samples were extracted from the cable, coming out from the NPP storage, that is of the same type of cables in use in the Belgian NPP.

The type of cable is a low voltage ERR cable (E-energy; R-insulation made of EPDM; R- jacket made of EPDM). These cables were produced by Kabelwerk Eupen AG (Belgium) during seventies and eighties. They are known as a second generation of Eupen cables.

The cable was designed in a way that outer insulation-jacket envelops four inner insulations, with similar composition, but different in colour. The industrial cable samples were extracted from the outer insulation (jacket) in a form of dumbbells and also from the black inner insulation in a form of tubular samples.

The data about cable composition were partly provided by ENGIE and partly experimentally investigated. Basic polymer component is EPDM, but there is also ethylene-vinyl acetate which contains 50% of vinyl acetate. It is known that EPDM type is NORDEL 2722, with ethylidene norbornene (ENB) as a diene. This type of EPDM was produced by DOW Chemicals, but it is not in production anymore. Higher amounts of VA are typical when EVA is planned to be used as an elastic material, because VA decreases crystallinity and increases polarity of EVA [95]. A high quantity of aluminium hydroxide (ATH) is present. ATH is well known for being used as a fire retardant filler. It starts decomposing at temperatures around 250 ^0C and gives water and alumina (aluminium oxide). This sample composition was cured by peroxide (dicumylperoxide). The main differences between outer and inner insulation is found to be in EPDM and EVA ratio and in ATH content. The chemical composition of the cable insulation material, estimated according tho the performed chemical investigation and some indication obtained by ENGIE Laborelec, is presented in Table 2.1: It has to be emphasized that no original data indicating the exact composition of the cable insulation was available.

Table 2.1: *Insulation material chemical composition.*

insulation	EPDM (wt%)	EVA (wt%)	ATH (wt%)
outer ins.	~ 40	$\sim$2	~ 58
inner ins.	~ 45	$\sim$10	~ 45

The dumbbell shaped samples were chosen due to uniaxial tensile testing

and formed from the cable outer insulation using stamping ("punch out") type tool. This tool contains hammer-like part with replaceable cutting system on the top, where it is possible to exchange several standard dimensions of dumbbell sample. Dimension of the dumbbells used in this study are in accordance with the dimensions for a "small dumbbell test piece" from the IEC International standard 60811-1-1 [71]. The total length is 50 mm length of the narrow part 17 mm, and the width of the narrow part is 4 mm see Fig. 2.1. Because they were extracted from a real cable insulation, which has a hollow cylinder shape, dumbbells are not perfectly flat. The thickness of the dumbbell is 2 ± 0.2 mm.

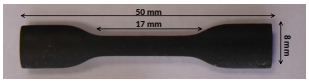

Figure 2.1: *Example of the industrial EPDM dumbbell sample made out of cable outer insulations.*

The tubular shaped samples were made from black inner insulation, in a way that the conductor was pulled out from the insulation. Length of the tubes is 10 ± 1 cm and thickness is 1 ± 0.2 mm (see Fig. 2.2).

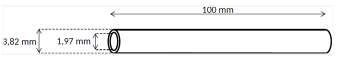

Figure 2.2: *Example of the industrial EPDM tubular sample made out of cable inner insulation.*

2.1.2 Laboratory samples/ Neat polymer

An attempt was made to obtain more detailed information about the chemical reactions, occurring during the ageing, in the polymer itself. The investigated cable insulation polymer has rather complex structure. For that reason, the neat polymer materials, chosen to match the characteristics od the EPDM component of the investigated cable polymer, were aged and investigated.

The neat samples were made out of "as received" pellets, without adding any cross-linking agent, filler or additive. Two types of polymer materials, equivalent to NORDEL 2722, were provided by DOW chemicals. First one is NORDEL 3722 that is in production nowadays and it is designed to match characteristic of NORDEL 2722 [72]. It has low content of diene (0.5 wt%) and it is semi-crystalline, with the crystallinity of 15 wt%, reported by DOW Chemicals. The ethylene content of Nordel 3722 is 70wt%. Second type of polymer is ENGAGE 8100, a polyolefin elastomer that is an ethylene-octene copolymer. The reported percent of crystallinity is 18 wt%. Several main physical and mechanical characteristics, as reported by the producer, of both neat polymers are presented in Table 2.2:

Table 2.2: *The properties of neat polymers.*

Polymer	Density (g/cm^3)	Crystallinity (wt%)	Tm (^0C)	Strength (MPa)$^{(1)}$	Elongation (%)$^{(1)}$
Nordel 3722	0.87	15	46	8.1	275
Engage 8100	0.87	18	62	9.6	810

(1)Tensile at 510 mm/min

Materials were received in pellet form. Dumbbell type of samples, matching the dimensions of the industrial outer insulation samples, were made out of them. In order to get the adequate samples, 2 mm thick sheets were made and the dumbbell shaped samples were punched out of, using the same knife system as for industrial EPDM.

The neat EPDM polymer sheets were produced by melting and pressing of the pellets. In the frame-like mould shape, about 55 g of pellets was spread over. This system was then placed in the melting machine (see Fig. 2.3.) and it was melted for 5 minutes while slightly pressed.

Figure 2.3: *The machine for pellet melting and forming of polymer sheet.*

To get a compact sheet, melting is followed by pressing under pressure of 8-10 bar. The machine for pressing is of similar design as the machine for melting, just with a possibility to obtain higher pressure on a sheet in comparison to the pressure under melting process (see Fig. 2.4). An obtained polymer sheet was considered to be good if boundaries within melted pellets were not visually noticeable. Appropriate melting temperature and pressing time are important with respect to the quality of a produced sheet. They were established to be 160^0C and 3 minutes after few trials, varying several temperatures and pressing times.

2.1.3 Accelerated ageing of the samples

Simultaneous thermal and radiation ageing of samples was performed at the Belgian research center SCK • CEN. The irradiation was performed in the RITA (Radio Isotope Test Arrangement) or BRIGITTE (Big Ra-

Figure 2.4: *The machine for pressing.*

dius Installation under Gamma Irradiation for Tailoring and Testing Experiments) irradiation facility described in details previously [73]. The RITA facility comprises four 20 cm high cylindrical Co^{60} sources located at $\sim$ 6.5 m below the water surface. The experimental samples were placed in the water-tight irradiation container. To perform exposure to gamma-radiation this container is lowered into the underwater position in the center of the square formed by the Co^{60} sources. The size of the square can be changed to adjust the dose rate.

The BRIGITTE facility is similar to RITA with a difference that it comprises up to 10 Co^{60} sources and the dose-rate adjustment is made by changing the number of sources.

In both facilities the gamma-sources have a length shorter than the container height. As a result the dose rate inside the container has a vertical gradient with a flat dose rate area around the mid-plane. A desirable dose-rate can be obtained by changing the vertical position in the irradiation container. The actual dose rate at the sample location was mapped before the irradiation using Harwell Red Perpex

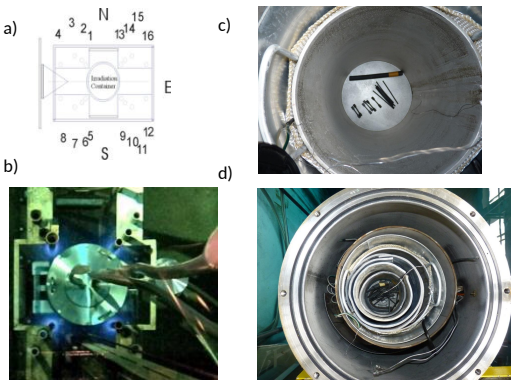

Figure 2.5: *a) Schematic description of the RITA irradiation facility with total of 16 source positions. (from [73]); b) The RITA irradiation facility. The irradiation container is surrounded by four 60Co sources and the plastic hoses contain the instrumentation and the cabling required to power the devices under test.(from [73]; c) The sample irradiation in RITA; d)The sample irradiation in RITA with lead shield added to decrease the dose-rate.*

dosimeters. The standard accuracy of the dosimetry is 5.5%. The non-uniformity of the dose-rate distribution over the samples was less than 5%. When under irradiation, the samples were located in a dedicated cylindrical furnace placed inside the irradiation container to allow for accurate temperature control throughout the experiment. This furnace is a thick wall Al tube with closed ends and a heating wire placed on the outside surface and covered with a thermal insulation. A high thermal conductivity of Al allows for a reasonably quick thermal response with a time of ~ 40 min to achieve stabilization at a desired temperature within $\pm 0.1^0 C$. The temperature under irradiation is maintained using a PID controller. The volume of this furnace is ~ 20 l. There was no air supply to the furnace: the irradiation was performed in stagnant air. Typically 10 samples with total mass of about 10 g are used for one irradiation condition.

The ageing matrices are given in Table 2.3 and Table 2.4 for industrial

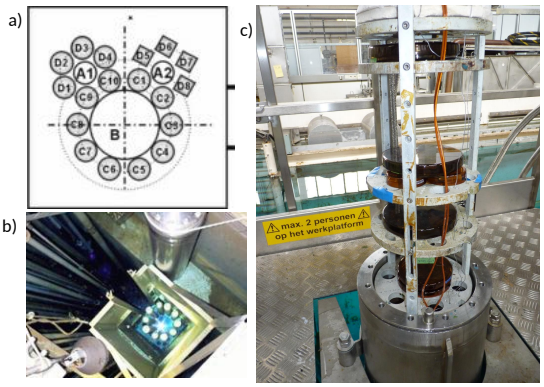

Figure 2.6: *a) Schematic lay-out of the BRIGITTE irradiation facility. (from [73]); b) The BRIGITTE gamma irradiation facility.(from [73]; c) The irradiation in the BRIGITTE - the placement of the samples in petri cups.*

and neat samples, respectively. The aging temperatures are in a range of 25^0C to 85^0C, and the dose rate from 106 Gy/h to 2760 Gy/h.

2.1.4 Diffusion limited oxidation

The possibility that some of the accelerated ageing conditions could cause limited oxygen diffusion and therefore heterogeneous oxidation of some samples is considered. Measurements of oxygen consumption and oxygen permeability could characterise an oxygen diffusion process during ageing and indicate if there is a possibility that the oxygen diffusion through an sample is limited. But it is not so simple to perform oxygen consumption or oxygen permeability measurements during an accelerated ageing, so there are methods that can be used to estimate possibility for DLO.

The IEC Technical Specification 61244-1 [50] offers one of the methods. It is based on theoretical estimation of the so-called "critical thickness" (Lc). This thickness is estimated for each applied condition: dose rate and temperature. This thickness is the maximal thickness for a

Table 2.3: *The ageing matrix of the indsutrial EPDM samples*

Dose rate (Gy/h)	Absorbed dose (kGy)	Temperature (^0C)	Irradiation facility
250	100 200 300 400 500 600	25	RITA
720	200 300 400 500 600 700 800 900 1000 1100	25	RITA
1390	200 300 400 600 800 1000	40	BRIGITTE
2760	317 466 793 1189 1586 2379	40	BRIGITTE
106	20 40 60 100 200 250	55	RITA
455	80 160 240 400 800 1000	55	RITA
106	20 40 60 100 200 250	70	RITA
455	80 160 240 400 800 1000	70	RITA
1390	200 300 400 600 800 1000	70	BRIGITTE
2760	320 470 800 1200 1600 2400	70	BRIGITTE
106	20 40 60 100 200 250	85	RITA
455	80 160 240 400 800 1000	85	RITA

Table 2.4: *The ageing matrix of the neat EPDM samples.*

Dose rate (Gy/h)	Absorbed dose (kGy)	Temperature (^0C)	Irradiation facility
450	52 76 129 194 258 388	40	BRIGITTE
1400	160 235 400 600 800 1200	40	BRIGITTE
2780	320 470 801 1201 1601 2402	40	BRIGITTE
450	50 75 125 200 250 400	70	BRIGITTE
1400	160 235 400 600 800 1200	70	BRIGITTE
2780	320 470 801 1201 1601 2402	70	BRIGITTE

given condition that should ensure homogeneous oxidation. If the actual sample thickness is equal or less than the critical is, then DLO is not expected; but if it is higher, then an importance of DLO effect should be considered. Eq. 2.1 is used to calculate Lc:

$$L_c = 2(pP_{ox}/R_{ox})^{0,5} \tag{2.1}$$

where p is the oxygen partial pressure of the surrounding atmosphere, P_{ox} is oxygen permeability of polymer and R_{ox} is polymer consumption rate for oxygen. Since P_{ox} and R_{ox} were not experimentally determined within this study, we used the values from literature. The values for P_{ox} are used from the work of Cellina and Gillen [67], and R_{ox} is $4.33x10^{-10}mol/g/s$ [75]. Table 2.5 gives the calculated Lc for the applied ageing conditions.

The thickness of outer insulation samples is about 2 mm, and for the

Table 2.5: *The values of critical sample thickness for the ageing conditions.*

Dose rate (Gy/h)	Temperature (^0C)	Lc (mm)	DLO in dumbbells	DLO in tubular
250	25	1.15	yes	no
720	25	0.68	yes	yes
1390	40	0.7	yes	yes
2760	40	0.5	yes	yes
106	55	2.95	no	no
455	55	1.42	yes	no
106	70	3.9	no	no
455	70	1.92	yes	no
1390	70	1.1	yes	no
2760	70	0.76	yes	yes
106	85	4.9	no	no
455	85	2.35	no	no

inner insulation samples the wall thickness is about 1 mm. For the cases where the critical thickness is higher than the actual thickness of the samples, DLO is expected.

2.2 Experimental methods

For the purpose of monitoring the condition of cable insulation polymer material, several Condition Monitoring techniques were used. The effort was made to select the potentially effective CM techniques, on the basis of the expected ageing behaviour of the studied materials. The choice of a suitable CM technique should be made in a way that it measures a property which is a good indicator of the material degradation. The focus was given to the study of mechanical and physico-chemical properties of the investigated materials. Additional accent was put on the techniques that are non or low destructive and can be used on-site in NPP.

The uniaxial tensile procedure and set-up are presented in Section 2.2.1 including the paragraph related to the development of the optical method to monitor test and double check the results, and the paragraph related to the description of model applied on the elongation at break data. Methods used to measure indenter modulus are described in Section

2.2.2. The techniques for investigation of physico-chemical properties are presented in sections from 2.2.3 to 2.2.8 in following order: TGA, FTIR, TGA coupled with FTIR, swelling test, DSC, DMA.

2.2.1 Uniaxial tensile test

The uniaxial tensile test is performed on the Lloyd LR10K machine presented in Fig. 2.7, at room temperature (22^0C). The employed load cell was supporting up to 5 kN.

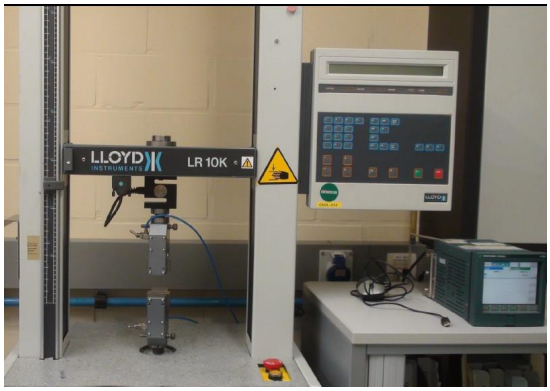

Figure 2.7: *The Lloyd LR10K tensile machine.*

Pneumatic gripping (clamping) system was used in order to ensure higher clamping force and equal pressure on sample ends that are gripped during the test. Two types of jaw faces were varied: pyramid and diamond. Pyramid inserts were used for non - aged and low aged samples. Generally, for softer samples that require better "bite". When samples became very brittle (rigid) and tended to slide from gripping system, more invasive - diamonds inserts, were employed. In Fig. 2.8 the pneumatic gripping system, together with the pyramid (Fig. 2.8b) and diamond (Fig. 2.8c) inserts (gripping jaw faces) are presented.

No extensometer was used, since it can leave traces on soft materials. The crosshead displacement was measured by tensile machine and transported to the data loader. In addition, the test was recorded optically,

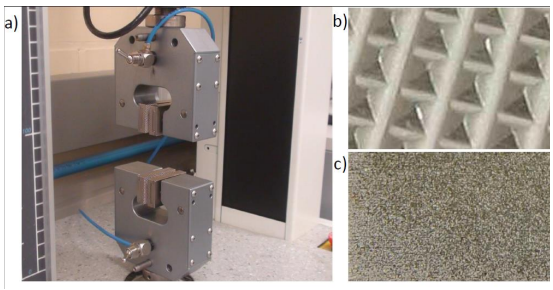

Figure 2.8: *a) The pneumatic gripping system; b) The pyramid type of jaw face; c) The diamond type of jaw face.*

which will be discussed later.

In order to obtain a good repeatability, it is recommended to use 5 samples [31] per each sample type (in our case per ageing condition). However, within this study two samples were tested per ageing condition, since number of samples per ageing condition is limited (6 outer insulation and 6 inner insulation samples) and tensile test is destructive. With "only" two samples per condition, the obtained data gave the expected trend, and they have been considered to be good considering the error bar. For this reason, the number of samples that were tested for each ageing condition was not further increased.

The absolute elongation at break is calculated as the total elongation at the fracture point, divided by the initial sample length and multiplied by 100 to get a percentage. The elongation at the break point is expressed as the length of the sample at the break point minus the initial sample length. Since no extensometer was employed for the absolute elongation at break determination, the crosshead displacement at break divided by non-clamped sample length. To obtain the relative elongation at break, the absolute value is divided with the elongation at break of a chosen reference sample, which is a non-aged sample in this case. It is worth mentioning that the last recommendation [29] defines the end-of-life criteria as 50% of absolute elongation at break value, but relative values are convenient for comparison of the data between different materials.

Beside the elongation at break, the ultimate tensile stress (UTS) and elastic modulus (Young's and modulus at a certain stress or strain level) were also determined. The ultimate tensile stress was calculated as the force at the break point divided by the initial sample area, which is known as an engineering (nominal) stress value.

An extensometer was not used during the tensile test, so the true values of the parameters were not recorded. Nevertheless, if one assumes that the investigated material, as a rubber, is incompressible and has the Poisson's ratio of 0.5; then the existing conversion (Eq. 2.2) from nominal to true stress can be applied together with the conversion from nominal strain to true strain (Eq. 2.3). [78]

$$Truestrain = ln(1 + nominalstrain) \tag{2.2}$$

$$Truestress = (nominalstress) * (1 + nominalstrain) \tag{2.3}$$

The Young's modulus was calculated as the slope of the initial linear part of the tensile curve. "The initial linear part" was determined to be up to the point where stress reaches 2 MPa in the case of outer insulation samples, and in the case of inner insulation up to the 4 MPa. In the case of elastomers, it is common to calculate the modulus at certain stress level as the ratio of stress to strain (for example, the point where the stress reaches 1 MPa, or where the elongation at break reaches 100%). For elastomers, stress to strain ratio decreases with strain increasing, because of that, the modulus calculated as the slope of the initial part of the curve are overrated in comparison to the modulus calculated at some stress level. Several modulus values are compared as a function of the dose for the samples aged at 25^0C and 250 kGy, and presented in Fig. 2.9. It could be observed that they all follow similar trends, regardless the value.

Test procedure for outer insulation specimens

The displacement rate applied to the outer insulation specimens was 10 mm/min. Displacement rates from 5 to 50 mm/min were tested and

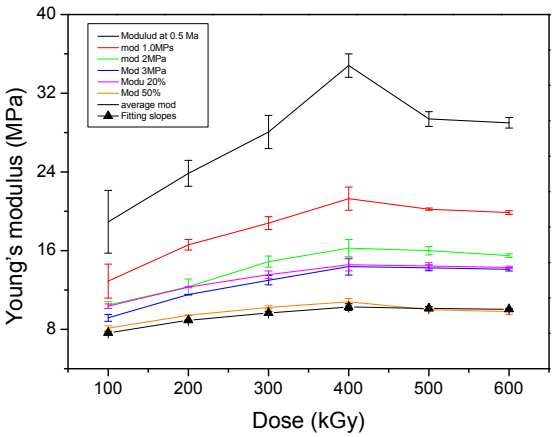

Figure 2.9: *The variation of Young's modulus, defined in various ways, as a function of dose for the outer insulation samples aged at* 25^0C *and 250 kGy.*

no significant influence on the elongation at break and stress level was observed. Still, for the speed of 10 mm/min most of the samples break in the middle of the gauge length. The samples were always clamped at 8 mm from each end of the specimens, (see Fig. 2.10).

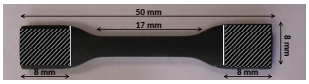

Figure 2.10: *The clamped part of the outer insulation specimen.*

Test procedure for inner insulation specimens

Generally, the sample geometry (dumbbell vs. tubular) is not expected to influence tensile test results [94]. Before actual test procedure was

determined, several testing parameters, like the gauge length (sample clamping length), displacement rate, were changed in order to define the best possible test condition.

Two series of samples were tested with respect to the gauge length. The first one with the samples of 60 mm the gauge length (specimens were clamped on 20 mm from each side) and the second one with the samples that were clamped 30 mm from each side, leaving 40 mm of gauge length. No important influence on the obtained results and data trend was observed, but to ensure that sliding is avoided (minimised), the series with samples having 40 mm of the gauge length (see Fig. 2.11) was chosen for inner insulation, since higher amount of the sample is clamped in that case.

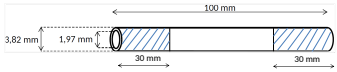

Figure 2.11: *Clamped part of the tubular specimen.*

Tubular samples often tend to break in the vicinity of the clamped part of the sample, where the tubular geometry is lost due to clamping. Several attempts were made to minimise this artefact: inner and outer inserts were placed inside/around the clamped part of the sample and several displacement speeds were used. Placing of the inserts was not practical and it was not helping in all the cases with respect to the sample rigidity. Increasing of the displacement rate to 250 mm/min was found to allow getting fracture inside the gauge length, without affecting the tensile data value. Only the samples that break at least 10 mm away from the clamped part were considered as valid.

The absolute elongation at break was calculated as the crosshead displacement at break divided by non-clamped sample length, which is in the case of tubular samples 40 or 60 mm. The UTS, defined as the force

at the break point divided per initial sample cross-section surface i.e. ∼8,3 mm^2, was calculated.

Optical extensometer development

Total elongation obtained for a sample by uniaxial tensile test, consists of a two components: uniform (before necking) and localized (from the moment when necking begins). For a fixed necking extension, the total elongation will depend on the gauge length. For the shorter gauge length, influence of the localized extensions will be greater. For a very precise determination of deformation with respect to the gauge length (extension of a gauge length and decrease of a gauge diameter) extensometers are used.

For rubbery materials, percentages of elongation are very high (couple of hundreds). Those materials are highly elastic, and after deformation they can return to their previous form easily (no trace of a necking can be noticed). To measure the elongation of a rubbery sample crosshead displacement can be used. It is possible sometimes that a deflection of the machine influences obtained values, but for such high elongation, as in the case of rubbery materials, it should not have important impact. Still, it is very important to avoid slipping of the sample from a gripping system, because that would influence elongation value.

In uniaxial tensile tests performed within this study no extensometer was used. Elongation was measured using crosshead displacement, because contacting type extensometers leave marks on the samples. Attempt is made to develop a system analogue to optical extensometer (non-contacting) to prove validity of the values obtained by using the crosshead displacement.

The test is recorded with the high speed camera, with resolution 2304x1296 px. The gauge length marks were imprinted on the samples, by a white soft marker. In such a case, the gauge length was not equal to the total non-clamped sample length. The initial distance between the marks (the exact gauge length) was precisely measured with an optical microscope. For outer insulation dumbbell samples, the gauge length was about 14

mm. For the inner insulation tubular samples the gauge length was about 20 mm. Change of the initial gauge length with time, during the tensile test was then recorded by the camera, which is schematically presented in Fig. 2.12.

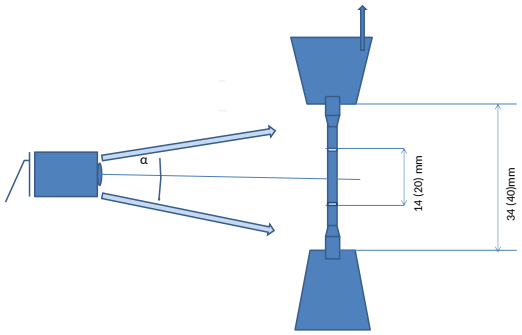

Figure 2.12: *The schematics of optical recording of an tensile test.*

Several time frames were extracted from the video and the distance between marks was measured on the picture (frame) at a given magnification, which is presented in Fig. 2.13.

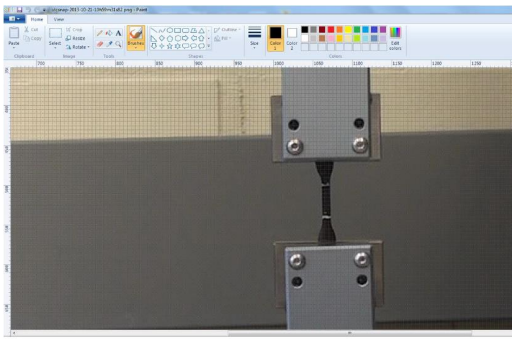

Figure 2.13: *The example of time frame extracted from the video which is covered by the grid system for calculating the distance between the marked points.*

The distance calculated from the time frame is then compared to the value of the crosshead displacement obtained from the machine, for a particular time. For this, the times between the video and the machine data for each tensile test were harmonized. This is done by calculating the time starting form the point of rupture backwards. The example of time calibration/harmonization is given in Table 2.6.

Table 2.6: *The calibration of the tensile test time.*

Video record		Machine
Rupture time: 05:39 (min:s)		Rupture time: 15:11:19 (h:min:s)
Time of the frame	Time between two consecutive frames (t_{delta})	Machine rupture time - (t_{delta})
5:20	19s	15:11:00
4:36	44s	15:10:16
3:58	38s	15:09:38
2:46	72s	15:08:26
1:42	64s	15:07:22
1:18	24s	15:06:58
0:12	66s	15:05:52

The crosshead displacements obtained by the machine and optical extensometer were compared as a function of the time and this is presented in Fig. 2.14. The displacement follows linear dependance as a function of time, which is expected since the deformation rate is constant. It was observed that the displacement obtained by optical measurement deviates from the displacement value obtained by the machine. The deviation increases almost linearly with time. It was assumed that the deviation between displacement values exists because the extension of sample out of the marked length(gauge length) was not included in optically measured data. The additional calculation, that includes the entire sample length between the crossheads, was performed. Indeed, the deviation decreased for this calculation, but it was still present. This was assumed to be the consequence of increasing the angle (see α, Fig. 2.12) between the camera and sample initial position with test time. The distance between marks and the distance between crossheads were calculated on the basis of the initial angle i.e. prior extension, but during the test this angle constantly changes (increases) with time, because the sample is pulled upwards.

It is demonstrated that, by using this optical method, one can always

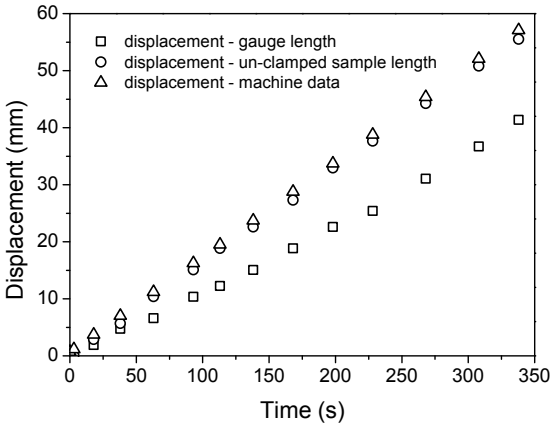

Figure 2.14: *The comparison between displacement versus time curves obtained by the machine and optical extensometer.*

confirm the validity of measurements performed on tensile machine within the error that is a consequence of using optical images that are always different form realistic.

Elongation at break modeling

Accelerated test is a common tool in a reliability studies. In the case of residual life assessment for the I&C cable employed in NPP, accelerated ageing was applied in the mind of exposing the cable samples to temperatures and dose rates that exceed the operational ones. Data obtained from the accelerated experiments are then extrapolated to the service conditions (moderate temperatures and low dose rates) using several methods [29].

Four basic methods of predicting the radiation aging behavior of cable materials have been developed in the last two decades, based on laboratory aging test [1, 29]: the power law extrapolation method, the superposition of time dependent data, the superposition of dose to equivalent damage (DED) data. the kinetic model. The methods differ mainly in the amount of data required for predicting the behavior of cable materials and in the way the test data are extrapolated to the service

conditions. The power law extrapolation method utilizes data obtained at a single temperature over several dose rates. The method based on superposition of time dependent data, also known as time - temperature - dose rate superposition, uses data on elongation at break as a function of time in a range of combined temperature/dose rate conditions. The method uses the superposition principle, which has been used extensively for thermal aging: the data of the elongation against the logarithm of time are superposed, to yield a master curve. The shift parameters required to form this master curve are found to be related to the test temperature and dose rate by a semi-empirical equation which has been verified for a number of cable materials. The method based on superposition of DED data also comes from the time - temperature - dose rate superposition. DED values are reported against dose rate in a log-log plot, and the data are superposed using a shift factor determined by the Arrhenius relationship. All mentioned methods are in details described in IEC Technical report 61244-2 [29] together with application areas, benefits and drawbacks. The kinetic model is based on Dakin's law. where superposition of the data is obtained using equations based on the chemical kinetics of the degradation. The analysis of the different rate constants (radiation, thermal, pressure etc.) allows to draw up a predominance diagram for the material. The main limitation in its wider application is the extensive matrix of test data required [30].

In order to predict a long-term behaviour, the kinetic equation of degradation evolution with time(Eq. 2.4), suggested by Menlow and Dakin [24, 25, 76], is used:

$$\delta e/\delta t = -Ke^{\beta} \tag{2.4}$$

In his work Dakin has demonstrated that it is possible to quantitatively describe the deterioration of the insulation using generalized chemical reaction rate laws, [76].

In Eq. 2.4, e represents a material property whose time variation is correlated to the ageing process of material. In majority of cases, when mechanical parameters are used for insulation ageing prediction, this

property is ultimate elongation at break. K is a pseudo reaction rate-constant, β is the overall order of the degradation process and t is the ageing time.

The elongation at break at $t = 0$ is denoted as e_0. On the basis of β value, the resolutions of Eq. 2.4 follows:

a) $\beta = 0; e/e_o = Kt$

b) $\beta = 1; e/e_o = exp(-Kt)$

c) $\beta \neq 0, \beta \neq 1; e/e_o = (1 + ((\beta - 1)Kt))^{1/(1-\beta)}$

It is assumed that the rate constant K includes Arrhenius (activation) type thermal and irradiative contributions:

$$K = K_{th} e^{(-E_{ath}/(k_b T))} + K_{irr} e^{(-E_{airr}/(k_b T))} \tag{2.5}$$

The E_{ath} and E_{airr} are thermal and irradiative activation energies, respectively. The K_{th} and K_{irr} are pre-exponential factors of thermal and radiative contribution parts, respectively.

This model is used in EDF ageing studies [24, 25] and because of this, it is applied to the experimental results here obtained. It follows similar principe as the "Superposition of time dependant data" method from the IEC Technical report 61244-2 [29].

2.2.2 Indenter modulus (IM)

The indenter modulus within this work was measured in two ways. Using the classical "industrial" procedure the variation of IM with ageing dose and time was determined for the industrial EPDM samples. Additionally, several samples were send to the "Sandia National Laboratories", California, where the modulus profiling was performed by measuring the tensile compliance, which is reciprocal of Young's modulus.

An anvil, moving at a fixed velocity, is pressed into the side wall of the material while the force is monitored. A load cell or similar force-measuring device connected to the anvil monitors the force applied. Once the anvil touches the material, its total travel is normally limited

to a fraction of a mm in order to keep within a range of a reasonably linear proportionality between stress and strain and to avoid permanent effects on the material. The indenter modulus is calculated by dividing the change in force by the change in position during inward travel.

Indenter modulus is measured in a way that while a thin probe goes into the sample, the depth and force of the controlled rate penetration are measured. These values (Force, N â“ depth, mm) are then plotted and the slope of the most linear part of the curve is calculated as IM value, see Fig. 2.15. The term "modulus" typically refers to the modulus of elasticity, defined as the ratio of the increment of unit stress to increment of unit deformation (stress-strain) and is expressed in N/m^2. However, it has become common practice to use the term in relation to the indenter system for describing the ratio of the change in applied force to material deformation, expressed in N/mm [33].

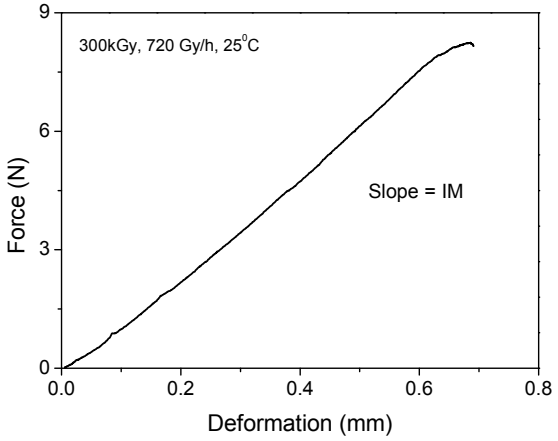

Figure 2.15: *Example of the Indenter Modulus calculation.*

Parts of the indentation instrument are needle (probe, indenter) and clamping system. Within this study the AMS IPAM 4 indenter from ENGIE Laborelec was used (see Fig. 2.16). The clamping system of this machine is made out of aluminium. Tests are performed at room temperature. Speed of the penetration is 5 mm/min and penetration depth was up to 1 mm. Indenter needle is in the conical shape. For the samples that are not perfectly flat (which was the case for the studied

samples, extracted from the real cable) it is recommended to perform the test on side that is more convex because needle - sample surface contact is better on this side, and this recommendation was followed.

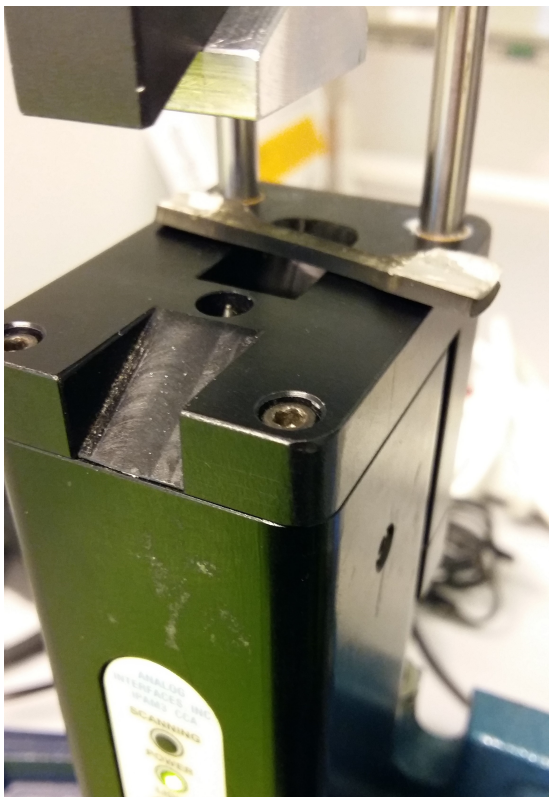

Figure 2.16: *The indenter machine on which tests were performed.*

The indentation was performed on the "head" of each dumbbell sample (see Fig. 3.10), which means that 12 IM values were obtained for one ageing condition (6 samples with two "heads") and the mean value is calculated. In order to perform the measurement on the one wall thickness of the tubular samples, the tubular specimens had to be cut across the length prior measurement. Two measurements were performed on each tube. Because test performance required sample cutting (destruction of the sample) it was performed on two samples per each ageing condition, which gave 4 IM values in total for one ageing condition. The mean value

was then calculated. Due to practical reasons, only few batches of the tubular specimens were tested in order to confirm the trends obtained for dumbbell samples.

The modulus profiling was performed by "Sandia National Laboratories", using the instrument, which is based on modifications of a thermomechanical analyser, which is in detail described [35, 50]. The apparatus measures the indentation of a tiny, paraboloidally-tipped indenter into the sample. Indentation measurements under a chosen load are made at selected locations across the cross-sectioned surface. Pressing of probe onto a sample at time 0 with a small contact mass is followed by the addition of a larger mass at time t_1. The change in penetration occurring between t_1 and $2t_1$ allows calculation of the tensile compliance, which is reciprocal of Young's Modulus. The result is modulus (N/m^2) as a function of the probe position from an outer edge (in mm).

2.2.3 Thermogravimetry

TGA test provides the measurements of sample mass change as a function of the temperature and time, while the sample is heated in a controlled environment. Sample can be heated in a controlled heating rate or weight change can be measured isothermally. Test can be conducted either in nitrogen or in air atmosphere. The experimental record is a thermal curve of some form of weight change (in mass units or in percents) versus time or temperature. Analysis is often extended by calculating the first derivative of mass loss.

TGA was performed on METTLER TOLEDO TGA/SDTA 851e machine, presented on the Fig. 2.17, in nitrogen and air, which flow was 50 ml/min, at the constant heating rate of 20^0C/min in a temperature range between 30^0C - 600^0C. Initial mass of the samples was about 10-15 mg, and the mass loss is presented in percentages. The samples were cut in a way that the total cross-section was measured.

Figure 2.17: *The TGA machine used in this study.*

2.2.4 FTIR

The ATR FTIR was performed on the Nicolet NEXUS 870 with Continuum FTIR Microscope System. The crystal in the system is a silicon crystal (penetration depth 2-6 . From the dumbbell samples, the non-aged sample and the two samples aged at 40^0C and 1390 Gy/h up to the doses of 600 kGy and 800 kGy were tested. Regarding the aged samples, sample surface and bulk were tested in order to attempt to determine the sample heterogenity/homogeneity. From the insulation samples the non-aged sample was tested.

Both types of samples (dumbbell and tubular) were cut transversally (0,5 mm thickness), taped on a glass slide and placed under the instrument microscope, see Fig. 2.18.

The measurements were performed on three spots alongside the samples with an average of 128 spectra at a 16 cm^{-1} resolution.

2.2.5 FTIR coupled with TGA

Experiment where the TGA was coupled with FTIR was performed in order to detect volatile compounds, that are evolving during the TGA decomposition. It was possible to perform this coupling only for TGA under the nitrogen atmosphere. FTIR to TGA coupling was made by connecting the gas-measuring cell of FTIR to the gas flow system of

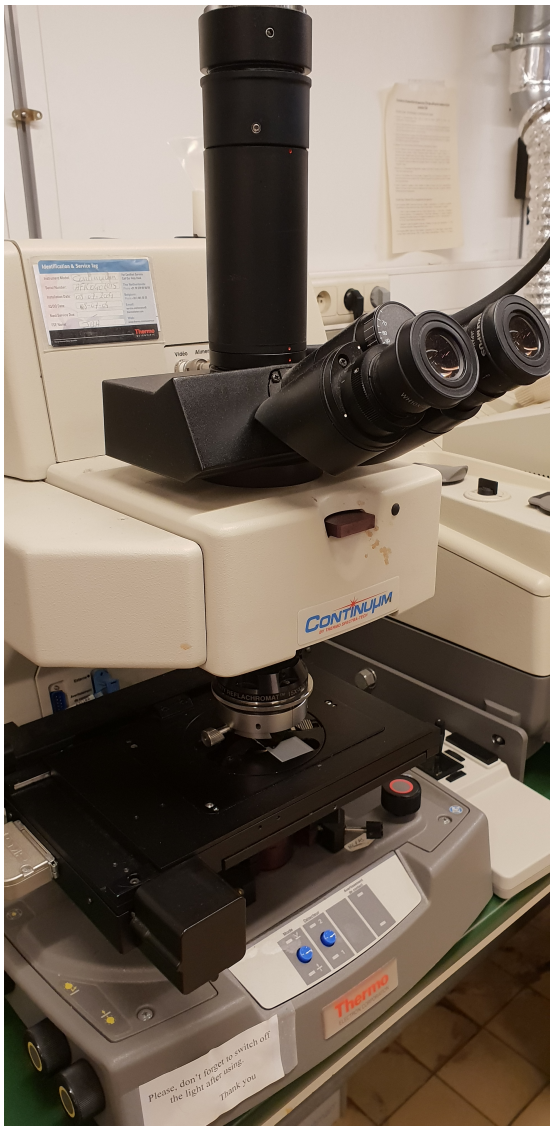

Figure 2.18: *The FTIR machine used in this study.*

the thermobalance. At the end of experiment, the Evolved Gas Profile (EGP) can be constructed from the stored interferograms according to Gram Schmidt [51]. Comparison of the EGP as a function of time with

the TGA and DTG curves is often performed in order to characterize the processes responsible for the mass loss.

2.2.6 Swelling test

The industrial EPDM samples were swollen in xylene following the method C. from ASTM D2766 95 standard [77]. Swelling was done for 48h in boiling xylene (see Fig. 2.19) and samples were dried at 80^0C in vacuum for 24h (see Fig. 2.20).

Figure 2.19: *The Swelling bench used in this study.*

In order to make the evaluation of the swelling parameters involving the surface and bulk contributions, the samples for swelling were made by cutting the sample across the cross-section.

The sample weights were measured before the swelling, then right after swelling they were placed in a tight container to avoid outgassing of the xylene and weighted again. Finally, they were weighted after drying in vacuum. It was assumed that filler does not swell, so the mass of the filler was excluded from the calculation.

The swelling ratio and gel fraction were calculated out of the measured weights using the Equations 2.5 and 2.6 (28.1 and 28.2 in the standard) from the ASTM D2766 95 standard, Method C. [77]

$$Swellratio = [(W_g - W_d)/(W_0 - W_e)]K + 1 \tag{2.6}$$

Figure 2.20: *The oven for drying the swollen sample used in this study.*

$$Gel fraction = 100 - percentextractextract, \% = [(W_s - W_d)/W_0] * 100 \quad (2.7)$$

W_o in the equations is original polymer weight (this weight does not include the weight of the other sample components, except polymer!); W_g is the weight of swollen gel after the immersion period; W_d is the weight of dried gel; W_e is the weight of extract (amount of polymer being extracted from the specimen in the test i.e. $W_s - W_d$, where W_s is the total weight of sample, including additives) and K is the ratio of polymer density to the solvent density at immersion temperature.

2.2.7 Differential Scanning calorimetry(DSC)

DSC technique is based on measurement of difference in the amount of heat required to increase the temperature of a sample and amount of heat required to increase the temperature of a reference, as a function of temperature. It was performed in order to characterise the sample crystalline structure. Heating rate applied was 20 ^0C/min, which is typical for this type of material. The samples were cut in a way that the

total cross-section is included in a measurement. They weighted 10-15 mg.

$$D = \delta H_{sample}/\delta H(PE) \tag{2.8}$$

Heat flux versus temperature curve was obtained as a result of DSC test. Peak related to the crystalline melting process was observed and crystallinity is calculated on the base of melting enthalpy of sample, which was calculated as an integral of the surface below crystalline melting peak. Since only PE part of material can give crystallites in EPDM, the enthalpy of 100 % crystalline PE (290 J/g) was used as a reference enthalpy, see Eq. 2.7.

2.2.8 Dynamic Mechanical Analysis (DMA)

DMA is a technique where a sinusoidal force or stress is applied and resulting sinusoidal deformation or strain is monitored. DMA measures changes in stiffness and dumping, that are reported as modulus (G) and tan delta ($tan\delta$). The strain response lags behind input stress and this lag is known as phase angle, δ. The ratio of the dynamic stress to dynamic strain gives a complex modulus. Complex modulus has two components: storage and loss modulus. Storage modulus measures the elastic properties of sample - stiffness and it describes ability of the material to store energy. Loss modulus is related to the dumping characteristics of the sample and it is related to the heat dissipated by the sample as a result of the material molecular motions. Tan delta is a ratio of the loss and storage modulus. Peaks on tan delta - temperature curve are representing different relaxations of the material. All these values (storage modulus, loss modulus and tan delta) depend on temperature and time, since polymers are viscoelastic materials.

DMA test is performed only on industrial outer insulation samples, on three types of samples: non-aged, aged at 25^0C, 250 Gy/h for dose of 600 kGy and aged at 25^0C, 720 Gy/h for dose of 1100 kGy . A shear stress was applied. The investigated temperature range was from -120^0C

to 75^0C and heating rate 5 ^0C/min. The machine on which test was performed is shown in Fig. 2.21.

Figure 2.21: *The DMA machine used in this study.*

The $tan\delta$ and storage modulus as a function of the temperature were obtained for all tested samples.

Chapter 3

Experimental investigation of the industrial EPDM material

3.1 Introduction

This study addresses the ageing of cable insulating polymer materials, especially ones installed in NPP facilities. Accordingly, the study is focused at the investigation of the industrial EPDM materials. Industrial EPDM is used to name the cable insulation material with EPDM being the main component. The samples are extracted out of cables obtained from the Belgian NPP storage. Two types of samples are created: dumbbells (dog bone samples), which are extracted out of the cable outer insulation - jacket; and tubular, which are extracted out of cable inner insulation. The accelerated ageing of the samples is performed and the mechanical and physicochemical properties after thermal and radiochemical ageing are investigated.

Within this Chapter the results of the industrial EPDM experimental investigation will be presented and discussed. Section 3.2 is devoted to the investigation of the outer cable insulation. The experimental investigation starts with the mechanical tests: tensile and indenter modulus measurement. Afterwards, an empirical model is applied to the elongation at break experimental results. Finally, physicochemical analyses

are performed (TGA, FTIR, TGA coupled with FTIR, swelling, DMA and DSC), in order to analyse the ageing effect at microstructural level. Section 3.2.4 is devoted to the discussion of the results obtained by the experimental investigation. The results of the experimental investigation of the inner insulation are presented in Section 3.3 with the detailed result discussion given in Section 3.3.4. General discussion and conclusions on results for industrial EPDM polymer together with the proposed procedure for cable life-time prediction is presented in Section 3.4

3.2 Experimental investigation of the industrial EPDM material - outer cable insulation

3.2.1 Mechanical properties

Uniaxial tensile tests, as the industrial benchmarking tests, and indenter modulus measurements, as potentially non destructive cable condition monitoring techniques, were performed on the industrial outer sheath samples.

Uniaxial tensile test

The typical nominal (engineering) stress - strain curves of the non-aged and aged EPDM polymer materials are shown in Fig. 3.1. The stress increases monotonously, in a non-linear way, up to the failure point, with a behaviour typical of elastomers. The mean value of elongation at break for the unaged sample is 125.5 $\pm$10 % and the mean value for the ultimate tensile strength is 6.7 $\pm$1.5 MPa. It is already evident from Fig. 3.1 that the strain of aged samples decreases in comparison to the non-aged one.

Using Eq. 2.2 and 2.3, true stress and true strain values were calculated from the experimentally obtained - nominal ones. True stress - true strain curves for the non-aged and several aged samples are presented in Fig. 3.2.

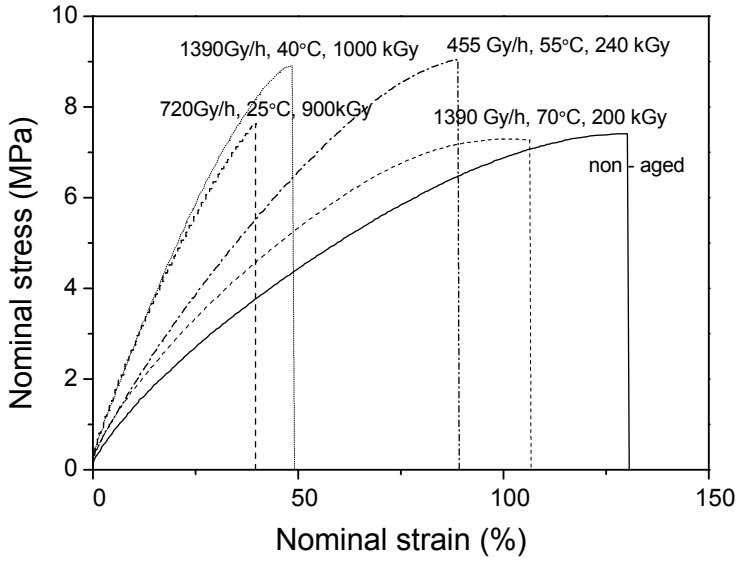

Figure 3.1: *The nominal stress - strain curves of several samples, aged at different temperature and dose rates - outer insulation.*

In Fig. 3.3 the elongation at break data in absolute values are given. The most recent recommendation suggests the use of absolute values for elongation at break data, especially in end of life criterion determination [29]. If the end of life criterion is defined as the point where elongation at break reaches 50 % (and the most frequently it is), then for most polymers used in commercial applications there is a significant difference for the end-of-life point if relative values are used. The decrease of the total elongation as a function of the dose is clearly observed, which is in a good agreement with previous results reported in the literature [24–26]. The reduction of the elongation at break to 50 % is reached at different doses ranging from 200 kGy up to the 1200 kGy depending on the ageing condition. The dose at which the end-of-life criterion is reached is called "dose to equivalent damage" or DED. The estimated approximate DED values for applied ageing conditions are given in Table 3.1 starting from the lowest DED toward higher.

For several batches the end-of-life criterion defined as 50 % absolute

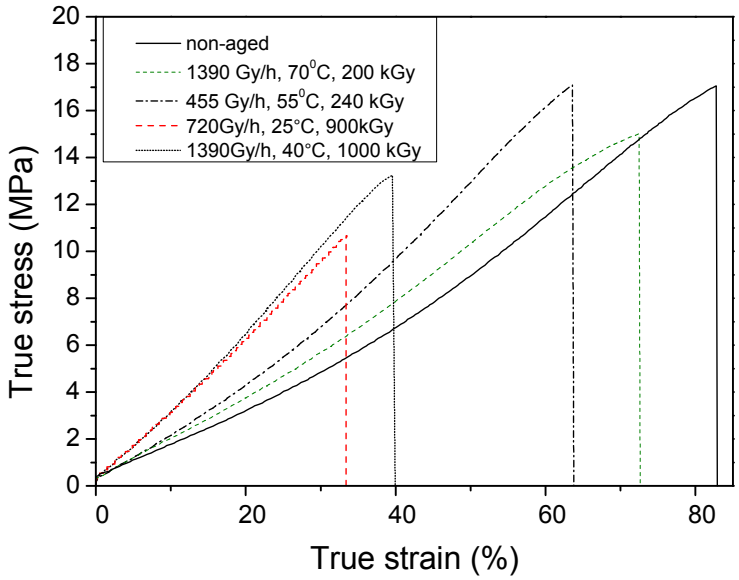

Figure 3.2: *The true stress - true strain curves of several samples, aged at different temperature and dose rates - outer insulation.*

elongation at break, was not reached. The batches aged at 55^0C 106 Gy/h and 70^0C 106 Gy/h, that are both aged up to the dose of 250 kGy, are still away from the threshold value; while the batches aged at 40^0C 1390 Gy/h and 70^0C 1390 Gy/h are almost reaching it, since their elongation drops to about 54% absolute value when they are aged up to the 1000 kGy. It could be observed that the end of life criterion is reached at the lowest doses for samples aged at higher temperatures and lower dose rates i.e. samples aged at 85^0C 106 Gy/h and 85 ^0C 455 Gy/h. Contrary, the samples aged at the highest dose rate within the applied ageing matrix (2760 Gy/h), have much higher DED values.

For dose rate of 2760 Gy/h, the divergence in DED value between the samples aged at 40^0C and 70^0C is very small. Although the samples aged at 1390 Gy/h 40^0C did not reach the end of life criteria, it could be assumed (or even the data extrapolation could be made) that they might reach it for the similar DED as the samples aged at 2760 Gy/h. This could indicate that the DED does not differ much for the samples

Table 3.1: *The estimated DED values for applied ageing conditions.*

Ageing temperature,^0C	Ageing dose rate, Gy/h	DED, kGy
85	106	250
85	455	275
70	455	400
25	250	600
55	455	800
25	720	800
40	2760	1190
70	2760	1200

aged at high dose rates at different temperatures.

From the available data it could be assumed as well that for the samples aged at high temperatures but low dose rates, the DED does not differ much. For the samples aged at 85^0C and the dose rates of 106 Gy/h and 455 Gy/h, the divergence in DED value does not seem to be large, especially in comparison to the samples aged at 25^0C at dose rates of 250 Gy/h and 720 Gy/h.

The elongation at break can be presented as normalized toward the non aged value, see Fig. 3.4, in order to facilitate the comparison with previous studies [24–26]. It can be observed that elongation at break monotonously decreases with increasing dose. Additionally, the decrease of elongation at break by increasing the dose is less pronounced for high dose rates and for low dose rates the reduction of elongation at break seems to be enhanced by ageing at high temperatures. This means that we clearly observe the "dose rate effect" (i.e. the difference in the measured parameter value for the samples aged up to the same dose, but for different dose rates), the potential cause of which will be discussed later.

The evolution of nominal ultimate tensile stress (nUTS) data as a function of the dose for different dose rate and temperature ageing condition is presented in Fig. 3.5 providing additional argument for dose rate effect appearance. The nominal ultimate tensile stress of the EPDM samples, aged at different temperatures at the medium dose rates is shown in Fig. 3.5 a). By increasing the dose, the nUTS first increases and then decreases, exhibiting a local maximum at about 500-600 kGy for the

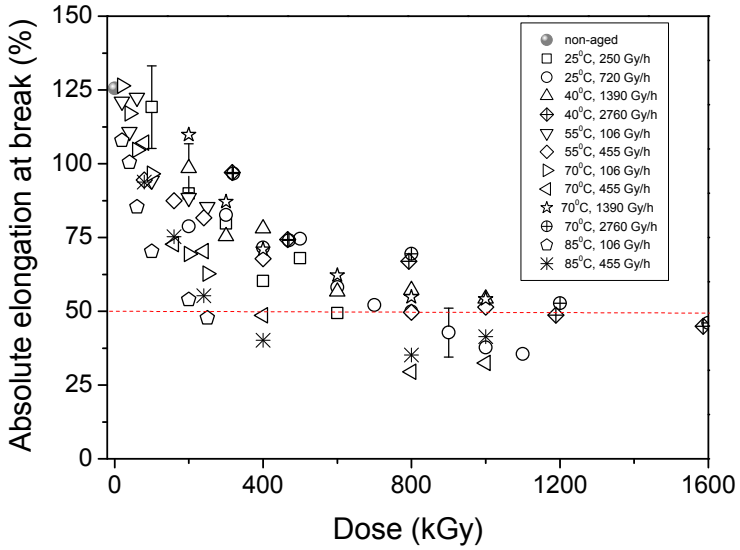

Figure 3.3: *The variation of absolute elongation at break as a function of dose, for different dose rate and temperature ageing conditions - outer insulation.*

temperature of 25^0C. By increasing the ageing temperature the region of nUTS increase is gradually suppressed, and the local maximum is shifted to a lower dose. The nominal ultimate tensile stress of the samples aged at different dose rates, at low and high temperatures is presented in Fig. 3.5 b) and Fig. 3.5 c), respectively. For the samples aged at low temperatures, 25-40^0C, shift of the local maximum to a higher dose, or equivalently the increase of nUTS at high dose with increasing the dose rate, is observed. Similar behavior is observed for the samples aged at high temperatures, 70-85^0C, but for these batches clear increase of the nUTS is observed only for the highest dose rates (1390 Gy/h and 2760 Gy/h).

The variation of the true ultimate tensile stress (tUTS) as a function of dose, for samples aged at similar doses and several temperatures ranging from 25 to 85^0C, is presented in Fig. 3.6 a). In comparison to the tUTS value measured for the non-aged sample, the values of the samples aged at 25^0C do not change gradually at the low doses. Thereafter the tUTS

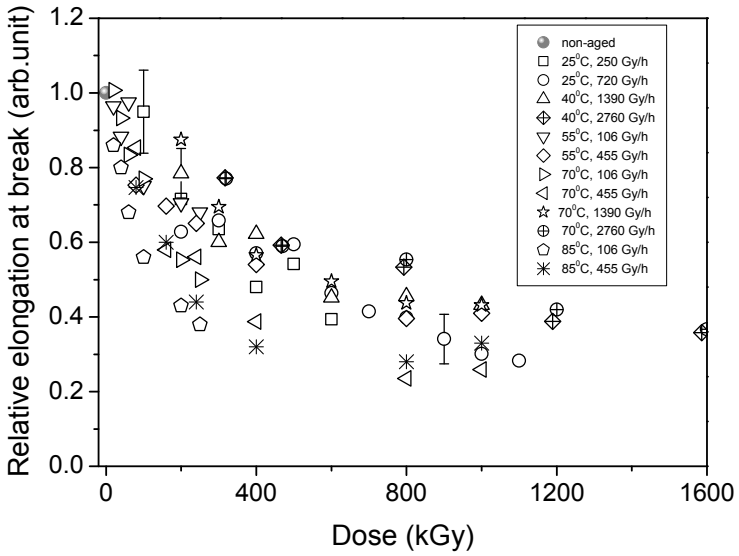

Figure 3.4: *The variation of relative elongation at break as a function of dose, for different dose rate and temperature ageing conditions - outer insulation.*

decreases at the higher doses. Comparing to the evolution of nominal ultimate tensile stress, there the clear increase of nUTS is observed at low doses. For the samples aged up to the same dose, the tUTS value decreases with increasing the ageing temperature, which is in accordance with nUTS data. The true ultimate tensile stress of the samples aged at different dose rates, at low temperatures is presented in Fig. 3.6 b) The initial increase in UTS value, observed at low doses for the nUTS data, is rather moderate for the true ultimate tensile stress data. While the nUTS value of the aged samples never falls below the value of the non-aged sample within the investgated dose range, the tUTS of aged samples at high doses is observed to be below the one of the non-aged. The evolution of the tUTS for the samples aged at the high temperatures (70 and 85^0C) at several dose rates is presented in Fig. 3.6 c). The tUTS of the samples aged at 1390 Gy/h does not vary much in comparison to the non-aged sample, within the investigated dose range. The data for the samples aged at 2760 Gy/h reveal that there is a drop in tUTS

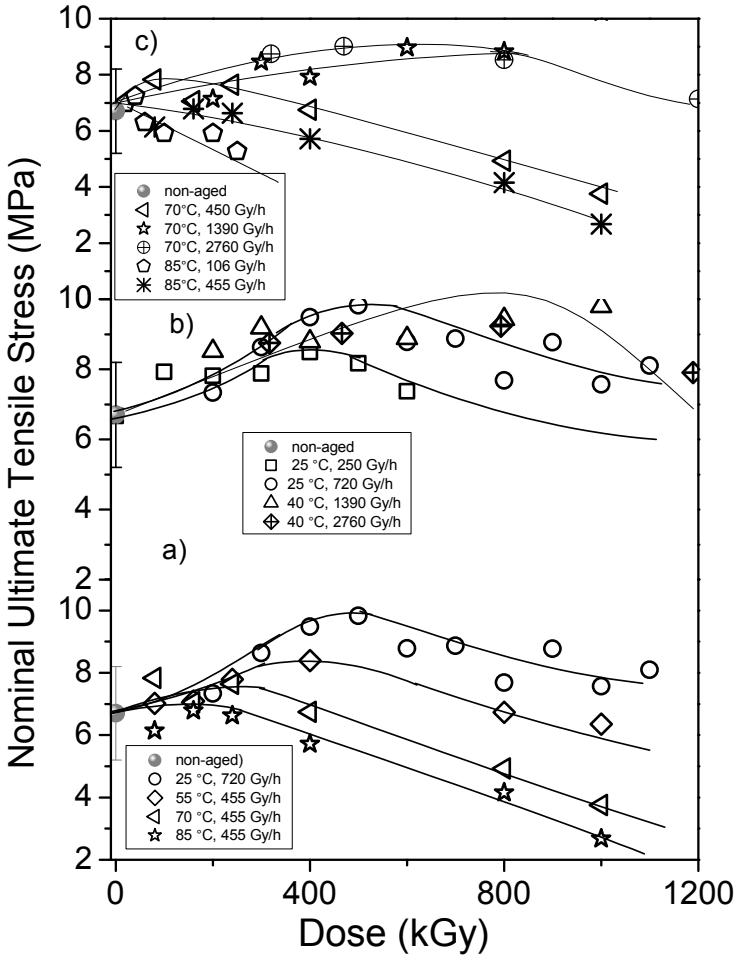

Figure 3.5: *The variation of the nominal ultimate tensile stress with dose at a) different temperatures for middle range of dose rates b) different dose rates in the low temperature range c) different dose rates in the high temperature range - outer insulation. The full line is a guide for an eye.*

value for the samples aged at high dose rates, but it happens at higher dose rates. Specifically for the samples aged at 2760 Gy/h the tUTS decrease can be observed from $\sim$ 1200 kGy, see Fig. 3.7. The rest of

the samples, aged at the high temperatures and at moderate or low dose rates, show dominantly decrease of the tUTS with increasing dose. Within the studied dose range the dose rate effect is observed for the tUTS data in a way that for the samples aged up to the same dose, the tUTS value increases with increasing the dose rate.

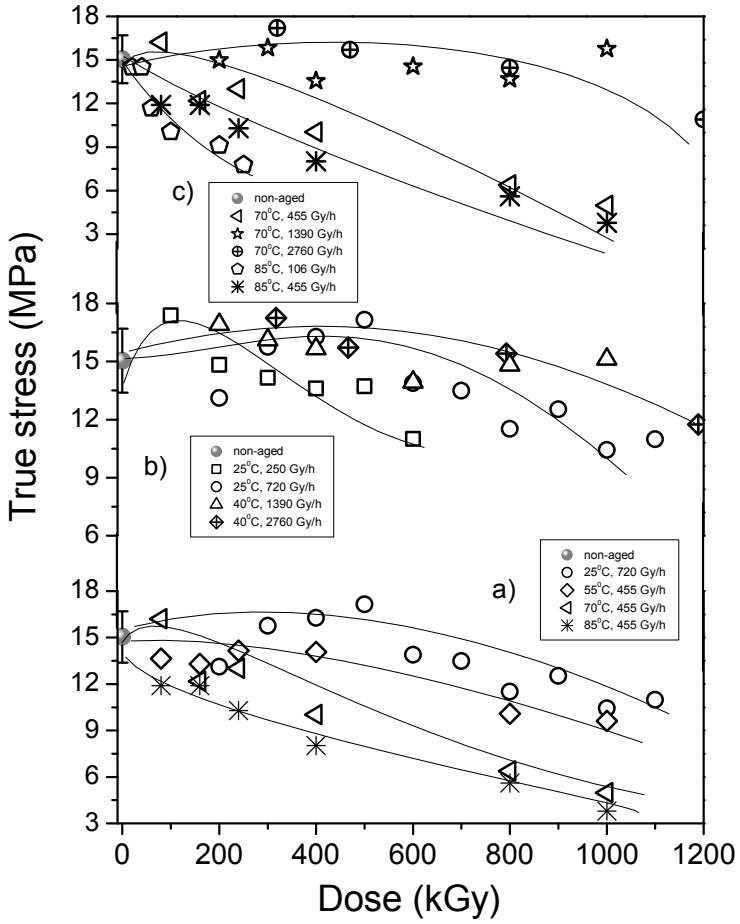

Figure 3.6: *The variation of the true ultimate tensile stress with dose at a) different temperatures for middle range of dose rates b) different dose rates in the low temperature range c) different dose rates in the high temperature range - outer insulation. The full line is a guide for an eye.*

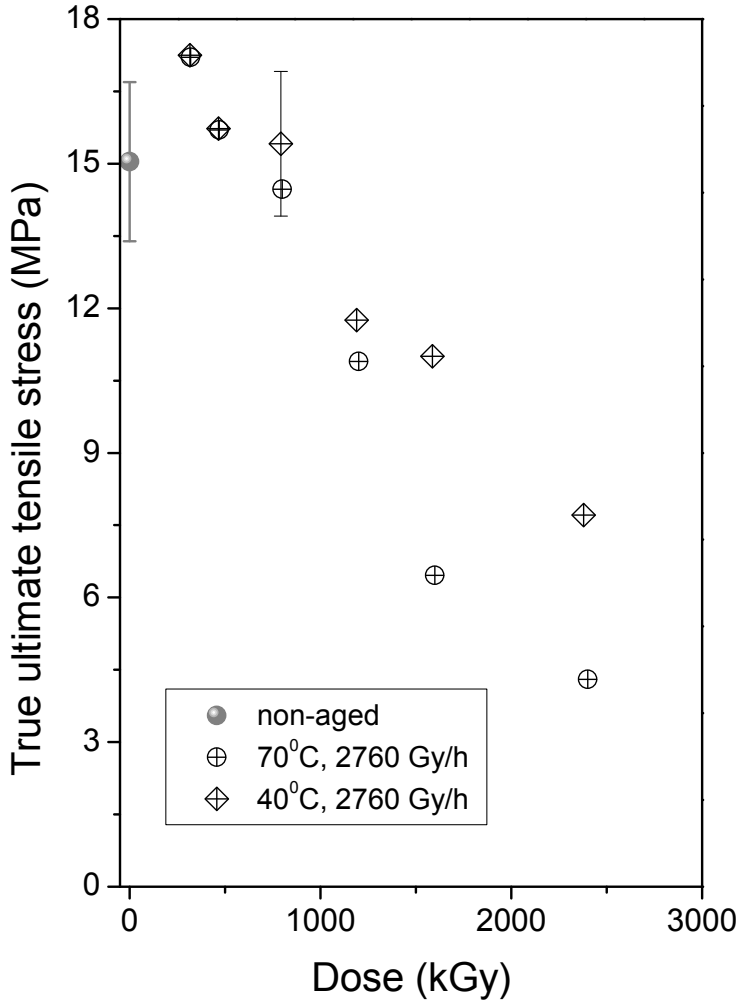

Figure 3.7: *The variation of the true ultimate tensile stress for the samples aged at 2760 Gy/h - outer insulation.*

The Young's modulus can be calculated from the tensile test data. Since the tensile curve of rubbery materials is not linear all to the break point, the slope of the initial linear part was calculated and presented as Young's modulus. For elastomers it is very common to calculate modulus at any point of the curve as the ratio between stress and strain, but this modulus is not Young's sense modulus. These values are named after

the point at which measurement is taken. For example modulus can be calculated at the point where stress is 1 MPa or at the point where strain is 100%. The Young's modulus can be used as an indicator of the sample stiffness and it can be correlated to the concentration of elastically active chains in the case of unfilled, amorphous rubbers [11]. Beside cross-links, chain entanglements are also contributing to the Young's modulus and the exact correlation has been investigated [79, 80]. Moreover, in the case of filled polymer it gets even more trickier to establish the exact contribution. The change of Young's modulus (calculated as a slope of the part of tensile curve up to the stress of 2 MPa) as a function of dose is presented in Fig. 3.8. Fig. 3.8 a) shows the samples aged at high temperatures and various dose rates, 3.8 b) samples aged at low temperatures and various dose rates, while samples aged at the same (middle) dose rate but on various temperatures are presented in Fig. 3.8 c).

Generally, it could be observed that initial increase of the Young's modulus (YM) is followed by a decrease, exhibiting a maximum. Similar behaviour was observed for the ultimate tensile stress data. Contrary to the evolution of the UTS, where decrease of the UTS was dominantly observed for the samples aged at high temperatures already at low doses, clear increase of the YM at low doses is observed for these batches. Interestingly, clear shift of the maximum as a function of dose rate was not observed. What is observed regarding the dose rate effect is the increase in YM for the samples aged at 720 and 1390 Gy/h in comparison to the samples aged at 250 Gy/h, noticed for the samples aged at low temperatures. No important influence of the ageing temperature on the YM variation with dose is observed. Moreover, very often the YM values of some aged up to the same dose are matching. This is the reason why all symbols are not presented in the same size (they often overlap).

Indenter modulus

Non-destructive cable monitoring would be very beneficial and convenient for the industry. In that respect the measurement of indenter modulus provides the possibility for on-site monitoring at outer cable insu-

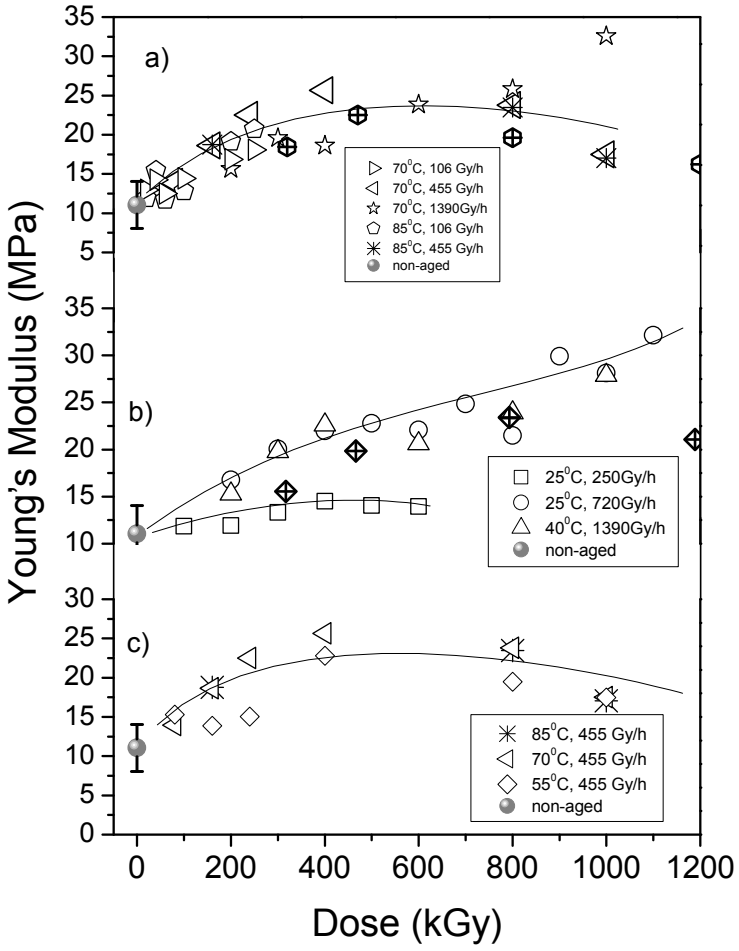

Figure 3.8: *The variation of the Young's modulus with dose at a) different dose rates in the high temperature range b) different dose rates in the low temperature range c) different temperatures for middle range of dose rates - outer insulation. The full line is a guide for an eye.*

lation in the nuclear power plant. Hence the measurements of indenter modulus of industrial outer insulation samples is performed.

The IM values, obtained by measurements performed in ENGIE Labore-

lec are expressed as N/mm, since IM is calculated as the slope of the penetration force versus penetration distance (the ratio of compressive stress to compressive strain below the proportional limit). The change of the IM as a function of time and dose is presented in Figures 3.9 and 3.10, respectively.

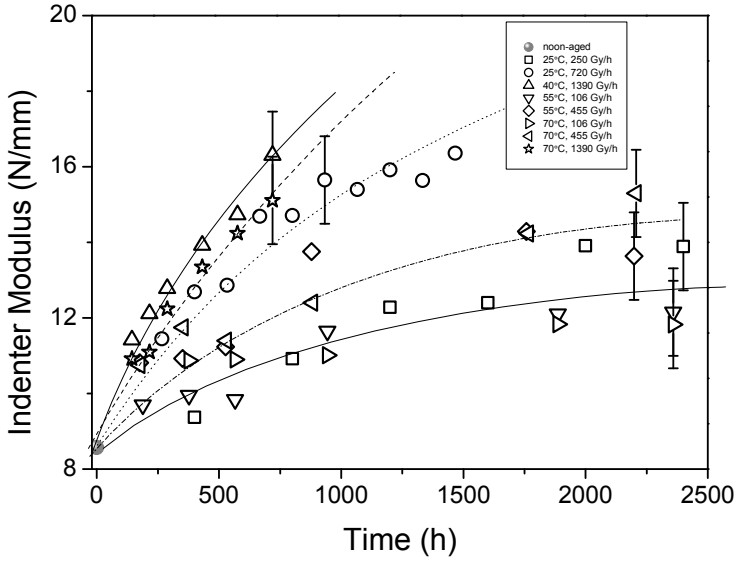

Figure 3.9: *The variation of indenter modulus as a function of the ageing time - outer insulation.*

The constant increase of IM by increasing the ageing time and dose is observed.

Regarding the dose rate effect, it seems to be less pronounced for the IM data, in comparison to the elongation at break data.

Thanks to a collaboration with Sandia National Laboratories, modulus profiling was performed for several selected samples in order to attempt to demonstrate the heterogeneity of the samples. Profiling is done by measuring the tensile compliance at several points across the sample cross section and then calculating the inverse tensile compliance, a quantity that is closely related to the much more commonly measured modulus. IM measured by this test is expressed as N/m^2. These results

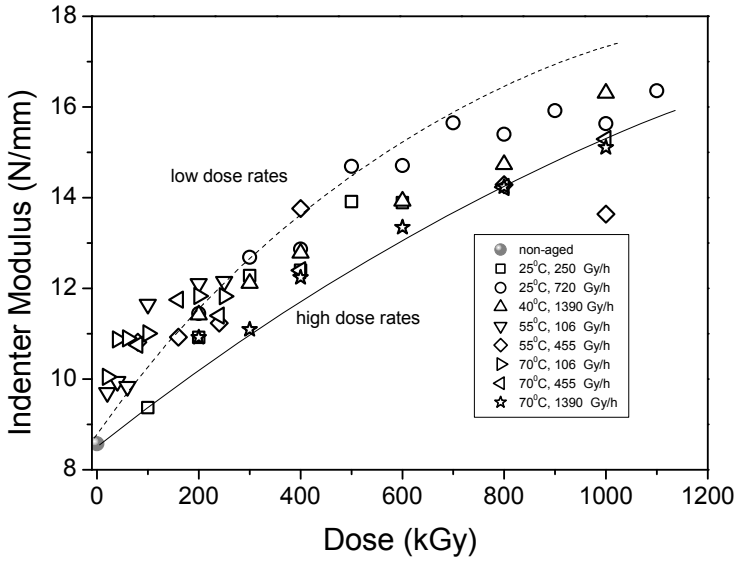

Figure 3.10: *The variation of indenter modulus as a function of the ageing dose - outer insulation.*

are presented in Fig. 3.11.

Samples which were chosen for modulus profiling are aged at the high dose rates 720 Gy/h (25^0C) and 2760 Gy/h (40^0C) up to the high doses 1100 kGy and 1186 kGy, respectively.

The modulus for the non-aged outer insulation sample is observed to be around 5 MPa and it does not change through the sample thickness, which is expected for the sample that has not been exposed to accelerated ageing. Modulus increases for the aged samples in comparison to the non-aged. The modulus change through the cross-section of aged samples could be clearly observed. The modulus increases from the sample edges towards the bulk and there is no significant change of a profile depth as a function of the dose rate.

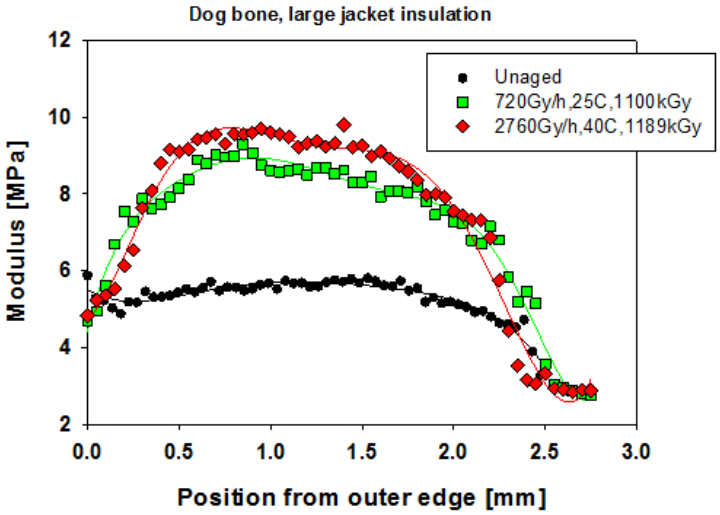

Figure 3.11: *The variation of indenter modulus profile trends for non-aged and several aged samples - outer insulation.*

3.2.2 Elongation at break modeling

Elongation at break are analyzed on the basis of the model developed by Menlow and Dakin [25, 76], which presents the kinetic equation of degradation evolution with time (Eq. 3.1). The formulas used for calculation are presented by the Equations 3.1 and 3.2. e represents the material property whose time variation is correlated to ageing process of the material, which is in this case, relative elongation at break. The K is a pseudo reaction rate-constant, β is the overall order of the degradation process and t is the ageing time.

$$\delta e/\delta t = -Ke^{\beta} \tag{3.1}$$

It is assumed that rate constant K includes Arrhenius (activation) type thermal and irradiative contributions:

$$K = K_{th}e^{(-E_{ath}/(k_bT))} + K_{irr}e^{(-E_{airr}/(k_bT))} \tag{3.2}$$

The E_{ath} and E_{airr} are thermal and irradiative activation energies, respectively. The K_{th} and K_{irr} are pre-exponential factors of thermal and radiative contribution parts, respectively.

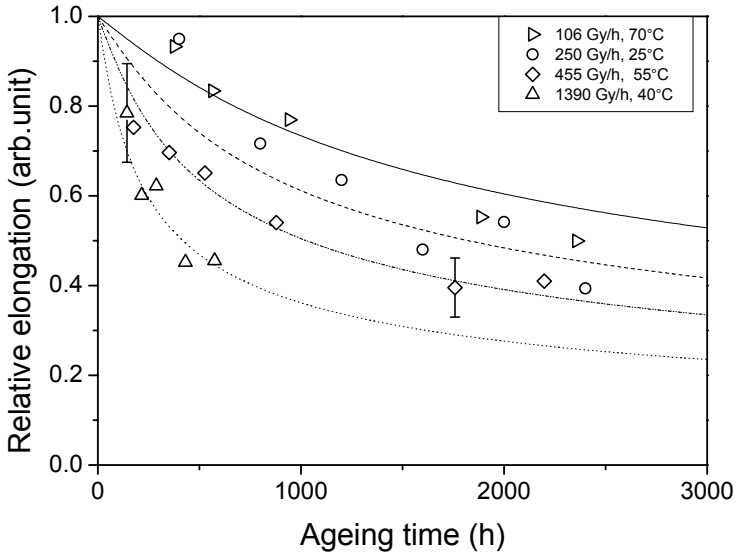

Figure 3.12: *The relative elongation as a function of the ageing time at different dose rates and temperatures - outer insulation.*

The values of the activation energies were obtained by ENGIE Laborelec, from the documentation received by the cable producer. The values of the pre-exponential factors (K_{irr} and K_{th}) and the β parameter were obtained by varying the parameter values to fit the experimental curves. Using the computing program Wolfram Mathematica, the variation of the, experimentally obtained, relative elongation at break with time, was compared to the relative elongation at break data calculated by presented model. This was performed for all investigated ageing conditions. The attempt was made to determine the values of the parameters in a way that general model, that can be used to calculate elongation at break evolution with time for all ageing conditions, is obtained. Fig.

3.12 shows examples of comparison between experimental values and the values calculated using the model, for several batches aged at different dose rates and temperatures.

The relative elongation at break is observed to decrease with time, as expected. The decrease rate increases for the samples aged at high dose rates. This is expected, since a total absorbed dose is reached faster for a higher dose rates (dose fluxes).

Very good agreement between calculated and measured elongation at break data was found. Essentially, all experimental results could be reproduced with Eq. 3.2 by varying one parameter, the pre-exponential factor of the irradiation rate constant, K_{irr}. All other parameters from Eq. 3.2 are kept constant. They are collected in Table 3.2. Both thermal and radiative activation energies, as well as the thermal reaction rate constants were found to be in a very good agreement with previous findings [24], which are also presented in the Table 3.2.

Table 3.2: *The parameters used in the calculation according to the model described by Equation 3.2. - outer insulation*

Parameter	Value	Value [24]
E_{ath}	1.07 eV	0.954 eV
K_{th}	50×10^9 h^{-1}	2.08×10^9 h^{-1}
E_{airr}	0.065 eV	0.043 - 0.087 eV
β	3.5	5 or 10

A single value for β parameter of 3.2 was obtained, ensuring the applicability of the model and indicating that single process is responsible for the change of elongation at break. Evidently, in the context of the present model, the decrease of the relative elongation is governed by the radiative term. All relative elongation values follow similar behaviour, irrespective of the irradiation temperature and dose rates.

3.2.3 Physicochemical properties

Thermogravimetry

The typical mass loss curves as a function of the temperature of non-aged and aged polymers were obtained by the TGA tests performed in air and under nitrogen atmosphere, see Fig. 3.13 a) and 3.13 b), respectively. The sample mass decreases as a result of the thermal decomposition at high temperatures ($> 250^0C$). This proceeds by the release of mainly carbon dioxide, water, and small organic parts. The mass loss is monotonous, with two major step decompositions. The first decomposition step begins at about 250^0C with the maximum weight loss at 350^0C. According to the literature, the first decomposition step can be associated with acetic acid evaporation from EVA polymer component [100–102], and/or with the decomposition of ATH (fire retardant filler) [100, 101]. The ATH decomposes by forming alumina and water vapor. The mass loss during the first decomposition step is of about 20% which corresponds to the sum of mass percents of water parts from ATH and acetate parts from EVA (in agreement with the polymer composition). The second decomposition step occurs at about 430^0C and 480^0C, when the TGA is performed under air and nitrogen atmosphere, respectively. The polymer mass loss during the second decomposition stage can be associated to the polyolefinic main chain scission / decomposition of polymer macromolecules. The decomposition in air occurs at a lower temperature in comparison with the decomposition in nitrogen, because the polymer decomposition path via peroxide decomposition requires lower activation energy [103] in comparison with random chain scission polymer decomposition which occurs under the nitrogen atmosphere.

Interestingly, the polymer decomposition temperature profile, measured by the TGA in air, gradually shifts towards the high temperatures with increasing the irradiation dose, see Fig. 3.13 a). For the dose higher than about 800 kGy, the polymer decomposition profile in air can not be distinguished from that in nitrogen. On the contrary, the decomposition of aged EPDM under the nitrogen atmosphere shows no change as a function of the dose (Fig. 3.13 b)). For the dose up to 800 kGy, the

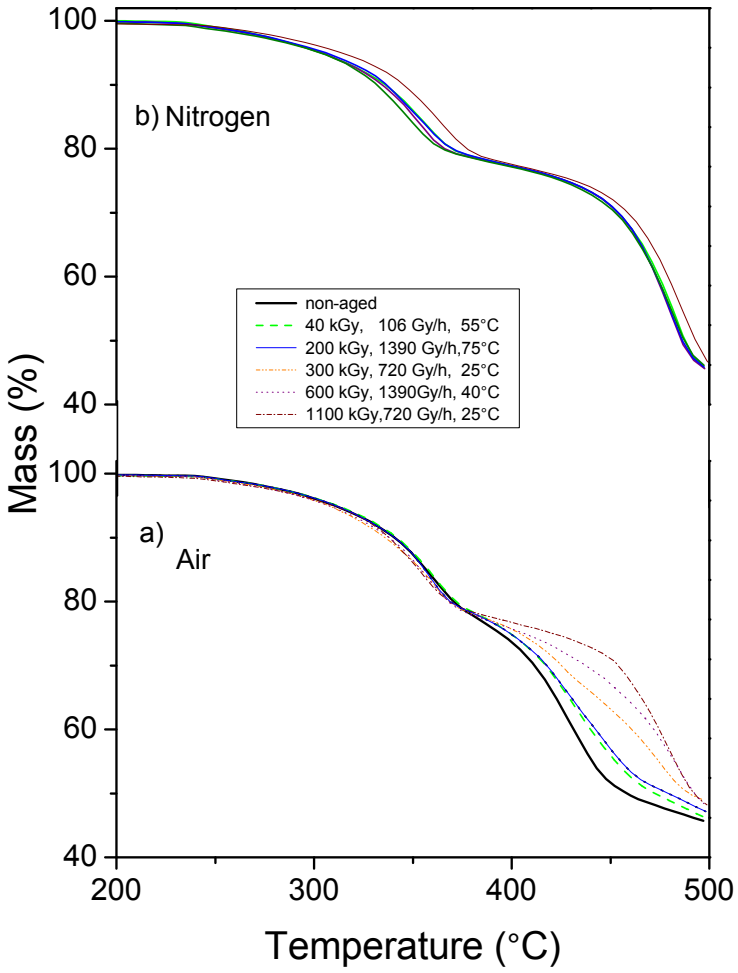

Figure 3.13: *Thermogravimetry curves of non-aged and aged samples under nitrogen and air atmosphere - outer insulation.*

polymer decomposition exhibits complex, multistage profile, which is further analyzed on the basis of the first derivative thermogravmetry (DTG) curves (derivative of the mass loss).

The DTG curves measured under the air atmosphere of the non-aged and aged polymer, for various doses and dose rates, aged at 25^0C and 70 ^0C are presented in Fig. 3.14 a) and b), respectively. As expected, the

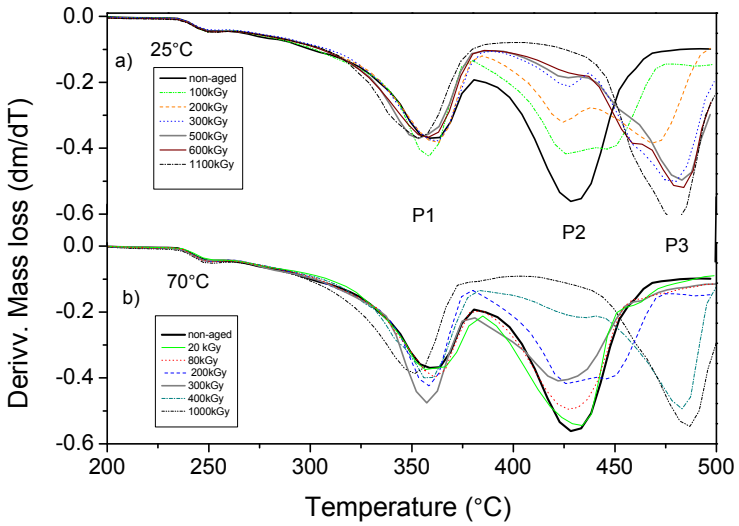

Figure 3.14: *The derivative of the mass loss measured in air for the EPDM samples irradiated at 25 ^0C and 70 ^0C at various dose rates - outer insulation.*

DTG curves exhibit peaks (defined as the minimum of derivative curve) at the temperatures which correspond to the maximum decomposition rate of the TGA decomposition stages discussed in the previous paragraph. The integrated intensities of the peaks can be correlated to the total mass loss during the decomposition stages. Three peaks have been observed at about 350^0C, 430^0C, and 480^0C, and enumerated as P1, P2, and P3, respectively. The P1 peak at 350^0C corresponds to the first decomposition stage, while the P2 and P3 peaks are associated to the second decomposition stage. Remarkably, by increasing the dose, the P2 and P3 intensities dramatically change in the way that the P3 intensity increases at the expense of the P2 peak decrease. In addition, the P2 and P3 peak position slightly increase in temperature by increasing the dose.

FTIR

FTIR spectroscopy is a main method for characterization and quantification of chemical groups [51]. Carbonyl and hydroxyl chemical species are known to be the main products of polymer oxidation. FTIR is then often used to quantify changes in the presence of these groups in aged material with respect to the non-aged material in order to detect extent of oxidation. Normally, this is a simple procedure to perform for neat polymers. More complex situation is to apply FTIR for industrial samples, especially when these samples contain carbon black, which is the case for the industrial samples studied within this thesis. Still, detection of chemical groups may contribute to the characterization of the sample chemical composition and it was performed. When samples are carbon filled, ATR (attenuated total reflectance) infra red is one of the ways to perform IR analysis on them. Carbon black is a strong absorber of IR radiation. It raises the refractive index of the sample, and simply reduces the amount of sample available for examination. Additionally, many overlaps of the peaks could be expected since the industrial samples are very complex regarding the composition. The average of three obtained spectra of non-aged dumbbell samples is presented in Fig. 3.15.

The absorptions at 3700 - 3260 cm^{-1} and the peaks from 1100-650 cm^{-1} can be attributed to the ATH [84–86]. The four peaks around 3450 cm^{-1} are related to the stretching of OH groups. The two peaks at 2915 cm^{-1} and 2850 cm^{-1} are related to the stretching vibrations of C-H bond from $-CH_2$ groups, so the two could be related to both EPDM and EVA polymer. The peak at 1740 cm^{-1} is specifically related to the EVA polymer since it it attributed to the stretching of carbonyl group from vinyl acetate. The scissoring vibration of C-H bond from $-CH_2$ groups is attributed to the peak at 1466 cm^{-1} and stretching of the C-H from $-CH_3$ to the peak at 1372 cm^{-1}. The peak at 1,241 cm^{-1} is present due to vibration of C-O-C group from EVA. The peak at 1560 cm^{-1} could indicate presence of an amino type antioxidant, although peak in this area might be an absorption of aromatic double bond, or C-O from carboxylates. The C-O stretching vibration, that can be related to

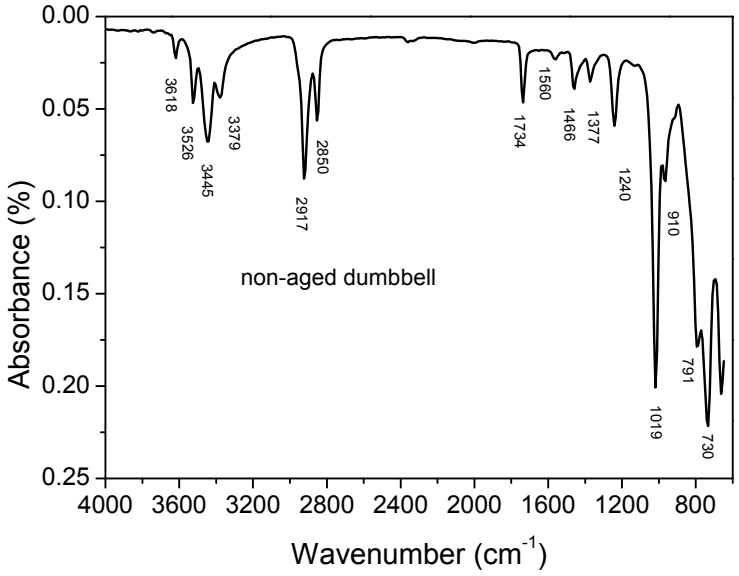

Figure 3.15: *The ATR-FTIR spectrum of non-aged industrial EPDM sample - outer insulation.*

the EVA is observed as absorption peak at 1019 cm^{-1}. Still, this peak together with the peaks at the lower wavenumbers i.e. 1019-600 cm^{-1} appear at the ATH spectrum. [84, 87].

The FTIR spectrum of non aged outer insulation sample demonstrates that the main components of the cable jacket are EPDM, EVA and ATH. In order to attempt to distinguish spectrum of non-aged versus aged sample and observe changes in sample chemistry resulted from ageing, the FTIR of aged samples is performed as well. In Fig. 3.16 the spectrum of non-aged outer insulation is compared to the spectra of the samples aged at 1390 Gy/h, 40^0C, up to the 600 kGy and 1390 Gy/h, 40^0C, up to the 800 kGy.

No important variation between the spectra was observed, except that in the area around 1630 cm^{-1}, which is domain of carbonyl family, the new peak seems to be formed, which is the most obvious for the sample aged at 800 kGy. An absorption peak about 1630 cm^{-1} is also characteristic of water, but water exhibit an broad -OH band, that is by far more intense

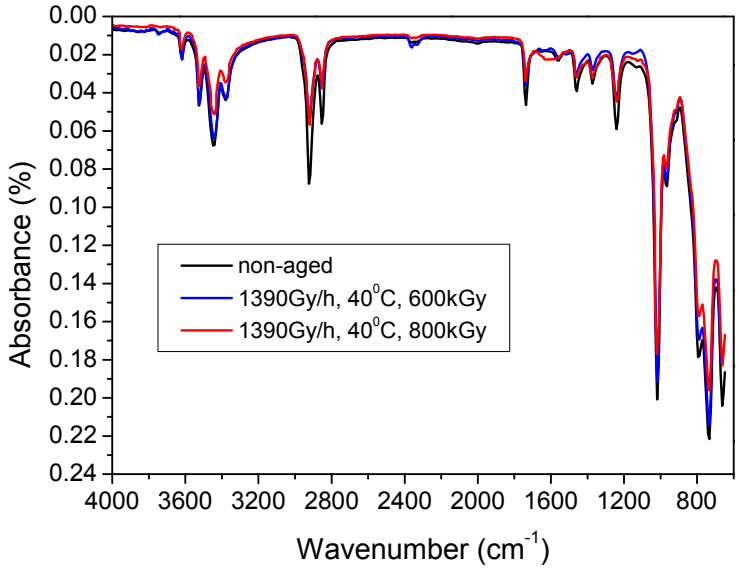

Figure 3.16: *The comparison of ATR-FTIR spectra of non-aged and aged industrial EPDM samples - outer insulation.*

than the peak at 1630 cm^{-1}, which is not clearly observed in this case. Thus, the 1630 cm^{-1} peak could be an indication of the formation of oxidation products. Still, more clear indication of the oxidation is not observed.

FTIR can be also used as mapping or profiling technique. The FTIR spectrum of the sample surface can be compared to the FTIR of the sample bulk, and possible differences might indicate sample heterogeneity. In the case of sample inhomogeneity due do the DLO it is expected to observe stronger absorption peaks in area of carbonyl and hydroxyl groups, which are the main oxidation products, at the sample surface in comparison to the sample bulk. The comparison of surface and bulk spectrum was done for the samples aged at 1390 Gy/h, 40^0C, up to the 600 kGy and 1390 Gy/h, 40^0C, up to the 800 kGy and it is presented in Fig. 3.17 a) and b), respectively.

The absorbances at 2915cm^{-1} and 2850cm^{-1} are taken as a reference, and the bulk versus surface spectra were quantified and compared ac-

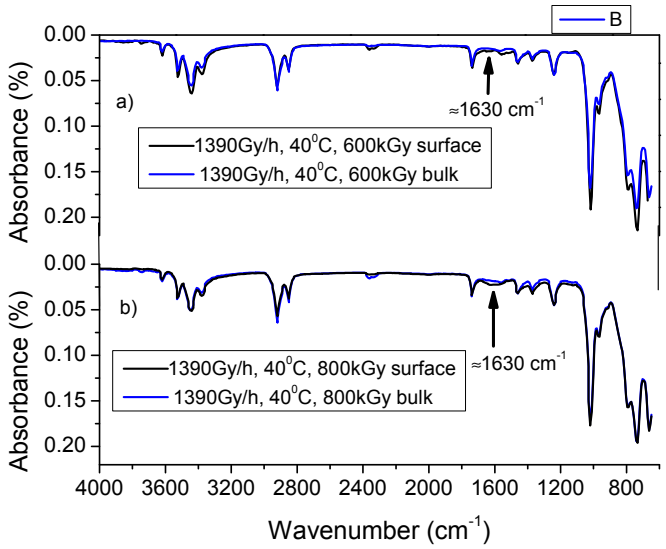

Figure 3.17: *The comparison of ATR-FTIR surface and bulk spectra of non-aged industrial EPDM samples - outer insulation: a) sample aged at 1390Gy/h and 40^0C up to the 600kGy; b)sample aged at 1390Gy/h and 40^0C up to the 800kGy .*

cording to these peaks, which are correlated to the $-CH_2$. For the sample aged at 1390Gy/h, 40^0C, up to the 600kGy (Fig. 3.17 a)) the increased absorbance was observed for the sample surface in the O-H and ATH area, together with the appearance of the peak in carbonyl area, at 1630 cm^{-1}. This could be an indicator of the increased oxidation of the surface in comparison to the sample bulk, but it is also possible that distribution of the $Al(OH)_3$ is not quite homogeneous through the sample. The same was observed in the case of the sample aged up to the 800 kGy, see Fig. 3.17 b). Indeed, due to this observations, it could be assumed that there is a difference in the oxidation extent at the sample surface and in the sample bulk and it could be related to the DLO during the ageing.

FTIR coupled with TGA

In order to analyse and characterise volatile compounds during the TGA test TGA was coupled with FTIR. Principle of this coupling is explained in Section 2.2.5. It was only possible to couple the two techniques when TGA is performed under nitrogen. The aim is to analyse the volatile products, that are evolving during TGA thermal decomposition, via FTIR. As a final result Evolved Gas Profile (EGP) can be constructed and comparison of EGP as a function of time with TGA and DTG curve can be done. The zero at the time axis is adjusted to the 0^0C point at the temperature scale, and the heating rate was 20^0C/min .

The intensity of the absorption between 3200 and 3800 cm^{-1} as a function of the time is presented in Fig. 3.18 a). These peaks can be correlated to the -OH species, mainly from the ATH, which gives water during its decomposition. The distribution of the evaporation indicates that the decomposition of ATH takes place at about 350 ^{0}C (17.5 min), as it was assumed after the TGA test. The intensity of the absorptions between 2750 and 3100 cm^{-1} which are attributed to the aliphatic chain parts are presented in Fig. 3.18 b). The peak can be observed between 400 and 600^0C, with the maximum at the 480 ^{0}C. This might indicate at which temperatures the break of the aliphatic chains is the most intensive.

The absorptions of the spectra between 2200-2450 cm^{-1} is attributed to the CO_2 and the distribution of its intensity is presented in Fig. 3.18 c). Several peaks are observed on the GEP versus time graph. The first one is positioned at 12.5 min ($\sim 250^0$C), and it can be observed only for aged samples, not for the non-aged ones. The second peak is positioned at 16.5 min or approximately 330^0C. The third one, with the highest intensity, is observed at 440^0C for non-aged sample and 450^0C for the aged ones. Carbonyl group characteristic peaks are observed at wavelengths between 1600 and 1800 cm^{-1} and the distribution of the evaporation of carbonyl species is presented in Figure 3.18 d). The high intensity peak can be observed at about 350^0C (17.5 min), and it can be correlated to the evaporation of acetic acid from EVA. The second peak is positioned at about 475^0C.

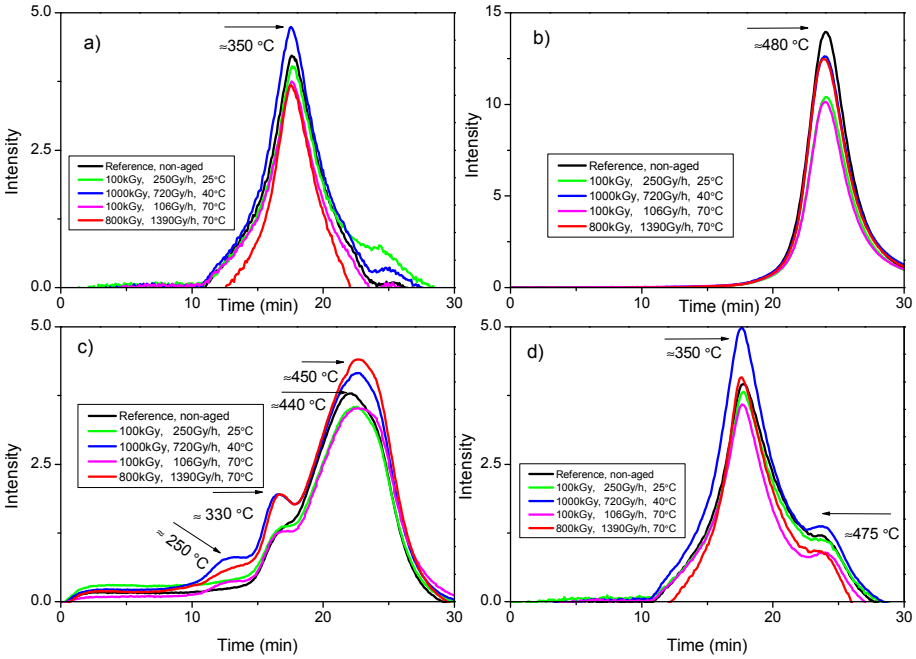

Figure 3.18: *The distribution of spectra intensity for specified wave lengths as a function of time: a) -OH species; b) aliphatic chain parts; c) CO_2; d)carbonyl species.*

According to the FTIR-TGA experimental results it could be confirmed that the thermal decompositions of the ATH and EVA are taking place at about 350^0C, while the macromolecular chains seem to decompose at temperatures between 400-600^0C, with the maximum decomposition rate at about 480^0C.

Swelling measurement

The effects of ageing on EPDM polymers were also analysed by swelling measurements. The measurement of the swelling ratio can help to monitor the changes of soluble and insoluble parts of aged EPDM in xylene. Higher values of swelling ratio indicate lower degree of cross-linking i.e. high molecular weights between the cross-links (lower network chain

density). Gel fraction and sol fraction parameters are indicators of unsoluble (crosslinked) and soluble (non-crosslinked chains) fraction of the polymer matrix. It was assumed that filler does not swell, so the calculation is made only for the polymer part of the industrially formulated samples. In Fig. 3.19. the change of swelling ratio as a function of dose for non-aged and several samples aged at: 25^0C, 250 Gy/h; 25^0C, 720 Gy/h; 80^0C, 106 Gy/h, is presented.

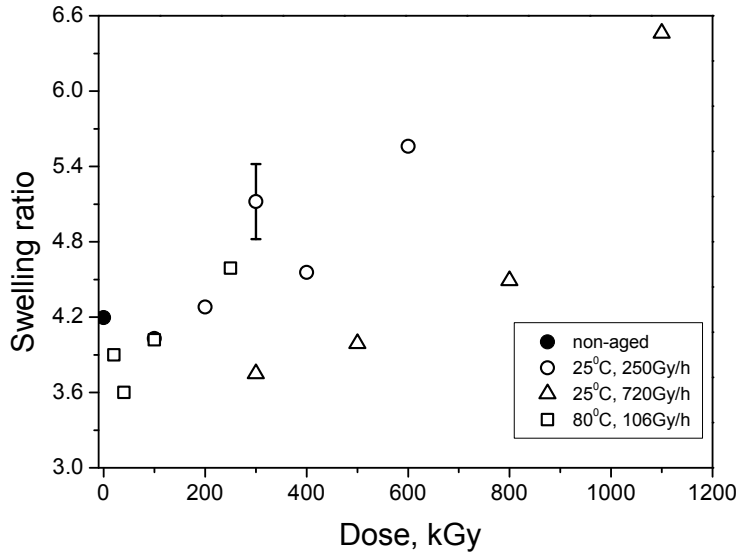

Figure 3.19: *The variation of swelling ratio as a function of dose for non-aged and several aged industrial EPDM samples - outer insulation.*

In comparison to the swelling ratio of non-aged samples, the swelling ratio of aged samples first decreases and then increases. Accordingly, it can be assumed that at the beginning of the ageing network chain density increases and then it decreases. Interestingly, the dose rate effect can be observed, in a way that the swelling ratio increase is becoming slower with increasing the ageing dose rate.

The evolution of gel fraction parameter with increasing dose is presented in Fig. 3.20:

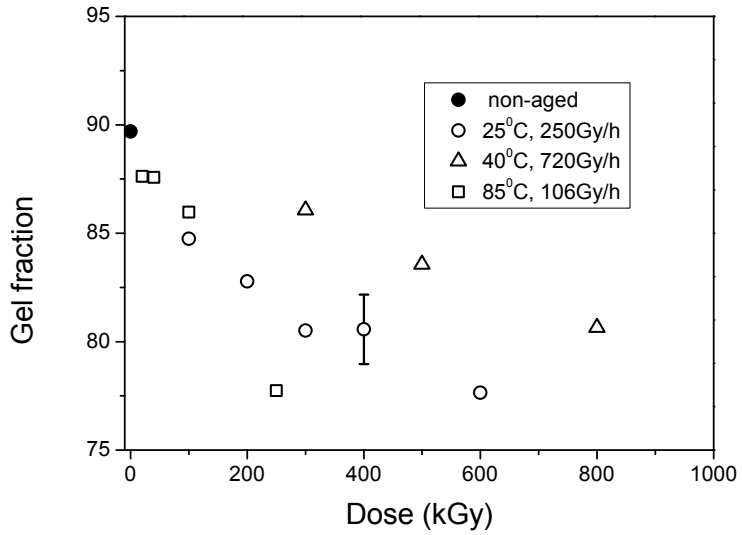

Figure 3.20: *The variation of gel fraction as a function of dose for non-aged and several aged industrial EPDM samples - outer insulation.*

The gel fraction value of non-aged sample is around 90% which could indicate that most of the network of non-aged sample seem to be cross-linked. For all aged samples a decrease of the gel fraction is observed, indicating a decrease in insoluble fraction with increasing the dose. The faster decrease of gel fraction for the samples aged at the low dose rates in comparison to the ones aged at the high dose rate can be observed.

Differential Scanning Calorimetry

DSC measurement is a way to determine the glass transition and melting transition (Tm) point of polymer material, as well as the percent of crystallinity for semi-crystalline materials. The DSC was performed on the samples aged at 25^0C, for the dose rates of 250 Gy/h and 720 Gy/h and the heat flow-temperature curves are presented in Fig. 3.21.

The calculated percent of crystallinity is very low 0.6 %, which was expected. EPDM is generally made as an amorphous material rather

than semi-crystalline, but exceptions are possible. The second matrix polymer in studied industrial samples is EVA, which crystallinity may vary, but when used in cable insulation purposes it is designed to be lower, so that material exhibits rubber-like behavior. Lower crystallinity of EVA is achieved by increasing VA concentration, since it hinders tendency of PE chains to align.

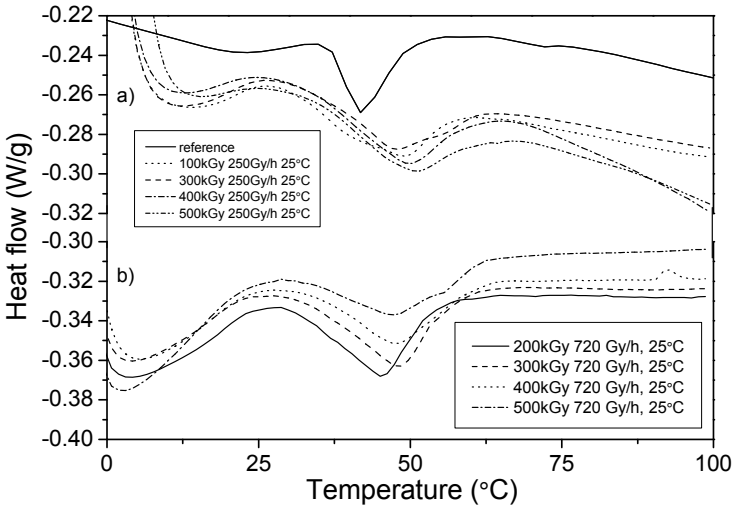

Figure 3.21: *The DSC curves of industrial EPDM samples - outer insulation a) non-aged sample and samples aged at* 25^0C*, 250 Gy/h b) samples aged at* 25^0C*, 720 Gy/h.*

The Tm of non-aged sample is found to be around 42^0C and it seems to increase with increasing ageing dose. Regarding the evolution of percent of crystallinity as a function of dose, no regular behaviour was observed. The value varies for different samples, and it goes from 0.4 up to the 0.99 %. The increase of Tm might indicate that slightly thicker crystallites are formed with ageing, probably due to some polymer fragments rearrangements. It must be noted that the DSC is performed on samples which were aged at 25^0C, so the crystalline structure was probably in majority preserved during the ageing, while for the other samples, which were aged at higher temperatures it can be assumed that the crystalline structure was melted during the ageing process and recrystallised after

the accelerated ageing was done. Still, the percent of crystallinity is very small, so the obtained trends are questionable and the samples might be considered as amorphous.

Dynamic Mechanical Analysis

DMA test is used to monitor relaxation behaviour and elastic modulus variation, which are expected to change with polymer ageing as a consequence of change in polymer macromolecular structure [54–56]. DMA has potential as low destructive technique that can monitor changes on microstructural level.

Fig. 3.22 presents the evolution of dumping ($tan\delta$) and storage modulus of non-aged sample and two samples aged at 25^0C at the dose rate of 250 kGy/h up to the total absorbed dose of 600 kGy and at the dose rate of the 720 Gy/h up to the 1100 kGy.

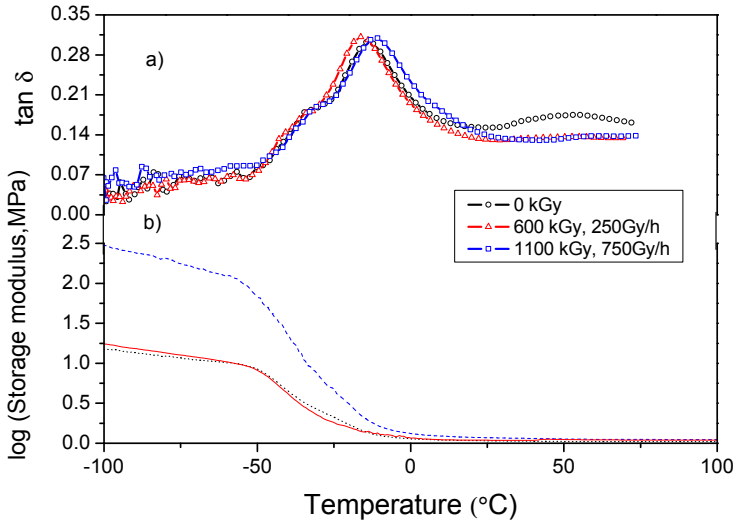

Figure 3.22: *The evolution of a)dumping and b)storage modulus with temperature of non-aged and several aged industrial EPDM samples - outer insulation.*

Three peaks can be observed on the tan δ versus temperature curves.

Each peak is assigned to a different relaxation process in the material. Changes in peak amplitude and position (temperature) are monitored. The most obvious peak is assigned to the glass transition process of the EPDM [54]. For the non-aged sample position of the peak associated with glass transition is at about -14.4^0C. Small shoulder-like peak can be observed at about -35^0C. It could be also attributed to the glass transition of EVA containing sequences. Third peak appears at about 50^0C, and it is linked to the crystalline melting peak, which is also in agreement with DSC measurement. Shoulder-like peak (P_1) seems to be the same for all three samples, but the glass-transition peak (P_2) exhibits a little change as a function of temperature. For the sample aged at 250 Gy/h up to the 600 kGy it is shifted toward left and for the sample aged at 720 Gy/h up to the dose of 1100 kGy it is shifted toward right in comparison to the non-aged sample. The third peak, related to the crystalline structure, is very lightly observed for the aged samples.

Regarding the storage modulus, it does not change considerably for the sample aged up to the 600 kGy, in comparison to the non-aged sample. But the storage modulus of the sample aged up to the 100 kGy clearly increases.

3.2.4 General discussion on the experimental investigation results of the industrial EPDM - outer cable insulation

Within this section, behaviour of the outer layer of the industrial cable, with thermal and radiative ageing, will be discussed, on the basis of mechanical and physico-chemical experimental investigation. The application of the condition monitoring techniques, used to investigate non-aged and aged samples, will be also discussed.

Mechanical properties

The variation of the uniaxial tensile elongation at break with ageing is investigated, as it is the most used criterion, within the mechanical properties, for assessing the state of the NPP cable insulation, see Section 3.1.1. The elongation at break is observed to decrease as a function

of the ageing dose, as expected. Elongation at break usually decreases gradually with insulation polymer degradation induced thermally, by radiation or by both ageing factors [19, 21, 24–28, 74]. Additionally, the decrease of elongation at break by increasing the dose is observed to be less pronounced for the high dose rates and for the low dose rates the reduction of elongation at break seems to be enhanced by ageing at high temperatures.

One can observe that the ageing conditions (dose rate and temperature) cause the difference in elongation at break evolution with ageing dose. The investigated mechanical property is observed to differ for samples aged up to the same dose, for different dose rates, which is defined as the "dose rate" effect. This can be analysed using the dose to equivalent damage (DED), which is observed to differ for samples aged under different ageing conditions, see Table 3.1. For the samples aged at lower dose rates and high temperatures, the DED are observed to be the lowest, while for the samples aged at the highest dose rate (2760 Gy/h), the DED are observed to be higher. Moreover, judging by the low divergence between the DED values for the samples aged at the high dose rates and different temperatures, it seems that the effect of temperature is reduced when the ageing is performed at the high dose rates, within the studied ageing conditions. By the same means, one could tell that the dose rate effect is reduced for the samples aged at the high temperatures, since the DED values is observed not to differ much for the samples aged at different dose rates at the high temperatures.

The ultimate tensile stress (UTS) data variation as a function of dose provide additional argument for the dose rate effect appearance. Two distinct regions are observed: at the beginning of ageing i.e. for the low ageing doses, the nUTS (nominal UTS) is observed to increase and the tUTS (true UTS) is observed to be rather stagnant; this region is followed by a decrease of the UTS (nominal and true) at higher doses i.e. for longer ageing times, creating a local maximum for the nUTS data or a decay point for the tUTS data. The dose at which the UTS begins to decrease depends on the ageing conditions. An increase of the dose rate leads to the gradual enhancement of the UTS increase region, which is manifested by the shift of the local maximum to a higher dose,

or equivalently by the apparent increase of ultimate stress values for the samples aged at the same dose, with increasing the dose rate. To investigate the effect of the temperature, the variation of the UTS data for the samples aged at similar dose rates is investigated. It can be observed that by increasing the ageing temperature the region of the UTS increase is gradually suppressed.

According to the literature, this increase of the UTS could correspond to the domination of the cross-linking as an ageing mechanism and the regime where chain scission dominates can be correlated to the decrease of UTS [24, 26, 55, 58, 59]. Cross-linking and chain scission modify the macromolecular chains of the material and the consequence is a change in the mechanical properties. Additionally, if the property is stagnant it is considered that the cross-linking and chain scission are in competition without a significant domination one of the mechanisms. [58] Still, one has to be careful while interpreting the results of the tensile test. Nominal (engineering) values are the most often used in industrial practise, but the true values have physical meaning. An evolution of nominal values clearly differs from true. True elongation at break values are also lower than engineering (see Fig3.2), therefore when a criteria is set up according to the elongation at break, this has to considered.

Next to the UTS values, Young's modulus values are used in order to estimate which degradation mechanism dominates. The increase of the Young's modulus is very often correlated to the increase in cross-linking and it often supports what was observed by the evolution of the UTS data [11, 58, 59]. The Young's modulus can be used as an indicator of the sample stiffness and it can be correlated to the concentration of elastically active chains in the case of unfilled, amorphous rubbers [11], but beside cross-links, chain entanglements are also contributing to the Young's modulus and the exact correlation has been investigated [79,80]. Moreover, in the case of filled polymer it gets even more trickier to establish the exact contribution. Still, YM is used as an reliable indicator of a polymer structure modification with ageing. The variation of the YM as a function of dose was investigated and it is observed that the YM behaviour is similar to the one observed for the UTS. Generally, the increase of the YM observed for low doses, is followed by its decrease at

high ageing doses. For the samples aged at the high temperatures, the increase of YM was observed, which is opposite to the UTS that was dominantly decreasing (see samples aged at 70 and 85^0C). An obvious dose rate or temperature effect was not observed for the YM data, within the studied ageing conditions. This could indicate that the dose rate effect could be better observed and investigated on the basis of ultimate mechanical properties like elongation at break or ultimate tensile stress.

Cross-linking and chain scission are well established as frequent ageing mechanisms of the cable insulation polymers, see Section 1.5.2. Cross-linking appears as a consequence of mutual interaction between macro-radicals (alkyl radicals) created in the polymers by γ - irradiation. However, they also easily react with oxygen creating peroxy radicals and hydroperoxides. These products can further react with the polymer chain causing chain scission (rupture of original bonds), or react with one another and terminate oxidation process. Which process will be dominant depends on the quantity of absorbed oxygen and concentration of alkyl radicals. Generally, the high production of radicals (high dose rate) and low oxidation will promote the cross-linking, while the high temperature and long exposures in oxidizing conditions (usual conditions when achieving the high dose at low dose rates) will promote the chain scission. The fact that the chain scission overcomes the cross-linking effect above certain dose has been confirmed earlier [16,17,55]. The crossover in neat EPDM films that are irradiation aged is measured through an increase in gel fraction as a function of the irradiation dose and found to be of about 100 kGy [16]. The relaxation measurements by Celette et al. [55] on 100 μm thick samples indicate the transition to be at about 200 kGy. Additionally, both authors correlate the promotion of cross-linking to the double bond presence in EPDM. In some cases, the crossover between cross-linking and chain scission is observed to appear at certain critical dose rate [24–26]. Ageing at 40^0C for dose rates between 10 - 2500 Gy/h up to 100 kGy, showed the existence of two distinct regimes: an ultimate stress decay for low dose rates (10 and 100 Gy/h) and ultimate stress increase for dose rates higher than 500 Gy/h [26]. Similar observation is also reported by Pinel and Boutaud [24,25]. Our results rather show that the crossover gradually changes, without threshold dose-rate

or temperature values, through an interplay of dose rate and ageing temperature. They both seem to affect the crossover in similar way: an increase of the temperature shifts the transition to lower dose, while an increase of dose rate shifts the transition to higher dose. The existence of a crossover is essentially observed in entire dose range considered in this study.

Indenter modulus is measured as a non-destructive technique, that could be potentially used as good ageing indicator for some cable materials. Increase of the IM with dose, and ageing time was observed, which was expected according to the experiences gathered from industry and previous studies [2,3,81,82] and it is often correlated to the cable insulation polymer hardening with ageing.

Unlike the Young's modulus, that is observed to decrease at high doses, IM is observed to dominantly increase, within the studied irradiation dose range. The correlation between YM and IM is analysed and presented in Fig. 3.23. It seems that a linear correlation exists, but only for samples aged at the high dose rates: 25^0C, 720 Gy/h; 40^0C, 1390 Gy/h; 70^0C, 1390 Gy/h, see Fig 3.23. a). Note that the IM measurements were not performed for the samples aged at the dose rate of 2760 Gy/h, which was the highest ageing dose rate applied during the accelerated ageing. The IM and YM values of the samples aged at lower doses, do not show clear correlation, see Fig 3.23. b).

The evolution of the IM as a function of ageing time (dose) is often compared to the evolution of other (well established) ageing indicators in order to confirm reliability of the IM as an ageing indicator. Indenter modulus is very often correlated with elongation at break, when cable ageing is studied, and the good correlation was often observed in previous studies [2, 3, 81, 82]. The correlation between IM and elongation at break (relative elongation at break)is presented in Fig. 3.24. Essentially, their mutual dependance can be described with linear function: $IM = -0.07e + 17.5(\pm 2)$. The IM is apparently better correlated to the evolution of elongation at break with ageing than with the evolution of YM. The possible reason could be explained by investigating the origin of the correlations.

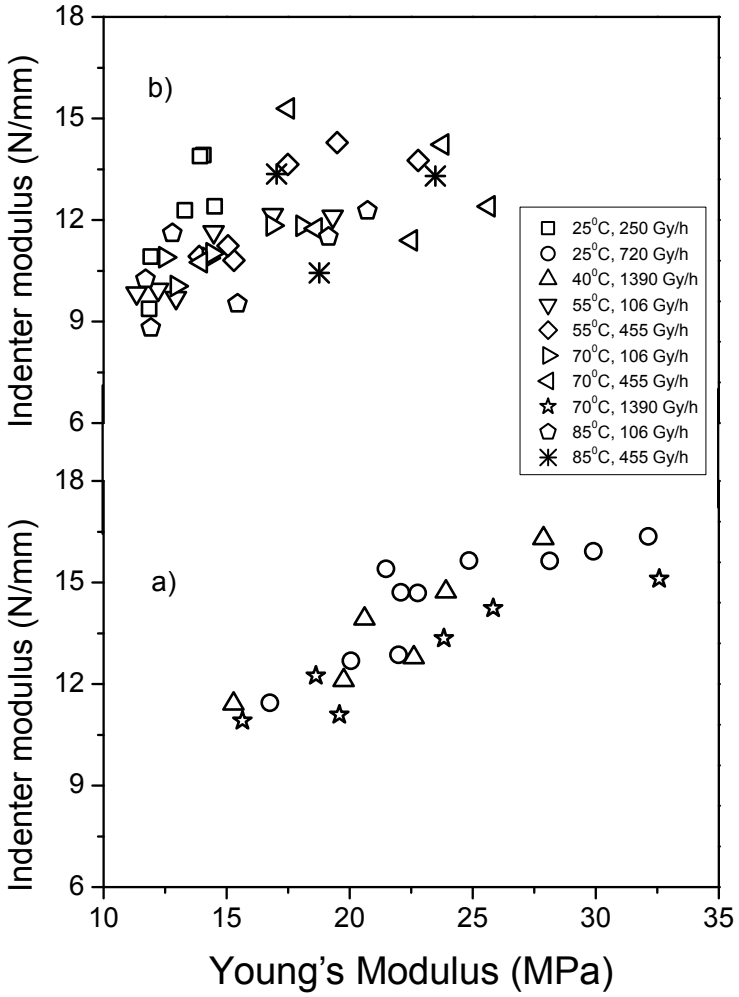

Figure 3.23: *The relation between Young's modulus and Indenter modulus - outer insulation: a) samples aged at high dose rates; b) samples aged at low dose rates*

In the study related to the investigation of non destructive, in situ techniques [81], the elongation at break, indenter modulus (expressed as N/mm), capacitance and dissipation factor were measured on a set of 47 aged flame-resistant EPR samples and the correlation between the IM

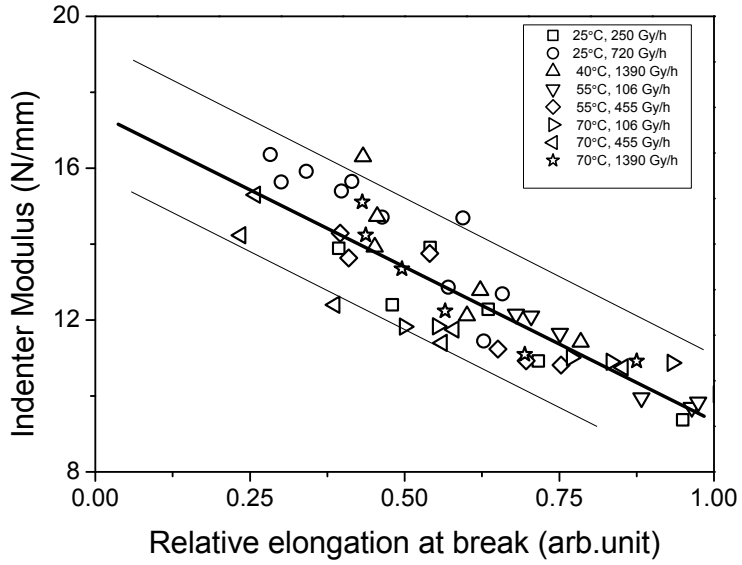

Figure 3.24: *The relation between Indenter modulus and elongation at break - outer insulation.*

and other parameters was made. It was observed that the elongation at break decreases with ageing, while the IM, capacitance and dissipation factor are increasing as a function of ageing time. Moreover, the correlation magnitudes between the IM and other parameters were calculated and the calculation showed that there is a higher correlation between the indenter modulus and dissipation factor (dimensionless property of a dielectric, that is determined by the insulator's structure) than between the indenter modulus and elongation at break. Previous studies have assumed that an increase in a dissipation factor with ageing time is due to the increase in sample polarity, which is a consequence of material oxidation during ageing [56].

As elongation at break and indenter modulus are well correlated, it could be assumed that the oxidation is the cause for IM increase as well as for the elongation at break decrease. Moreover, correlation between IM and tensile properties may be strongly dependant on heterogenity/homogenity of the oxidation. For the same material aged under

different conditions, these conditions play an important role in the oxidation process. Diffusion limited oxidation, where the oxygen consumption rate is higher than the oxygen supply rate through diffusion, is often discussed as one of the main limitations for accelerated ageing, since it might lead to the heterogeneity of the aged samples. Heterogeneous oxidation is more important at high dose rates where because of the rapid ageing only sample surface is affected by oxidation, and this oxidized layer thickness is smaller. More homogeneous oxidation appears at lower dose rates, where longer ageing times are required to achieve the same dose, so there is more time for oxygen to diffuse deeper and oxidized layer thickness increases. Additionally, temperature increase (up to certain values) is considered to enhance oxidation diffusion. So for low oxidation thickness cross-linking will prevail, which could be possible observed when measuring UTS and YM, by the increase in their value. Thick oxide will mean promotion of the chain scission. In fact, as already mentioned - oxidation thickness is what governs elongation at break and IM, so the correlation between them could be established through the oxidized layer. The correlation of the elongation at break decrease to the oxidation was proposed earlier [74], on the basis of measurement of the electrical properties. Thickness of oxidized layer depends on many parameters that affect oxygen diffusion process through the sample bulk. Some of these parameters are dependent of a material itself and the other on the atmosphere surrounding the sample during the ageing (first of all concentration of the oxygen).

The IM, expressed as N/mm, was measured by a indenter technique with a set-up standardly employed within the NPP industry. During measurement, the indentation apparatus was set up as it normally is when standard tests are performed on the NPP cables and the probe was penetrating about 1 mm into the sample. The thickness of outer sheath samples that are investigated herein is about 2 mm, which means that the probe goes up to the half sample. Indenter modulus value obtained in such a way enables to have more general information, because both oxidized and non-oxidized parts of the material are measured. This might also explain such a good correlation with the elongation at break. Young's modulus has entropic origin in the case of rubbers. Entropy is a

measure of the degree of disorder within a system. When it is extended under stress, rubbery material tends to go back to higher entropy state. During the extension the entangled and cross-linked chains straighten and align, less disordered system is formed and entropy lowers. When the applied stress is removed the system goes back to its thermodynamically preferred state [8]. Accordingly, the area of YM decrease might indicate the decrease in " sample disorder" i.e. decrease in number of bonds and entanglements due to an extensive chain scission.

The more precise tools were used for obtaining the profiles of IM (N/mm^2). Modulus profiling is performed for non-aged sample to confirm its homogeneity. No profile was observed, as expected. For the samples that are aged at the high dose rates heterogeneity, due to the uneven oxidation level was expected, so the profiling is performed for two samples aged at 720 Gy/h (25^0C) and 2760 Gy/h (40^0C) up to the doses 1100 kGy and 1186 kGy, respectively. The modulus is observed to increase from the sample edges towards the bulk and there is no significant change of a profile depth as a function of the dose rate. The modulus profile indicates that the heterogeneous oxidation occurs through the sample thickness [22, 50]. More oxidized material at sample edges shows less modulus increase than the sample bulk, which undergoes cross-linking due to the more inert ageing atmosphere. Still, these data have to be interpreted carefully, since the possibility of having a measurement artefact near the sample edges is not known for sure (there is a possibility that the sample holder effects the results).

The indenter modulus clearly has a potential as a control monitoring technique. According to the presented data, this potential is coming from the possibility to correlate the extent of the sample oxidation to the IM evolution with ageing. Further analysis are also possible using more precise tools and probes (micro or nanoindenters), like in the case of modulus profiling, which also enables cross-sectional investigation of the material. This analysis can reveal distribution of the oxidation through the sample thickness.

Predictive modelling

Predicting of the cable behaviour with ageing is one of the main goals for the NPP and this is why accelerated measurements are performed. As the elongation at break is widely accepted as reliable cable ageing indicator, its change with ageing time is analysed in order to predict the behaviour of the cable insulation with ageing. The evolution of the elongation at break with ageing time is described using a standard model, see Section 3.2.2. When elongation at break data were modeled, it was indicated that it seems that single process is responsible for the change of elongation at break and the decrease of the elongation at break is governed dominantly by the radiative term for our ageing conditions. According to the experimental results of the mechanical properties and modeling radiation induced oxidation is considered to be the main reason for elongation at break decrease.

When comparing to the work of B. Pinel and F. Boutad [24], which use the same model, they predict the behaviour of the elongation at break describing the predominant ageing mechanism. Namely, they obtain two values for the β parameter (which is the overall order of the reaction, see Section 3.2.2.), which depend on the dose rate. Below the critical dose rate, which was observed to be about 500 Gy/h, the β was found to be 5, and above the critical dose rate β was 10. The existence of the two β values was correlated to the difference in degradation processes above and below the critical dose rate. It is considered that at low dose rates, below the critical dose rate, the oxidation process leads predominantly to a chain scission and the degradation is homogenous; while above the critical dose rate the degradation process is considered to be controlled by the oxygen diffusion, which causes the predominance of the cross-linking in the sample bulk. The critical dose rate was observed and determined on the basis of ultimate tensile stress data [24].

According to our identification, all the model parameter (including β) are determined as constants within investigated ageing conditions, except the K_{irr}. The behaviour of K_{irr} with dose rate is analysed. K_{irr} parameter, obtained from the fitting of the experimental data, as a function of the dose rate is shown in Fig. 3.25 (symbols). By increasing the

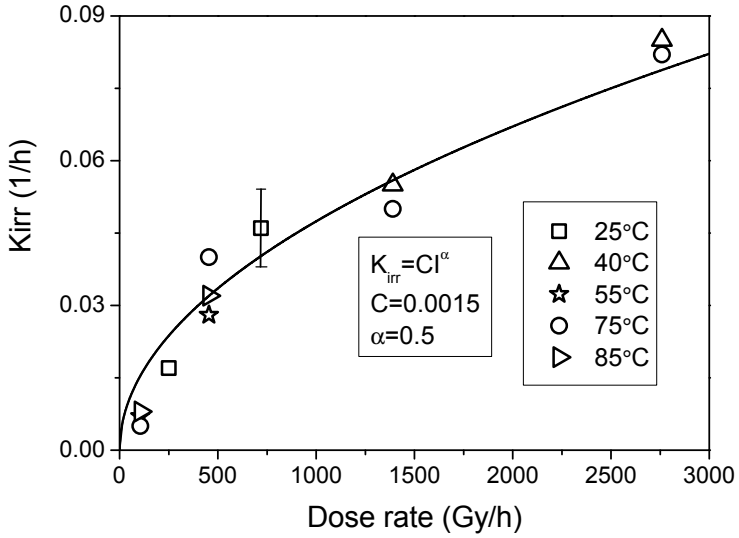

Figure 3.25: *The variation of the radiative reaction rate constant as a function of dose rate: experimental data - symbols and the square root fit - line; outer insulation.*

dose rate the K_{irr} parameter increases monotonously in order to fit the data, irrespectively of the irradiation temperature. This behavior is analyzed on the basis of $K_{irr} = CI^{\alpha}$, where I is dose rate, α is dose rate exponent and C is a constant (see Fig. 3.25, line). It is found that the K_{irr} follows a square root dependence ($\alpha = 0.5$) as a function of the dose rate, see full line in Fig. 3.25. This result agrees well with the dose rate dependance of the oxygen consumption [83]. Accordingly, the elongation at break decrease could be strongly correlated with the oxygen consumption i.e. oxidation induced degradation.

Still, for low dose rates, slight discrepancy between the K_{irr} values obtained by fitting and ones calculated via square root dependance, can be observed. Theoretically, for very low dose rates, the K_{irr} weights toward infinity. A linear dependance seems to be more suitable to describe the evolution of the K_{irr} with increasing dose rate, for low doses. The evolution of the K_{irr}, can be described via two distinct linear functions, within the total investigated dose rate range, see Fig. 3.26. The linear

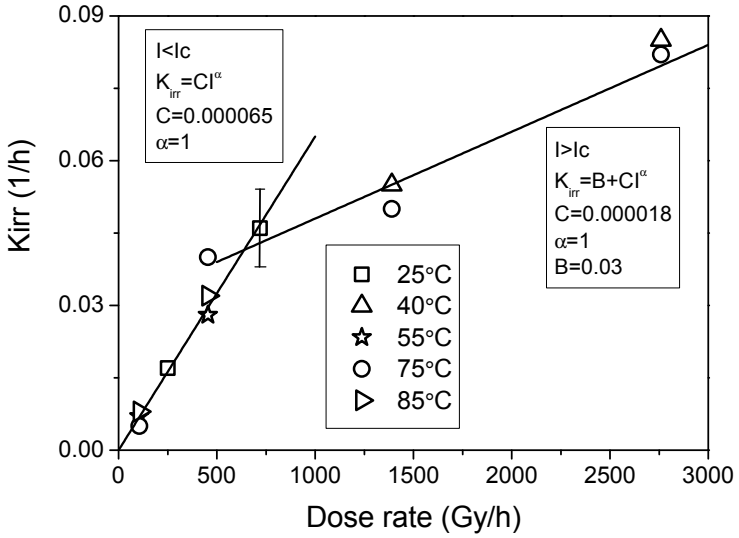

Figure 3.26: *The evolution of radiative reaction rate constant as a function of dose rate: experimental data - symbols and the linear fit - lines; outer insulation.*

dependance $K_{irr} = 6.5x10^{-5}$I, can be used for the low dose rate, and the function $K_{irr} = 1.8x10^{-5}$I + 0.03, can be used for the high dose rates. The dose rate at which there is a transition of the linear functions describing the variation of the K_{irr} with dose rate, can be entitled as critical dose rate. For the investigated data, the critical dose rate would be between $\sim$ 500 - 750 Gy/h. This is in agreement with the previous studies [24, 25], that report the critical dose rate about 500 Gy/h.

Physico-chemical properties

The thermogravimetry performed under nitrogen and air is one of the techniques used for the physico-chemical characterisation of non-aged and aged industrial polymer samples. For the samples that were thermally decomposed under nitrogen no significant difference in the decomposition between non-aged and aged samples was observed. On the contrary, when the decomposition was performed under air, the polymer decom-

position temperature profile is observed to gradually shifts towards the high temperatures with increasing the irradiation dose. On the DTG curves, two peeks related to the macromolecular chain decomposition are observed and entitled as P2 (positioned at $\sim 430^0$C) and P3 (positioned at $\sim 480^0$C). The peak intensities are found to be dose dependant in a way that P3 intensity increases at the expense of the P2 intensity decrease, with increasing dose. To depict that, the P2 and P3 intensities as a function of the dose are presented in Fig. 3.27.

By increasing the dose, the P2 intensity gradually decreases, simultaneously wwith the increase of P3 intensity. Both the P2 and P3 intensity changes seem to exhibit the dose rate effect, see Fig. 3.27 a) and 3.27 b), respectively. Namely, for the samples irradiated at low dose rates, the changes of P2 and P3 intensities look like they are more pronounced in comparison with the changes at high dose rates. Moreover, the P2 peak intensity behavior as a function of dose, temperature and dose rate fully mimics the behavior of the elongation at break. The variations of P2 and elongation at break with dose are compared in Fig. 3.28.

The relation between P2 peak intensity and elongation at break is pictured in Fig. 3.29. and it indicates the existence of a linear correlation.

The existence of an apparent correlation between the P2 and elongation at break indicates that the reduction of the elongation at break of industrial EPDM polymer is probably related to the reduction of the P2 i.e. polymer material part which decomposes at 430^0C in air. Since the mass loss at 430^0C is observed to be the main decomposition step of non-aged polymer, the reduction of the elongation at break is probably linked to the gradual increase of the oxidized part of the EPDM polymer. During the ageing, the polymer undergoes radiative and thermally mediated oxidation and internal sample oxidation increases with the dose. Therefore, the increase of the dose decreases the portion of the non-oxidized polymer part, causing the decrease of the P2 peak intensity when the TGA is measured under air atmosphere. Similarly, the ageing increases the oxidized part of the polymer, causing the increase of the polymer mass loss at higher temperature, of about 480^0C (P3 peak). The oxidized part of the polymer during ageing is not affected by the presence of oxygen during the TGA measurements. Because of that, the temperat-

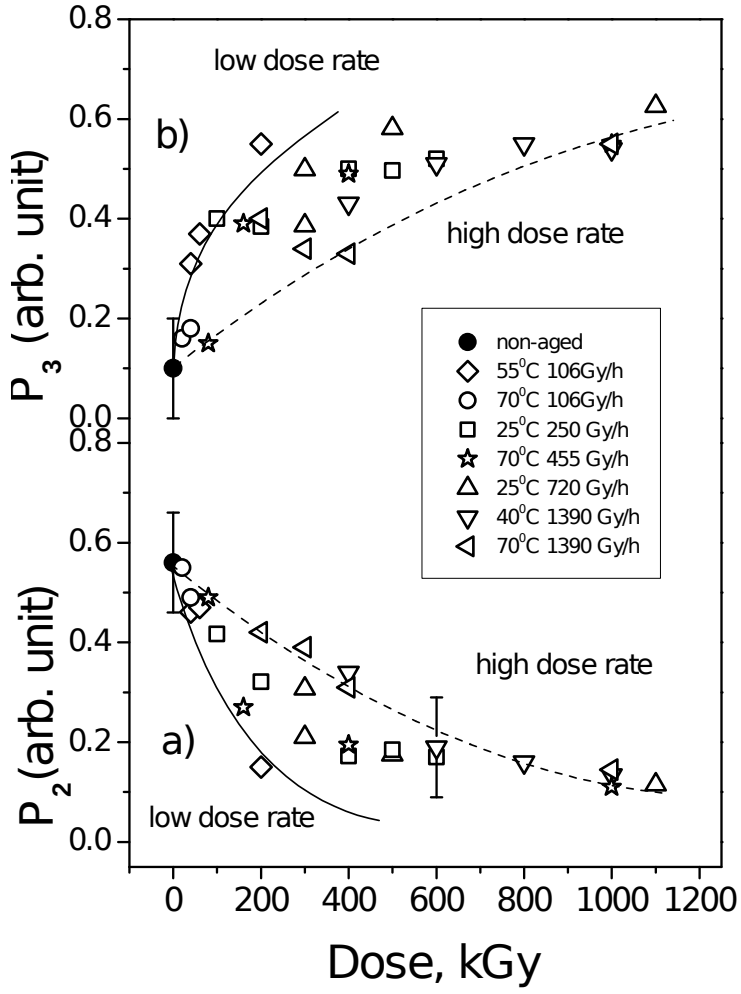

Figure 3.27: *The peak intensities at a) 430 ^0C (P_2 peak) and at b) 480 ^0C (P_3 peak) as a function of the dose - outer insulation.*

ure position of the P3 peak can be correlated to the temperature at the second decomposition stage when the TGA is measured under nitrogen atmosphere. Similar reasoning explains why the decomposition under the nitrogen atmosphere does not show the dose dependence. Finally, the radiation and thermally mediated polymer oxidation is responsible

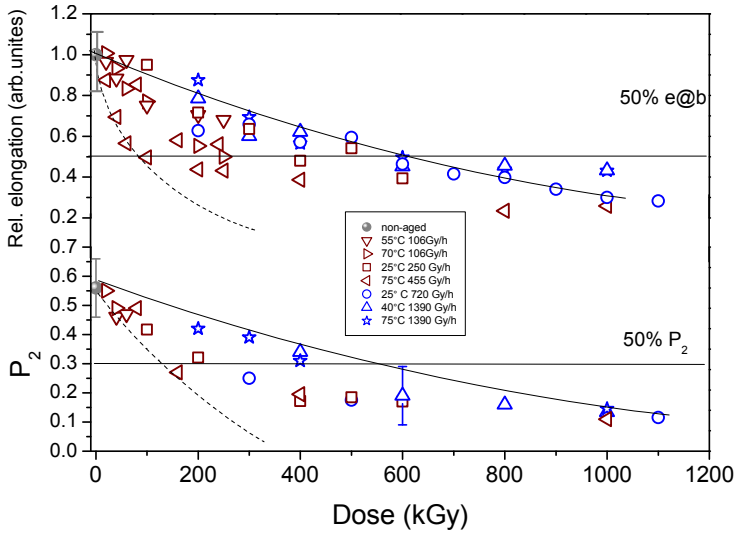

Figure 3.28: *The variation of the a) relative elongation at break and b) P2 intensity as a function of the dose, for samples aged at different temperatures and dose rates.*

for the appearance of the dose rate effect in aged industrial EPDM polymer. In that respect, the high dose rates limit the polymer oxidation because of the DLO and short radiation exposure times, while the high temperatures enhance the oxidation because of the increase of oxygen diffusion. By increasing the oxidation, the number of oxidized bonds in the polymer increases, causing the gradual destruction of the polymer network and reduction of the total elongation. This also explains the previous observation that elongation at break as a function of the ageing time can be described by a single model parameter.

According to what was discussed within the previous paragraph, the two decomposition mechanisms will be proposed for thermal decomposition under air. The first, related to the main mass loss at about 430^0C, is considered to be oxidation. The second, with the major mass loss at about 480^0C a random chain scission.

These results provide a direct link between the mechanical and physicochemical properties of aged cable polymer. The observed correlation

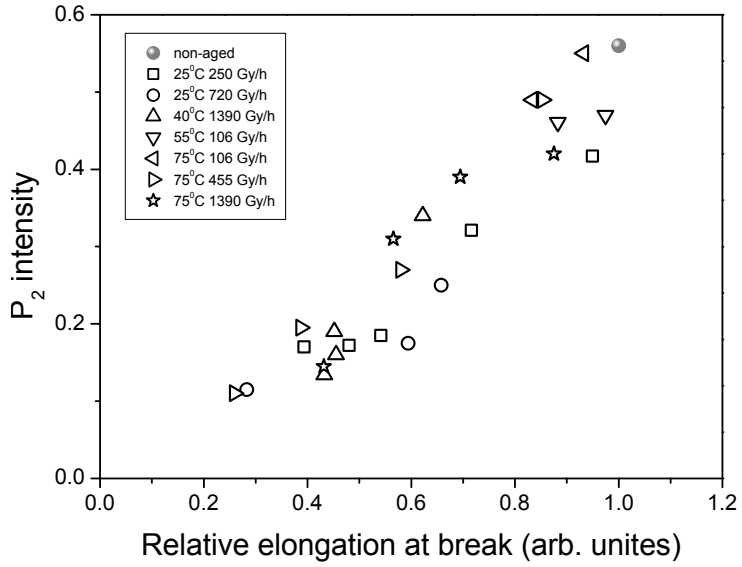

Figure 3.29: *The relation between intensity of P2 peak and relative elongation at break.*

clearly demonstrates the importance of thermally and radiochemically mediated oxidation degradation processes for long term operation, and provides very useful methodology for the evaluation of cable conditions.

The ATR-FTIR and the TGA coupled with FTIR were used in order to characterise the non-aged and aged samples. FTIR has potential to be used as a technique to qualitatively, and even quantitatively distinguish sample degradation level, by detecting the chemical species created by oxidation i.e. oxidation products and possibly, some other chemical changes created during sample ageing. According to the obtained spectra it was possible to confirm that the main components of the investigated cable outer insulation are EPDM, EVA and ATH. Still, no important variation in the composition between aged and non-aged samples is observed. When the spectrum of the aged samples surface was compared to the spectrum of the bulk, a slight indication of increased oxidation at the sample surface is observed via increase in peaks related to the carbonyl species (1630 cm^{-1}). The increased oxidation

of the samples surface in comparison to the sample bulk, would be an indicator of the DLO during the accelerated ageing, but the differences between spectra are not strong. Actually, when samples with complex structure (industrial) are studied, spectral modifications between more aged, less aged and non-aged samples are in principle small, which influences effectiveness of the FTIR, as CM technique. Still, there are studies reporting employment of multivariate analysis methods (mathematical procedures) for better interpretation of the FTIR spectrum [84, 90, 91].

By coupling of TGA and FTIR, in order to analyse the evolving volatile compounds during the TGA, performed under nitrogen, four components were clearly detected: -OH species, aliphatic chain parts, CO_2 and carbonyl species. The distribution of their spectra with increasing TGA temperature (and time) is obtained. The -OH species and carbonyl species spectra intensities are observed to be the highest at about 350^0C. The two were correlated to the evaporation of water from the ATH, and the acetic acid from EVA, respectively. This confirms, what was previously proposed on the basis of the literature, that the first decomposition step from the TGA (or the P1 from the DTG), is related to the decomposition of the ATH and EVA. Strong aliphatic chain spectrum intensity peak is observed at about 480^0C, confirming that the polymer chain decomposition is ongoing at that temperature, and it can be correlated with the second decomposition step from the nitrogen TGA, or the P3 from the air TGA.

The investigation of the changes in polymer network structure induced by ageing, is often done by performing the swelling test. The variation of the swelling ratio and gel fraction with increasing dose is investigated. The swelling ratio is observed to decrease for low doses, and it is correlated to the increase in polymer network chain density. Increase of chain density could be a consequence of dominance of cross-linking as an ageing mechanism, which is in agreement with UTS and YM increase, that is observed at low doses. The swelling rate decrease is followed by its increase at higher doses, which is related to the destruction of polymer network. This is in agreement with the assumption that with ageing time concentration of oxygen in the material increases, and chain scission increases, overcomes cross-linking and network density reduces.

Moreover, the dose rate effect is observed. And the doses at which the cross-over from cross-linking to chain scission domination happens, are observed to be dependant on the ageing dose rate, which is probably related to the DLO during ageing at the high dose rates.

The gel fraction is observed to decrease for all the tested ageing conditions, indicating the decrease in the unsoluble sample fraction, i.e. the destruction of the polymer network. According to the tensile data and swelling ratio evolution with dose, initial increase of gel fraction could be expected. Still, the initial value of the gel fraction is already very high ($\sim$90%). Possibly it is difficult to expect strong increase of gel fraction when the initial value is so high, but the results from tensile test (UTS and YM) indicated the cross-linking domination in the beginning of ageing process (for the short times). Uncertanties of swelling test have to be considered here. The dose rate effect is observed in a way that decrease of gel factor is fastest for samples aged at low dose rates and it gets slower with dose rate, which is in accordance with the tensile data.

It was indicated in previous studies that the swelling measurement, even often done, is considered to have big uncertaintities [11, 58], especially for industrial samples, which have many inclusions next to the polymer matrix that influence solvation process and obtained swelling parameters as well as for the highly oxidised sample, which normally have increased polarity in comparison to the non aged sample. For these reasons, the values of the parameters have no quantitative meaning, but they can still be used as a support to other techniques, giving useful information about network evolution with ageing.

Measurement of the sample crystallinity by the DSC reveal that the investigated samples are dominantly amorphous, and the same was confirmed by the DMA. Thus the monitoring of the crystalline structure evolution with ageing is not expected to give an important information about the ageing mechanism.

DMA monitors relaxation behaviours, and their evolution with ageing could be used to describe changes in sample structure caused by ageing. Shift of the relaxation peak toward higher temperatures, which is ob-

served for the sample aged up to the 1100 kGy, implies decrease in the sample chain motion. This is considered to be a consequence of cross-linking as a dominant ageing mechanism. Due to cross-linking molecular motions are hindered and their mobility decreases. Accordingly, in the case of chain scission predominance, relaxation peak is expected to be shifted toward lower temperatures, as it is the case for the sample aged up to the 600 kGy. This means that for the sample aged at 25^0C, 720 Gy/h, up to the 1100 kGy cross-linking is expected to be the dominant mechanism and for the sample aged at 25^0C, 250 Gy/h, up to the 600 kGy, chain scission. This result is in accordance with the tensile data. In the previous studies [54–56] broadening of the glass transition peak together with its decrease in height were observed. These are also indicators of decreased dumping in the material, which is characteristic of decrease in molecular mobility and consequence of cross-linking. Important changes of peak hight and width were not observed from presented results.

Storage modulus results are in accordance with $tan\delta$ data. The sample aged at 720 Gy/h up to the 1100 kGy is found to have the highest value of storage modulus and sample aged at 250 Gy/h up to the 250 kGy the lowest. Storage modulus is expected to increase as a consequence of cross-linking process, because it means forming of more rigid structure. Chain scission dominance is usually seen as a decrease in modulus value.

Theoretically, DMA seems to have good potential as a low destructive CM technique, but its sensitivity when it is applied on industrial sample could be the issue. The observed changes in monitored parameters are much less for the industrial samples in comparison to the non-industrial, "laboratory produced" samples, [54–56] probably due to the difference in the samples composition complexity.

According to the investigation of the mechanical and physisco-chemical properties of the non-aged and aged cable outer insulation samples, together with modelling of the elongation at break data with time; it can be concluded that the insulation (industrial EPDM) polymer degradation is probably caused by the thermally and radiochemically mediated oxidation process. The changes in sample structure, that are causing the changes in the material performance, are considered to be driven by

cross-linking and chain - scission mechanisms, that both occur simultaneously during the ageing, but with the predominance of one of them. Which mechanism will dominate depends mainly on ageing conditions (dose rate, temperature, oxygen concentration) and material properties. This is tightly related to the homogeneoity/heterogeneity of the sample oxidation through the sample thickness. The diffusion limited oxidation, where the oxygen consumption rate is higher than the oxygen supply rate, due to the ageing conditions and material properties influencing the diffusion process, is often discussed as one of the main limitations when accelerated ageing is applied. It is not considered to be representative of an ageing under operation conditions, for which DLO is not expected. The extent and the distribution of the material oxidation are considered to be the responsible for the evolution of the mechanical and chemical properties with ageing for the cable outer insulation made out of the EPDM.

3.3 Experimental investigation of the industrial EPDM material - inner cable insulation

The inner cable insulation is extracted from the cable and tubular form of the specimens is made and aged together with the outer layer (so the ageing conditions were identical).

3.3.1 Mechanical properties

The mechanical properties of the non-aged and aged inner insulation samples are investigated. The same type of the experiments is performed as it was for the outer insulation: tensile and indenter modulus test.

Uniaxial tensile test

Some representative nominal stress - strain curves of the non-aged and aged specimens were plotted in Fig. 3.30. The behaviour of the nominal stress - strain is observed to be similar to the outer insulation samples.

Namely, the stress increases monotonously up to the breaking point. The mechanical behaviour is mainly elastic, and it is significantly altered by thermal and radiation ageing. The elongation at break decreases with ageing and the changes of ultimate tensile stress were also observed.

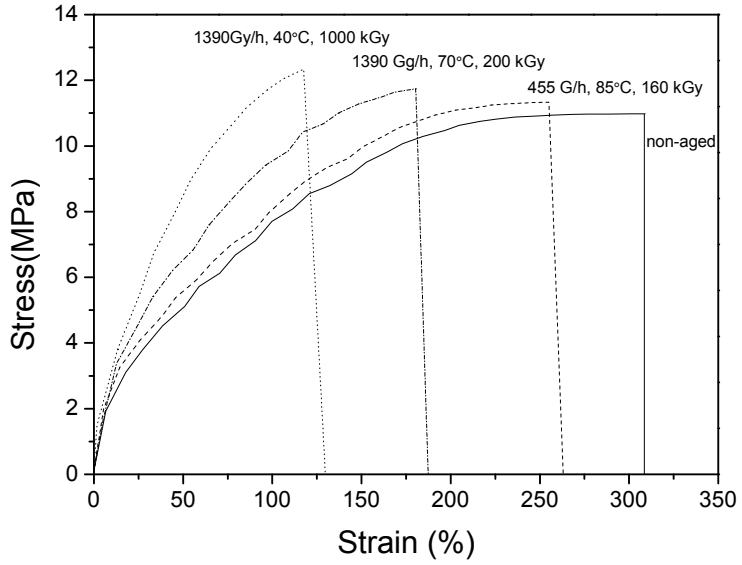

Figure 3.30: *The nominal stress - strain curves of several samples, aged at different temperatures and dose rates - inner insulation.*

The mean nominal absolute elongation at break and ultimate tensile stress values for non-aged inner insulation are higher in comparison to the values obtained for the outer insulation. The average elongation at break for the inner insulation non-aged (reference) samples is 279.1 % ± 33 % , while for the outer insulation it is 125 ±10%. The reference nUTS for the inner and outer insulation samples are 11.2 MPa and 6,7 MPa, respectively.

The 50 % absolute elongation (taken as the end-of-life criteria) was never reached for the investigated doses in the case of inner insulation samples, see Fig 3.31. The relative elongation as a function of the dose data are presented in Fig. 3.32.

The elongation at break as a function of dose seems to follow rather

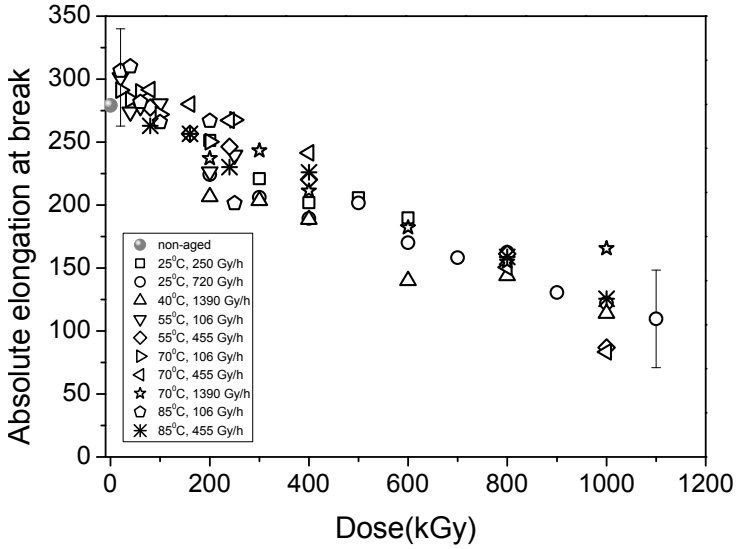

Figure 3.31: *The variation of absolute elongation at break as a function of dose for different dose rate and temperature ageing conditions - inner insulation.*

linear-like dependance than exponential, which was observed for the outer insolation as previously discussed (see Fig. 3.4). The decrease of elongation at break of the inner insulation samples, within the investigated total absorbed dose range, looks similar to the decrease of the elongation at break of the outer insulation samples at small doses. Since the 50 % absolute elongation was not reached for the inner insulation, the doses at which 50 % relative elongation is achieved will be analysed. It seems that if the extrapolations of the curves that did not reach the 0.5 e/e_0 would be made, all relative elongation versus dose curves (including the curves that do reach the 0.5 e/e_0) reach it at the dose of about 800 $\pm$ 50 kGy. This indicates that the evolution of the elongation at break as a function of dose seems to be less dependant on the ageing conditions, in comparison to the outer insulation.

The change of nominal ultimate tensile stress with dose is presented in Fig. 3.33. The samples aged at various dose rates and low temperatures are shown in Fig. 3.33a). By increasing the dose, the nUTS seems to

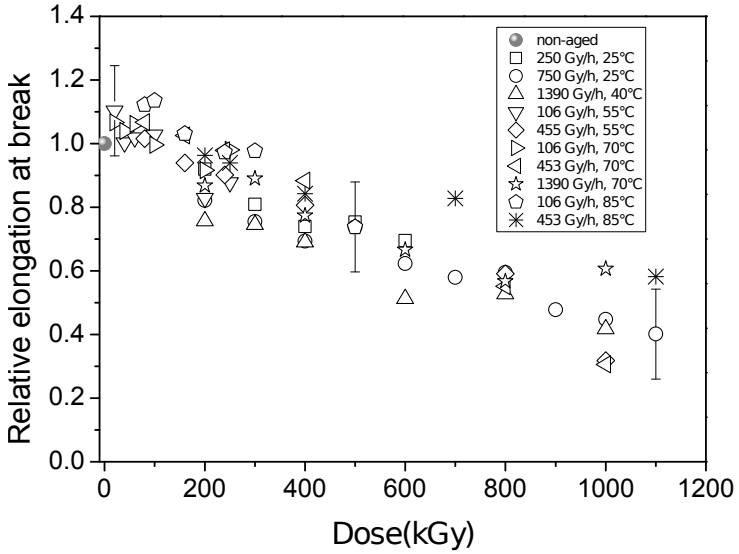

Figure 3.32: *The variation of relative elongation at break as a function of dose for different dose rate and temperature ageing conditions - inner insulation.*

have the tendency to increase at the beginning. The nUTS for the aged samples in comparison to the nUTS of non-aged sample does not seem to differ much. Initial increase of the nUTS at low doses is strongly reduced in comparison to the one observed for the outer insulation. At high doses the decrease of nUTS is observed for the batch aged at 720 Gy/h and 25^0C. Generally, the observed changes of nUTS for inner insulation aged at low temperatures (25^0 C and 40^0C), are moderate in comparison to the one observed for the outer insulation samples.

Similar behaviour is observed for the samples aged at high temperatures (Fig. 3.33 c)), but here the initial stagnant nUTS value changes abruptly at high doses for the samples aged at 70^0C, 455 Gy/h. For the samples aged at 85^0C the UTS constantly decreases for the investigated dose range. The effect of temperature to similar dose rate is presented on Fig. 3.33 b). It seems that the drop of nUTS is enhanced at high ageing temperatures.

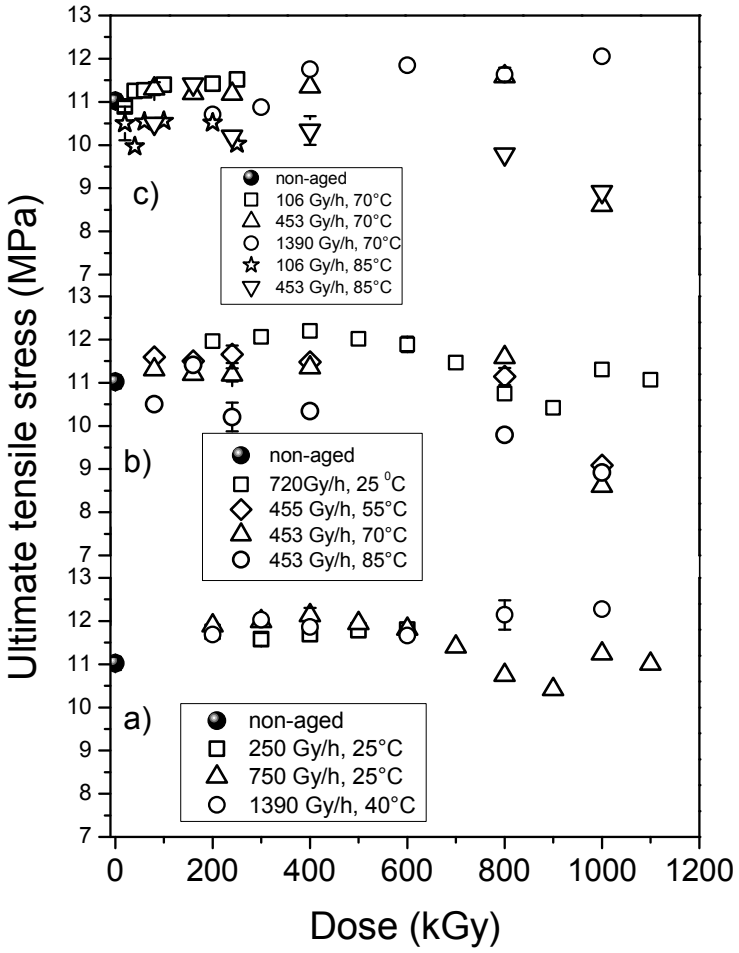

Figure 3.33: *The variation of nominal Ultimate Tensile Strength as a function of dose for different ageing conditions - inner insulation.*

The variation of the calculated true ultimate tensile stress with dose is presented in Fig. 3.34.

Generally, it can be observed that the changes of the tUTS with ageing dose are much higher in comparison to the nUTS data. It seems that the tUTS slightly increases up to the about 100 kGy, but then a clear decrease with increasing dose is observed. The variation of the tUTS

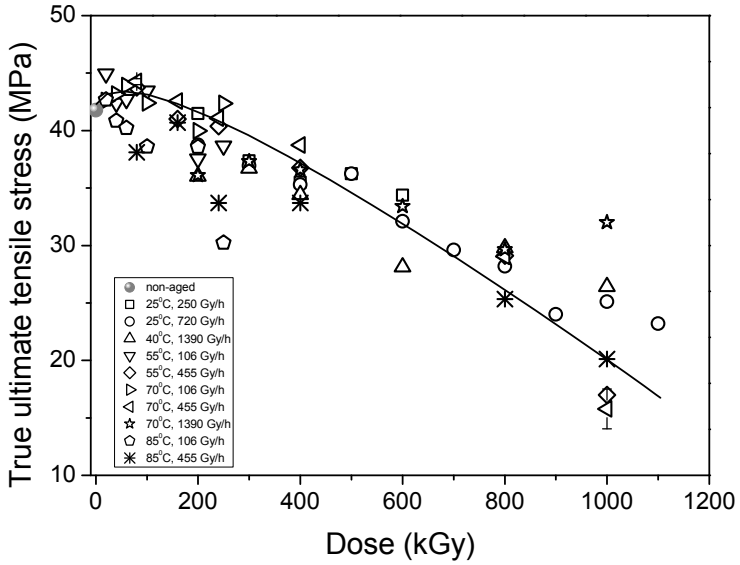

Figure 3.34: *The variation of true ultimate tensile strength as a function of dose for different ageing conditions - inner insulation.*

with dose is observed to be similar for all samples, regardless the ageing conditions.

The variation Young's modulus, calculated as the slope of the initial part of the nominal stress - strain curve, with ageing is analysed. Fig. 3.35 presents the YM versus dose data. The effect of the ageing temperature on the YM evolution with dose is analysed for the samples aged at the similar dose, but different temperatures, see Fig 3.35 a). Considering the error bar, significant change of the YM can be observed from about 800 kGy, when the YM increases. No effect of the ageing temperature on the YM evolution data is observed. The exceptions are the samples aged at 25^0C, for which the YM is higher in comparison to the YM of non-aged samples for all the investigated doses. But, for this batch clear increase of the YM with increasing dose can be observed only at about 1000 kGy. The YM is significantly higher in comparison to the non-aged sample, but it is rather constant for all aged samples within the batch. It has to be highlighted that the dose rate of the batch aged

at 25^0C is higher in comparison to the dose rate of the other batches within the temperature effect analysis segment. The YM variation with doses for the samples aged at low temperatures and different dose rates is presented in Fig. 3.35 b). The YM of all the aged samples is higher in comparison to the YM of the non-aged sample. Considering the error bar, the YM value is similar for all aged samples up to the higher doses (800 $\pm$ 200 kGy) where a bit stronger YM increase can be observed. Regarding the samples aged at high temperatures and different dose rates, YM is observed to be rather constant up to the doses about 600 kGy, from which YM significantly increases for the batches aged at 455 Gy/h and 1390 Gy/h (both 70^0C); while this decrease is less for the samples aged at 455 Gy/h and 85^0C.

Clear does rate effect is not observed for the elongation at break, ultimate tensile stress and Young's modulus data in the case of inner insulation.

Indenter modulus

For the samples aged at 85^0C standard industrial indenter modulus test is performed. The IM test set-up that is used has been designed for monitoring the IM of cables outer insulation, by testing the whole cable i.e. without stripping out the insulation. Whole cable samples are larger and much thicker comparing to the extracted inner insulation samples. Hence, it is possible that the obtained IM values for the $\sim$ 1mm thick inner insulation samples investigated herein, are influenced by the sample holder system, originally designed for thicker samples. The variation of the IM as a function of dose is presented in Fig. 3.36. Samples aged at 106 Gy/h do not exhibit a significant change of IM within the investigated dose range, except for the 250 kGy, where a slight increase can be observed. The IM increase is clear for the samples aged at 455 Gy/h. The increase of the IM with dose is expected to express exponential behaviour (as in the case of outer insulation samples), but according to the presented data it could be described as linear. The guides for an eye are given in the figure in order to describe the possible trends.

For several samples the modulus profiling trends were obtained thanks

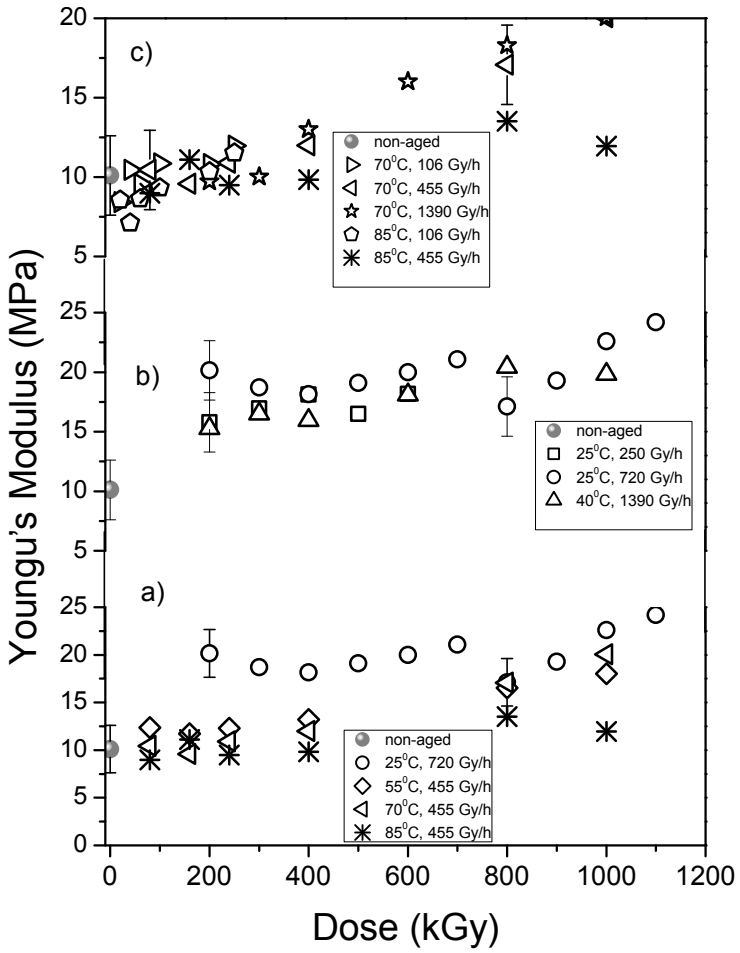

Figure 3.35: *The variation of Young's modulus as a function of dose for different ageing conditions - inner insulation.*

to the collaboration with Sandia National Laboratories. These modulus profiles are presented in Fig. 3.37. The machine used for measuring the IM (N/mm^2) profiles is designed for testing the extracted cable insulation samples. Still, the thickness of the inner insulation is low, so the influence of the sample holder to the sample modulus value is expected, especially on the sample edges.

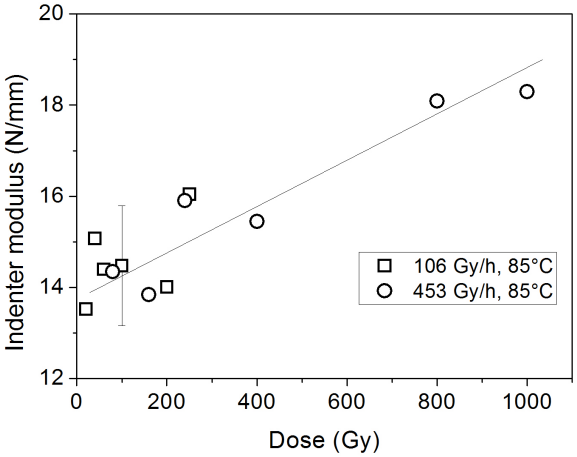

Figure 3.36: *The variation of the indenter modulus as a function of dose for samples aged at 85^0C - inner insulation. The full and doted lines are guide for an eye.*

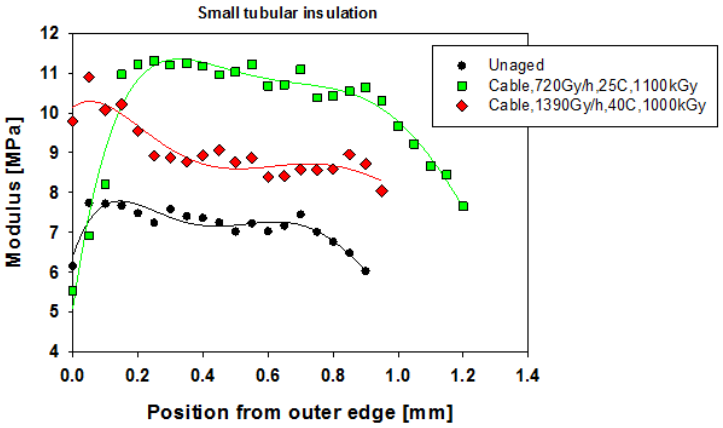

Figure 3.37: *The indenter modulus profile trends for non-aged and several aged samples - inner insulation.*

Samples which were chosen for modulus profiling are aged at the high

dose rates 720 Gy/h (25^0C) and 2760 Gy/h (40^0C) up to the high doses 1100 kGy and 1186 kGy, respectively. The IM of the non-aged inner insulation sample is observed to be about 7.5 MPa , which is higher comparing to the IM of non-aged outer insulation ($\sim$5 MPa). For the aged samples, IM increase is observed. It does not seem that there is a profile of IM. The modulus value is rather constant through the cross-section, which could indicate that the inner insulation specimens are more homogeneously aged.

3.3.2 Elongation at break modelling

The elongation at break variation with time for the inner insulation is analysed using the same model and the same fixed model parameter values that were used for the outer insulation data, see Section 3.2.2. The experimentally obtained and calculated elongation at break data are presented in Fig. 3.38. The parameters from the model that are fixed are collected in the Table 3.3. It was possible to fit all the experimental data with the data calculated by the model, by varying only one model parameter: the pre-exponential factor of the radiation rate constant, K_{irr}. It has to be noted that the optimal K_{irr} values for each irradiation condition were obtained using the same values for the fixed parameters as in the case of outer insulation (see Table 3.2).

Table 3.3: *The parameters used in the calculation according to the model described by Equation 3.2*

Parameter	Value
E_{ath}	1.07 eV
K_{th}	50×10^9 h^{-1}
E_{irr}	0.065 eV
β	3.5

Good agreement between calculated and experimentally measured elongation at break data is observed. It was confirmed that a single value of β parameter can be used for the data identification, indicating that single process is responsible for the change of elongation at break of inner insulation samples.

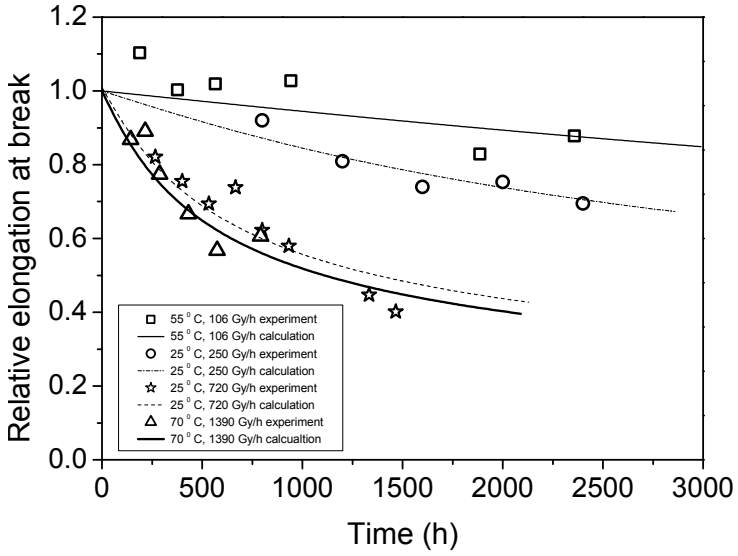

Figure 3.38: *The experimental and calculated relative elongation data as a function of the ageing time at different dose rates - inner insulation.*

3.3.3 Physicochemical properties

FTIR

ATR-FTIR is performed on the non-aged inner insulation, in order to check if there is a difference in the chemical composition between non-aged inner and non-aged outer insulation. The measurements are performed on three adjacent spots of one sample with an average of 128 spectra and a 16 cm^{-1} resolution, as it was done in the case of outer insulation samples. The average of the three obtained spectra from non-aged inner insulation sample is compared to the average spectrum of non-aged outer insulation in Fig. 3.39.

The majority of peaks of the non-aged inner insulation sample absorbance spectrum matches the ones of the outer insulation non-aged specimen, and the position of the peaks indicates that indeed EPDM, EVA and ATH are the main components of both cable insulation polymers. If

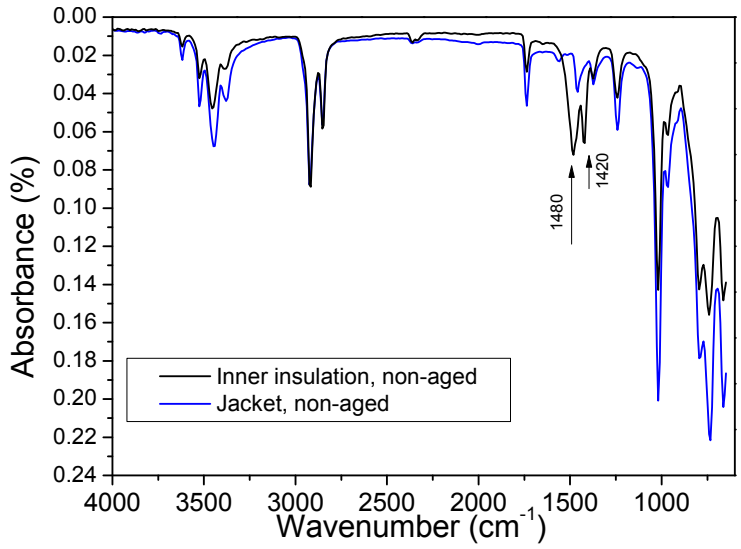

Figure 3.39: *The comparison between ATR-FTIR spectrum of non-aged inner insulation and non-aged outer insulation samples.*

the peaks positioned at at 2915 cm^{-1} and 2850 cm^{-1} are taken as reference peaks, it could be indicated that there is more ATH and EVA component in the outer insulation. Higher presence of mineral filler in the jacket (outer insulation) in comparison to the inner insulation is common for insulation formulations, due to the fact that jacket is rather expected to contribute to the protection of the inner insulation. Accordingly, inner insulation formulation is focused on ensuring quality of the insulation properties, while outer insulation formulation is focused to satisfy mechanical properties. The spectrum of the non-aged inner insulation sample exhibits new peaks at 1480 cm^{-1} and 1420 cm^{-1} which might indicate the presence of hydromagnesite ($Mg_5(CO_3)_4(OH)_2 * 4H_2O$) as the second fire retardant [88].

Thermogravimetry properties

Beside providing information about thermal stability and thermal decomposition steps, TGA measurements in nitrogen and air showed ap-

parent correlation with the elongation at break in the case of outer insulation samples. Thus the same measurements were performed on inner insulation samples. The mass loss curves during thermal decomposition in nitrogen and air are presented in Fig. 3.40.

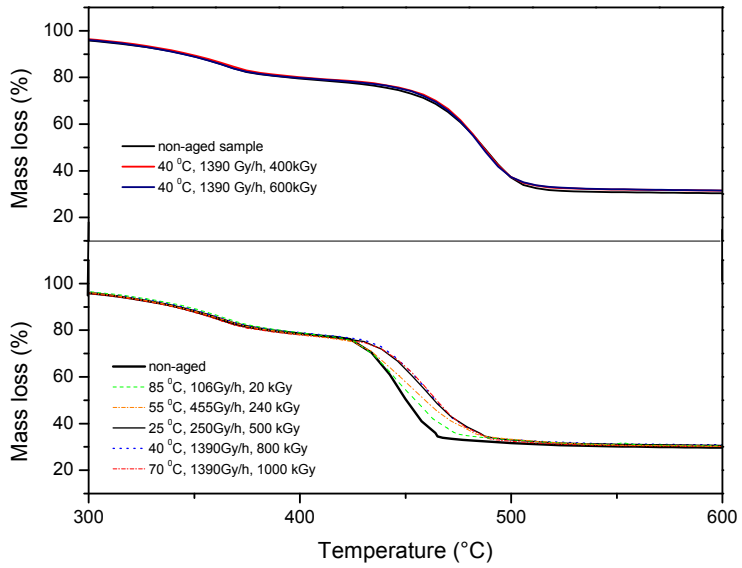

Figure 3.40: *Thermogravimetry curves of non-aged and aged samples under a) nitrogen and b) air atmosphere - inner insulation.*

The mass loss occurs monotonously with two major steps. The first major decomposition step takes place in the temperature range between $\sim 300^0C$ - 400^0C, with the maximum weight loss at about 360^0C. The second major degradation step follows the first one, with the maximum weight loss at 450^0C - 460^0C when the TGA is performed under air, and at 485^0C when the TGA is performed under nitrogen atmosphere. These two main decomposition steps are associated with the same mass loss process as in the case of outer insulation. According to the literature, the first decomposition step is related to the degradation of ATH and EVA [100, 101]. ATH degrades by forming alumina and water evaporation and EVA by evaporation of acetic acid. Polyolefinic main chain decomposition is associated to the second decomposition region, and it proceeds by the release of mainly carbon dioxide, water, and small or-

ganic parts. Due to the higher decomposition temperatures, one could instantly observe that the inner insulation is more thermally stable in comparison to the outer insulation samples. At the end of the TGA (nitrogen or air atmosphere), which is at 600^0C, the residue mass was $\sim$30% in the case of outer insulation, while it is about 20% in the case of inner insulation. If one assumes that this residue is mostly alumina (product of ATH decomposition), the difference in residue quantity may indicate that there is about 10% more filler in outer insulation layer.

As expected, the decomposition in air occurs at the lower temperature in comparison with the decomposition in nitrogen, see Fig. 3.40. Under air the polymer decomposition is enhanced by the presence of oxygen, and it requires lower activation energy in comparison with random chain scission polymer decomposition which occurs under the nitrogen atmosphere.

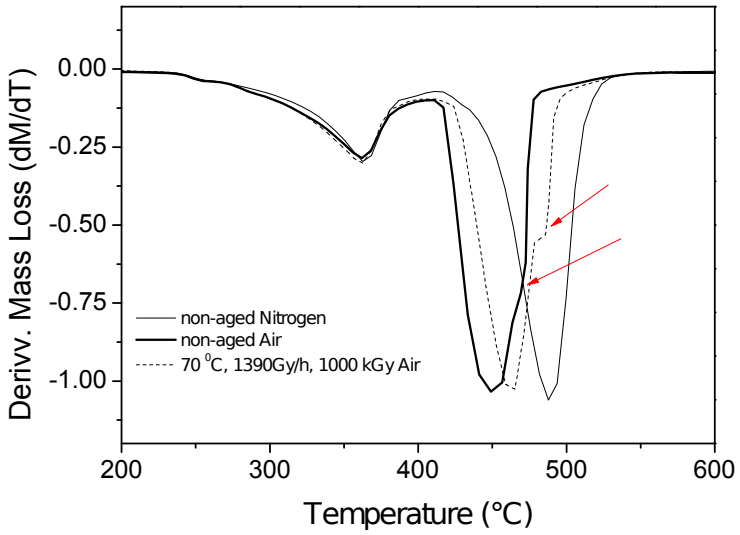

Figure 3.41: *The derivative mass loss under air and nitrogen - inner insulation.*

Moreover, the DTG curves under air show additional complexity with respect of thermal decomposition. Namely, the decomposition peak at about 450^0C exhibits a shoulder at the high temperature side of the

peak, see Fig. 3.41. This additional decomposition step is not observed when the measurements are performed in nitrogen. In the case of outer insulation samples, similar behaviour is observed, with that difference that for the same resolution (heating rate) the two peaks were better resolved.

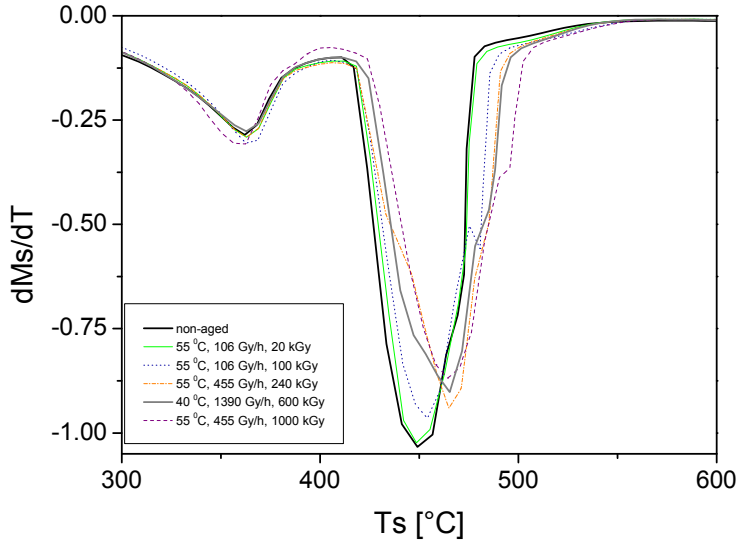

Figure 3.42: *The derivative mass loss under air for samples aged under different ageing conditions - inner insulation.*

The observed minima of inverted peaks on DTG curves are analysed, see Fig. 3.42 The peak temperature corresponds to the maximum decomposition rate and the peak intensity (integrated area) can be correlated with the total mass loss in given temperature range. The peak at the 360^0C (P_1) does not change with the ageing and the same was observed for the outer insulation. The P_2, is located around 440^0C for non-aged or little aged tubular samples. The intensity of the P_2 decreases and it shifts toward $\sim 460^0C$ by increasing the dose.

Swelling measurement

The variation of swelling ratio as a function of dose for inner insulation is presented in Fig. 3.43 and the variation of Gel fraction is presented in Fig. 3.44.

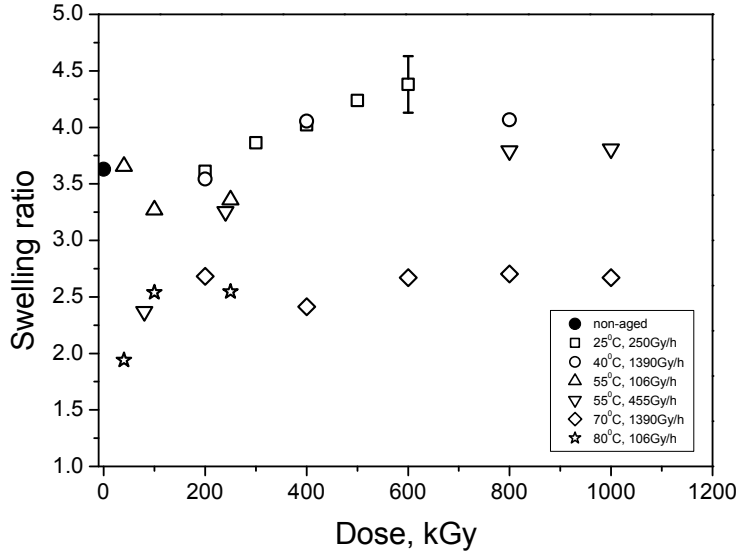

Figure 3.43: *The variation of swelling ratio as a function of dose for non-aged and several aged industrial specimens - inner insulation.*

The swelling ratio of non-aged inner insulation sample is lower with respect to the outer insulation. The values are 3.36 and 4.2 for the inner and outer insulation, respectively. This could indicate the network structure density of non-aged inner insulation material is slightly higher. For the batches aged at low temperatures, 25 and 40^0C, the swelling ratio dos not seem to change importantly for the low doses (up to about 300 kGy), but afterwards it clearly increases. Contrary, for the samples aged at high temperatures, 70 and 85^0C, the swelling ratio is observed to decrease for all measured doses. With respect to the samples aged at 55^0C: for the samples aged at 106 Gy/h significant change of the swelling ratio is not observed for the investigated doses, and for the samples aged at 455 Gy/h the initial drop of the swelling ratio is followed

by its increase. The dose rate effect is not observed on swelling results of tubular specimens.

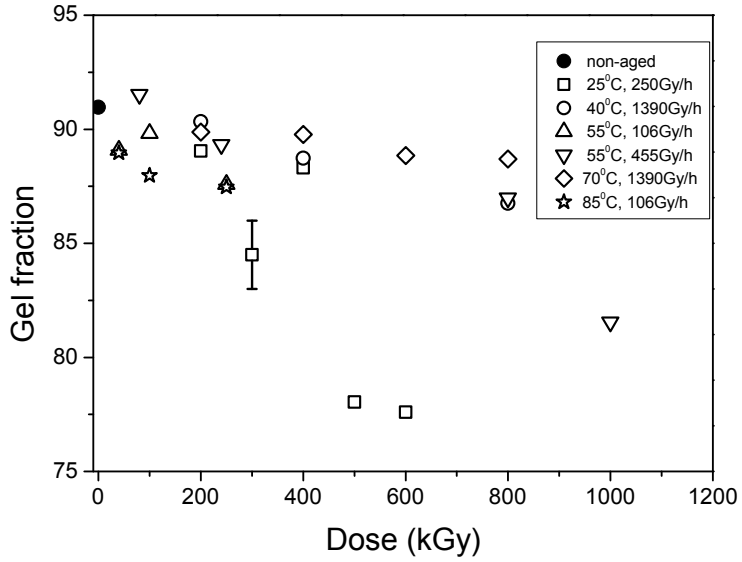

Figure 3.44: *Gel fraction as a function of dose for non-aged and several aged industrial tubular specimens.*

The gel fraction data are presented in Fig. 3.40. After the initial stagnation period, the gel fraction value mainly decreases. Similar was observed for the outer samples. The gel fraction of the non-aged sample is high, about 92 %, which might indicate that the initial density of the tubular insulation network is rather high, while the evolution of the gel fraction might indicate the destruction of this network with ageing. The dose rate effect is observed as slower decrease of the gel fraction for samples aged on the high dose rate versus faster decrease for sample aged at lower dose rates.

3.3.4 Discussion on the experimental investigation results for industrial EPDM - inner insulation

Composition of the inner insulation

Next to the outer insulation of the investigated NPP cable, the inner insulation was extracted, aged and analysed. The outer and inner insulation of the investigated cable are supposed to have similar composition, with EPDM, EVA and ATH being the main components. This is confirmed, primarily by the ATR-FTIR spectra. The differences between the inner and outer insulation are observed when measuring the mechanical properties and by chemical analysis. The ATR-FTIR indicates that it is possible that outer insulation contains more ATH. The TGA residue is considered to mainly originate from the fire retardant decomposition, possibly including a small amount of carbon black since the samples are black. After the TGA up to 600^0C was performed, the residue mass percent was higher for the outer insulation (40%), than for the inner (30%). Accordingly, it can be assumed that the outer insulation has more fire-retarding filler. This assumption is in accordance with the industrial practise to make the outer insulation more mechanically and fire resistant, since the main expectation out of jacket is to protect the inner layers. Moreover, there is an indication that additional fire retardant is present in the inner insulation, since two ATH-FTIR peaks could be related to presence od hydromagnesite. Hydromagnesite decomposes releasing water at about 220^0C, which is similar to the decomposition of ATH. Additional mass loss steps, related to the release of carbon dioxide, should follow [89]; but the mass loss expected at temperatures about 515 - 640 ^0C was not observed on TGA curves. It can be concluded that, if there is some hydromagnesite in the formulation of inner insulation, its quantity can be assumed to be low. Furthermore, estimation of the EVA content was made according to the TGA mass loss within the temperature range where VA and water release are expected from EVA and ATH, respectively (between 250 - 380 ^0C), and the assumption that the residue is mostly a product of a fire retardant decomposition (Al_2O_3). This estimation indicated higher EVA content in the inner insulation than in outer, see Table 2.1.

The tensile and indenter test revealed that the ultimate tensile stress and IM are higher for the non-aged inner insulation, with the elongation at break being significantly higher. The differences in the tensile test procedure and in the sample shape are not expected to be the reason for the observed mechanical parameter variations between the two. The difference in the composition and structure might be. The results of the swelling test: lower swelling ratio and slightly higher gel fraction value for the inner insulation, could indicate that the non-aged inner insulation is a bit more cross-linked in comparison to the non-aged outer insulation. Moreover, the cable from which the samples are stripped out, was placed in a storage for about 30-40 years prior testing, and it is possible that the outer insulation aged more during this time, in comparison to the inner one, since the outer is more exposed to the environmental ageing stressors.

Mechanical properties

Regarding the evolution of the mechanical parameters with ageing dose, it is observed that the changes of all investigated parameters are less dependant on the ageing conditions, in the case of inner insulation. Contrary to the observation for the outer insulation materials, where the dose rate effect was found to be significant, in the case of inner insulation samples dose rate effect seems to be strongly suppressed. In the case of outer insulation the 50 % absolute and relative elongation was reached at the range of the doses starting from about 250 kGy up to the about 1200 kGy, depending on the ageing conditions (primarily dose rate). The range of the doses at which 50 % relative elongation is achieved for the inner insulation samples seems to be much narrower in comparison to the one of the outer insulation. Quasi-linear elongation at break decrease with dose is observed and, according to the previous study, it could originate from more homogeneous oxidation [67].

For the inner insulation samples it seems that nominal UTS stays stagnant or just slightly increases up to the decrease point, which seems to be sharp. The increase of the nUTS, observed for the low doses, seems to be more significant for outer insulation data. The true UTS increases

up to the 100 kGy, and then decreases. The tUTS variation with dose seems to be very similar for all the sample batches, regardless the ageing conditions. The evolution of Young's modulus with increasing dose supports the nUTS data up to some extent. For the samples aged at higher temperatures (higher than 40^0C), no important change of the YM is observed up to about 800 $\pm$ 200 kGy. From this dose range the YM is observed to increase. For the samples aged at 25^0C and 40^0C, the YM of aged samples is observed to be significantly higher in comparison to the non-aged sample. Even being significantly higher, the YM is rather constant with the dose increasing up to about 900 $\pm$ 100 kGy. From this dose range it increases slightly more. The same reasoning for the correlation of the tensile parameter changes to the sample structure changes will be applied for the inner insulation as it was in the case of outer insulation, see Section 3.2.4. Accordingly, observed evolutions of the UTS and YM seem to indicate that cross-linking and chain-scission are in competition, without significant dominance of one of them, for most investigated samples up to the high doses.

Swelling test is observed to be good as a technique to support the investigation of the network structure evolution with ageing. The increase of swelling ratio with dose indicates decrease of cross-linking density, while the decrease normally indicates the increase in polymer network density, which is the most often due to cross-linking prevalence. At the doses where no significant change of the swelling ratio is observed cross-linking and chain scission are supposed to be in competition. Accordingly, the evolution of the swelling ratio with dose should indicate following processes during ageing: for the batches that are aged at the low temperatures the period of cross-linking to chain scission competition is followed by a chain - scission dominance; for the batch aged at 55^0C and 106 Gy/h chain scission and cross-linking seem to be in competition, without significant dominance of any mechanism; for the batch aged at 55^0C and 455 Gy/h the dominance of cross-linking is followed by a dominance of chain scission; while for the batches aged at the high temperatures, the dominance of cross-linking is observed. The gel fraction is observed to dominantly decrease for all investigated samples, which is an indicator of the network destruction with ageing. Similar is

observed for the outer insulation. For both insulations, the initial gel fraction i.e. the gel fraction of the non-aged samples is already rather high. This could be a reason why an important increase in gel fraction, which could be expected in some cases at low doses on the basis of the tensile and swelling ratio data, is not observed.

The analysis of the IM data indicates that inner insulation hardens with ageing, i.e. the IM increases with the ageing dose. The correlation of the IM with the elongation at break, observed for the outer insulation, seems to be valid for the inner insulation material. IM versus elongation at break for the inner insulation data is presented in Fig. 3.45 and indeed a linear correlation is observed, and can be presented by the equation: IM = -6.6e + 19.2

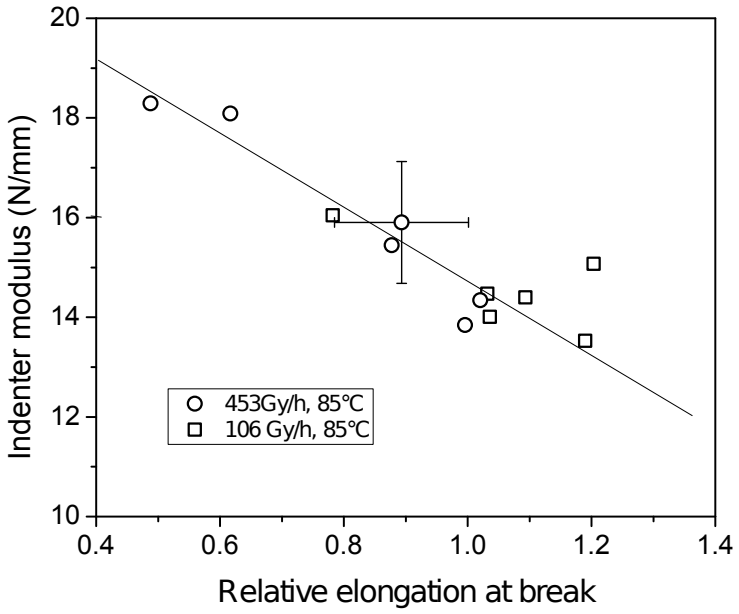

Figure 3.45: *The relation between indenter modulus and relative elongation at break for samples aged at 85^0C - inner insulation.*

When IM profiles are analysed, no profile is observed, which could confirm that the inner insulation samples age rather homogeneously. Regarding discussion about the indenter modulus as a potential control

monitoring technique for the inner insulation, it seems that it has potential since the property is observed to be suitable as an ageing indicator for this type of material. But IM investigation of the inner insulation requires dismantling of a small cable part. Due to the fact that generally, the thickness of inner insulation of a low voltage cables is small, some instrument modification would be welcome, especially for the instruments used in industry that are in majority of cases designed to measure the IM of jacket and whole cable samples.

3.3.5 Predictive modeling

In order to attempt to describe and predict the behaviour of insulation with ageing, the elongation at break variation with ageing time is analysed. The attempt is made to identify all the experimental data using the same model and model parameters that are used for the outer insulation. Good agreement is observed between the experimental data and data calculated using the fixed parameter values previously determined for the outer insulation. According to our identification, all the model parameters are determined as a constants within investigated ageing conditions, except the K_{irr}. The behaviour of K_{irr} with dose rate is analysed and K_{irr} as a function of the dose rate is shown in Fig. 3.46.

By increasing the dose rate, the K_{irr} parameter increases monotonously irrespectively of the irradiation temperature. This behavior is similar as for the outer insulation samples. The full line presented in Fig. 3.46 is simulation of the equation $K_{irr} = CI^{\alpha}$, where I is dose rate, α is dose rate exponent and C is a constant. The K_{irr} versus dose rate function is observed to be linear within the investigated dose rate range and it could be described by the equation: $K_{irr} = 2\text{x}10^{-5}\text{I}$. Linear like dependance is observed to be better for describing the evolution of the K_{irr} with dose for outer insulation at lower dose rates, in comparison to the square root function that could be used as well.

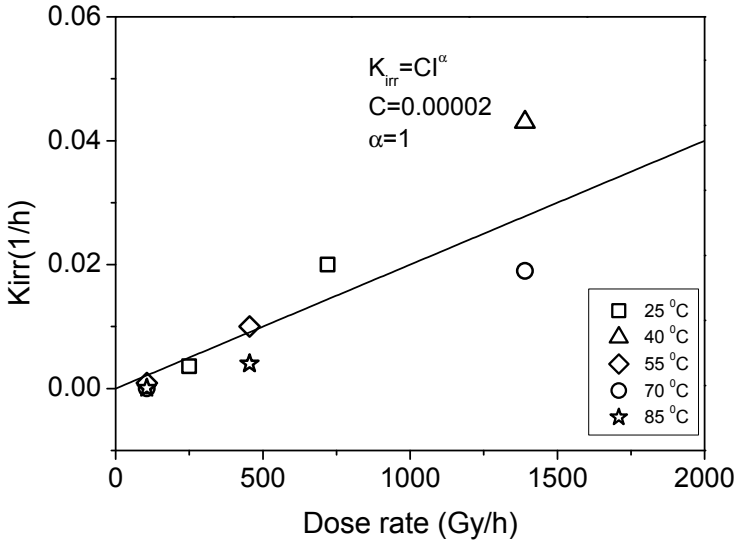

Figure 3.46: *Radiative reaction rate constant as a function of dose rate - inner insulation.*

3.3.6 Physico-chemical properties

The thermal decomposition data of the inner insulation are observed to follow similar behaviour to what was observed for the outer insulation. The mass loss rate, for the air TGA, is observed to depend on the material total absorbed dose. On the contrary, no important difference is observed between the mass loss curves of the non-aged and samples aged under different ageing conditions, up to the different doses, when TGA was performed under nitrogen. Since the thermal decomposition is observed to be dose dependant for the oxygen containing atmosphere, it is assumed that the degree of the sample oxidation previously accumulated during the accelerated ageing, could be the cause for the observed behaviour. The analysis of DTG curves provided more details about the mass loss variations between the non-aged and aged samples, thermally decomposed under air. Two peaks are observed. No important change with the ageing was observed for the first peak, P_1 (observed at about 360^0C). The intensity of the P_2 is observed to decrease while it shifts

toward higher decomposition temperatures, by increasing the dose. In addition, a small shoulder at the high temperature side of the P_2 peak is observed.

In order to analyse the P_2 and the observed "shoulder", and compare their evolution as a function of the dose with what was observed for the outer insulation, the DTG curves were fitted using two Gaussian peaks, numerated as P_2' and P_2'', see Fig. 3.47 a, b. The obtained fit showed that with sample ageing the P_2' decreases while the P_2'' increases by increasing the dose. This is similar to the evolution of the P_2 and P_3 from the outer insulation data, with the difference that for the same decomposition rate (resolution), the two peaks were observed as clearly resolved for the outer insulation, while for the inner insulation a peak with a shoulder is rather observed. Moreover, clear shifts of both Gaussian peaks toward higher decomposition temperatures with increasing the dose is observed for inner insulation. This means that the activation energy for the sample decomposition increases with dose. This was not so clearly observed in the case of the outer insulation.

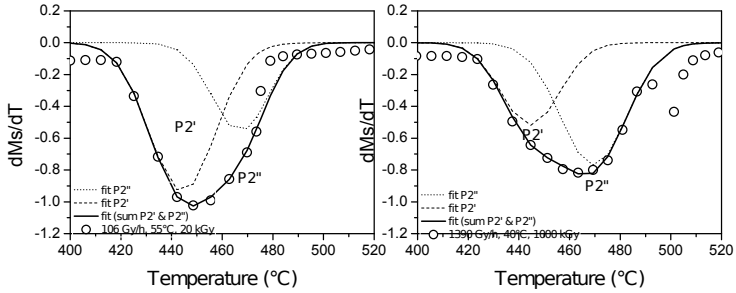

Figure 3.47: *a)Gaussian fit with two peaks P2' and P2" for very low dose. b) Gaussian fit with two peaks P2' and P2" for high dose.*

The evolution of the P_2' and P_2'' peak integrated intensities as a function of the dose are presented on Fig. 3.48. It can be observed that the dose rate effect is less pronounced in comparison to the outer insulation data.

The mass loss correlated to the P_2' is assumed to be related to the thermal decomposition that occurs via oxidation, as the main decomposition mechanism, because it take place at lower decomposition tem-

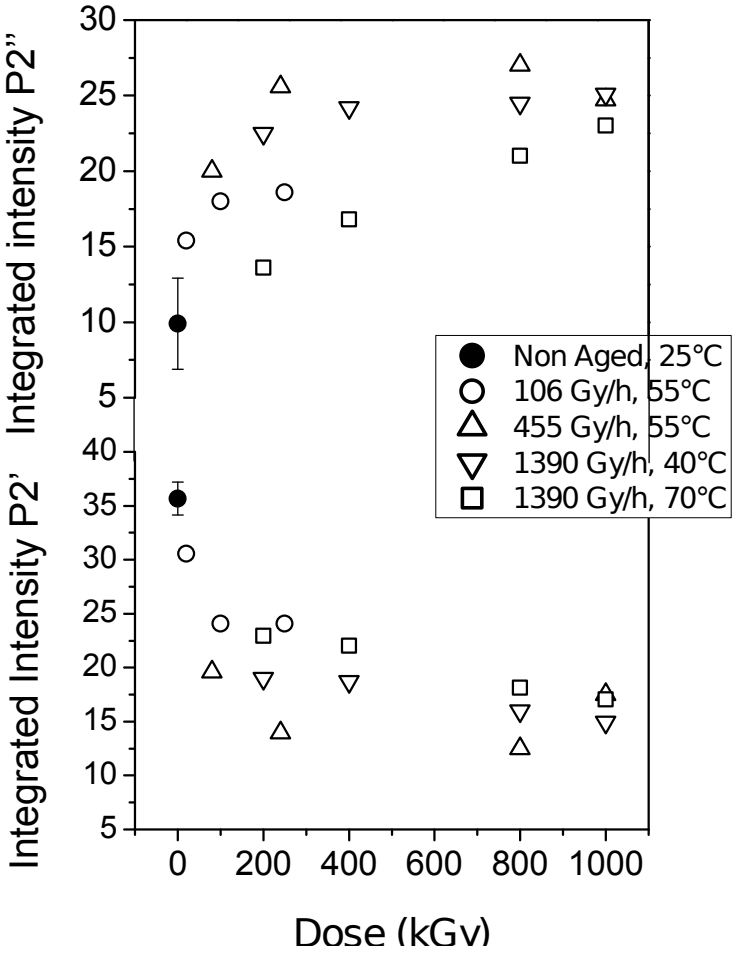

Figure 3.48: *The variation of the P_2' and P_2'' peaks as a function of dose - inner insulation.*

perature in comparison to the P_2", that is assumed to be related to the decomposition via random chain scission mechanism, that requires higher activation energy in comparison to the oxidation and takes place at higher temperature. This is further related to the decomposition of the two portions of the material: a) the first portion that was not oxidised during the accelerated ageing is assumed to dominantly decompose

via oxidation (P_2') and b) the second portion that already undergo oxidation during the accelerated ageing and that decomposes dominantly via random chain scission mechanism during the TGA (P_2''). Moreover, the activation energy for both processes seem to increase with ageing.

Oxidation is assumed to be the main ageing mechanism for the inner insulation, but it is supposed that the oxidation during accelerated ageing is more homogeneous within the inner insulation material, in comparison to the outer insulation. The difference in the composition could be one of the reasons for the observed differences in the oxidation extent and distribution with ageing. But the main reason is assumed to be the sample thickness. The inner insulation samples are about two times thinner in comparison to the outer insulation, and it is assumed that oxygen diffuses faster and distributes more evenly through the thickness. Additionally, if the concentration of filler is less in comparison to the outer insulation layer, as it is indicated by the FTIR and TGA, then it could also enhance the oxygen diffusion.

3.4 General discussion and conclusions on results for industrial cable polymers and proposed procedure for cable life-time prediction

Accelerated, simultaneous radiation and thermal ageing, under various dose rates and temperatures, was performed on the industrial cable insulation samples. Two type of samples were studied: 2 mm thick dumbbell shaped, stripped out of the cable outer insulation; and 1 mm thick tubular, made out of the cable inner insulation. The cable was made around '70s or '80s and stocked in the NPP cable storage prior the accelerated ageing.

Although both type of samples have very similar composition and they were aged under same ageing condition, a variation in the ageing behaviour was observed. Starting with mechanical properties, it was firstly observed that the elongation at break and ultimate tensile stress values of the non-aged samples were higher in the case of the inner insulation

specimens. This could indicate that during the non-accelerated ageing (while cables were stored) the outer insulation aged more, probably because it is more exposed to the environmental ageing stressors. The difference was observed in the decrease rate of the elongation at break with dose, which was more equal for the inner insulation in comparison to the outer insulation specimens under all applied ageing conditions. When the range of the doses at which the elongation at break reaches 50% relative value was compared it was observed that it is much more narrower in the case of inner insulation samples (800 $\pm$ 50 kGy), in comparison to the outer insulation ($\sim$ 250 kGy to $\sim$ 1250 kGy), where this dose was very dependant on ageing conditions, especially dose rate. In total, the evolution of the mechanical properties with dose was observed to be much more dependant on the applied ageing conditions, especially the dose rate dependant, in the case of the outer insulation. It was supposed that the inner insulation specimens, which are thinner than outer insulation ones, age more homogeneously under applied ageing condition.

The predictive modelling of the elongation at break data was based on the Menlow and Dakin kinetic model [24, 25, 76]. The radiative term was observed to be more dominant ageing stressor in comparison to the thermal one, which could be expected for the applied temperatures, according to the literature [24]. For both type of samples, inner and outer, all experimental results were reproduced by varying one parameter, the pre-exponential factor of the irradiative rate constant, K_{irr}. Accordingly, it was assumed that the radiation induced oxidation is the main degradation mechanism for industrial EPDM samples.

Regarding the application of the indenter modulus as non-destructive cable condition monitoring technique, it was observed that it has a good potential, especially for an outer insulation i.e. the cable jacket. The resolution of IM measurement is important regarding its application. In the case where IM was penetrating deep in the samples bulk (standard industrial IM parameter), a linear correlation with elongation at break was observed, and it was assumed to originate from the extent of the sample oxidation i.e. the increase of the oxidation layer thickness causes increase of the IM and decrease and the elongation at break. When more

precise tools are applied, like micro or nanoindenters, cross-sectional investigation is possible and it is convenient for the mapping the oxidation distribution through the sample thickness.

The investigation of the evolution of physico-chemical properties provided a direct link between the mechanical and physicochemical properties. While the thermal decomposition of the samples was not dependant on ageing when it was performed under nitrogen, it was observed to be dependant on the ageing evolution when it was performed in air. The thermal decomposition curve were observed to shift toward higher decomposition temperatures with increasing the dose, for both, inner and outer insulation samples. This was supposed to be a consequence of a difference in the extent of the oxidised portion of the samples, which was supposed to increase with dose i.e. ageing time. The observed peaks from the DTG curves were related to the decomposition process, considered to be dominantly responsible for the mass loss at the temperature on which the peak is positioned. The P_1 with the maximum weight loss at 360^0C was related to the decomposition of the ATH and evaporation of the acetic acid from EVA. No variation of the P_1 was observed with increasing the dose. The following peaks that appear at higher temperatures were related to the decomposition of the polymer chains via two different processes. The first polymer chain decomposition process, that is ongoing at lower temperature (correlated to P_2 for outer and P_2' for inner insulation) and requires lower activation energy is supposed to be the decomposition of the polymer through the reaction with oxygen contained in the TGA atmosphere (which was air), while the second decomposition process (correlated to P_3 for inner and P_2" for inner insulation), activated at the higher temperature is correlated to the scission of the polymer bonds. It was observed that the intensity of the peak correlated to the thermal decomposition via oxidation gradually decreases with the dose, while the intensity of the peak correlated to the thermal decomposition via random chain scission gradually increases. Additionally, it was observed that for the same resolution (the same TGA heating rate) the two polymer decomposition related peaks were more closer for the inner insulation samples. Interestingly and unexpectedly, the evolution of the P_2 and P_2' intensity with the dose

was observed to mimics the evolution of the elongation at break. Even the observed dependance of the elongation at break data on the ageing conditions (the dose rate and temperature) i.e. the "dose rate effect" could be observed for the decrease of the peaks with the dose.

The observed evolution of the mechanical and physico-chemical properties together with the data obtained by the elongation at break modelling indicated that the main degradation mechanism in both type of the samples is oxidation, mainly induced by the radiation. It was also observed that the degradation (oxidation) seems to be more homogeneous in the inner insulation samples, which is thought to be related primarily to the difference in the thickness - the inner insulation is about two times thinner in comparison to the outer insulation. The rather heterogenous oxidation, assumed for the outer insulation samples aged under the high dose rates and low temperatures, is most probably caused by the diffusion limited oxidation. The oxidation diffusion is known to depend on many factors, primarily the polymer diffusion coefficient and oxygen permeability, but also on the ageing conditions. For the high dose rates, and high temperatures, the creation of the radicals at the sample surface is high, and then it may happen that the oxygen is gradually consumed within the surface, which hinders it diffusion toward the sample bulk. For the short ageing times and under the low-oxygen concentration atmosphere, the bulk of the sample might stay non-oxidised under irradiation, and for the EPDM, it means that the cross-linking process will predominate. Contrary, the sample surface where the oxygen is gradually consumed, will dominantly undergo chain-scission. This creates degradation heterogeneity within the sample. Very important factor, regarding the DLO is certainly the sample thickness. It is logical that the oxidation is expected to be more homogeneously distributed within the thinner sample.

Regarding the temperature influence, within the studied range, thermal oxidation term is not expected to have an important influence as the degradation factor, especially comparing to the influence of the radiative term. But it is expected that the diffusion of oxygen is enhanced with the temperature increase. Also the influence of the temperature on the once started decomposition reaction has to be accounted for, especially

the effect of the high temperatures on the hydroperoxide decomposition. Both, increased oxygen diffusion and enhanced hydroperoxide decomposition, lead to an increased oxidation and oxidation layer thickness.

The TGA measurement, under air atmosphere, could be used to measure the extent of the oxidation and ratio between the oxidised versus non-oxidised portion of the material. This measurement could be further related to the changes in the mechanical properties, and used in material life-time prediction modelling.

Upon the ageing during which the oxidation is thought to be the main mechanism, depending on the ageing conditions, ageing time and sample characteristics, the extent and the distribution of the oxidised portion of the material differ, but unless the material undergoes complete degradation, it could be stated that there are always oxidised and non-oxidised portions of the material. The oxidised layer thickness is considered to govern elongation at break, IM (measured as by standard industrial technique), and the thermal decomposition evolution with ageing, which explains the observed correlations of these parameters.

3.4.1 Proposed procedure for cable life time prediction

In order to evaluate the life time of the cable, the first step is to determine if DLO took place during the accelerated ageing. Thshica can be determined based on TGA measurements or profiling (e.g. IM) measurements at the cable cross-section. The cable life time prediction assumes the hypotheses in force during accelerated ageing conditions that ensure homogeneous oxidation of the samples remain applicable, since it is considered to be the case for the operational conditions.

If the existence of DLO is not confirmed, the life time estimation should be based on the modeling performed in the case of inner insulation in the second step.

The appropriate parameters from the Eq. 3.4 should be determined. For a given dose rate, the variable parameter (pre-exponential factor of radiative contribution of the pseudo reaction rate constant) K_{irr} should be calculated from the K_{irr} versus dose rate graph (relation). Here, the

evaluation is made assuming the operational conditions corresponding to the temperature of 40^0C and dose rate 1 Gy/h, [4].

The values of the fixed parameters used are already presented in Table 3.2, for the outer insulation; which are exactly the same as the one from the Table 3.3, for the inner insulation. The K_{irr} in this case will be calculated from the Fig. 3.26 for the outer insulation and 3.46. for the inner insulation. For a given dose rate of 1 Gy/h the K_{irr} is 6x10^{-5} h^{-1} and 2x10^{-5} h^{-1}, for the outer and inner insulation, respectively.

On the basis of end of life criterion set to be the e_t/e_0=0.5 (50% relative elongation at break), the time is calculated based on Eq. 3.2 at which this criterion is reached is calculated to be only about 36 year for the outer insulation and about 101 year for the inner insulation.

Then, the end of life is estimated to be at about 2.8 times lower in the case of outer insulation in comparison to the inner insulation. Possible reason could be that the prediction is made using the parameters obtained by accelerated ageing of the polymer that was already aged. It was already discussed that the initial elongation at break is much higher in the case of inner insulation in comparison to the outer (279.1 $\pm$ 33 % inner versus 125.5 $\pm$ 10 % outer). This was explained by the fact that the tested cable was produced about 30-40 years ago. Since then it was stored in the NPP cable storage. During this time the cable aged, in the way that the outer cable insulation degraded more than inner, since it is exposed to the environment. Original initial value of the elongation at break for non-aged insulation samples are not known, but it can be evaluated based on the inner insulation elongation at break (it corresponds to elongation at break of the nowadays produced cable, see Appendix A, Figure A.6).

As a result we propose to use the parameters obtained for the inner insulation. The time to failure may be also calculated using the 50 % absolute elongation, which would then give even less conservative values. In this case, the time to reach this end of life criteria is about 1000 and about 60 years, for the inner and outer insulation, respectively.

The time to failure may be calculated using the 50% absolute elongation, which would give even less conservative values. The time to reach this

end of life criteria, for the inner insulation, goes to about 1000 year, and for the outer, to about 60.

The use of IM is reliable only if DLO does not play the role. IM value can be transformed to an elongation at break value through an existing correlation, which further can be applied to calculate life time. For example, the measured IM value for the non-aged outer insulation EPDM is 8.6. Using the linear function which describes the IM versus elongation at break relation (IM = -0.07e + 17.5 $\pm$2) the elongation at break is calculated to be 127.14 %. Time to reach 50% absolute elongation at break under the normal operating conditions (40^0C and 1 Gy/h) can be calculated using the Equation 3.2, and it is about 75 years, observed in the case of outer insulation for evaluation of the cable life time.

Chapter 4

Experimental investigation of the neat EPDM material

Due to the complexity of industrial samples, regarding their chemical composition, similar ageing procedure was applied on more simple samples produced in the laboratory of the UCL and named "neat EPDM polymer" samples. Tensile test and TGA were applies as monitoring techniques and performed on the non-aged and aged neat polymer samples. Two types of "EPDM - like" polymer materials: Nordel 3722 and Engage 8100, were recommended for this study and kindly provided by "Dow chemicals", see Section 2.1.2. The samples were produced in the form of 2 mm thick dumbbells and samples were aged under the three different dose rates and two temperatures. Section 4.1 is devoted to the experimental investigation of Nordel and Section 4.2 to the Engage. General discussion of the results obtained by the experimental investigation of neat polymers is presented in Section 4.3.

4.1 Experimental investigation of Nordel 3722

4.1.1 Mechanical properties

Uniaxial tensile test

Examples of typical nominal stress - strain curves of the non-aged and aged Nordel are shown in Fig. 4.1. Clear difference is observed in the tensile behaviour and ultimate tensile values between the industrial and neat EPDM. The industrial EPDM had significantly lower elongation at break value (see Sections 3.2.1 and 3.3.1), compared with the Nordel. This is expected knowing that the industrial polymer contains additives that inhibit chain mobility and extension properties. The mean strain value for Nordel is 975 $\pm$20 %.

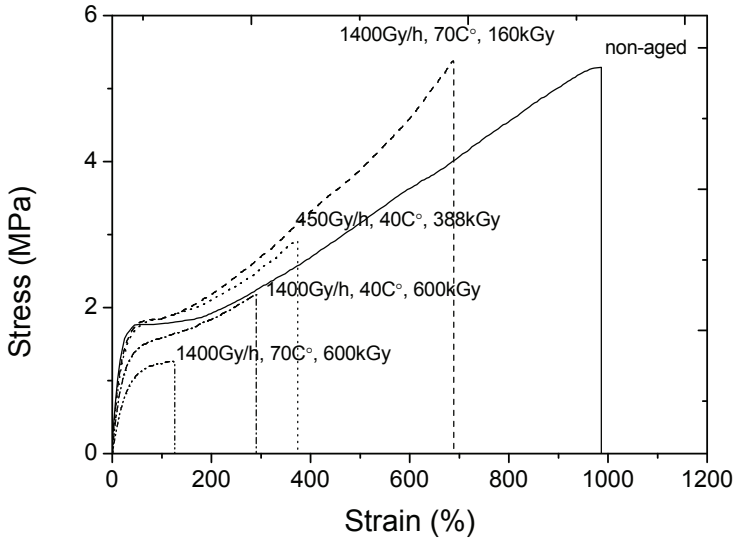

Figure 4.1: *The nominal stress - strain curves of several samples, aged at different temperature and dose rates - NORDEL.*

A yield point can be observed in the tensile curve of non-aged Nordel as a consequence of its semi-crystalline structure. For semi-crystalline polymers, the necking mechanism involves orientation and destruction of

semi-crystalline morphologies, resulting in the existence of a yield point [7]. Yielding point disappears at high doses. The appearance of necking during the mechanical testing of Nordel samples is illustrated in Fig. 4.2. While the industrial EPDM after rupture completely recovers its initial shape, the Nordel samples irradiated to low dose exhibit macroscopic plastic deformation/necking. On the contrary, at high irradiation dose both Nordel and industrial EPDM broke in elastic region of the stress strain curve.

The evolution of relative elongation at break as a function of the ageing dose is presented in Fig. 4.3 for two ageing temperatures 40^0C and 70^0C. The elongation at break decreases monotonously and for the applied ageing conditions the total destruction of the sample is reached. For the samples that were aged up to the very high doses (1601 kGy and 2402 kGy), the measurements could not be performed since the samples were disintegrated and sticky. For the industrial samples, which were aged under similar conditions, much less decrease of the elongation at break was observed and the total disintegration was certainly not observed (the lowest value of the relative elongation at break was 0.25). It is clearly demonstrated that Nordel is less stable in comparison to the industrial EPDM.

The dose rate effect is not clearly observed for the sample aged at 40^0C, while it seems to be present for the samples aged at 70^0C. Namely, it seems that the elongation at break of the samples aged at 450 Gy/h and 70^0C decreases slightly faster in comparison to the samples aged at 1390 Gy/h and 2780 Gy/h. In general, within the entire ageing matrix applied, the elongation at break decrease rate is the highest for the samples aged at 450 Gy/h and 70^0C.

In Fig. 4.4 the ultimate tensile stress as a function of dose data of Nordel are presented. The ultimate stress value of non-aged Nordel is slightly lower in comparison with the one of non-aged industrial EPDM (outer insulation), which could be expected since industrial sample is cross-linked and contains mineral fillers. For the dose rate of 450 Gy/h, the initial increase in UTS, up to about 100 kGy, is observed, which is then followed by the UTS. The UTS increase is higher for the samples aged at 40^0C. The UTS dominantly decreases for the samples aged at

Figure 4.2: *Necking behaviour observed in neat polymer aged to low dose (white samples). The total recovery in industrial EPDM (black samples).*

1400 Gy/h and 2760 Gy/h.

Regarding the dose rate effect, it seems that the samples aged at the lower dose, exhibit faster UTS decrease with dose, in comparison to the ones aged at the higher dose rates. This behaviour seems to be enhanced for the samples aged at 70^0C. The ultimate tensile stress data are in accordance with the elongation at break data and both are proposing that

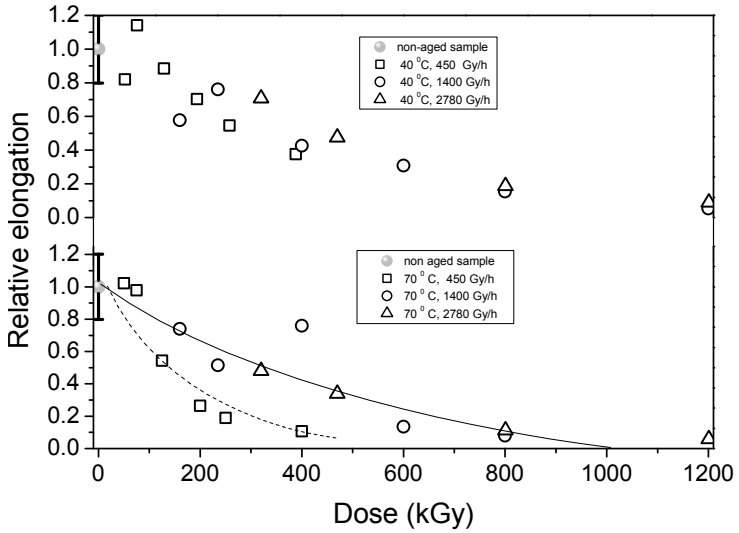

Figure 4.3: *The variation of the relative elongation at break as a function of dose for different temperature and dose rate conditions-Nordel. The lines are guide for an eye.*

the sample degradation is enhanced at the higher ageing temperature, where additionally the dose rate effect seems to be stronger.

Modelling of mechanical results

The same type of identification of elongation at break experimentally obtained data with the data calculated using the basis of Menlow and Dakin model [24, 25, 76].

The comparison between the experimental results and calculations based on Eq. 2.2 is presented for the industrial EPDM and Nordel at Figure 4.5 a) and Figure 4.5 b), respectively.

Very good agreement between the calculated and measured elongation at break data is osberved for both materials. Essentially, all experimental results could be reproduced with Eq. 2.2 by varying single parameter, pre-exponential factor of the irradiation rate constant, K_{irr}. All other parameters from Eq. 2.2 were kept constant in the calculation. They

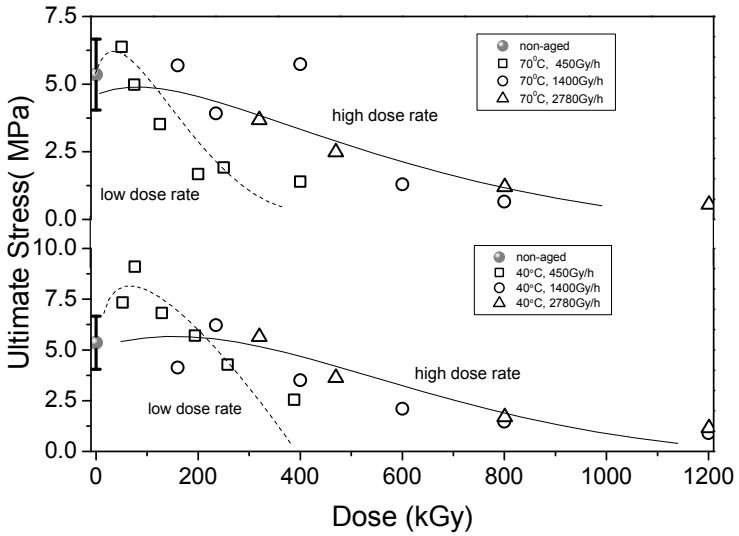

Figure 4.4: *The evolution of the nominal ultimate tensile stress with dose of aged at 40^0C 70^0C - Nordel. The lines are guide for an eye.*

are collected in Table 4.1. In comparison to the industrial EPDM, there is the difference in the parameter β value, which is 2 for the Nordel, while it is 3.5 in he case of the industrial EPDM.

Table 4.1: *The parameters used in the calculation according to the model described by Equation 2.2.*

Parameter	Value industrial EPDM	Value neat EPDM
E_{ath}	1.07 eV	1.07 eV
K_{th}	50×10^9 h^{-1}	50×10^9 h^{-1}
E_{irr}	0.065 eV	0.065 eV
β	3.5	2

By increasing the dose rate the K_{irr} parameter increases monotonously, see Fig. 4.6. K_{irr} follows a linear dependance as a function of the dose rate in the case of Nordel.

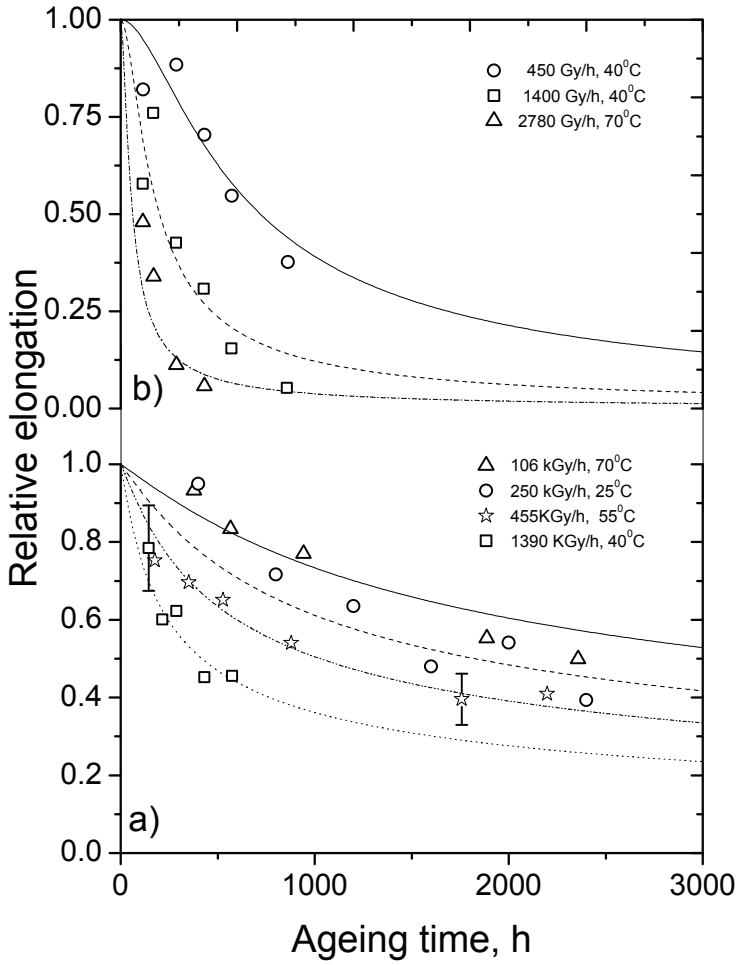

Figure 4.5: *The comparison between relative elongation as a function of the ageing time between a) industrial EPDM, outer insulation and b) Nordel.*

4.1.2 Physicochemical analysis

Thermogravimetry

Similar TGA and DTGA analysis as in the case of industrial EPDM polymer are performed on neat polymers. The results are compared with

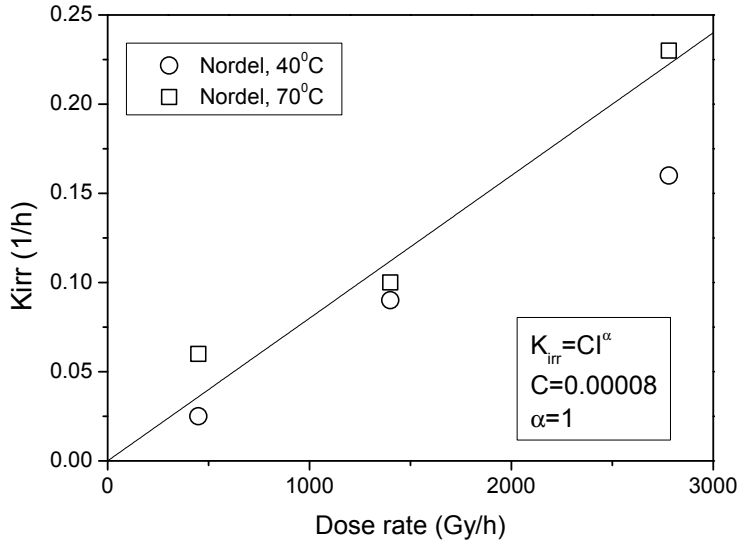

Figure 4.6: *The radiative reaction rate constant K_{irr} as a function of the dose rate - Nordel.*

the industrial ones. The mass loss curves during thermal decomposition in nitrogen and air are presented in Fig. 4.7.

During the TGA test Nordel was completely decomposed. At about 500-600^0C mass drops to zero. This is in contrast to what was observed for the industrial polymers where residue was about 20 and 30 % of the initial mass for the inner and outer insulation, respectively. The thermal decomposition of the Nordel starts at about 300^0C, contrary to the industrial EPDM, where sample mass starts to decrease at about 250^0C. Mentioned variations in the thermal decomposition of Nordel and industrial EPDM are because the composition of the industrial polymer includes EVA and ATH, which start to decompose at lower temperatures in comparison to the EPDM ($\sim$ 250^{0}C). Decomposition of ATH proceeds by formation of aluminium oxide, and it is considered to be the main component of the industrial sample residue upon the TGA.

In nitrogen, degradation process proceeds via one step, reaching its maximum decomposition rate at about 490^0C for non-aged sample, which is similar to what was observed for the decomposition of the non-aged

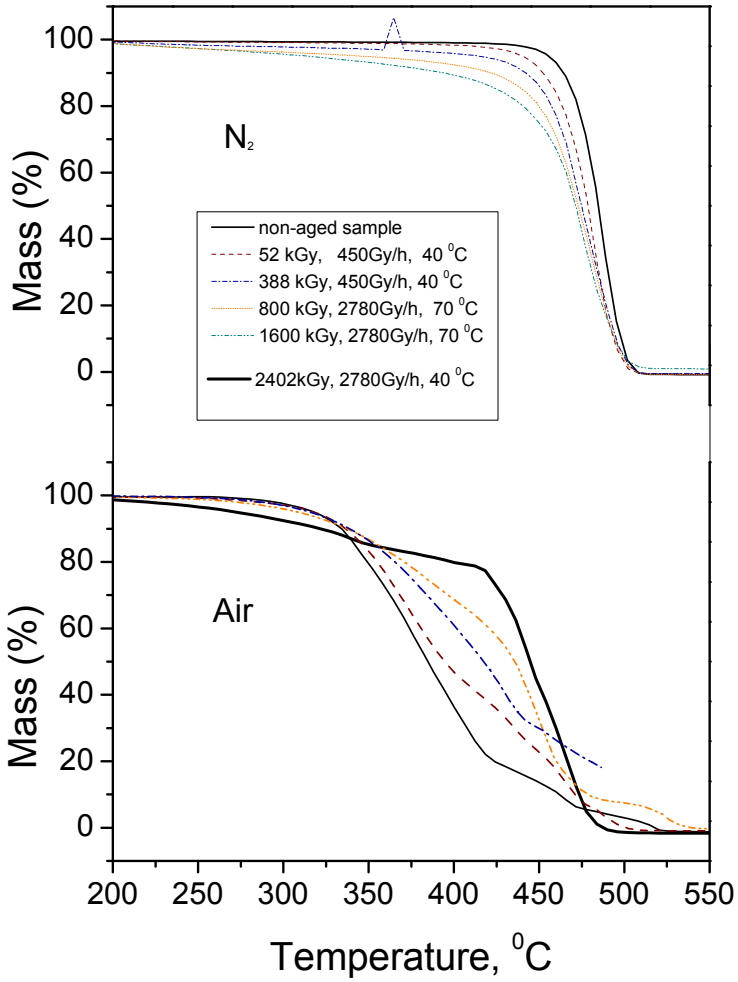

Figure 4.7: *Thermal decomposition of NORDEL under air and nitrogen .*

industrial EPDM polymer chains under nitrogen. Interestingly, the decomposition of Nordel in nitrogen is dose dependant, in a way that it shifts toward lower decomposition temperatures with increasing the dose. Moreover, the DTG analysis show that the DTG peak decreases, broadens and shifts toward left (peak temperature decreases) as a function of the dose, see Fig. 4.8. The broadening of the DTG peak with

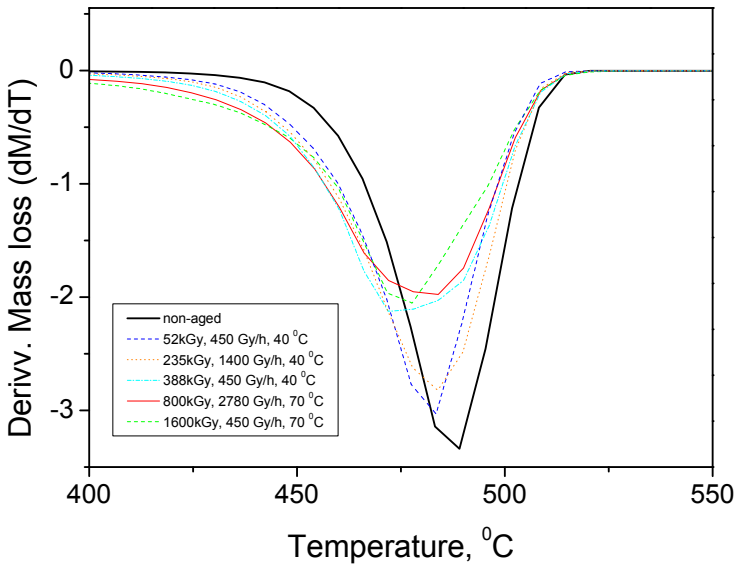

Figure 4.8: *Derivative of the mass loss curves under the nitrogen atmosphere - Nordel.*

ageing could be a consequence of the widening of the distribution of the chain length due to the chain length shortening caused by ageing. This could mean that, with ageing, less thermally stable material is created, probably by shortening of the chain length, which was not the case for the industrial EPDM.

As expected, the decomposition in air is faster in comparison to the nitrogen one and enhanced by the presence of oxygen. However, the decomposition curves of Nordel seem to be more complex in comparison to what was observed for the industrial EPDM, with more than two decomposition steps. Still, the shift of the curves toward higher decomposition temperatures could be observed. For further analysis the DTG curves were calculated and presented in Fig. 4.9.

The DTG peaks could be clearly distinguished and resolved for Nordel, but more peaks were observed in comparison to the industrial EPDM, which was anticipated considering the TGA curves. The peaks above 450^0C will be neglected, since the percent of the sample mass there is

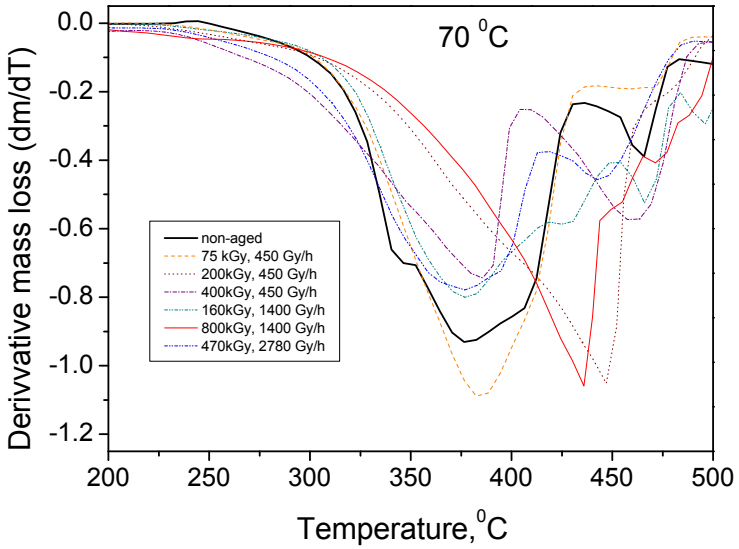

Figure 4.9: *Derivative of the mass loss curve for the thermal decomposition under air - Nordel.*

very small. The position of the first polymer chain decomposition peak is shifted toward left (lower temperatures) in comparison to the industrial EPDM. For non-aged Nordel the first peak appears at about 390^0C and for the industrial EPDM it was at 430^0C. This probably indicates that polymer macromolecules of Nordel are more sensitive to the thermal decomposition in oxygen in comparison to the polymer macromolecules from industrial EPDM.

DSC

The crystalline structure in produced Nordel dumbbells was analysed by the DSC with the heating rate of 10^0C/min. The heat flux versus temperature curves for the non-aged and two aged samples are presented in Figure 4.10. The percent of crystallinity is calculated to be about 10% and the crystalline structure melts in the temperature region from about 46^0C to 70^0C with the melting point (observed as the minimum of the peak) at about 50^0C.

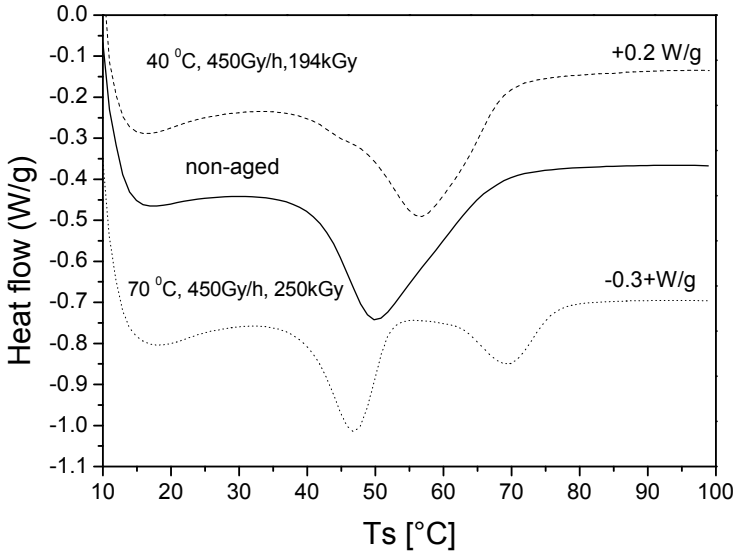

Figure 4.10: *The representative DSC curves of non-aged and aged samples - Nordel.*

4.2 Experimental investigation of Engage 8100

4.2.1 Mechanical properties

Uniaxial tensile test

Several representative nominal stress-strain curves of the non-aged and aged Engage samples are presented on the Fig. 4.11. It could be observed that, with ageing, tensile behaviour changes from ductile to brittle. This change of the tensile behaviour could be caused by the decrease of the molecular weight. According to previous studies [92], this type of copolymer will display a ductile deformation for molecular weights greater than about 30000 and brittle for lower molecular wights.

For the non-aged and samples aged up to the low dose dominant strain - hardening region could be observed. Strain - hardening slope decreases with ageing and for samples aged up to higher doses strain-hardening could not be observed. In the case of Engage an rather diffused yield

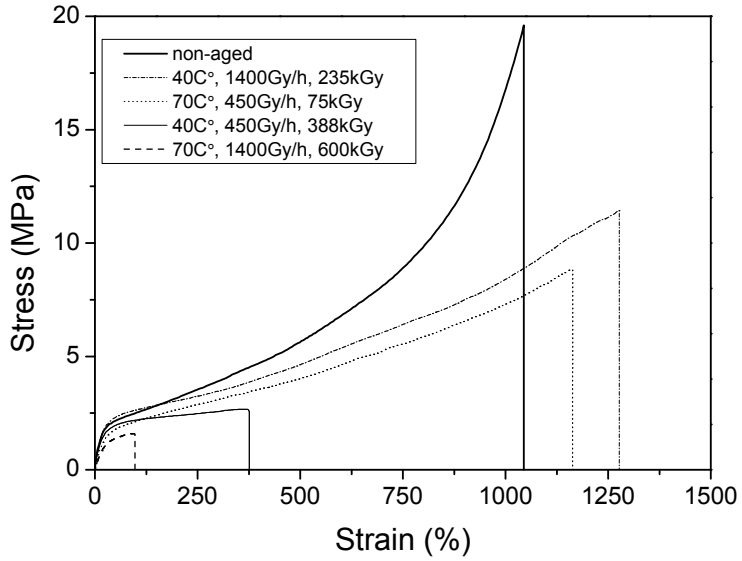

Figure 4.11: *The nominal stress - strain curves of several samples, aged at different temperature and dose rates - Engage.*

region, in comparison to the Nordel, can be observed.

The evolution of the relative elongation at break with ageing dose is presented in Fig. 4.12. The Engage has much higher values of the absolute elongation in comparison to the industrial EPDM. This is expected, considering the differences in composition and it was already observed in the case of Nordel. The elongation at break data of Engage batches aged at 40^0C do not exhibit clear decrease as a function of the dose before 300-400 kGy, and the samples aged at 70^0C before about 150 kGy. In the case of EPDM and Nordel, the decrease of elongation at break started at lower doses, in comparison to the Engage aged under similar ageing conditions, especially when one compares the samples aged at 40^0C. It is possible that this is a consequence of the competition between the chain scission and cross-linking. Indeed, after the period during which elongation at break of the aged samples does not change significantly in comparison to the non-aged one, the elongation at break drops abruptly to the lower values. It could be observed that with ageing, the

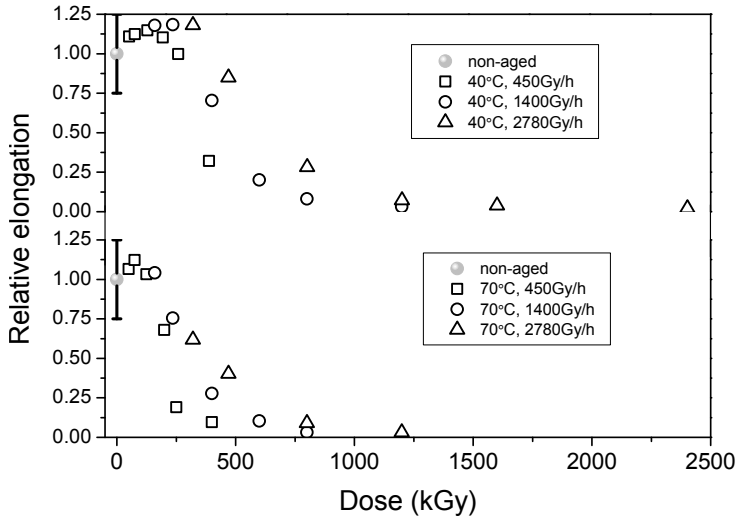

Figure 4.12: *The variation of relative elongation at break as a function of dose, for samples aged at different dose rate and dose rates - Engage.*

elongation at break of Engage approaches to zero (instant break of the sample), which means that for a given ageing conditions, the sample structure was completely destroyed. Several samples, aged at 70^0C up to the high doses, became sticky and disintegrated upon ageing, so the measurements could not be performed. What concerns the dose rate effect, it seems to exist but, it is strongly reduced in comparison to the industrial EPDM.

For the non-aged Engage, an unexpectedly high ultimate tensile value is observed (about 17 MPa), see Fig. 4.13. It is significantly higher in comparison to the industrial EPDM and Nordel. According to the stress-strain curve, the strain hardening is observed to be pronounced, and it is assumed to be the reason for increased ultimate tensile stress, with respect to the values for other non-aged investigated samples. The ultimate tensile stress value clearly decreases with ageing and the dose rate effect could be observed in a way that the decrease of stress is faster for the lower dose rate. Again, the dose rate effect is reduced in comparison to the industrial EPDM.

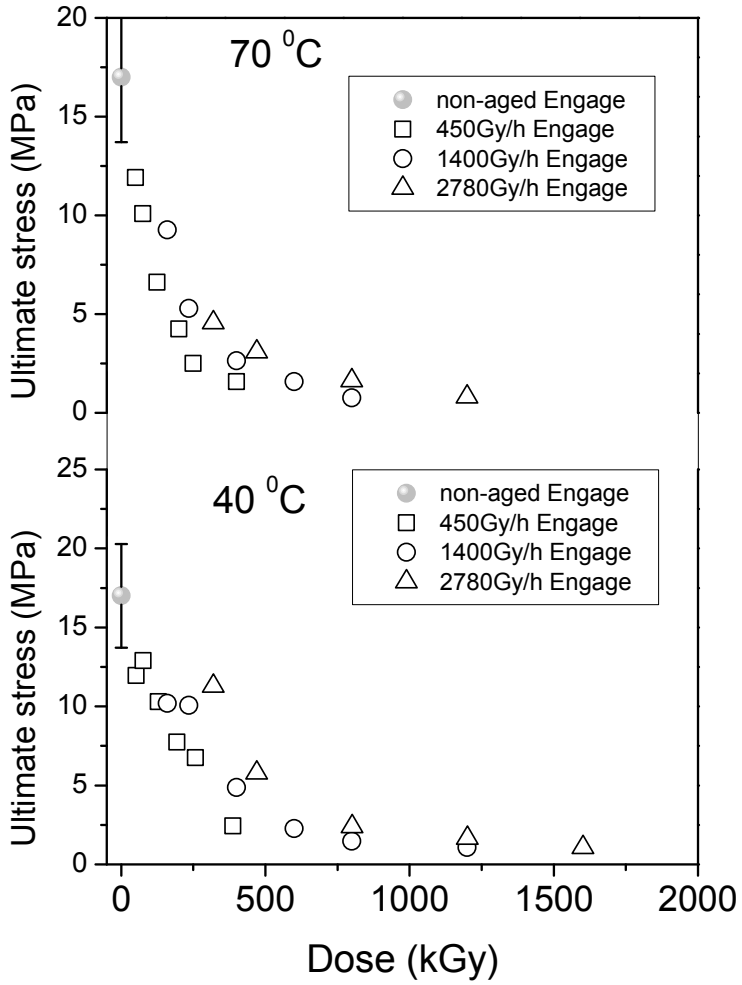

Figure 4.13: *The variation of nominal ultimate tensile stress as a function of dose, for samples aged at different dose rates and temperatures - Engage.*

Elongation at break modeling

The calculation of elongation at break value was done using the Eq. 2.3. Very good agreement between the calculated and the measured data is observed (see Fig. 4.14). All the parameters, except K_{irr}, are kept

constant and they are identical to the ones used for Nordel data, see Table 4.1. The values of these parameters are in agreement with the ones for industrial EPDM (see Table 3.2 or Table 3.3, except for the β parameter.

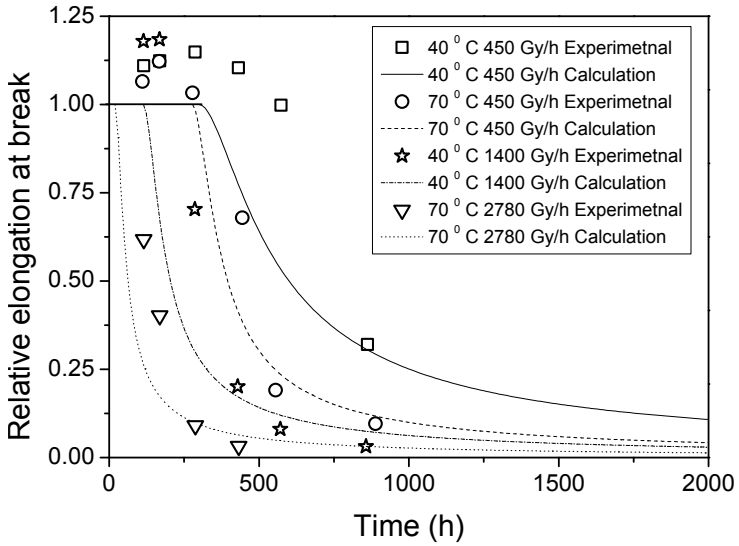

Figure 4.14: *The relative elongation as a function of the ageing time - calculated and experimental data - Engage.*

It was already observed that the elongation at break as a function of the dose behaves differently, in comparison to the industrial EPDM and Nordel. In the case of Nordel, the elongation at break value is observed to be stagnant with increasing the dose, up to about 300-400 kG, and after that it abruptly decreased below 50 %.

The evolution of the K_{irr} parameter as a function of dose is presented on the Fig. 4.15

As in the case of tubular industrial samples and Nordel, the K_{irr} for Engage is observed to follow the linear trend as a function of the dose rate.

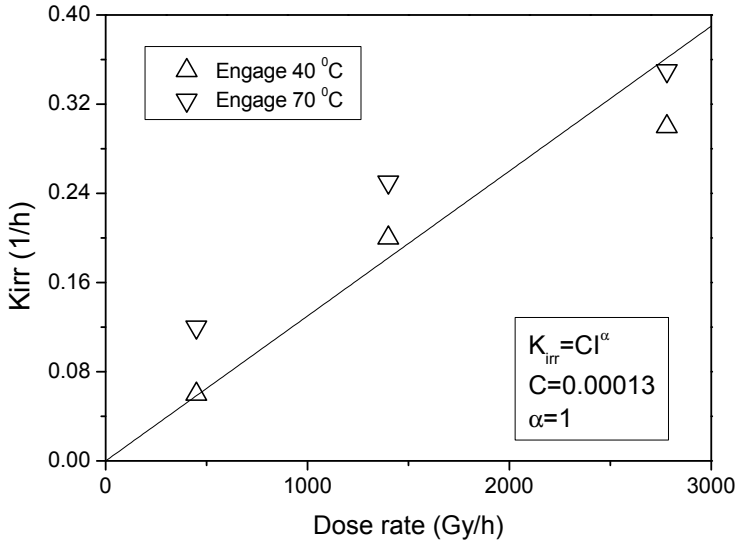

Figure 4.15: *The radiative reaction rate constant Kirr as a function of the dose rate - Engage.*

4.2.2 Physicochemical analysis

Thermogravimetry

The thermal decomposition of Engage in nitrogen is presented in Fig. 4.16. The mass loss as a function of the temperature and the first derivative of mass loss are shown in the figure. Both confirm that the Engage behaves similarly to the Nordel during the thermal decomposition in nitrogen. The decomposition can be described as a one step process, with the maximal decomposition rate at about 480^0C. With ageing i.e. by increasing the dose, the thermal decomposition curves shift toward lower temperatures. This means that less thermally stable material is created as a result of ageing, possibly by shortening the macromolecular chains (decreasing the average molecular mass).

The representative mass loss curves, for the decomposition in air, are presented on the Fig. 4.17. The thermal decomposition is dose dependant, but the dose dependance changes within the decomposition tem-

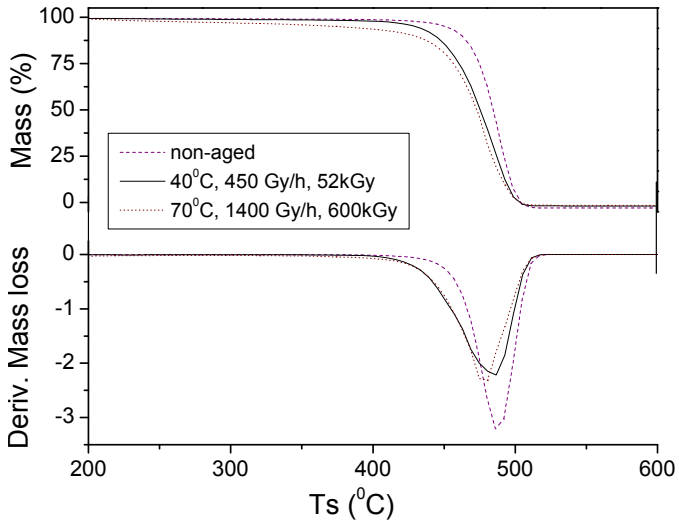

Figure 4.16: *The thermal decomposition in nitrogen: the mass loss as a function of decomposition temperature and the first derivative of the mass loss - Engage.*

peratures. At the beginning the dose dependance is similar to the one observed in the nitrogen - with increasing the dose thermal stability of the samples decreases. But as decomposition temperature increases, behaviour switches in a way that thermal stability increases with the dose i.e. ageing time. It could be assumed that, at least two different factors, caused by the accelerated ageing, affect the thermal decomposition in air. The proposed ones are decrease of the molecular average mass with ageing and the oxidation. Increased stability during the thermal decomposition in the air with ageing was observed previously for the industrial materials and it was explained by the difference in the radiation induced oxidation extent.

Further analysis is done by calculating the DTG curves, for mass loss in air. The maximum degradation rates can be characterized through inverted peaks. The peak position and intensity are monitored. For non-aged sample, the one broad peak appears at about 440^0C (P1), with a shoulder at about 390^0C (P1'), see Fig. 4.18. For the samples aged up

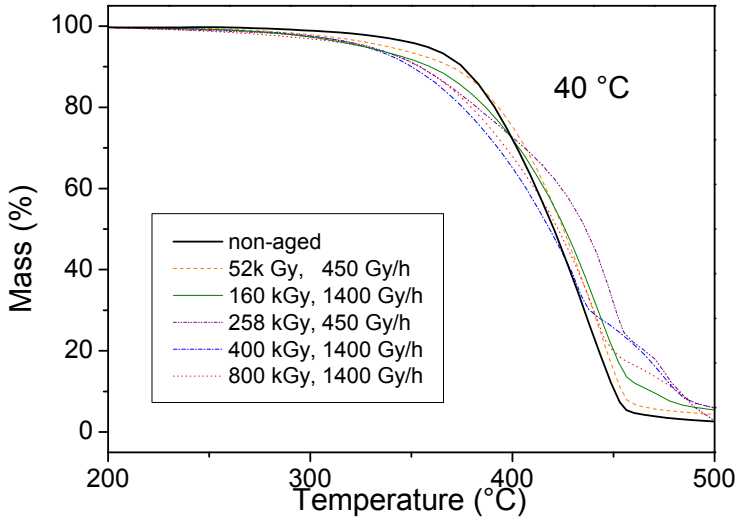

Figure 4.17: *The thermal decomposition in air: mass loss as a function of the decomposition temperature - Engage aged at 40^0C.*

to the small doses, the P1 seems to increase and shifts toward higher temperatures, while for the samples aged up to the higher doses, P1 seems to be shifted toward lower temperatures with decreased intensity. Several peaks appear about 500^0C, but since the polymer mass is very low at that temperature, they will be neglected.

On the basis of the mass loss curves, it was assumed that several factors affect the thermal decomposition of Engage in air. In such a case, these factors act simultaneously in the similar temperature range, so it is difficult to distinguish DTG peaks and correlate them to the certain decomposition process. Still, it seems that the decomposition tends to shift toward higher temperatures, with increasing the ageing dose.

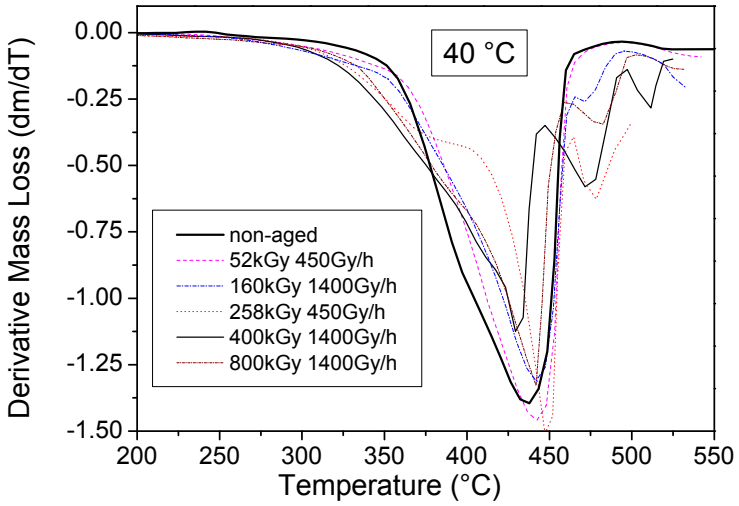

Figure 4.18: *The thermal decomposition in air: the first derivative of the mass loss for the samples aged at 40^0C - Engage.*

4.3 General discussion and conclusions on results for neat cable polymers

The two types of neat polymer samples, made out of "as received" pellets: Nordel 3722 and Engage 8100, were produced. The same ageing conditions as for the industrial samples (which main components are Nordel 2722, EVA and ATH), were applied in order to compare the evolution of mechanical and physico-chemical properties with ageing. It was assumed that, due to the less complex composition, it will be easier to analyse the monitored property data.

The nominal stress - strain behaviour of Nordel and Engage was observed to differ in comparison to the industrial EPDM. With respect to the low strain field: for Nordel a yield point was observed, while in the case of Engage it is rather more diffuse yield region, which has been observed for this class of copolymers [92]. For Nordel a bit sharper yielding point was observed, with some, not to prominent, strain softening. The tress - strain behaviour of non-aged Engage and Engage samples aged up to the low dose, manifest dominant strain - hardening region. The observed

strain - hardening is assumed to be a reason for very high ultimate tensile stress, observed in the case of non-aged Engage.

The elongation at break of Nordel is observed to decrease as a function of ageing dose, as expected. Moreover this decrease is observed to be stronger for samples aged at 70^0C. What was explained as a "crossover between the cross-linking and chain scission domination" in the case of outer insulation, and depicted as a maximum on UTS-dose graph, could be observed for Nordel samples aged at 450 Gy/h and 40^0C, at rather low dose. Cross-linking to chain scission crossover, at low doses, has been confirmed earlier for non-industrial polymers. The crossover in neat EPDM films that are irradiation aged is measured through an increase in gel fraction as a function of the irradiation dose and found to be of about 100 kGy [16]. The relaxation measurements by Celette et al. [54] on 100 μm thick samples indicate the transition to be at about 200 kGy. The mechanical measurements of Nordel, aged at 450 Gy/h and 40^0C, agree well with these results. For the other samples, the ultimate tensile stress rather decreases considering the error bar, and the decrease is observed to be slightly faster for samples aged at 70^0C. The ultimate tensile stress data are in accordance with the elongation at break data, obtained for Nordel, and both are proposing that the sample degradation is enhanced at the higher ageing temperature, where additionally, the dose rate effect seems to be stronger.

The evolution of ultimate tensile parameters investigated for Engage, exhibit somewhat different behaviour, comparing to the what was observed for Nordel and industrial EPDM. The elongation at break decrease is observed to be "delayed" i.e. for the samples aged at 40^0C and 70^0C, the elongation at break does not decrease up to about 350 $\pm$50 kGy and 150 kGy, respectively. The UTS of non-aged sample is observed to be very high, which is assumed to be related to a strain-hardening observed for Engage, and it significantly decreases with ageing. High values of the strain - hardening slopes are often related to the density of the chain entanglements. For the semi-crystalline polymers, which do not display strain softening the amorphous phase is in the rubbery state [93]. Accordingly, it could be assumed on the basis of the tensile behaviour, that the structure of the Engage obtained upon the sample

production is more cross-linked in comparison to the Nordel.

Nevertheless, for both neat polymer samples, the stress-strain behaviour shifts from ductile toward brittle with ageing. For the high ageing doses samples break at low ultimate tensile stress, without exhibiting a plastic deformation. The stress-strain curves of samples aged up to the low doses exhibit rubbery like behaviour and the one aged up to the high doses brittle. The decrease of strain - hardening slope with increasing the dose is observed for Engage. It has been previously observed that a strain - hardening slope decrease culd be a consequence of the decrease in polymer molecular weight [92]. This could indicate that indeed molecular weight of Engage decreases with ageing i.e. chain length is shortening. The same can be assumed for Nordel. For the same ageing conditions, the industrial EPDM is much more stable in comparison to the neat polymers, which is explained as a consequence of the sample composition industrial vs. neat polymer.

For both neat polymers, a good agreement is observed between the experimentally obtained elongation at break and the elongation at break calculated on the bases of the same model, that was previously used for the identification of industrial EPDM elongation at break data, Eq. 2.2. All the constant model parameters were kept same, except for the β (the overall order of reaction), which was determined to be 3.5 for industrial and 2 in the case of neat polymers. This might be an indicator of a difference in the ageing mechanism between the neat and industrial polymers. The K_{irr} is observed to follow a linear like dependance as a function of the dose rate. It would be interesting to compare the constants (C, 1/Gy) of the K_{irr} - dose rate linear functions determined for Engage, Nordel, inner insulation EPDM and for outer insulation at low dose rates. The values of constants are: 0.00013 Gy^{-1}, 0.00008 Gy^{-1}, 0.00006 Gy^{-1}, 0.00002 Gy^{-1}, for the Engage, Nordel, outer insulation and inner insulation, respectively. According to the constant values, the K_{irr} of Engage, changes the most with increasing the dose rate. Interestingly, the Nordel 3722, designed to match the properties of Nordel 2722 [72], which is used for the production of industrial EPDM cables, has the most similar constant to the outer insulation industrial EPDM. These two sample types have the same thickness. The inner insulation

is also made out of Nordel 2722 (forerunner of Nordel 3722), but the thickness of inner insulation is about two times lower in comparison to the outer insulation industrial EPDM and Nordel 3722. Moreover, the inner insulation is observed to have the lowest constants of the K_{irr} - dose rate linear functions, which means that its ageing is the least dose rate dependant, among the investigated materials. This might be related to its thickness, which seem to allows uniform ageing, with respect to the sample cross-section.

The thermal decompositions under nitrogen and air, observed by TGA, could indicate that instead of a "moderate" (gradual) oxidation process, rather excessive chain scission occurs during ageing of neat polymers. This was assumed on the bases of the decreased thermal stability, observed for the aged neat polymers, when TGA is performed in nitrogen. The shift of the nitrogen TGA curves toward lower decomposition temperatures with increasing the dose could be a consequence of chain length shortening induced by an accelerated ageing. This certainly would affect the thermal decomposition of aged neat samples in air, so the observed shifts of the polymer decomposition temperature profiles as a function of the irradiation dose, are not so easy to interpret in comparison to the analysis done for the industrial EPDM.

Interestingly, it seems that the correlation between the mechanical and physicochemical results can be established through the thermal decomposition in nitrogen. The decrease of the peak intensity as a function of the dose, observed for nitrogen DTG curves, seems to mimic the behavior of the elongation at break as a function of the dose. This is presented for Nordel in Fig. 4.19.

The red points on the elongation at break vs. dose graph present the elongation at break values for the samples for which thermal decomposition in nitrogen was performed. This correlation could indicate that indeed the oxidation is not dominant mechanism responsible for the decrease of elongation at break, and that the decrease of elongation at break is governed by the massive chain length shortening.

According to the evolution of the tensile behaviour and thermal decomposition with ageing, it was assumed that excessive chain scission, led to

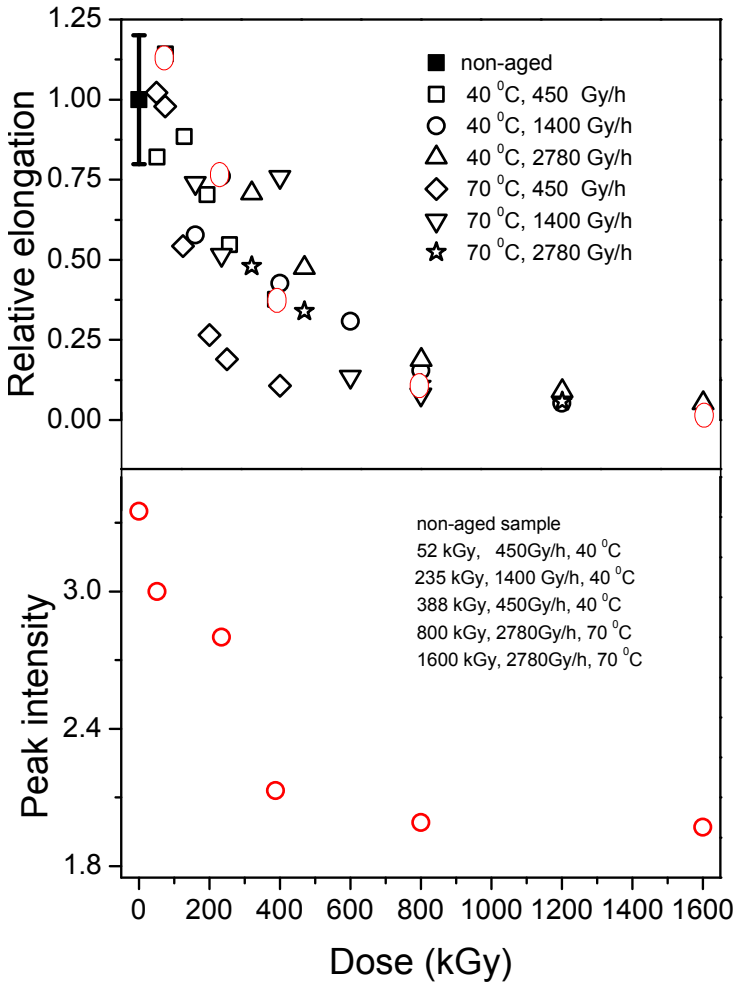

Figure 4.19: *The comparison of the changes of the elongation at break and the DTG peak intensity from nitrogen thermal decomposition as a function of the ageing dose - Nordel.*

a significant shortening of the chain length and even total decomposition of the neat polymer samples at higher doses. Neat material degradation, caused by the accelerated ageing, was observed to be significantly higher in comparison to the industrial EPDM, so the obtained data are only partially comparable.

Chapter 5

General discussion and conclusions

5.1 General discussion

Accelerated simultaneous thermal and radiation ageing was performed on industrial cable insulation samples, as well as on the neat EPDM polymer samples, with the aim to validate the cables for extended lifetime operation in nuclear power plants. The focus was given to the study of mechanical and physico-chemical properties of these materials, as well as to the development of semi-empirical ageing model that can be used for preliminary assessment of the cable lifetime. Ageing conditions were designed in order to reach the end-of-life criteria, and to have a variety of ageing conditions, broad enough for the evaluation of dose rate effect.

What concerns industrial EPDM polymer, two types of the samples were investigated: (1) Those extracted from outer insulation in the form of dumbbell, and (2) those from inner insulation in the form of tubes. Regarding the neat EPDM polymer, two types of raw material in the form of pellets were obtained thanks to the "DOW Chemicals": (1) NORDEL 3722 and (2) ENGAGE 8100. From both, the samples matching the size and shape of the industrial EPDM outer insulation (2mm thick dumbbell) samples were produced in the laboratory by pellet melting and pressing.

The experimental investigation included mechanical and physico-chemical

tests performed in parallel with modelling of the elongation at break data in order to predict the remaining cable lifetime. Mechanical tests were performed utilizing tensile test bench primarily for the measurements of elongation at break, which is already established as appropriate parameter for assessing cable condition. Indentation was applied as non-destructive technique that could be of use as on-site test method. Thermogravimetry was performed in order to evaluate if there is an influence of the ageing on the polymer thermal decomposition. Studying of the material viscoelastic properties was performed using the DMA in order to assess the sample structural changes. Swelling was used in order to monitor the evolution of the polymer network with ageing. FTIR was used to analyse sample chemistry on the molecular level and to investigate the changes in sample chemistry caused by ageing. Experimental data were analyzed based on the model of Menlow and Dakin which uses generalized chemical reaction rate laws to quantitatively describe the deterioration of the insulation.

The elongation at break decreases by increasing the total absorbed dose (i.e. ageing time) for all the applied ageing conditions. The variation of ultimate tensile stress and Young's modulus with ageing was observed to be somewhat more complex in comparison to the elongation at break. For both parameters periods of stagnation or more or less significant increase were observed for low doses, typically followed by a parameter value decrease at higher doses. The evolution of the tensile parameters was considered to depend on interplay of cross-linking and chain-scission mechanisms, which generally become dominant at low and high doses, respectively. Cross-linking and chain scission interplay was assumed to depend on the ageing conditions and sample characteristics. The dose rate effect was observed as the difference in the measured parameter (elongation at break, UTS or YM) value for the samples aged up to the same dose, but under different ageing conditions. The dose rate effect was observed to be the most significant for the outer insulation samples, while it was observed to be strongly suppressed for the inner insulation of the investigated industrial cable. Regarding the neat polymers, it was observed to be more significant for the Nordel, but still it was less significant in comparison to the industrial EPDM samples obtained by

the extraction from the outer cable insulation, see Fig 5.1. These can be easily observed when one compares the dose to equivalent damage (the dose required to reach set end - of - life criterium). In Fig. 5.1, 50 % elongation at break is established as an end - of - life criterium (presented with red lines). It can be observed that in the case of EPDM outer insulation, and Nordel insulation aged at 70 ^0C, there is a range of doses equivalent to the ded, which depend on ageing conditions. Contrary, for the inner EPDM insulation this range is rather narrow, or even one dose can be determined as ded, with a suitable error bar.

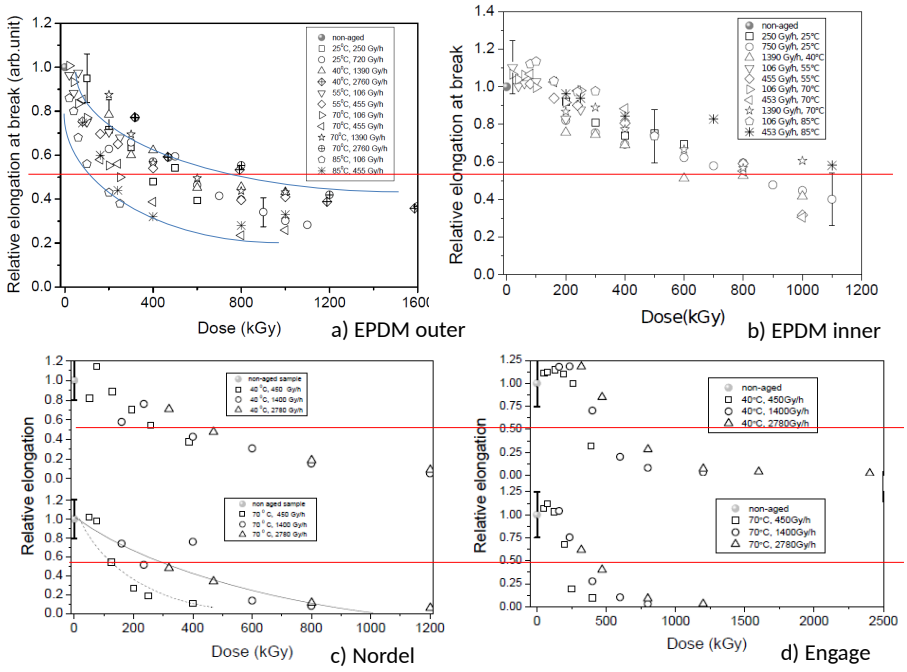

Figure 5.1: *The evolution of relative elongation at break with dose for a)EPDM outer insulation, b)EPDM inner insulation, c)Nordel and d)Engage.*

The indentation was performed only for the industrial samples. The resolution of IM measurement was observed to influence its application. In the case where IM was penetrating deep in the samples bulk (standard

industrial IM), the monotonous increase of the IM was observed, which was found to be very well correlated with the decrease of the elongation at break (linear correlation was observed). Both, increase of IM and increase of elongation at break are considered to be caused by the increase in sample internal oxidation. The correlation od IM and YM, analysed for the outer insulation samples, was observed to be weak for the samples aged under rather low dose rate. Due to this, it was assumed that the elongation at break versus IM is dependant on sample heterogeneity: and it is stronger for the sample where DLO is more pronounced. When more precise tools are applied, like micro or nano - indenters, cross-sectional investigation is possible and it is convenient for the mapping the sample homogeneity through the sample thickness, see Fig 5.2.

The DMA and swelling results supported the assumption that the original network structure is being changed, with ageing, by simultaneous creation of new intermolecular bonds and destruction of the original ones, where one of these processes dominates depending on the ageing conditions, atmosphere and sample characteristics. By the ATR-FTIR it was confirmed that the main components of the industrial EPDM samples are EPDM, EVA and ATH. No significant difference between the non-aged and aged industrial samples was observed by the ATR-FTIR.

Regarding the physico-chemical investigation, the most interesting results were obtained by the TGA measurement. For the thermal decomposition of the industrial EPDM samples in nitrogen atmosphere it was observed that it does not depend on the sample ageing state i.e. no dose, dose rate or temperature dependance of the TGA curves was observed. For all the samples, mass loss versus temperature curves followed very similar trend. The two main decompositions stages were observed. The first one with the maximum decomposition rate at about $T = 360^0C$ was related to the evaporation of the water from the ATH and acetic acid from the EVA; and the second to the decomposition of polymer macromolecular chains, with the maximum decomposition rate at about $T = 480^0C$. The TGA-FTIR coupling results, used to analyse the products evolved during the TGA, supported the proposed thermal decomposition

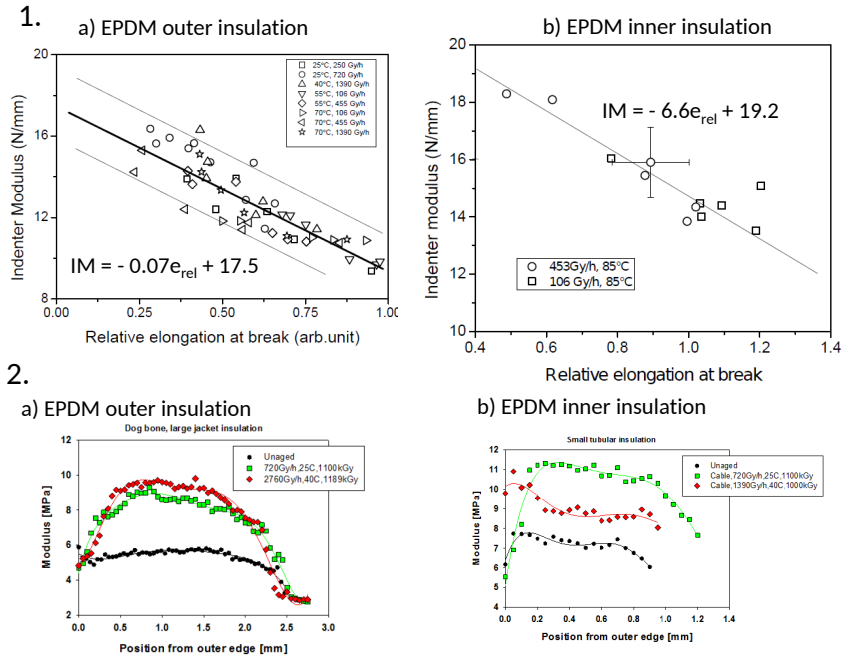

Figure 5.2: *1. The correlation of IM with elongation at break for a)EPDM outer insulation, b)EPDM inner insulation; 2. The IM profiling for a)EPDM outer insulation and b) EPDM inner insulation.*

scheme. Interestingly, the polymer thermal decomposition temperature profile, measured by TGA in air, gradually shifts towards the high temperatures with increasing the irradiation dose, see Fig. 5.3.

Further analysis of the first derivative of the mass loss revealed that there are two main decomposition steps related to the decomposition of the polymer macromolecular chains. The first polymer chain decomposition process, observed at the temperature of 430^0C in the case of outer insulation, and 450^0C for the inner insulation, requires lower activation energy is assigned to the decomposition of the polymer through the reaction with oxygen. The second decomposition process, activated at the temperature of about 480^0C in the case of outer and inner insulation,

is correlated to the scission of the polymer bonds. It was observed that the rate of mass loss related to the thermal decomposition via oxidation (P_{OX}) gradually decreases at the expense of the increase of random chain scission driven thermal decomposition (P_{CHSC}). Interestingly the evolution of P_{OX} with the dose was observed to mimics the evolution of the elongation at break, see Fig 5.4. Moreover, the observed dependance of the elongation at break data on the ageing conditions i.e. the dose rate effect could be observed for the decrease of the P_{OX} with the dose. This result provided very important link between the evolution of the mechanical and physico-chemical properties with ageing. These results show: 1) under the ageing conditions investigated in this study, the dose rate effect originates from the thermo-radiative oxidation process; 2) macroscopic mechanical behaviour, in particular elongation at break, can be fully assessed by performing TGA in air.

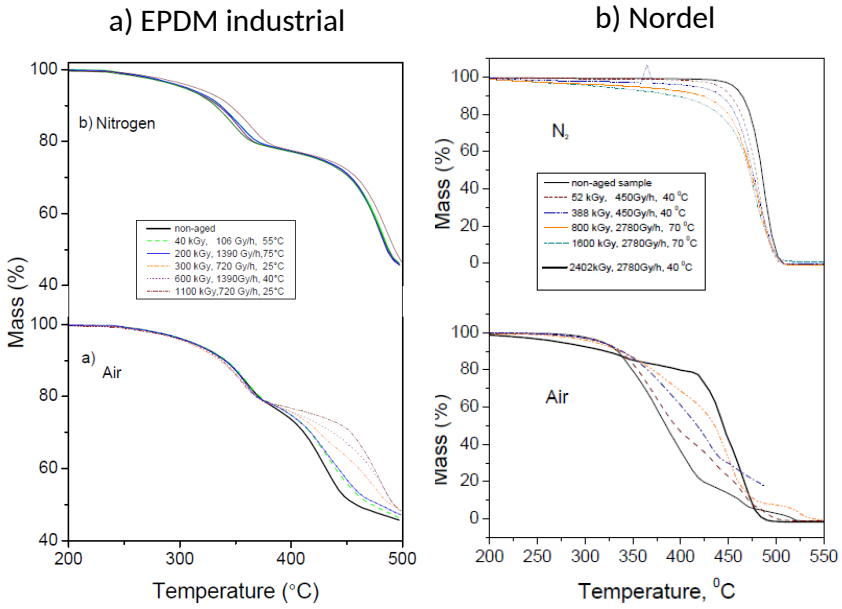

Figure 5.3: *The evolution of mass loss under nitrogen and air for a) EPDM outer insulation and b) Nordel.*

Moreover, regarding the DTG, it was observed that the peaks related to the macromolecular chain decomposition via oxygen reaction can be better resolved, for the same resolution (heating rate), from the peaks related to the chain decomposition via random chain scission of the polymer bonds, for the outer insulation i.e. in the case where dose rate effect is considered to be more significant. Accordingly, TGA has potential to be used not just for assessing the level of sample oxidation, but also to estimate the level of DLO. Additionally, for the samples where oxidation seems to be the most homogeneous, the correlation between P_{OX} (P_2) and elongation at break seems to be weaker, see samples aged at 55 ^{0}C, Fig 5.4 b).

Contrary to industrial polymer, thermal decomposition of aged neat polymer exhibited the dose dependance under both, air and nitrogen, see Fig 5.3 b). For the neat polymer the TGA curves under nitrogen were observed to shift toward lower temperatures by increasing the dose. This behaviour is associated to low thermal stability. It is assumed that less thermally stable material is created with the ageing, probably by shortening the chain length. Moreover, the TGA curves of neat polymer, obtained under air, were observed to be more complex in comparison to the industrial samples. The observed evolution of the neat polymer thermal decomposition in air and nitrogen with the ageing indicated the existence of several overlapping degradation effects, which differs from the industrial EPDM, where oxidation seems do be dominant.

The proposed process for assessing the end-of-life time is schematically presented in Fig. 5.5. The applied model on the elongation at break data indicated that for the investigated ageing conditions, the radiative term is the main cause for the decrease of elongation at break. All the experimental data were calculated by varying only one model parameter: pre-exponential factor of the irradiation rate constant, K_{irr}.

It was observed that pre-exponential factor of the irradiation rate constant increases monotonously with increasing the dose rate irrespectively of the irradiation temperature, within the studied temperature range. It was found that the pre-exponential factor of the irradiation rate constant as a function of dose rate follows linear dependance, see Fig 5.6. For the general prediction process, the curve obtained for the EPDM

inner insulation is chosen to be included, since it is considered that accelerated ageing of inner insulation EPDM samples is the most representative with respect to the operational conditions (the oxidation is rather homogeneous for inner insulation EPDM).

Additionally, K_{irr} - dose rate, could be described by the square root dependance, in the case of outer insulation. The square root dependance should be interpreted carefully, because it can not be used for the elongation at break prediction at very low dose rates ($K_{irr} \rightarrow 0$). Nevertheless, it can be used to compare it with the square root function that describes oxygen consumption - dose rate dependance, previously observed [83]. This comparison provides direct link between oxygen consumption (oxidation) and evolution of elongation at break with ageing time.

a) EPDM outer insulation

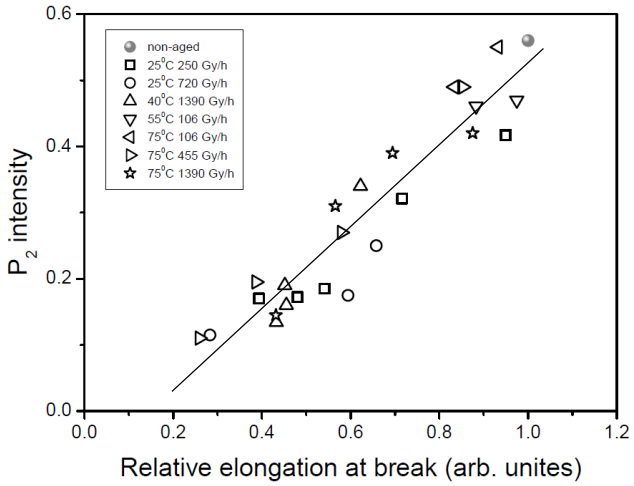

b) EPDM inner insulation

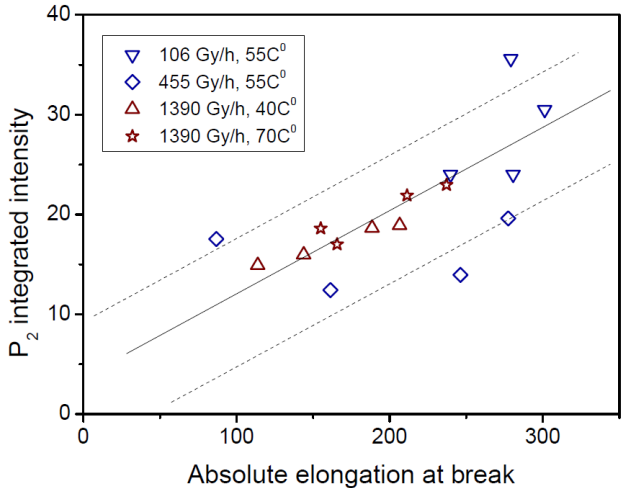

Figure 5.4: *The correlation of TGA parameter with elongation at break for a)EPDM outer insulation, b)EPDM inner insulation.*

$$e/e_o = (1 + ((\beta - 1)Kt))^{1/(1-\beta)}$$

$$K = K_{th}e^{(-E_{ath}/(k_bT))} + K_{irr}e^{(-E_{airr}/(k_bT))}$$

Parameter	Value
E_{ath}	1.07 eV
K_{th}	50×10^{9} h^{-1}
E_{airr}	0.065 eV
β	3.5

$$t = \frac{0.4\sqrt{\frac{e_o}{e}} - 1}{2.5K}$$

K_{irr} = f(I)

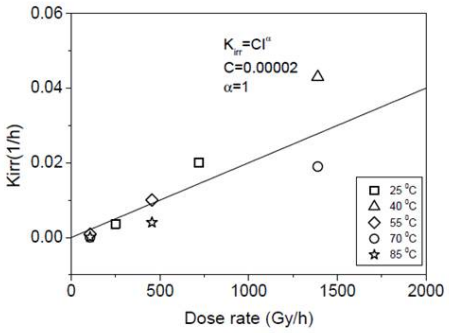

e = f(IM) Has to be established for a particular material !

Figure 5.5: *An cable end-of-life prediction tool - general scheme.*

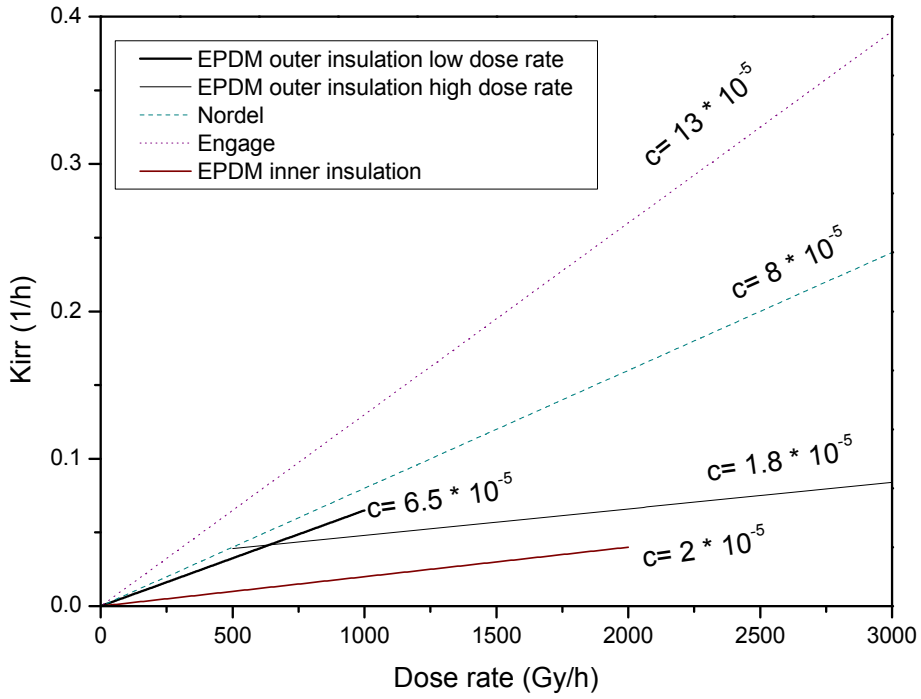

Figure 5.6: *The evolution of K_{irr} as a function of dose rate.*

5.2 Conclusion and perspectives

Accumulated results from both, mechanical and physisco-chemical properties of the non-aged and aged industrial EPDM insulation samples, together with modelling of the elongation at break data as a function of time demonstrated that the polymer degradation is caused by combined thermally and radiochemically mediated oxidation processes. One of the main arguments for such scenario is based on the correlation between the decrease of the elongation at break and the decrease of the rate of mass loss related to non-oxidised part of the polymer, observed by TGA experiments.

Accordingly, the dose rate effect observed for the outer insulation is explained on the basis of the diffusion limited oxidation (DLO) effect. The high consumption of the oxygen at the sample surface (enhanced oxidation at the sample surface) is usually caused by the creation of high amount of free radicals that are prone to react fast with the oxygen. High amount of radicals is typically created at high dose rates. When the oxidation process proceeds fast at the sample surface, the diffusion of oxygen toward the sample bulk is hindered (limited). This means that the dominant ageing mechanism at the sample surface will be the chain scission (because high oxygen concentrations promote chain scission in PE), while the cross-linking will prevail in the sample bulk, due to the lack of oxygen. This is known as diffusion limited oxidation effect, where the oxygen consumption rate is higher than the oxygen supply rate via diffusion. In the conditions of significant DLO, the sample oxidation is rather heterogeneous. For the EPDM type of samples it means that the sample surface is oxidised, while the sample bulk is dominantly cross-linked, because PE (the main EPDM component) tends to cross-link in the oxygen deficit atmosphere. As a result, the elongation at break decrease was observed to be more pronounced for low dose rates and high temperatures for the outer insulation. Low dose rates cause more oxygen diffusion through the sample and the increase of oxide thickness. On the contrary, at high dose rates, the decrease of elongation at break is observed to be slower, which is related to the low oxide thickness. Similar reasoning can be applied to explain why UTS and YM are observed to

increase with increasing dose rate for the samples aged up to the same dose. The increase of the dose rate promotes the cross-linking, which is related to the increase of UTS and YM. By increasing the ageing temperature, YM and UTS decrease for the samples aged up to the same dose, which was related to the promotion of the oxygen diffusion at high temperature.

Homogeneous oxidation is favoured when the samples are aged at low dose rates and for the thinner samples. This was confirmed by the experimental investigation of the inner insulation, which is about two times thinner in comparison to the outer insulation. The dose rate effect was not observed for the inner insulation samples that were aged under the same ageing condition as outer insulation. The elongation at break decrease was found to be independent on the ageing conditions, and no significant dose rate effect on the UTS and YM data was observed. Still, at the highest ageing temperature investigated (85^0C), the UTS and YM where observed to decrease, which can be related to the enhanced oxygen diffusion and chain scission promotion.

The dose rate effect directly influences the estimation of the cable life time. The first step is to determine the level of DLO, after accelerated ageing. This can be done via performing some profiling technique (IM, TGA). The estimation of the cable life time was performed based on extrapolation method to relative dose rate and temperature. For that purpose the model is developed K_{irr} as a function of dose rate was determined from the best agreement between calculated and experimental data. Since homogeneous oxidation is expected for the NPP low voltage cable operation conditions, K_{irr} vs. dose rate obtained for the inner insulation was used. According to the analysis presented in Section 3.4.1, the estimated life time of EPDM cable polymer is about 60 years.

In comparison to industrial EPDM cables, neat polymer samples produced without any additives and fillers, have different ageing mechanism for the same ageing conditions. More extensive shortening of the macromolecular chains seems to occur. This is most certainly the consequence of difference in composition, which indicates that one has to be careful when designing the "model" samples. Still, it is important to underline that the K_{irr} values of EPDM industrial outer insulation (at low dose

rates) and Nordel are the most similar among all, see Fig. 5.6. This could mean that two samples made out of same basic polymer (same polymer matrix) and with a same thickness, exhibit similar ageing behaviour as a function of dose rate, despite the fact that one of them contains additive and fillers (even more than 50%).

IM is confirmed to be suitable as ageing indicator and the relations proposed for the outer and inner insulation of the investigated cable could be used to calculate elongation at break from the measured IM, hence, to use calculated elongation at break for life time predictions.

Still, regarding the relation between the IM and elongation at break, the one obtained for a particular material is often not suitable for general usage. For the materials where IM and elongation at break evolution with ageing originates from the increase of the internal material oxidation, there might be a potential in establishing more general correlation, through an introduction of a parameter that is related to material oxidation evolution. The predictive model could be improved if measurements at low dose rates are performed.

An apparent correlation between TGA measurement in oxygen and evolution of elongation at break provides direct link between physico-chemical and mechanical properties. The observation of this correlation supports potential of TGA to be used as non - destructive technique that could be used to assess level of sample degradation, and possibly the DLO importance. Additionally, an oxidation related parameter could be potentially assessed via DTG peak, related to the polymer chain oxidation during the TGA.

Within an investigation of the cable polymer insulation degradation, a focus is often given to detect the ageing mechanism responsible for the degradation process. These materials are often elastomers, characterised by their polymer network structure, so the focus goes to the investigation of the processes responsible for the degradation of macromolecular networks. Evolution of many mechanical and physico-chemical parameters with ageing supports the assumption that the degradation goes through the simultaneous cross-linking and chain scission, with the domination of cross-linking at the beginning of ageing, followed by a domination of

chain - scission. The elongation at break is generally proven as a good cable polymer ageing indicator, but this is mostly empirically based. More fundamental understanding of the ageing process at relevant NPP conditions is needed to make more accurate predictions. In that purpose, prediction of the network evolution with ageing is often based on determining which of the ageing mechanism is supposed to dominate under ageing conditions of interest, for a given material, and how much is it critical, with respect to the insulation functionality dependence on the material structure. This prediction appears to depend on the parameter used as an ageing indicator, especially in the cases of industrial polymers, that are chemically and structurally rather complex. For example, the dose at which chain scission is expected to overcome crosslinking depends on the parameter used to detect it (UTS, YM, swelling ratio, gel fraction...) and the way this parameter is determined from the experiment (nominal, true values of tensile parameters; absolute, relative elongation at break ...). Preferably, universal criterion should be developed. With respect to the elastomers, regarding mechanical parameters, focus should go toward the ultimate properties, which address the material structure endurance toward environmental stressors. Fracture toughness evolution could have a good potential in understanding the fundamentals behind the structural degradation. With respect to the physico-chemical properties, investigation of the parameters appropriate for monitoring the oxidation distribution and extent with ageing seem to be of outmost importance when oxidation is the main degradation mechanism.

To sum up, regarding this thesis, the experimental investigation of accelerated aged cable insulation samples is performed using various condition monitoring techniques. Several physico-chemical, microstructural and mechanical properties are analysed in order to optimise the investigation process, with respect to the most appropriate ageing indicator. Non-destructive techniques were investigated together with their correlation with the current benchmark parameter (elongation at break). Accelerated ageing conditions were analysed with respect to the dose rate effect and diffusion limited oxidation. The correlation between mechanical and physico-chemical properties is established as well as the

procedure for assessing the end - of - life time of the cable.

Chapter 6

List of references

Journal papers

1. T. Šarac, N. Quiévy, A. Goussarov, M.J. Konstantinović, *Influence of γ-irradiation and temperature on the mechanical properties of EPDM cable insulation.* In: Radiation Physics and Chemistry, Vol. 125, p. 151-155 (August 2016).

2. T. Šarac, N. Quiévy, J. Devaux, A. Goussarov, M.J. Konstantinović, *The correlation between elongation at break and thermal decomposition of aged EPDM cable polymer.* In: Radiation Physics and Chemistry, Vol. 132, p. 8-12 (March 2017).

3. T. Šarac, N. Quiévy, A. Goussarov, M.J. Konstantinović, *The study of temperature and radiation induced degradation of cable polymers: A comparison between the mechanical properties of industrial and neat EPDM*, 21st European Conference on Fracture, ECF21, 20-24 June 2016, Catania, Italy, Procedia Paper

4. T. Šarac, L. Remy, N. Quiévy, J. Devaux, A. Goussarov, M.J. Konstantinović, *Influence of γ-irradiation and temperature on the mechanical and physico-chemical properties of EPDM cable polymer: comparison between the outer and inner cable insulation*, to be submitted

Bibliography

Bibliography

[1] INTERNATIONAL ATOMIC ENERGY AGENCY (IAEA) Tchnical Reports. Assessing and Managing Cable Ageing in Nuclear Power Plants. *IAEA Nuclear Energy Series* NP-T-3.6, IAEA Vienna 2012.

[2] McCarter D., Shumaker B., McConkey B., Hashemian H. Nuclear Power Plant Instrumentation and Control Cable Prognostics Using Indenter Modulus Measurements. *International Journal of Prognostics and Health Management* 5(16), 2014.

[3] Prepared by Lofaro R., Bowerman B., Carbonaro J., Kasturi S., Lee B., Subudhi M., Ibylor J., Villaran M. Literature Review of Safety-Related Electric Cables. *U.S. Nuclear Regulatory Commission* NUREGICR-6384 2, April 1996.

[4] Willan A. Thue (Ed.). Electrical Power Cable Engineering, Third edition, *CRC Press*, 2011.

[5] Zuidema C., Keerise W., Fleming R. , Welker M., Boggs S. A short history of rubber cables. *IEEE Electricsl Insulation Magazine* 27(4):45-50, 2011.

[6] Mead J.L., Tao Z., Liu H.S. Insulation materials for wire and cable applications. *Rubber Chemistry and Technology* 17(4): 701-712, 2002.

[7] Callister W.D., Rethwisch D.G. Materials science and engineering - an introduction. *Wiley*, 2003.

[8] Plavsic M. Polimerni materijali. *Naucna knjiga*, 1996.

[9] Handbook of Cable Wire Producer

[10] http://scientificpolymer.com/density-of-polymers-by-density/

[11] A. Shabani, Ph.D Thesis, Thermal and Radiochemical Aging of neat and ATH filled EPDM., *Arts et MÃ©tiers ParisTech - Centre de Paris Laboratoire des ProcÃ©dÃ©s et IngÃ©nierie en MÃ©canique et MatÃ©riaux*, May 2013.

[12] PLANES E., CHAZEAU L., VIGIER G., FOURNIER J., STEVENSON-ROYAUD I. Influence of fillers on Mechanical Properties of ATH Filled EPDM During Ageing by Gamma-irradiation. *Polymer Degradation and Stability* 95(6):1029-1038, 2010.

[13] Makhils F.A. Radiation Physics and Chemistry of Polymers, *Wiley* 1975.

[14] Schanbel W. Polymer Degradation â“ Principes and Practical Application, *Hanser* 1982.

[15] Rivaton A., Cambon S., Gardette J.L. Radiochemical aging of ethyleneâ“propyleneâ“diene monomer elastomers. 1. Mechanism of degradation under inert atmosphere *Journal of Polymer Science Part A-Polymer Chemisrty*42(5): 1239-1248, 2004.

[16] Rivaton A., Cambon S., Gardette J.L. Radiochemical ageing of EPDM elastomers.2. Identification and quantification of chemical changes in EPDM and EPR films γ-irradiated under oxygen atmosphere. *Nuclear Instruments and Methods in Physics Research B* 227: 343-356, 2005.

[17] Rivaton A., Cambon S., Gardette J.L. Radiochemical ageing of EPDM elastomers. 3. Mechanism of radiooxidation. *Nuclear Instruments and Methods in Physics Research B*227: 357-368, 2005.

[18] Planes E., Chazeau L., Vigier G. Role of temperature during ageing under gamma irradiation of filled EPDM: consequences on mechanical properties. *Journal of Polymer Science Part B-Polymer Physics* 48(12):1319-1328, 2011.

[19] Seguchi T., Tamura K., Okhshima T., Shimada A., Kudoh H. Degradation Mechanisms of Cable Insulation Materials During Radiation-Thermal Ageing in Radiation Environemnt. *Radiation Physics and Chemisry* 80:268-273, 2012.

[20] Prepared by Subudhi M. Literature Review of Safety-Related Electric Cables. *U.S. Nuclear Regulatory Commission* NUREGICR-6384 1, April 1996.

[21] Masayukii I. Degradation of elastomer by heat and /or radiation. *Nuclear instruments and methods in physics research B* 80:227â“231, 2007.

[22] Clough R. L., Gillen K. T., Quintana C.A. Hterogeneous Oxidative Degradation in Irradiated Polymers. *U.S. Nuclear Regulatory Commission* NUREG/CR-3643 2, April 1984.

[23] Seguchi T., Hashimoto S., Arakawa K. Radiation Induced Oxidative Degradation of Polymersâ"I: Oxidation Region in Polymer Films Irradiated in Oxygen Under Pressure *Radiation Physics and Chemistry*17: 195-201, 1981.

[24] Pinel B., Boutaud F. A Methodology to Predict the Life Duration of Polymers Used in Nuclear Power Plant Stations. Industrial Needs and Their Approach. *Nuclear Instruments and Methods in Physics Research B* 151: 471-476, 1999.

[25] Pinel B., Boutaud F., Life Prediction of Electrical Cable Equipment EPR Insulating Material. *Conference Record of the 1994 IEEE International Symposium on Electrical Insulation, Pittsburgh, PA USA.* June 1994.

[26] Gueguen V., Audouin L., Pinel B., Verdu J., *Polymer degradation and stability* 1994, 46: 113-122.

[27] Clavreul F., Thermal ageing of Ethylene Propylene Copolymer, *Insulation and Dielectric Phenomena*, IEEE, 1996.

[28] Shimada A., Sugimoto M., Radiation ageing technique for cable life evaluation of Nuclear Power Plant, *Transactions on dielectric and electrical imsulation, IEEE*, 2012. 19(5): p.1768-1773

[29] IEC Technical report 61244-2. Determination of long-term radiation ageing in polymers - Part 2: Procedures for predicting ageing at low dose rates *International Electrotechnical Commission*, 2014.

[30] INTERNATIONAL ATOMIC ENERGY AGENCY (IAEA), Pilot study on the management of ageing of instrumentation and control cables, IAEA Austria, 1995.

[31] Standard Test Method for Tensile Properties of Plastics, 2010.

[32] Subudhi M., Literature Review of Environmental Qualification of Safety-Related Electric Cables, NUREG/CR-6384 BNL-NUREG-52480 Vol.1, Brookhaven National Laboratory, April 1996.

[33] Nuclear power plants - Instrumentation and control important to safety - Electrical equipment condition monitoring methods - Part 2 : Method descriptions - Indenter modulus, 2008.

[34] Toman, G.J., Hunsader, S., Peters, D. In-Plant Indenter Use at Commonwealth Edison Plants. *EPRI Workshop on Cable Condition Monitoring* EPRI TR-102399, 1993.

[35] Kenneth G.T., Clough R.L., Quintana C.A., Modulus Profiling of Polymers, *Polymer Degradation and Stability* 1987, 17: 31-47

[36] Abadir E.F., *Journal of Thermal Analysis and Calorimetry*, 2013, 144: 1409-1413

[37] Pistor V., Fiorio R., Ornaghi F.G., *Journal of Applied Polymer Science*, 2011, 122: 1053â“1057

[38] Gamlin C., Markovic M.G., Dutta N.C., *Journal of Thermal Analysis and Calorimetry*, 2000, 59: 319-Â–336

[39] Gamlin C., Dutta N., Choudhury N.R., *Thermochimica Acta*, 2001, 367(368): 185-193

[40] Nabil H., Ismail H., Enhancing the thermal stability of natural rubber/recycled ethyleneâ“propyleneâ“diene rubber blends by means of introducing pre-vulcanized ethyleneâ“propyleneâ“diene rubber and electron beam irradiation, *Materials and design*, 2014. 56: p. 1057-1067

[41] Maysa M., Shaltout N.A., El Miligy A.A., The effect of gamma irradiation and particle size of CaCO3 on the properties of HDPE/EPDM blends, *Arabian journal of chemistry*, 2011. 4: p. 71-77

[42] Shun Z., Min N. and all., The influence of γ-irradiation on the mechanical, thermal degradation, and flame retardant properties of EVA/LDPE/ATH blends, *Journal of thermal analysis and calorimetry*, 2015. 119: p. 167-173

[43] Gheysari D., Behjat A., The effect of high-energy electron beam irradiation and content of ATH upon mechanical and thermal properties of EVA copolymer, *European polymer journal*, 2002., 38: p. 1087-1093

[44] Vinicius P., Rudinei F., and all., Degradation Kinetics of Vulcanized Ethyleneâ“Propyleneâ“Diene Terpolymer Residues, *Journal of applied polymer science*, October 2011., 122(2): p.1053-1057

[45] Rybinski P., Janowska G., Effect of the spatial network structure and cross-link density of diene rubbers on their thermal stability and fire hazard, *Journal of thermal analysis and calorimetry*, 2014. 117: p. 377-386

[46] Hull T.R., Price D., Liu Y., Wills C.L., Brady J., An investigation into the decomposition and burning behaviour of ethylene-vinyl acetate copolymer nanocomposite materials, *Polymer degradation and stability*, 2003. 82: p.365-371

[47] Seguchi T., Tamura K., Ohshima T.,Shimada A., Kudoh H., Degradation mechanisms of cable insulation materials during radiation-thermal ageing in radiation environment, *Radiation physics and chemistry*, 2011. 80: p.268-273

[48] Monchy â“ Leroy C.,Therond P., Nuclear cables and life time simulation, *7th International conference on insulated power cables*, 2007, Versailles-France

[49] Zaharescu T., Giurginca M., Setnescu R., The radiation stability of the ethylene â“propylene type rubbers during their gamma ray aging , *Romanian journal of chemistry*, 1995. 40 (2): p. 181-190

[50] IEC Technical report 61244-1.Determination of long-term radiation ageing in polymers - Part 1: Techniques for monitoring diffusion-limited oxidation *International Electrotechnical Commission*, 2014.

[51] Litvinov V.M., Prajna P.,Spectroscopy of Rubbers and Rubbery Materials, *Rapra Technology Limited*, 2002.

[52] Sharif J., Sharif H., Kamaruddin H., Radiation effects on LDPE/EVA blends, *Radiation Physics and Chemistry*, 2000. 58: p. 191-195

[53] Seguchi T. and all, Fast neutron irradiation effect â“ II. Crosslinking of polyethylene, ethylene-propylene copolymer, and tetrafluoroethylene-propylene copolymer, *Radiation physics and chemistry*, 1985. 266(2): p. 221-225

[54] Celette N., Stevenson I., Davenas J., Relaxation behaviur of radiochemically aged EPDM elastomers, *Nuclear instruments and methods in physics research B*, 2001., 185: p. 305-310

[55] Celette N., Stevenson I., David L., Davenas J., Vigier G., Seytre G., *Polymer International* 2004, 53: 495-505.

[56] Chailan J.F., Boiteux G., Viscoelastic and dielectric study of the thermally aged ethylene-propylene diene monomer (EPDM) compounds, *Polymer degradation and stability* 1995., 47: p. 397-403

[57] Bsrtonicek B., Hnat V., Placek V., Ageing monitoring of plastics used in nuclear power plants bu DSC, *Journal of thermal analysis and calorimetry*, 2001., 64: p. 571-576

[58] E. Planes Ph.D Theses: Influence des charges sur l^{TM}evolution des propriétés mécaniques des EPDM chargÃ©s lors de leur vieillissement par irradiation., *L^{TM}Institut National des Sciences Appliquées de Lyon*, 2008.

[59] Seguchi T., K. Arakawa, M. Ito, N. Hayakawa, S. Machi, *Radiation Physics and Chemistry* 1983, 21(6), pp. 495-501.

[60] Seguchi T., K. Arakawa, N. Hayakawa, *Radiation Physics and Chemistry* 1982, 19(4), pp. 321-327.

[61] Davenas J., Stevenson I., Celette N., Cambon S., et al., Gardette J.L., Rivaton A., Vingoud L., *Nuclear Instruments and Methods in Physics research B* 2002, 191, 653.

[62] Davenas J., Stevenson I., Celette N.,Vigier G., David L., Influence of the Molecular Modifications on the Propoerties of EPDM Elastomers Under Irradiation., *Nuclear Instruments and Methods in Physics research B*, 2003. 208, pp. 461-465.

[63] Seguchi T., K. Arakawa, N. Hayakawa, *Radiation Physics and Chemistry* 1981, 18(3-4), pp. 671-678.

[64] Bouguedad D., Mekhaldi A.,Boubakeur A.,Jbara O., Thermal Ageing Effects on the Properties of Ethylene- Propylene-Diene Monomer (EPDM).,*Annales de Chimie Sciences des MatÃ©iaux*, 2008., 33(4), pp: 303-313.

[65] Bouguedad D., Mekhaldi A., Jbara O.,Rondot S.,Hadjadj A.,Douglade J.,Dony Ph., Physico-Chemical Study of Thermally Aged EPDM Used in Power Cables Insulation, *IEEE Transactions on Dielectrics and Electrical Insulation* 2015., 22(6)

[66] Masayukii I.,Kaori U.,Kenkichi M., Application of chemical stress relaxation to the degradation of elastomers by heat and radiation, *Die Angewandte Makromolekulare Chimie*, 1998., 261/262, 4621. pp. 101-107

[67] Celina M., GillenK.T,. Oxygen Permeability Measurements on Elastomers at Temperatures up to 225^0Câ. *Macromolecules* 38:2754, 2005

[68] Gillen K.T., Bernstein R., Review of Nuclear Power Plant Safety Cable Aging Studies with Recommendations for Improved Approaches and for Future Work., SAND 2010-7266., Sandia National Laboratories, 2010.

[69] Celina M.C.,Gillen K.T.,Lindgren E., Nuclear Power Plant Cable Materials: Review of Qualification and Currently Available Aging Data for Margin Assessments in Cable Performance., SAND2013-2388., Sandia National Laboratories, 2013.

[70] Elenuc, LES CENTRALES NUCLÃ‰AIRES DANS LE MONDE/Nuclear power plants in the world, *ELENUC CEA*, 2010.

[71] International Standrd 60811-1-1, 2001. International Electrotechnical Commission.

[72] Robert Snyder, How New EPDM Technology is Meeting Customer Needs., Conference: EPDM Supply and demand into the next decade, Paper4., May 11th, 2000., Brussels, *RAPRA Technology Limited*

[73] Fernandez A.F., Ooms H., Brichard B., Coeck M., *Radiation Effects Data Workshop* 2002, IEEE, Reno, 2002, 171-176.

[74] Verardi L., Aging of Nuclear Power Plant Cables: In Search For Non-destructive diagnostic quantities., Ph.D Thesis., *ALMA MATER STUDIORUM Â· UNIVERSITY OF BOLOGNA*., 2012-2013.

[75] Arakawa K. Oxygen Consumption and Gas Evolution by Radiation-Induced Oxidation in Ethylene-hpylene-Diene Terpolymers *Journal of Polymer Science Part A-Polymer Chemisrty.* 251: 1713-1716, 1987.

[76] Dakin T.W., Electrical Insulation Deterioration treated as a Chemical Rate Phenomenon., *AIEE Transaction*, 1948., 67., pp. 113-122

[77] ASTM D2765 - 95; Standard Test Methods for Determination of Gel Content and Swell Ratio of Crosslinked Ethylene Plastics, 1996.

[78] Roylance D., Mechanical Properties of Materials, MIT, 2008.

[79] Langley N.R., Polmanteer K.E., Relation of elastic modulus to crosslink and entanglement concentrations in rubber networks., *Journal of Polymer Science Polymer Physics Edition.*, 1974.,12(6), pp.1023 - 1034

[80] Klueppel M., Wartewig S., Helmis G., Trapped entanglements in polymer networks and their influence on the stress-strain behavior up to large extensions., Physics of Polymer Networks., *29th Europhysics Conference on Macromolecular Physics, Merseburg, Germany*, 1992. 137-143

[81] Bowler N., Liu S., Aging Mechanisms and Monitoring of Cable Polymers., *Materials Science and Engineering Publications - Iowa State University Digital Repository., 2015.*

[82] Tao L., Fei H., Haining S., Xinming J., Condition Assesment of NPP Cables Through Indenter Modulus and Break-Elongation Test., 18th International Conference on Nuclear Engineering ICONE18., May 2010., Xi'an, China

[83] K. Arakawa, T.Seguchi, Y. Watanabe, N. Hayakawa, *Journal of polymer science Part A-Polymer chemistry*, 1981, 19, pp. 2123-2125

[84] Leveta A., Colombiana J., Duponchel L., Studying radiolytic ageing of nuclear power plant electric cables with FTIR spectroscopy., Talanta., 2017. 172, pp 139â“146

[85] Gibin G., Arunjunairaj M., Anandhan S., Use of nano-ATH as a multi-functional additive for poly(ethylene-co-vinyl acetate-co-carbon monoxide., *Polymer Bulletin.*,2014., 71(8), pp 2081â“2102

[86] Guihua L.,Bo-hao Z., et al., Surface properties of superfine alumina trihydrate after surface modification with stearic acid., International *Journal of Minerals Metallurgy and Materials.*, 2015., 22(5)., pp 537-542

[87] Hosseinkhani O., Kargari A., Sanaeepur H., FacilitatedtransportofCO_2 throughCo(II)-S-EPDMionomermembrane., *Journal of Membrane Science.*, 2014., 469 pp 151â“161

[88] Lanas J., Alvarez J., Dolomitic lime: thermal decomposition of nesque-honite., *Termochimica Acta* 2004.,421, pp 123-132.

[89] Hollingbery L.A., Hull R., A review of the structure and thermal decomposition of hydromagnesite and hunite., *Thermochimica Acta* 2010.,509, pp 1-11.

[90] Peng H., Yan X., Puming Z., Chunhua X., Thermal degradation of syndiotactic polypropylene and the influence of stereoregularity on the thermal degradation behaviour by in situ FTIR spectroscopy., *Polymer degradation and Stability* 2005., 88(3), pp 473-479

[91] Miranda T., Goncalves A.R., Amorim P., Ultraviolet Induced Crosslinking of Poly(Vinyl Alcohol) Evaluated by Principal Component Analysis of FTIR spectra, *Polymer International* 2001., 50(10), pp 1068-1072

[92] Kennedy M.A., Peacock A.J., et al., Tensile Properties of Crystalline Polymers: Random Copolymers of Ethylene., *Macromolecules.*, 1995., 28, pp 1407-1421.

[93] Janssen R., Deformation and Failure in Semi-Crystalline Polymer Systems - Master Thesis, *Eindhoven University of Technology, MT 02.14*, 2002.

[94] Holt W.L., McPherson A.T. Toggle clamp for rubber tensile specimens. *Journal of research of the National Bureau of Standards* 22:543-552, 1939.

[95] Alothman O.Y. Processing and Characterization of High Density Polyethylene/Ethylene Vinyl Acetate Blends with Different VA Contents. *Advances in Materials Science and Engineering*, 2012.

[96] Ed. Sidel A. Characterization and analysis of polymers, *Wiley* 2008.

[97] Clough R.L., Gillen K.T., *Journal of Polymer Science, Part A*, February 1985, 23(2): 359-377

[98] Seguchi T., Arakawa K., *Radiation Physics and Chemistry*, 1981, 18: 671-678

[99] Zaharescu T., *Revue Roumaine de Chimie*, 1998, 43(10): 909-912

[100] Shun Z., Min N., Xiaofeng W., *Journal of Thermal Analysis and Calorimetry*, 2015, 119: 167-173

[101] Hull T.R., Price D., Liu Y., *Polymer Degradation and Stability* 2003, 82: 365-371

[102] Ray I., Roy S., Chaki T.K., Khastgir D., *Journal of ELastomers and Plastics*, 1994, 26: 168-182

[103] Peterson J.D, Vyazovkin S., Wight C.A., *Macromolecular Chemistry and Physics* 2001, 202: 775-784

Appendix

Results on material from IAEA benchmariking program

The benchmarking test programme was a part of the IAEA coordinated research programme on Qualification, Condition Monitoring and Management of Ageing of low voltage cables in Nuclear Power Plants. The test programme was made in such a way to cover some of the cable condition monitoring methods that are currently in use or are being investigated for future use in nuclear power plant. Within the program SCK•CEN with Laborelec performed thermal ageing and tensile testing on the cable materials. This program is not directly related to the subject of the thesis. Still, the investigated data are used to confirm the reliability of the performed tensile test. Even the elongation at break is widely used as an ageing indicator, discrepancies in its value are observed to appear often, for test performed by different subjects. These mainly depend on the sample preparation and tensile test set - up. When the data obtained from the tensile measurements at the SCK•CEN were compared to the others, they were observed to be in a good accordance with majority of other benchmark measurements.

.1 Materials

The cable materials that were tested within the programme represent a range of materials that are either in use in current NPPs or are likely to be used in new NPPs. They are manufactured by various companies, world wide. While the industrial cable material (EPDM) studied in this work was taken off shelf, these cable materials are freshly produced. Table A.1 gives the overview of the tested cable materials (jacket and inner insulation) including their producers.

Table 1: *Cable materials and manfuacturers.*

Insulation/Jacket	Manufacturer
XLPE/CSPE	Rockbestos, USA
EPR/EVA	Eupen, Belgium
XLPO/XLPO	Shanghai Special Cable, China
EPR/EPR	Changzhou Bayi Cable Co., China

.2 Ageing conditions

Only thermal ageing was performed on the "IAEA" samples. The ageing temperature and time were calculated by IAEA using the activation energy for the given cable material, on the basis of Arrhenius equation. The minimum temperature that can cause a significant degradation within available timescale was chosen. Few ageing times were proposed by the IAEA on the basis of experience with the ageing of particular material, and the rest of the aging times were chosen during the ageing procedure depending on the results (magnitude of the decrease of the elongation at break) obtained up to that moment. The suggested ageing temperatures and the ageing times are presented in Table A.2 for each material.

Table 2: *The ageing temperatures and times for each material.*

Material	Temperature	Ageing times
CSPE	120	176, 337.5, 511.5, 784, 912, 1056, 1248, 1464, 1824
EVA	120	2103, 2803, 3450, 4175, 4932, 5544, 7004
XLPE	135	2419, 3173.5, 3696, 4723, 5424, 5945, 6040
EPR, Eupen	135	2225.2, 2588, 3864, 4556, 5155, 5860, 6504
EPR, Changzhou Bayi Cable Co.	135	2205, 2588, 3888, 4556, 5155, 5860, 6495

.3 Tensile testing

Two shapes of samples were tested: dumbbell and tubular. The same test bench was used as for the industrial and neat EPDM polymers, see Section 2.2.1

.3.1 Rockbestos: XLPE/CSPE

The inner insulation of Rockbestos cable was made of XLPE and the samples were cut off in dumbbell form. The few representative engineering stress- engineering strain curves of non-aged and aged material are shown in Figure A.1.

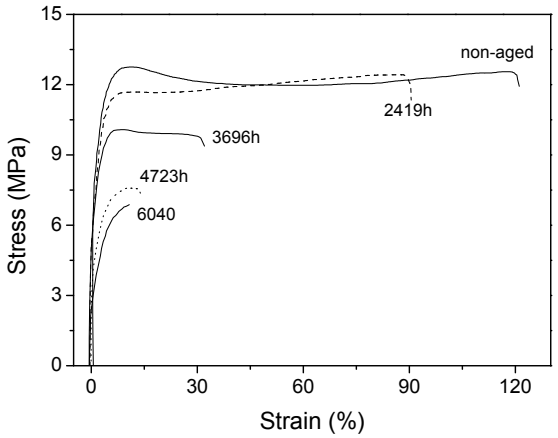

Figure 1: *Examples of engineering stress- engineering strain tensile curves of non-aged and aged XLPE from Rockbestos cable.*

The tensile behaviour changes with ageing as expected: the elongation at break decreases and the modulus increases. Samples seem to became brittle with ageing. Yield stress also disappears with ageing, which was already observed for the Nordel sample.

The change of elongation at break with ageing is given in Fig. A.2. It is important to notice that end-life criteria - 50 % of absolute elongation,which was required by the program plan, is achieved, for the samples aged more than 3500h. Moreover, the elongation at break almost approached zero value, for ageing time at about 5000-6000h.

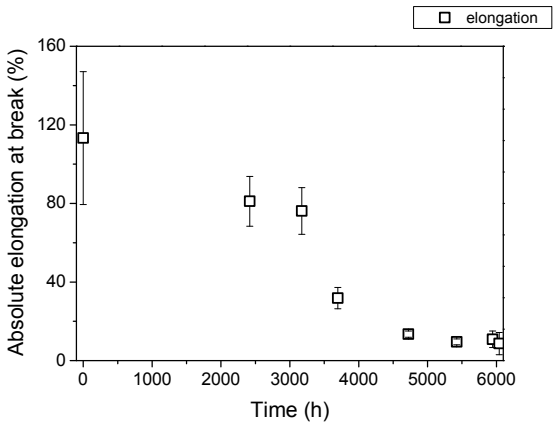

Figure 2: *The absolute elongation at break as a function of the ageing time of non-aged and aged XLPE from Rockbestos cable.*

The jacket material is made of Chlorosulfonated Polyethylene (CSPE). CSPE is commercially known as Hypalon rubber. It consists of a modified polyethylene backbone with chloro- and sulfonyl chloride side groups. The stress-strain curves of the non-aged and aged samples are given in Fig. A.3.

The stress-strain curves seem to follow linear dependance. The decease of elongation at break and stress at the break with ageing are clear, while tensile modulus seem to increase with ageing time. The change of elongation at break with ageing time is presented in Fig. A.4. The error bar is not large in comparison to the results from other rubbery polymers, even when the elongation at break values are large. The

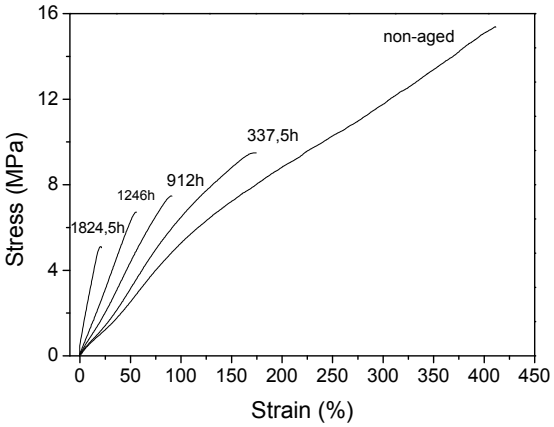

Figure 3: *Examples of engineering stress- engineering strain tensile curves of non-aged and aged CSPE from Rockbestos cable.*

ageing sequences were approximately the same (around 170 h between two successive ageing times), but still the largest change of the elongation at break is observed after the first ageing step. The elongation at break drops ~ 157 % after the first ageing step and about 86 % after the second ageing step. It could be assumed that this high drops of elongation at break are due to the elimination of chlorosulfone and chlorine sites, which is assumed to be the main degradation mechanism, for this type of an insulation material.

.3.2 Eupen: EPR/EVA

Inner insulation, made of EPR were prepared as tube samples, aged and tested. Four types of inner insulations could be found in a cable. The difference was only in colour (pigment used during the manufacturing) and the sample colours were: black, blue, red and yellow-green. The stress-strain curve trend was the same for all type of colours. Because of this similarity the tensile curves will be presented only for the black non-aged and aged insulation, see Fig. A.5. Tensile test was performed at the speed of 500mm/min, which ensured that most of the samples break at the middle rather than near the grip. As a consequence the

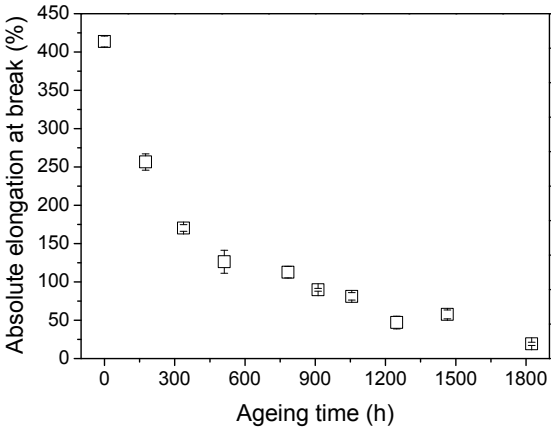

Figure 4: *The absolute elongation at break as a function of the ageing time of non-aged and aged CSPE from Rockbestos cable.*

resolution was not perfect, so the curves look broken-like sometimes. Still, the trend could be clearly observed and the samples are found exhibit rubber-like behaviour.

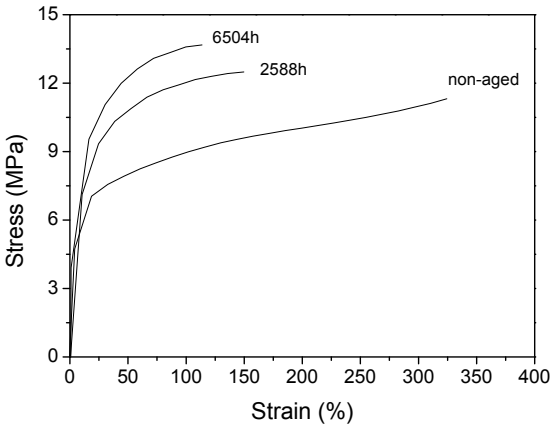

Figure 5: *Examples of engineering stress - engineering strain tensile curves of non-aged and aged EPR from Eupen cable.*

With ageing, the samples get brittle and the elongation at break decreases.It is interesting to compare the change of elongation at break as

a function of ageing time for the samples with different colours, see Fig A.6.

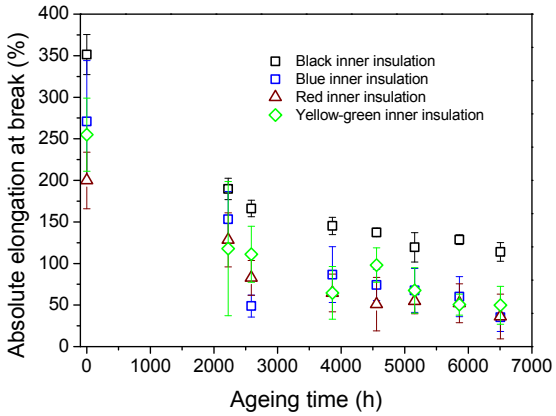

Figure 6: *The absolute elongation at break as a function of the ageing time of non-aged and aged EPR from Eupen cable.*

The difference in elongation at break value between the samples with different colour was observed, even though the only difference is sample colour (pigment). So, the black samples have the highest value of the elongation at break. All the rest behave similarly, but the red sample seems to have the lowest values of elongation at break. This observation points out the importance of chemical composition of the sample, and role of each component on the material behaviour. End of life criteria was reached for the blue, red and yellow-green samples, but not for the black one, even after approximately 6500h of ageing time. Interestingly, after ageing time of about 4000h no big change of the elongation at break value with the ageing time as found.

Outer sheet of Eupen cable is made of EVA material. Since it contains VA it is expected that ageing mechanism includes elimination of acetic acid. Several eng. stress- eng. strain curves of non-aged and aged EVA samples are presented in Fig. A.7.

There is a clear change in the elongation at break value as a function of the ageing time, but big change of the ultimate tensile stress is not observed even for the highes ageing time ($\sim$ 7000h). Interestingly, yield

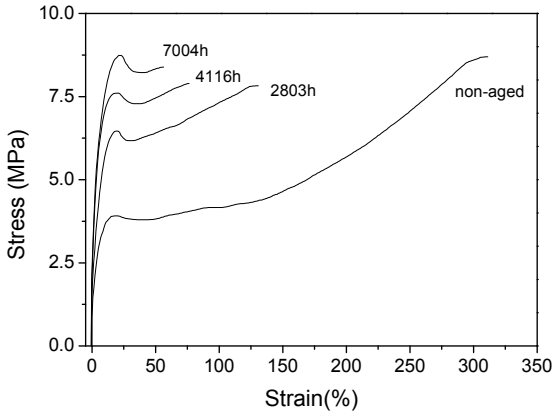

Figure 7: *Examples of engineering stress - engineering strain tensile curves of non-aged and aged EVA from Eupen cable.*

point appears for all aged samples and it seems to increase with the ageing time. It is expected to have crystalline structure in the EVA since it contains PE, and it seems that this structure is not destroyed with thermal ageing as it was observed before for some other semi-crystalline polymers.

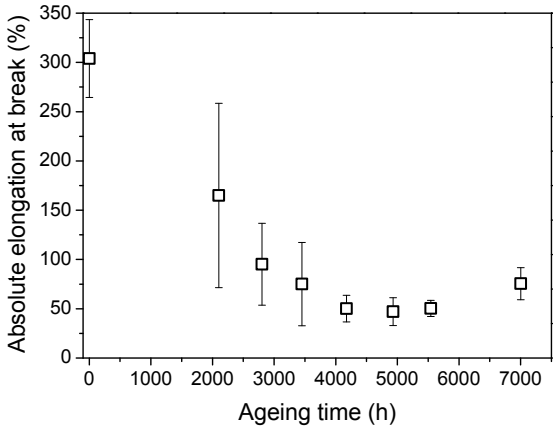

Figure 8: *The absolute elongation at break as a function of the ageing time of non-aged and aged EVA from Eupen cable.*

The existence of the yielding for highly aged samples might be correlated to another observation. Namely, it is observed that the initial decrease of elongation at break with ageing time is followed by its stagnation or even increase for the ageing time higher than about 5000h (see Fig. A.8). Interestingly, this transit from the decrease to the increase of elongation at break with ageing time occurs at about end of life criteria - 50 % of absolute elongation at break value. It seems that there is a recovery mechanism involved in the ageing.

Considering the complexity of the EVA structure: presence of VA and crystalline structure due to the PE, numerous ageing mechanisms could be involved: chain scission, cross-linking, changes in crystalline structure (like melting or chemi-cristallisation),oxidation, evaporation of acetic acid... Further analysis, including the physico-chemical ones, are necessary in order to assay the behaviour of elongation at break with the ageing time.

.3.3 Shanghai Special Cable - SSC: XLPO/XLPE

Even if the same polymer is used as a matrix polymer, it is obvious that there is difference in final industrial material of inner and outer insulations, see Fig. A.9 The huge difference in the elongation at break value is explained by the fact that inner insulation has probably higher polymer content and its main purpose is to satisfy the dielectric properties while the desired flame retardancy in the case of outer layer is mainly obtained by the introduction of mineral filler in high quantities.

The decrease of the elongation at break with the ageing time and reaching the end of life criteria is observed for both: dumbbell and tubular samples, as it was expected. Values of the elongation at break of XLPO dumbbell samples from SSC cable are close to the XLPO samples from Habia cable. Just in the case of SSC material after initial drop of elongation at break, it is stagnant around the same value (50% absolute)before it drops to about 7%, and in the case of Habia material change of elongation at break with ageing time seemed to be linear.

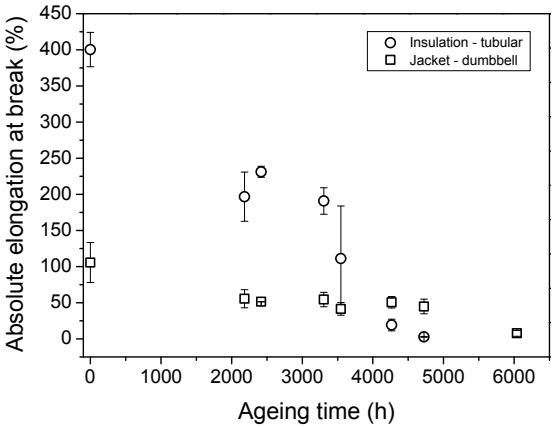

Figure 9: *The absolute elongation at break as a function of the ageing time of non-aged and aged XLPO from the SSC cable.*

.3.4 Changzhou Bayi Cable Co-CBC: EPR/EPR

Outer and inner insulation of CBC cable are made out of EPR material. The representative eng. stress- eng.strain curves for inner, tubular insulation are shown in Fig. A.10.

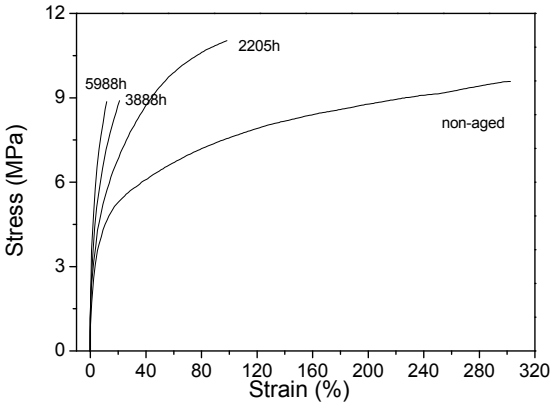

Figure 10: *The absolute elongation at break as a function of the ageing time of non-aged and aged inner insulation EPR from the CBC cable.*

As expected, elastic type behaviour is observed. With ageing the elongation at break clearly decreases and the modulus increases. With respect to the ultimate tensile stress it seems that the initial increase is followed by decrease, as a function of the ageing time. Similar result was observed for the industrial EPDM previously (see Chapter 3.).

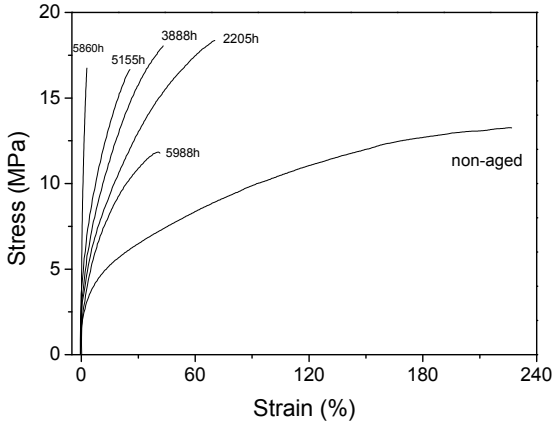

Figure 11: *The absolute elongation at break as a function of the ageing time of non-aged and aged outer insulation EPR from the CBC cable.*

It is interesting to observe what happens in the case of jacket material, see Fig A.11. Similar behaviour could be observed, but in the case of jacket material the ageing time is longer (there is one more ageing time) and significant drop of modulus is observed for this ageing time (5988h) and moreover the sudden increase of the elongation at break. The structural change that caused this change of macroscopic parameters was acting as a recovery (healing) mechanism, but since we don't have any information about important structural properties (percent of crystallinity, degree of cross-linking, presence of fillers), mechanism of this process couldn't be specified.

The change of elongation at break with ageing is presented in Fig A.12 Interestingly, even if important difference in the elongation at break of non-aged insulation and jacket samples is observed, after thermal ageing is applied similar values of elongation at break are obtained for both

insulations.

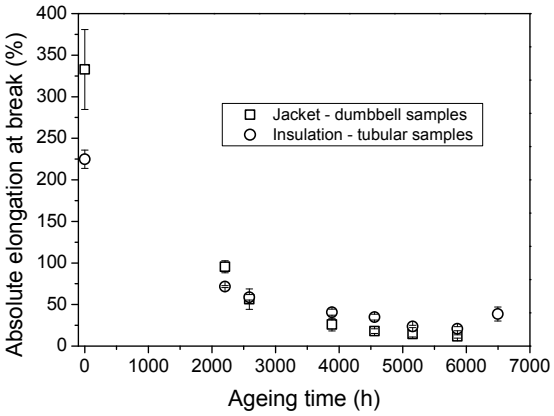

Figure 12: *The absolute elongation at break as a function of the ageing time of non-aged and aged EPR from the CBC cable.*

The absolute elongation at break of non-aged EPR jacket material is about 225 %, while for the non-aged industrial EPDM it was about 125.5 % for outer insulation and 279.1 % for inner insulation.